Unravelling new oncogenic functions of IKKα: towards a better understanding of colorectal carcinogenesis

Carlota Colomer Montañà

TESI DOCTORAL UPF / 2017

Thesis supervisors:

Dr. Lluís Espinosa Blay

Dr. Anna Bigas Salvans

Programa de Recerca en Càncer,

Institut Hospital del Mar d'Investigacions Mèdiques

Per vosaltres, que sempre heu confiat en mi

“I have not failed. I’ve just found
10.000 ways that won’t work”

Thomas A. Edison

“Que tot està per fer i tot és possible”

Miquel Martí i Pol

ACKNOWLEDGEMENTS

AGRAÏMENTS

Si alguna cosa saben els doctors, és el que comporta fer una tesi. Esforç, dedicació i perseverança, molta perseverança. I tot això, només s'aconsegueix quan s'està ben rodejat de les millors persones i professionals. Aquest camí no hagués estat el mateix sense totes les persones que d'una manera o altre, s'han creuat en ell.

Començaré pel principi. Maria del Món gràcies a tu vaig arribar al Bigas lab! Gràcies pels consells i ajudar-me a decidir en un moment que estava ben perduda professionalment.

Gràcies Lluís i Anna per donar-me la oportunitat de treballar al lab. Al principi només era per un parell de mesos... i al final han passat 4 anys. La veritat és que des del primer moment ho vaig tenir clar. Va costar, però gràcies als dos per dipositar en mi la confiança perquè em pogués quedar al lab. Lluís, admiro la passió que tens per la ciència, amb un director de tesi com tu és impossible perdre la motivació! Gràcies per ser-hi sempre que et necessitem, i per ensenyar-nos tant. I Anna, gràcies per ser la veu de la consciència, sempre amb bons consells que t'ajuden a millorar cada dia. M'heu ensenyat tot el que em converteix en la petita científica que sóc avui i per això us estaré sempre agraïda. He après a ser crítica amb la meva feina i amb la dels altres, a saber transmetre els meus resultats i una de les coses que més valoro, a fer equip. El lab no seria el mateix sense aquest grup tant magnífic de persones que s'ha creat, i això és en part gràcies a vosaltres.

A tots els que hem compartit poyata i el dia a dia del lab. Leonor, llegué a tiempo para conocerte, y tuve suerte, porqué eres LO MÁS. Lista, con muy buen humor y los más importante, con connections haha. Al principi, també vaig coincidir amb el Ricard i la Cristina Rius. Va ser una llàstima que els dos abandonéssiu el lab! A partir d'aleshores les tardes es van convertir en avorrides. Cristina gràcies per transmetre tanta energia i Ricard gràcies per compartir tot el que saps i totes les idees que se't passen pel cap (tot i que a vegades descabellades jaja). Et desitjo molta sort amb la tesi! I'm not forgetting about Bing. It was good to have you around! També a la Rosa, tu ens vas donar la gran idea de fer un MS per buscar fosforilacions de quinases. A partir d'aquí va sorgir bona part del meu projecte, així que gràcies perquè si no potser encara m'estaria barallant amb els endosomes. Lierni, fue genial tenerte en el laboratorio, nos abandonaste pero me encanta poderte seguir viendo tan a menudo! Christos, at the beginning it was difficult to get to know you (even see you haha), but at the end we end up having some interesting conversations, and I discovered a very nice guy. Thanks for all your advice and all the things I learned from you. I hope everything is going well with you! Another one I miss is Roshani, the good Roshani. There is no doubt you are one of the nicest and strongest women I ever met. I admire you, and I hope our paths will cross again sometime in the future. Thank you for always being so helpful. Y Erika, ¡Cómo te

echamos de menos! Has sido mi mentora después de que se fuera Pol. Gracias por la paciencia, por estar dispuesta siempre a enseñarme y ayudarme. Tampoco me olvido de las charlas, risas y aventuras varias en el lab! Gracias. También a Francesca, me fui a Londres y cuando volví ya no estabas! Fue un placer conocerte y tenerte por aquí, te deseo lo mejor para tu futuro!

I ara ve el torn de la Lab Crew, els meus compis actuals. Els dos pilars del lab, la Jessi i la Cristina; les post-docs: Cristina P i Anna; els PhDs, la Laura i el David; els estudiants, la Sara; els sèniors, el Joan i els nouvinguts, la Kitty, la neus i la Irene. Vaya equip! Gràcies a tots!

Jessi, gràcies per ajudar-me sempre amb el què faci falta, per compartir tots els cotis (jijijij) i per tots els moments innumerables al lab! Els de fer el tonto, de riure, de comentar-la.. you are the best! Cris, como ya sabes, al principio es complicado conocerte pero una vez lo consigues, descubres a una gran persona, que se preocupa por los suyos. Gracias por todos los consejos, por siempre ser tan sincera, por ayudar siempre que te necesitamos y por todas las interminables horas de conversaciones, que siempre llevan a alguna parte. Ahora no eres nada sin tus dos cacahuetas, Nora y Elsa, gracias por dejarnos disfrutar de ellas de vez en cuando! ☺ Vaig estar molt contenta amb l'arribada de la Laura al team Espinosa, ets una persona discreta però sempre estàs allà quan algú et necessita. I el David, que al final ens va abandonar! Però me n'alegro molt que aconseguissis una beca per quedar-te al lab, encara que fos a "l'altre bàndol"! Tot i així ja sabem que podem comptar amb la teva ajuda sempre que necessitem ;) Anna Vert, amb tu van arribar els reforços!! Recordo el dia que ens va arribar el primer tumor.. i deu ni do ara quin show que tens muntat! Gràcies per tota la grandíssima ajuda, no nomes amb els tumoroids, sempre estàs disposada a ajudar amb el que faci falta si algú ho necessita. The super post-doc, Cristina P. Thanks for your help, I wish you all the best in your next step! Joan, tot i no poder-hi ser sempre, gràcies per l'interès que mostres per nosaltres i per tots els projectes.

Volia donar-vos les gràcies en especial a les meves estudiants, que no podíeu ser millors! Grazzia, although at the beginning it wasn't easy, you were a great student and you helped me a lot! La Raquel, sempre tan feliç! Tenir-te pel lab era una alegria, gràcies per ser una persona tan fàcil segur que et quedarà un TFG molt xulo. Kitty, you didn't arrive at the best moment, but I have been lucky to have you around at this time! Although you just arrived, your help has been enormous. Y por último, a mi sucesora (que no hubiera podido ser mejor), Irene. La verdad es que me recuerdas un poco a mi cuando llegué. Tienes mucha motivación por aprender lo que sea, y esto te hará llegar lejos! Me encanta dejar el proyecto en tan buenas manos.

Però no tot s'acaba al Bigas lab! M'agradaria agrair també a totes les persones que he tingut a prop al meu dia a dia, al Programa de Recerca en

Càncer. En especial vull agrair a la Gemma, vas ser la primera persona que vaig conèixer el primer dia que vaig arribar, i tot i marxar del lab, la nostra amistat no ha parat de créixer! Gràcies pels ànims quan ho he necessitat i per ser una de les meves confidents d'aquesta etapa. També a tots els veïns, els Snail i altre gent del departament, que sempre estan allà pel que necessitem, sigui per reactius, anticossos o simplement consells. Rubén, gràcies per alegrar-me sempre el dia! Et desitjo molta sort amb la tesi, que segur que acabarà sent TOP! Gràcies Raul, Guillem, Laura, Aïda, Jordi, Rocco, Lorena.. Gràcies també al chromatin team, que tant trobem a faltar! Joan Pau i Laura no és el mateix sense vosaltres! També gràcies al Joan, Neus, Judith i Sílvia.

També m'agradaria agrair als nostres col·laboradors, sobretot a l'Alberto per tota la feina amb els xenos, i sense la qual la meva tesi no seria el mateix. També a la Mar, per aconseguir-nos sempre mostres i ajudar-nos amb les immunos sempre que necessitem.

Gràcies també als jefes del departament, en especial l'Antonio per ser el meu tutor de tesi. Lorena i Silvia G, gràcies per solucionar tots els problemes amb tanta eficàcia. I en general a tots els professionals de l'IMIM que m'han ajudat amb temes de beques o RRHH.

I also want to thank the Boulton lab for having such a nice stay while I was in London. Specially, to Simon for giving me the opportunity to work in his lab and Graeme for the big help with the experiments.

I no em puc oblidar de les meves amigues, la família que tries. Amb vosaltres he passat els moments més divertits sens dubte. Gràcies per estar sempre allà, per preocupar-vos i valorar la meva feina i la tesi, i fins i tot per intentar entendre el que faig. LES AMIGUES: Ordeig, Laia, Blanca, Clàudia per trobar sempre un moment per veure'ns, Cris per les converses, i per preocupar-te sempre de com em van les coses. Mariona, gràcies pel teu humor que em fa plorar de riure, Núria, per la teva alegria, Sil per preocupar-te i per posar seny, Clara per interessar-te i per valorar tant la meva feina i Carlota, gràcies per ajudar-me i ser-hi sempre. Les nenes megliore pels viatges, els sopars, les festes... Mil moments indescriptibles que fan que t'oblidis de qualsevol problema. Tot i que sempre feu bromes, sé que en el fons sempre heu confiat en mi (o això vull pensar). Gràcies a l'insuperable GAS TEAM, conèixer-us ha set una gran sort!. Nora, Irene, Cris, Anna, Angi, Ari, per fer-te estimar tan fàcilment; Juls, per ser tan amiga de les teves amigues; Silvi, per ser-hi sempre, i acompanyar-me en totes les aventures; i la Clara per les hores de crossfit que ajuden a desconnectar, i per les converses setmanals que solucionen qualsevol problema. Us estimo molt a totes.

Gràcies també als Megliore, Ferran, Míriam, Iu, Titi, Guillem i Juli. Hem fet un gran equip! Gràcies per mostrar interès en la tesi i valorar la meva feina. I com no, gràcies per les festes que sempre estan a l'altura. Gràcies a en Javi per preocupar-se sempre pels ratolins i l'enzima.

Gràcies a les farmacèutiques! Cori, Bàrbara, Pilar, Nia, Silvi, Berta, Laura. Amb vosaltres va començar la meva carrera científica. Els moments que vam viure a la uni, ens han unit per sempre. M'encanten els nostres sopars de posar-nos al dia, totes hem acabat a llocs bastant diferents, però m'alegra veure-us a totes tant bé.

L'Eugènia, encara que sigui de tant en tant, veure't sempre és una alegria. La Carla, que des d'aquells inicis a la Sant Jordi t'has convertit en una peça essencial. I a la meva amiga de l'ànima, l'Imma. Tot i que no ens veiem tant com voldríem, sé que sempre ens tindrem l'una a l'altre.

Gràcies també als Conguitos, i en especial a en Jordi, per imprimir-me la tesi de la millor manera possible.

A la meva família, per preocupar-vos sempre per mi. Tiets, cosins i avis. En especial, l'avi Pere, que estaria molt orgullós, i a la iaia, gràcies per preocupar-te sempre i cuidar-nos tan bé. Als meus germans, en Rafa i l'Àlex, que malgrat que ens enfadem sovint no us canviaria per res, i sempre m'heu ajudat quan he necessitat alguna cosa. I la Carla, que t'has convertit en una més de la família. I els mes importants, els meus pares. No hi han paraules per agrair tot el què heu fet per mi. Sense tot el que m'heu donat i ensenyat, avui no seria on sóc. Gràcies per ser-hi sempre que he necessitat, per alegrar-vos sempre que les coses m'han anat bé i per preocupar-vos quan no ho han anat tant. Per escoltar-me i donar-me consells, sempre els millors. Per tot això i molt més, vull dedicar-vos aquesta tesi en part a vosaltres.

I per últim, vull donar-te les gràcies en especial a tu, Pol. Has viscut aquesta tesi amb la mateixa intensitat que he fet jo quasi, i sé que amb una tesi a la vida ja n'hi ha prou. Gràcies per ajudar-me sempre, per ensenyar-me tant, escoltar-me, per donar-me consells, per deixar-me una espatlla on plorar, per treure'm a sopar quan m'ha fet falta desconnectar, per fer-me riure, per ajudar-me a afrontar els problemes, per fer-me veure el cantó positiu de les coses quan les veia ben negres, en resum, per fer-me molt feliç. Has set el pilar més important en aquesta etapa, i per això aquesta tesi va en especial per tu.

Per tot això, i segurament més, aquesta tesi no hagués estat el mateix sense tots vosaltres. A tots, moltes gràcies!

ABSTRACT

ABSTRACT

Numerous studies have shown that the protein kinase IKKα is associated with cancer progression and metastasis in different models. However, the mechanisms underlying IKKα tumorigenic functions are poorly understood. We have here demonstrated that intestinal-specific deletion of IKKα does not affect intestinal homeostasis but greatly decreases tumour formation in the $Apc^{Min/+}$ background associated with reduced stemness and proliferation. In advanced human colorectal cancer (CRC), we identified a new oncogenic form of IKKα (p45-IKKα) that sustains CRC cell survival downstream of BRAF. We have here shown that p45-IKKα regulates phosphorylation of the DNA damage repair proteins 53BP1 and KAP1 thus facilitating DNA repair in CRC cells after genotoxic stress. Finally, we used patient-derived tumouroids and orthotopic xenograft models to demonstrate the possibility of using BRAF or IKKα inhibitors to enhance the effect of DNA damage-based therapies on CRC.

RESUM

Nombrosos estudis han demostrat que la proteïna quinasa IKKα està associada en diferents models de càncer, amb la progressió tumoral i la metàstasi. No obstant això, els mecanismes subjacents a les funcions tumorigèniques de IKKα són poc coneguts. Hem demostrat que l'eliminació específica de IKKα a l'intestí no afecta l'homeòstasi intestinal a l'hora que disminueix la formació de tumors en el model animal $Apc^{Min/+}$ associat a una disminució de cèl·lules mare i proliferació cel·lular. En el càncer colorectal (CCR) humà avançat, vam identificar una nova forma oncogènica de IKKα (p45-IKKα) que sustenta la supervivència de les cèl·lules de CCR per sota de BRAF. Hem demostrat que p45-IKKα regula la fosforilació de les proteïnes de reparació de dany a l'ADN, 53BP1 i KAP1, facilitant així la reparació del dany en cèl·lules de CCR després d'estrès genotòxic. Finalment, hem utilitzat tumoroids derivats pacients i models de xenògraf ortotòpic per demostrar la possibilitat d'utilitzar inhibidors de BRAF o IKKα per millorar l'efecte de les teràpies basades en el dany a l'ADN en el càncer colorectal.

PREFACE

PREFACE

Colorectal cancer (CRC) progression is a relatively well-understood process from a genetic point of view. Yet it remains the second leading cause of cancer-related death, which manifests that current therapies against advanced tumours are not totally effective. Thus, understanding the molecular mechanisms leading to CRC initiation and progression is of crucial importance to develop new drugs for treating patients. My work has been focused on delving into the role of IKKα in tumour initiation and progression. This is an essential step, not only to better understand colorectal carcinogenesis but also to develop new strategies to treat CRC. The identification of mechanisms that are unique in cancer cells, will lead to the development of new drugs for personalised therapies.

During my PhD I have been funded by the Ministry of Economy and Competitiveness of the Spanish Government with a FPI fellowship (BES-2014) and by the EMBO organization with a Short Term Fellowship to visit Simon Boulton laboratory's at the Francis Crick Institute (London). The IMIM-Hospital del Mar d'Investigacions Mèdiques funded the printing of this thesis.

The cover shows an intestine stained with Ki67 at the base of the crypts and it was designed by Pol Margalef.

TABLE OF CONTENTS

TABLE OF CONTENTS

FIGURES AND TABLES

FIGURES AND TABLES

INTRODUCTION

MATERIALS AND METHODS

IKKα inhibition reproduces the effects of BRAF inhibition in the DDR pathway

BRAF inhibition synergies the effect of standard chemotherapy on an in vivo human CRC PDX model

DISCUSSION

ABBREVIATIONS AND ACRONYMS

ABBREVIATIONS AND ACRONYMS

5-FU	5-fluorouracil
APC	Adenomatous polyposis coli
ASR	Age-standardized rates
ATM	Ataxia-telangiectasia mutated
ATR	ATM- and Rad3-Related
BAFF	B-cell-activating factor
BCC	Basal Cell Carcinoma
BER	Base excision repair
BME	β-mercaptoethanol
BRCA	Breast cancer
BRCT	BRCA1 carboxy-terminal
CaMKII	Ca2+/calmodulin-dependent protein kinase II
CAPIRI	Capecitabine and Irinotecan
CAPOX	Capecitabine and Oxaliplatin
CBP	CREB-binding protein
CC	Coiled-coil
CDK	Cyclin-dependent kinase
cDNA	Complementary DNA
cIAP	Cellular inhibitor of apoptosis
CIMP	CpG island methylator phenotype
CIN	Chromosomal Instability
CR	Conserved Region
CRC	Colorectal cancer
CSC	Cancer stem cell
CSR	Class switch recombination
DCC	Deleted in colorectal cancer
DD	Death domain
DDR	DNA damage response
DSB	DNA double strand breaks
DSS	Dextran sulphate sodium
DUB	Deubiquitinating enzymes
EGF	Epidermal Growth Factor
EGFR	Epidermal Growth Factor Receptor
ELKS	Protein rich in aminoacids E, L, K and S
ENU	Ethynilnitrosourea
ERα	Estrogen Receptor Alpha
FADD	Fas receptor-associated DD
FAP	Familial Adenomatous Polyposis

FGF8	Morphogen fibroblast growth factor
FISH	Fluorescence in situ hybridization
FOLFIRI	Folinic acid, 5-FU and irinotecan
FOLFOX	Folinic acid, 5-FU and oxaliplatin
GAP	GTPase activating proteins
GEF	Guanine nucleotide exchange factor
GI	Gastrointestinal
GMO	Genetically modified organisms
GSEA	Gene Set Enrichment Analysis
HCC	Hepatocellular carcinoma
HDAC	Histone Deacetylase
HLH	Helix-loop-helix
HNPCC	Hereditary Non-Polyposis Colon Cancer
HR	Homologous recombination
IF	Immunofluorescence
IFN	Interferon
IGF1R	Insulin Growth Factor Receptor
IHC	Immunohistochemistry
IKK	IκB kinase
IR	Ionizing radiation
IRAK4	IL-1R associated kinase 4
ISC	Intestinal stem cells
IκBα	Inhibitor of κB α
KAP1	KRAB-interacting protein
KD	Kinase-dead
KO	Knockout
LC	Liquid chromatography
LC-MS/MS	Liquid Chromatography-Tandem Mass spectrometry
LOF	Loss-of-function
LPS	Lipopolysaccharide
LT	Lymphotoxin
LT-β	Lymphotoxin-β
LUBAC	Linear ubiquitin assembly complex
LZ	Leucine zipper
mAbs	Monoclonal antibodies
MAPK	MAP kinase
mCRC	Metastatic CRC
Min	Multiple intestinal neoplasia
MMEJ	Microhomology-mediated end-joining
MMR	Mismatch repair

MS	Mass spectrometry
MSI	Microsatellite Instability
MyD88	Myeloid differentiation primary response 88
N-CoR	Nuclear Receptor Correpresor
NBD	NEMO-binding domain
NEMO	NF-κB essential modulator
NER	Nucleotide excision repair
NF-κB	Nuclear Factor kappa-light-chain-enhancer of activated B cells
NF1	Neurofibromin 1
NGS	Next-generation sequencing
NHEJ	Non-homologous end-joining
NIK	NF-κB inducing kinase
NLK	Nemo-like kinase
NSAID	Non Steroidal Anti-Inflammatory Drugs
PAGE	Polyacrylamide gel electrophoresis
PARP-1	Poly-ADP ribose polymerase
PDOX	Patient-derived orthotopic xenograft
PDX	Patient-derived xenografts
PEI	Polyethylenimine
PI3K	Phosphatidylinositol 3-kinases
PIASγ	Protein inhibitor of activated STATγ
PIDD	p53-induced protein with a death domain
PKA	Protein kinase A
PNA-FISH	Peptide Nucleic Acid FISH
PPAR	Peroxisome proliferator-activated receptor
PTM	Post-Translational Modification
qRT-PCR	Quantitative real time polymerase chain reaction
RAF	Rapidly Accelerated Fibrosarcoma
RANKL	Receptor activator for NF-κB ligand
RIPK1	Receptor-Interacting Protein Kinase 1
RNA-seq	RNA sequencing
RTK	Receptor tyrosine kinases
RUNX2	Runt-related transcription factor 2
SCC	Squamous Cell Carcinoma
SCF	Skp1-Cullin-F-box
SDD	Scaffold/dimerisation domain
Sh	Short hairpin
SMRT	Silencing mediator for retinoic acid and thyroid hormone receptor

SOS	Son of Sevenless
SRC-3	Steroid Receptor Coactivator 3
SSB	Single strand breaks
SUMO	Small Ubiquitin-related Modifier
TA	Transit amplifying
TAB3	TAK1 Binding Protein
TAK1	TGFβ–activated Kinase 1
TF	Transcription factors
TGF-β	Transforming growth factor-β
TIF	Telomere-dysfunction-induced foci
TIR	Toll/IL-1R
TLR	Toll-like receptor
TNFR	Tumour Necrosis Factor Receptor
TRADD	TNFR-associated protein with a DD
TRAF	TRNF-associated factor
TRIF	TIR-domain-containing adapter-inducing interferon β
UBC13	Ubiquitin-conjugating enzyme 13
UDR	Ubiquitination-dependent recruitment
UEV1A	Ubiquitin-conjugating enzyme E2 variant 1
UV	Ultraviolet
VEGFR	Vascular Endothelial Growth Factor Receptor
WB	Western blot
WTSS	Whole transcriptome shotgun sequencing

INTRODUCTION

INTRODUCTION

I1. The intestine

I1.1 The intestinal tract

The gastrointestinal (GI) tract is a muscular tube that extends from the mouth to the anus where food is processed and digested. It forms part of the digestive system, which includes the digestive organs and their accessory organs (such as teeth, tongue, salivary glands, liver, gallbladder and pancreas). Anatomically, it can be classified as follows: the upper GI tract, that consists of the **oesophagus**, **stomach** and duodenum[a]; and the lower GI tract, that comprises most of the small and large intestine. The intestine is the segment of the GI tract extending from the pyloric sphincter of the stomach to the anus and is composed by two segments, the **small intestine** and the **large intestine**. The small intestine is further subdivided into the duodenum, jejunum and ileum, while the large intestine is subdivided into the cecum (with the appendix), colon (right or ascending, transverse, left or descending, and sigmoid), rectum, and anal canal.

The major function of the GI tract is to ingest, digest and absorb nutrients from the diet, and excrete the waste products left. In addition to processing nutrients, it also has a prominent role in the immune system as an important barrier between the human host and the microbial of the intestinal lumen.

I1.2 Layers of the intestine

The GI tract has a specific histology that reflects its functional specialization. The **gastrointestinal wall** surrounding the lumen of the GI tract is made up of four concentric tissue layers, with functional differences in each specialised region:

- **Mucosa**: is the innermost layer of the gut. It comes into direct contact with the food, and is responsible for absorption and secretion. It is highly specialised in each part of the tract to deal with different conditions. It is protected by a layer of mucus secreted by goblet cells from the epithelium (See below). It can be further divided into **epithelium** (where

[a] From the Greek word οισοφάγος *(oisofágos)* which means "to carry, to eat".

most digestive, absorptive and secretory processes occur), **lamina propria** (connective tissue) and **muscularis mucosae** (thin layer of smooth muscle).

- **Submucosa**: consists of fibrous connective tissue, separating the mucosa from the surrounding muscles. Includes large lymphatic and blood vessels, as well as fine bundles of nerve plexuses.

- **Muscularis externa**: external muscle layer composed by two distinct layers of the smooth muscle: an inner circular muscle layer and the outer longitudinal muscle layer. Between the two muscle layers are the myenteric or Auerbach's plexus that control peristalsis[b].

- **Serosa** (intraperitoneal) or **adventitia** (retroperitoneal): are the outermost layers of the gut, containing a single layer of mesothelial cells and several layers of connective tissue. *Intraperitoneal regions* of the tract are covered with serosa; they have a clear boundary with the surrounding tissue and have a mesentery. These include most of the stomach, first part of the duodenum, small intestine, caecum and appendix, transverse colon, sigmoid colon, and rectum. *Retroperitoneal regions* are covered with adventia; they blend into the surrounding tissue and are fixed in position. These include oral cavity, oesophagus, pylorus, distal duodenum, ascending colon, descending colon and anal canal.

I1.3 Architecture of the intestinal epithelium

In the small intestine, the epithelial layer covers **finger-like villus** structures and adjacent invaginations called **crypts of Lieberkühn**[c] [**FIGURE I1**]. In contrast, the colonic epithelium does not contain villi and instead forms deeper invaginations that represent a compressed version of the crypt-villus architecture.
The intestinal epithelium contains differentiated cells that populate the villi and can be categorized based on their function: absorptive enterocytes, and four secretory cell types including paneth cells, goblet cells, enteroendocrine cells, and tuft cells [**FIGURE I1**].

[b] Involuntary constriction and relaxation of the muscles of the intestine, creating wave-like movements which push contents forward the canal.

[c] Named for Johann Nathanael Lieberkühn that first described these glands in 1745.

Enterocytes are responsible for the absorption of nutrients and their transport across the epithelium. They are also present in the large intestine where they are named **colonocytes**. They are polarised cells with microvilli on the apical surface facing the lumen (visible microscopically as a brush border) that increase the absorptive area[1]. **Goblet cells** are responsible for secreting a protective mucus barrier that allows the smooth passage of the intestinal content but also acts as a protective barrier for bacteria[2–4]. We can also find neuroendocrine[d] or **enteroendocrine cells** that release peptidic hormones and/or digestive enzymes. **Tuft cells** (or brush cells) were described long ago[5], and although their most stablished function is as chemoreceptors, they were described as a new secretory type of the intestinal epithelium. Moreover, three different studies revealed a key role for tuft cells in driving type 2 immunity by releasing IL-25, which starts an immune cascade[6–8]. Normally residing at the bottom of the crypts of Lieberkühn, **paneth cells**[9,10] mainly secrete anti-microbial peptides such as lysozyme[11] and α-defensins[12]. However, they are now emerging as components of the stem cell niche [13,14]. **Intestinal stem cells** (ISCs) reside at the bottom of the crypts and are capable of producing all **transit amplifying** (TA) progenitors, which can differentiate toward all epithelial lineages[15]. As cells begin to differentiate, they migrate toward the lumen and are eventually shed, either from the tip of the intestinal villi or from the surface of the colonic epithelium. Therefore, the crypt is mainly a proliferative compartment and is maintained by multipotent stem cells whereas the villus represents the differentiated compartment.

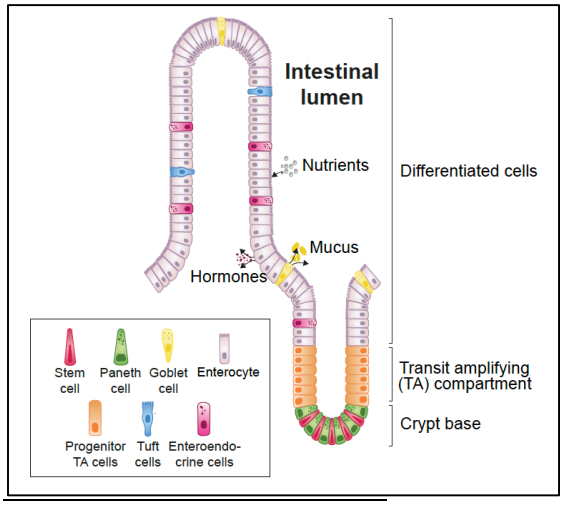

Figure I1. Schematic of the crypts and villi of the small intestine. The stem cells are located at the base of the crypt and the cell types of the intestinal epithelium line the villus.

[d] First termed **neuroendocrine cells**, they were once thought to originate from the neural crest, due to the similarities they share with neurons.

I2. Colorectal cancer

The intestinal epithelium is able to continuously self-renew while maintaining an excellent balance between cell differentiation, proliferation, migration and cell death. If one of these processes is altered, intestinal tumorigenesis can arise. **Colorectal cancer (CRC)** is characterized by an uncontrolled and abnormal cell growth with invasive capacities in the colon or in the rectum. Colorectal cancer is often asymptomatic, however, as the tumour grows, it may bleed or obstruct the intestine.

I2.1 Incidence and mortality

CRC is the third and the second most common cancer in men and women, respectively. According to the last Globocan Project from 2012[16], there are 746,000 cases reported (10% of the total worldwide) in men and 614,000 cases (9,2% of the total worldwide) in women and interestingly, almost 55% of them occur in more developed regions. This is due to differences in diet, physical activity, etc.[17,18], that makes the incidence across the world to differ depending on the location. Regarding its mortality, it is the fourth leading cause of death by cancer in men (374,000 deaths, 8% of the total) and the third in women (320,000 deaths, 9% of the total) [**FIGURE I2**].

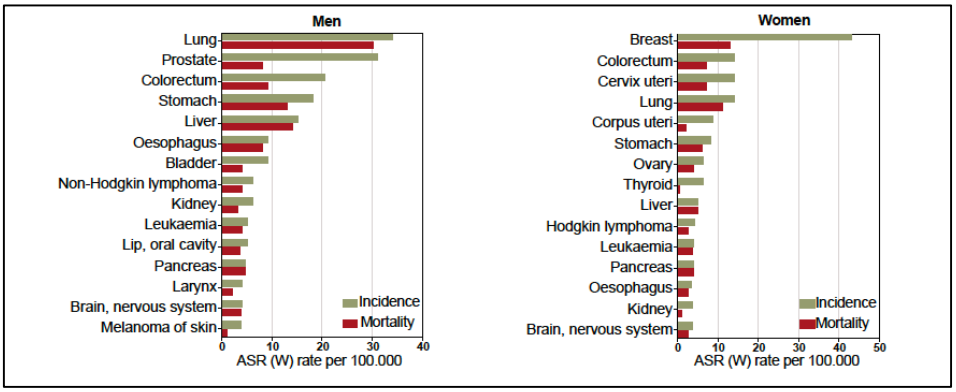

Figure I2 | Global cancer incidence and mortality. Estimated age-standardized rates (ASR) for incidence (green) and mortality (red) for men (left) and women (right). Adapted from Ferlay et al. 2015[19].

I2.2 Colorectal cancer development and progression: The adenoma-carcinoma sequence

The earliest identifiable event of colorectal neoplasia is a small dysplastic lesion formed in the colonic or rectal epithelium. This results in the formation of **aberrant crypt foci**[20,21] that expand over time to form macroscopically visible **adenomatous polyps**. Adenomas are neoplasms defined by an expansion of the proliferating compartment and defective differentiation of epithelial cells that protrude into the lumen from the intestinal epithelium[22]. Thus, the strict correlation between cellular phenotype and the position along the vertical axis of the intestinal crypt is totally disrupted. Indeed, it is now firmly established that most, if not all, colorectal carcinomas develop from a preceding non-invasive adenoma. Progressively, mutant cells acquire the ability to invade the basement membrane into the lamina propria, where they advance to the **carcinoma in situ**[23] stage. Overtly, invasive carcinomas often represent the first clinical presentation of colorectal tumours. Finally, these carcinomas are able to colonise other organs both locally or at distance, through the blood circulation, where they form a **metastatic carcinoma** [**FIGURE I3**].

I2.3 Genetics

From a genetic point of view, CRC is one of the best-understood solid malignancies. CRC arise as a consequence of the accumulation of genetic and epigenetic alterations that transform colonic epithelial cells into colon adenocarcinoma cancer cells. The loss of genomic stability is now recognised as an essential cellular feature that accompanies the acquisition of mutations in most types of CRC. In CRC, at least three distinct pathways of genomic instability have been described[24]. The most common (around 60% of CRC) is characterized by **Chromosomal Instability (CIN)**, that induce gross changes in chromosome number and structure, including deletions, gains, translocations and other chromosomal rearrangements[25]. Another mechanism, less common (around 20% of CRC), shows **Microsatellite Instability (MSI)** due to defective DNA mismatch repair (MMR)[26]. CRC also harbours epigenomic instability, either by global hypomethylation or as the **CpG island**[e] **methylator phenotype (CIMP)**

[e] Short interspread DNA sequences rich in CpG dinucleotide repeats and being predominantly nonmethylated. Most, perhaps all, are located within gene promoters.

(20% of total CRC), defined as DNA hypermethylation in CpG-rich promoters that result in loss of tumour suppressor gene expression[27,28].

Sporadic colorectal cancer: The sequence of genetic mutations

Sporadic CRC arise without known contribution from germline mutations or significant family history of cancer or inflammatory bowel disease. It represents about 70-80% of all CRC cases and patients usually develop the disease over 50 years of age[29].

In 1990, Fearon and Vogelstein proposed a multistep **genetic model for colorectal tumorigenesis**, describing genetic alterations essential to the development of CRC[30].

In this model, loss of function of the adenomatous polyposis coli (***APC***) gene is one of the earliest events required for colon adenoma formation and is found in up to 80% of all CRC patients[31,32]. APC is a protein that functions as a suppressor of the Wnt signalling pathway by catalysing the degradation of β-catenin[33–35]. In the presence of inactivating APC mutations, β-catenin is accumulated in the cytoplasm and translocated to the nucleus where it activates specific gene transcription. Alternatively, some colon cancers activate the pathway through mutations in the β-catenin gene that results in non-degradable variants. Genes induced by Wnt activation include *c-myc*, *cyclin D1* and *PPAR-δ*[36]. In normal epithelial cells, most of the cellular β-catenin protein is associated with the cell-adhesion transmembrane glycoprotein E-cadherin at the adherens junctions. E-cadherin is downregulated in a significant number of patients leading to altered β-catenin regulation[37,38].

The second step in the progression of this malignancy is the activating mutations in oncogene ***KRAS*** in exon 2 (codons 12 and 13) and to a lesser extend in exon 3 (codon 61). Mutations in each of the three codons lock KRAS in the active GTP-bound state.

Mutations in KRAS are present in about 40-50% of the patients with CRC, which leads to the aberrant activation of the MAPK pathway that controls cell proliferation[39].

Loss of the **18q chromosome** is frequently observed in advanced CRC and is associated with poor prognosis[40,41]. Importantly, **18q deletion results in** loss of *SMAD2/4* genes that are members of the TGFβ signalling pathway, which plays a tumour suppressor activity in epithelial cells. Unexpectedly, it

was recently demonstrated that high levels of TGFβ in the microenvironment of CRC tumours is an indicator of bad prognosis, as it associates with increased metastatic activity of cancer cells. In fact, TGFβ activity is primarily induced in stromal cells that then secrete factors that impact on CRC cells[42]. Another gene that is localized at chromosome 18q is *DCC* (deleted in colorectal cancer) that encodes a netrin[f] receptor that controls differentiation and tumorigenesis[43].

Finally, loss of tumour suppressor **p53** at a late stage may account for invasive carcinoma formation, associated with escape from cell cycle arrest, apoptosis[44] and therapy resistance[45,46] [**FIGURE I3**].

While mutation events are stochastic, the sequence in which they accumulate is not arbitrary, supporting the argument that only certain mutations confer a selective advantage at a given stage of tumour's natural history.

Sequencing studies have also revealed that many other mutations occur in individual CRC tumours, although at much lower frequencies. For example, a recent theory of CRC, referred to as the **Big Bang model**, describes tumour growth as an expansion populated by various heterogeneous subclones. All subclones carry initial "public" mutations in genes, such as APC and KRAS, and subsequent "private" mutations are acquired later in individual subclones[47]. The importance of several of these mutations is still unclear and many represent passenger mutations which might have no function[48–50].

A different group of sporadic tumours include those with MSI (~20% of sporadic colon cancers), which is commonly associated with **DNA mismatch repair (MMR) gene inactivation**, characterized by the loss of function of the MMR pathway[51]. Failure to repair replication-associated errors due to a defective MMR system allows persistence of mismatch mutations all over the genome, but especially in regions of repetitive DNA known as microsatellites, giving rise to the phenomenon of MSI. Loss of DNA MMR function can be caused by either mutations, deletions, or epigenetic silencing of both copies of one of the MMR genes, the most important ones being *MSH2*, *MLH1*, *MSH6* and *PMS2*[52,53]. Epigenetic modification of *MLH1* can serve as tumour marker and has been detected in

[f] Netrins are a class of proteins involved in axon guidance. They are named after the word "*netr*" which means "one who guides" in Sanskrit language.

the serum of MSI colon cancer patients[54]. BRAF mutations (usually V600E) are found in the majority of sporadic tumours with MSI[55] [**FIGURE I3**].

Hereditary colorectal cancer

Around 20-30% of CRC patients[56,57], are affected by a hereditary colorectal cancer syndrome caused by germline mutations in different genes that confer a high risk of developing CRC during their lifetime[58,59].

The most common syndrome in this category is the **Hereditary Non-Polyposis Colon Cancer (HNPCC) or Lynch syndrome**. This syndrome account for 2-4% of all CRC[60] and is characterised by germline mutations in components of the DNA MMR complex that induce MSI[52,61–63]. Carriers of these autosomal dominant mutations have an 80% lifetime risk of CRC and an increased risk of gastric and endometrial cancers. A well-planned cancer surveillance program is essential not only for these individuals but also for at-risk family members. DNA MMR inactivation induces a nearly 1000-fold increase in spontaneous gene mutation rates. This “mutator” phenotype reduces the time for colon cancer development to less than 36 months, creating mutational hotspots in the coding regions of some genes[64]. The prototypical example is the biallelic mutational inactivation of the type II TGF-β receptor[40,65].

The second most common hereditary colorectal cancer syndrome is the inherited **Familial Adenomatous Polyposis (FAP)** caused by germline mutations in one allele of the *APC* gene[40,65]. *APC*, a classic tumour suppressor gene, is then inactivated in the wild-type (WT) germline allele of these patients, most often by deletion. The majority of FAP associated *APC* mutations are nonsense mutations that truncate the APC protein, suggesting a critical tumour-suppressive role for the central and C-terminal domains of the protein. Different domains of the protein have been functionally characterized including the one that binds to and promotes the degradation of cytoplasmic β-catenin[66–68] in the context of a complex including AXIN, CK1 and GSK3β[69–72]. When the complex is active (APC WT), CK1 and GSK3β sequentially phosphorylate β-catenin at S33, S37, T41 and S45[72]. When *APC* is inactive, β-catenin accumulates in the nucleus of epithelial cells. FAP patients develop hundreds to thousands of colonic adenomas during the third to fourth decade of life, and the lifetime risk of colon cancer approaches 100%[34].

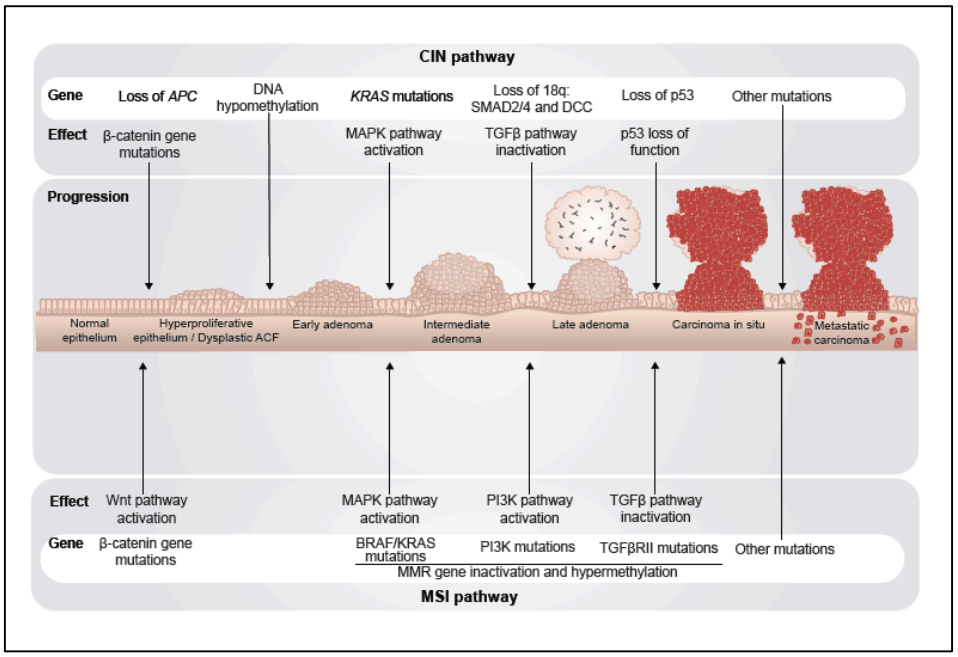

Figure I3 | Histopathology and genetic abnormalities of colorectal cancer: the adenoma-carcinoma sequence. Simplified model of colorectal carcinogenesis evolution. It aligns observed clinicopathological changes with genetic abnormalities in the progression of CRC. The initial step in tumorigenesis is the appearance of aberrant crypt foci upon APC loss. Adapted from Fearon & Volgestein, 1990[30].

Other classifications: The consensus molecular subtypes of CRC

Metastatic CRC (mCRC) patients can also be grouped into molecular subtypes based on gene expression profiles[73]. While some mutations are more common in certain subtypes, particular driver mutations appear to be less important than biological signatures associated with each category. Using this classification, patients can be grouped into MSI/immune (CMS1), canonical/Wnt (CMS2), metabolic (CMS3) and mesenchymal (CMS4) profiles. Although these subtypes are still not ready for introduction into standard clinical practice, they present an opportunity to guide targeted therapies with underlying biologic rationale and will hopefully help to improve the success of targeted agents in mCRC trials.

I2.4 Models for CRC

Models of intestinal cancer are powerful tools to recapitulate human intestinal tumorigenesis, understand its biology and to test potential therapeutic strategies.

Genetically modified organisms (GMO) have been long used to model human diseases. As mentioned above, mutations in *APC* gene are required to initiate FAP and are also important in sporadic CRC[33,56,74]. Given the high prevalence of *APC* mutation, several *Apc*-mutant mice have been generated to study the role of *Apc* and other involved genes in the initiation and progression of intestinal tumorigenesis. The most commonly used model to study FAP and CRC is the Min (Multiple intestinal neoplasia) model, referred to as $Apc^{Min/+}$. Min mice carry a ethynilnitrosourea (ENU)-induced mutation in the murine *Apc* gene[75] that encodes a stop codon at position 850 resulting in premature truncation of the polypeptide. Like humans with FAP syndrome, Min/+ mice (in a C57BL/6 background) develop hundreds of adenomas by 4 to 6 months of age[76]. Remarkably, adenomas are developed in the small intestine of the mice and only occasionally progress to invasive carcinomas[75,77] in contrast to human FAP patients that present predominantly colonic adenomas and usually do progress to invasive carcinomas. Despite these differences, this is still one of the best available models to study early events in colorectal tumorigenesis.

To specifically drive disease development to the large intestine, some groups have generated conditional *Apc* mice using specific Cre strains directly delivered in the colon[78–81]. Nevertheless, due to their bias toward the development of small intestinal tumours, these mouse models have been considered inadequate surrogates of human CRC. Probably, the model that recapitulates best the FAP syndrome until now is the one that conditionally suppressed *Apc* using a doxycycline-regulated shRNA. *Apc* suppression in Lgr5 expressing ISC produces adenomas in both the small intestine and colon, which in the presence of Kras and p53 mutations progress to invasive carcinoma[82]. Indeed, in this work it is demonstrated that restoration of *Apc* drives tumour regression even in the presence of *Kras* and p53 mutations, which proves that *Apc* loss is required not only for tumour initiation but also for tumour maintenance.

Further, mutations that mimic the adenoma-carcinoma sequence have been added to generate mouse models of invasive CRC that better reflect the human disease. These include combination of mutant *Apc* and mutated $Kras^{G12V/+}$ and $Kras^{G12D/+}$ [83–85], mutant *Pten*[86] and *Pi3kca*[87,88], as well as

inactivation of various components of the TGF-β signalling pathway (*Tgfbr2*, *Smad2*, *Smad3* or *Smad4*)[89–92] or loss of *Tp53*[77,93]. Collectively, all these mutations lead to increased tumour progression and development of adenocarcinomas in mice, although alone these additional mutations did not provoke rapid tumorigenesis. This observation further supports the concept that *Apc* mutation is indispensable for intestinal tumour initiation.

Apart from genetic mice models, many **chemicals** have been used, such as dextran sulphate sodium (DSS)[94], to induce CRC. The progression of these cancers depends on the duration and the dose of each chemical.

Another attempt to overcome the limitations of these models and study the mechanisms involved in tumour growth and metastasis is the use of **transplantation models**. In recent years, there has been a renewed interest in the development of xenograft models from different tumour types. Indeed, these models are becoming the preferred preclinical tool in an attempt to identify biomarkers, understand the mechanisms of drug resistance, drug development and screening, and are also emerging as applications for personalised medicine. Conventional cell-line based xenografts, although convenient and easy to use, have important limitations. The most relevant is their lack of representation of the broad molecular diversity of the disease. For this reason, there has been increasing interest in the application of more advanced preclinical cancer models such as patient-derived xenografts (PDX). Serially passaged PDXs show biological consistency with the tumour of origin, are phenotypically stable across multiple transplant generations at the histological, transcriptomic, proteomic and genomic levels, and show comparable treatment responses to those observed clinically[95]. While a vast majority of the studies have focused on subcutaneous implantation, others have explored the value of implanting the tumours in the same organ of origin (orthotopic implantation)[96] or in better-vascularised tissues such as the renal capsule[97]. Arguably, these more physiological implantation sites may better recapitulate some phenotypic features of the original tumours including the presence of an intestinal-specific micro-environment and their capacity to develop distant metastasis. To avoid xenograft rejection, PDX models are developed in immune-compromised mice, which makes it a major limitation given the increasing importance of the immune response for cancer therapy. In this line, an emerging approach would be the reconstitution of a human immune system in the mouse, although that still requires further innovation since current approaches are labour intensive and difficult to scale to higher throughput drug treatment studies[98]. Other major limitations of PDX models are the

replacement of human stromal components and the selective outgrowth of more malignant cells[99,100].

Finally, in 2009, Sato *et al.* published a robust method that enabled the production of self-renewing **intestinal organoids**, which could be expanded indefinitely[101]. In this system, intestinal crypts are cultured as organoids in non-adherent and serum free conditions in a 3D matrix that mimics the microenvironment of the crypt base in vivo. This method was soon optimised to enable the production of **tumouroids** from murine and human colorectal adenoma and carcinoma tissue that grow as undifferentiated spheres, as well as organoids from human colonic stem cells[102,103]. Later, in mid 2015, the generation of tumouroids derived from colorectal cancer patients arrived[104]. This enables the in-depth testing of a range of therapeutic compounds in a patient-relevant model. The ability to test a range of chemotherapeutics on actual patient-derived organoids could lead to patient-specific personalised therapy. On a broader scale, production of a range of patient-derived organoids from a variety of different genetic profiles will enable the exploration of specialised drug treatment plans post-biopsy, as well as enable the genetic manipulation using technologies such as CRISPR-Cas9 to isolate the genetic mutations responsible for specific cancer phenotypes. Interestingly, the successful introduction of each of the mutations (*APC, KRAS, SMAD4* and *P53*) by CRISPR-Cas9 confirmed the CRC progression model proposed by Fearon and Volgestein in 1990[105,106] [**FIGURE I3**]. By providing an easy-to-handle model in which genotype and phenotype can be directly compared in a short space of time, the use of organoid culture opens up an array of different experimental techniques which were previously not possible.

Together these models have been used to define fundamental processes involved in tumour initiation and metastasis. They have and will provide key insights to understand this complex disease and hopefully will lead to the discovery of new therapeutic strategies.

I2.5 Cancer stem cells

There is extensive evidence that most cancers are mainly heterogeneous, organized and sustained by a subpopulation of self-renewing cells that can generate the full repertoire of tumour cells[107–109]. Accordingly, two models have been proposed to explain tumour heterogeneity:

On the one hand, the **stochastic model** predicts that a tumour is biologically homogeneous and every tumour cell has the potential to be a **cancer stem cell (CSC)**. Clinically this means that both the actual CSCs and the bulk of the tumour cells need to be simultaneously removed to efficiently eliminate a tumour, because all cells have the potential to become CSCs.

On the other hand, the **hierarchy model** predicts that the tumour mimics the normal tissue development, retaining a hierarchical organization where only a distinct subset of cells have the potential to behave like CSC[110]. From a clinical point of view, this model raise the possibility to specifically target CSCs as an effective method to revert tumour growth and avoid resistance to therapies and tumour relapse[111].

Identification of subsets of tumour cells with CSCs activity can be done by different approaches. There is an in vivo approach involving the purification of specific cell populations (by the presence of cell surface markers) of colon cancer cells and testing their ability in tumour formation by xenotransplantation in mice. Alternatively, CSCs can be cultured in vitro as tumouroids. However, there is no clear consensus on what the intestinal CSCs are, as multiple subpopulations follow these same criteria.

Barker *et al.* suggested that only **Lgr5$^+$** stem cells carrying APC-deficiency, might lead to colorectal adenoma formation[112]. Lineage tracing experiments with an inducible GFP driven by the *Lgr5* promoter revealed that *Lgr5*$^+$ tumour cells have self-renewal and differentiation capacity and contribute to tumour regrowth[113]. A similar report demonstrated that tumours are maintained by proliferative Lgr5$^+$ cells that continuously attempt to replenish the Lgr5$^+$ CSC pool, leading to rapid re-initiation of tumour growth upon treatment cessation[114]. This was later demonstrated also for LGR5$^+$ human colon CSC[115].

Apart from Lgr5, **CD133** was initially described as a CSC marker for human colorectal cancer[116,117], and cells expressing CD133 display a similar capacity for tumour initiation as Lgr5+ in mice[112,118]. Likewise, a different report described that **EphB2** sorted ISC-like tumour cells, display tumour-initiating capacities in immunodeficient mice, and defines a CSC niche within colorectal tumours that play a central role in CRC relapse[119]. **Musashi 1 (MSI1)**, which was one of the first proposed intestinal stem cell markers[120–122], has also been described as a marker for tumour growth and maintenance[123–125]. Human CRC cells have been shown to require **BMI1** expression for tumour growth and maintenance[126]. Furthermore, **Sox9** has

also been proposed as a CSC marker although it has a controversial role because both oncogenic and tumour-suppressing functions of the protein have been described[127–131]. Other surface markers that have been demonstrated as human and/or murine colorectal cancer stem cell markers are **ALDH1** [132], **CD26** [133], **DCLK-1** [134] **KRT19** [135], **SOX2** [136], **CDCP1** [137] and **CD110** [137,138].

Although the terms CSC and '**tumour initiating cell**' (TIC or 'cancer initiating cell', CIC) have been used interchangeably, the term TIC more suitably denotes the cell of origin of a tumour. In human colorectal cancer, TICs have been described to express the markers CD133[118], LGR5[112], and KRT19[135] in a similar fashion to CSCs. However, CSCs have been the most extensively studied because of their clinical implications: if they are not eliminated with therapy or become resistant, they would have the ability to re-grow the tumour and account for relapse.

I2.6 Therapy

Treatment for CRC is largely based on the stage of the disease. Patients with non-metastatic CRC usually have **surgery** as the first option or are initially treated with neoadjuvant therapies that consist of the classical **chemotherapy** and/or **radiotherapy** before surgery. For chemotherapy, the first-line drug regimens consist of 5-fluorouracil (5-FU) or its precursor capecitabine plus leucovorin, together with irinotecan[g] and/or oxaliplatin[h] [139]. Folic acid or leucovorin is a vitamin B derivative that increases the cytotoxicity of 5-FU, which is a pyrimidine analogue that incorporates in the DNA and stops replication. Irinotecan is a topoisomerase I[i] inhibitor that prevents DNA from uncoiling and duplicating, and oxaliplatin is a platinum-based anti-neoplastic that causes crosslinking of DNA inhibiting its repair and synthesis.

In some patients, sequential single-agent therapy is a reasonable treatment approach that is comparable to the combination therapy[140]. Sometimes,

---

[g] Drug combination abbreviated as CAPIRI (CAPecitabine and IRInotecan) or FOLFIRI (FOLinic acid, 5-FU and IRInotecan). Some therapies include oxaliplatin to this combination, which is then called FOLFOXIRI

[h] Drug combination abbreviated as FOLFOX (FOLinic acid, 5-FU and OXaliplatin) or CAPOX (CAPecitabine and OXaliplatin). Folic acid or leucovorin is a vitamin B derivative.

[i] Type I topoisomerase are enzymes that cut one of the two strands of double-stranded DNA to catalyse the relaxation of negatively supercoiled DNA.

chemo drugs are given along with a targeted therapy drug. Nowadays, targeted therapies include monoclonal antibodies against VEGF and EGFR (further explained at section I3). Anti-VEGF antibodies play an antiangiogenic role and include the drugs bevacizumab[141], ramucirumab[142] and ziv-aflibercept[143]. On the other hand, cetuximab and panitumumab, the monoclonal antibodies against EGFR, are also an effective treatment in combination with irinotecan for patients with metastatic colon cancer [144–146]. Importantly, their use is restricted to RAS and RAF wild-type patients[147,148]. However, despite local recurrences being under control due to more invasive surgery (transmesorectal excision) and pre-operative adjuvant chemotherapy or radiotherapy, distant recurrences after surgery (~30% of stage II or III patients) still present a major problem and are often the ultimate cause of death for CRC patients[149,150]. Colorectal cancer therapy still needs a lot of research to improve CRC patient survival.

I3. NF-κB pathway

More than 30 years ago, in 1986, NF-κB was identified by David Baltimore´s laboratory[151]. Its name accounts for Nuclear Factor kappa-light-chain-enhancer of activated B cells. It was discovered as a DNA-binding factor in the nucleus of activated B cells that specifically recognizes an enhancer element found in the gene encoding the immunoglobulin-κ light chain. Initially, it was thought to be an important regulator of B cell activation and development. This has proved true[151], but it greatly underestimated the impact of NF-κB on different biological processes, such as inflammation, cell growth and apoptosis, as well as on pathological events such as cancer[152], arthritis[153] or asthma[154].

In mammals, the NF-κB family consists of five members: NF-κB1 (p105/p50), NF-κB2 (p100/p52), RelA (p65), RelB and c-Rel.

I3.1 Activation cascade

Classical NF-κB pathway

The classical or canonical NF-κB pathway is representative of the general scheme of how NF-κB is regulated. Upon ligand recognition, cytokine receptors, such as **TNF** receptor (TNFR), trigger signalling cascades that are mediated by a series of intermediary adapters. The cytoplasmic tail of TNFR1 exhibits several protein-binding domains, most notably a death domain (DD), that mediates signalling events following TNF binding[155,156].

After ligand binding, the DD of TNFR1 binds **TRADD** (TNFR-associated protein with a DD)[157] and the DD-containing kinase **RIP1**[158]. The mechanisms coordinating binding between the DDs of these elements are not fully understood. TRADD also provides an assembly platform for recruitment of another DD adapter protein, **FADD** (Fas receptor-associated DD)[159,160]. TNFR1 lacks a TRAF interaction motif, and **TRAF**s[j] (TRNF-

[j] To date, six distinct TRAF adaptor proteins (TRAF 1 to 6) have been identified in mammalian species. Although a novel protein was named TRAF7[182], the claim is controversial, as it does not have the TRAF homology domain that defines the TRAF family. With exception to TRAF1, they all contain an N-terminal RING finger domain. TRAF2, 3, 5 and 6 also act as E3 ubiquitin ligases, apart from adaptor proteins[573].

associated factors) recruitment is thus also dependent on TRADD, which has a TRAF-binding domain. Although RIP1 also has a TRAF-binding domain and may contribute to TRAF2 recruitment under some circumstances[161], it is generally thought that TRAF2 recruitment is primarily dependent on TRADD[161–163]. TRAF2 recruits **cIAP1** and **cIAP2** (cellular inhibitor of apoptosis), which are essential for IKK activation[164–166]. cIAPs can function as E3 ubiquitin ligases required for the recruitment of LUBAC[k] (linear ubiquitin assembly complex)[167–171], which catalyses the incorporation of linear polyubiquitin chains to NEMO leading to efficient activation of IKK by TNF. RIP1 and TRAF2 cooperate in the recruitment of **TAK1** (TGFβ–activated Kinase 1) through **TAB1**, **TAB2** and **TAB3** (for TAK1 Binding Protein)[172–174], and the **IKK** kinase complex. This complex is comprised by IKKα, IKKβ and the regulatory subunit, NEMO (or IKKγ). After recruitment, TAK1 is autophosphorylated[175] leading to IKKβ phosphorylation and activation, which will in turn phosphorylate IκBα (Inhibitor of κB α). Phosphorylation of IκBα occurs in two conserved serine (S) residues located in its terminal region, S32 and S36, leading to recognition by the β-TrCP F-box-containing component of a Skp1-Cullin-F-box (SCF)-type E3 ubiquitin-protein ligase complex, called **SCF$^{\beta TrCP}$**, resulting in polyubiquitination and subsequent degradation of phosphorylated IκBα by the 26S proteasome[176]. This liberates IκBα-bound NF-κB dimers **p50/RelA**(p65) that are now able to translocate into the nucleus and activate transcription of target genes. Strongly induced NF-κB target genes include those that encode the negative regulators IκBα and A20. After protein synthesis, IκBα binds to nuclear NF-κB complexes and inhibits their function by shuttling NF-κB back into the cytosol. To terminate signal transduction, deubiquitinating enzymes (DUBs) deubiquitinate RIP1, NEMO and TRAFs that prevents IKK activation[177–180] [**FIGURE I4**]. DUBs implicated in the regulation of signalling by TNFR and other receptors related with inflammation and immunity are **CYLD**, **A20** and **OTULIN**. While CYLD is a deubiquitinating enzyme that removes K63-linked polyubiquitin chains[179], A20 is a ubiquitin-editing enzyme that has the ability to remove K63-linked polyubiquitination and replace them for 48-linked polyubiquitin chains thereby targeting proteins for degradation[177]. Moreover, OTULIN was recently proposed to specifically antagonise LUBAC thus removing linear ubiquitination[181].

[k] LUBAC is an ubiquitin ligase complex composed of SHARPIN, HOIP and HOIL-1L that generates linear polyubiquitin chains which are linked through Met 1 and have established as important players of inflammatory signalling and apoptotic cell death.

In general, K63-linked polyubiquitination leads to NF-κB activation and promotes cell survival, whereas K48-linked polyubiquitin chains induce proteosomal degradation of target proteins, NF-κB suppression and cell death[182].

Alternative NF-κB pathway

The alternative or non-canonical NF-κB pathway is induced by specific members of the TNF cytokine family, including **CD40** ligand[183], **BAFF** (B-cell-activating factor)[184], **LT-β** (lymphotoxin-β)[185] and **RANKL** (Receptor activator for NF-κB ligand)[186]. In contrast to the canonical pathway, non-canonical NF-κB depends on IKKα but is independent of IKKβ and NEMO[187]. Alternative NF-κB activation requires stabilization of **NIK**[I] (for NF-κB inducing kinase), which is constitutively active but efficiently degraded to keep it at basal levels[188–190]. In the steady state, **TRAF3** recruits NIK into an ubiquitin ligase complex composed by **TRAF2** and **cIAP1/2**[191]**,** which are directly responsible for the degradative K48-linked polyubiquitination of NIK[164,192]. Ligand-receptor engagement results in the recruitment of the TRAF3-TRAF2-cIAP1/2 complex to the receptor, which leads to a rapid activation of TRAF2. TRAF2 will then ubiquitinate cIAP1/2 via a non-degradative K63-linkage and thereby enhance its ubiquitin ligase activity, which is now directed towards TRAF3. This will lead to the K48-linked ubiquitination and degradation of TRAF3[191]. Once TRAF3 is degraded, NIK can no longer interact with the TRAF2-cIAP1/2 complex, resulting in its stabilization and eventual autophosphorylation and activation. NIK will now phosphorylate and activate **IKKα**, and together they will phosphorylate **p100**[187,193] at specific c-terminal serine residues, resulting in its ubiquitination by the $SCF^{\beta TrCP}$ complex and partial proteasomal processing to **p52**. p52 will translocate to the nucleus as a dimer with **RelB**[194,195] to activate specific transcriptional programs. Whereas IKKβ-dependent degradation of IκBα occurs within minutes, IKKα-dependent processing of p100 requires several hours[196] [**FIGURE I4**].

[I] NIK was first identified and named for its ability to increase NF-κB activation in response to proinflammatory cytokines, but it was later demonstrated that it had no effect in response to TNFα or IL-1[574].

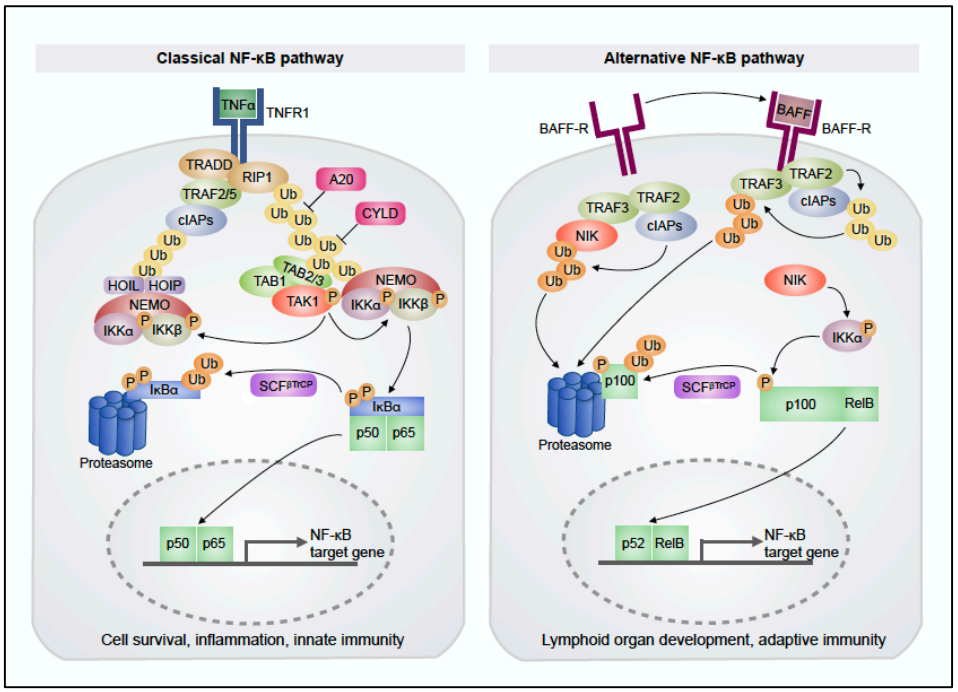

Figure I4 | Classical and alternative NF-κB pathways. Canonical activation of NF-κB by TNFα is mediated by the recruitment of TRADD, TRAF2/5, and cIAP1/2 together with RIP1 to the receptor. K63-linked polyubiquitination of RIP1 results in recruitment of TAK1 through TAB1/2/3 and the IKK complex that will get activated. IKK phosphorylates IκBα, which triggers its K48-linked polyubiquitination and subsequent degradation by the proteasome. This allows translocation of NF-κB (p50/p65 dimers) into the nucleus and activation of gene transcription. This includes transcription of IκBα and DUBs such as A20, that deubiquitinate RIP1, NEMO and TRAFs leading to disassembly of proximal NF-κB-activating complexes and shutting down the inflammatory response. Non-canonical NF-κB pathway can be activated by different ligands, such as BAFF. In the absence of BAFF, a complex consisting of TRAF2, TRAF3 and cIAP1/2 facilitate the degradation of NIK. Following BAFF interaction with BAFF-R, the complex is recruited to the receptor and TRAF3 will we ubiquitinated and consequently degraded. This releases NIK from degradation, which accumulates in the cytoplasm and phosphorylates IKKα. Together, NIK and IKKα will phosphorylate p100 leading to ubiquitination and partial degradation to p52. Active p52/RelB dimers are now able to migrate to the nucleus and initiate NF-κB specific gene transcription. Yellow Ub: K63-linked, Orange Ub: K48-linked Ub.

Additional TNFR-independent NF-κB cascades

Activation of NF-κB through members of the IL-1R and the Toll-like receptor (TLR) family

Members of the TLR family, such as TLR4 whose activation is mediated by **LPS** (lipopolysaccharide), and members of the IL-1R family, whose activation is mediated by **IL-1**, have a conserved cytoplasmic domain known as the Toll/IL-1R (TIR) domain[197]. TIR-containing receptors do not have catalytic activity and recruit intracellular adaptors, such as **MyD88** (Myeloid differentiation primary response 88) and **TRIF** (TIR-domain-containing adapter-inducing interferon β), to activate downstream effectors[198]. MyD88 is common to all TLRs, but TLR3 and TLR4 can also recruit TRIF to promote an alternative pathway leading to type I IFN (Interferon) production[199].

Receptor stimulation triggers the association of **MyD88** (myeloid differentiation primary-response protein 88) which in turn recruits **IRAK4** (IL-1R associated kinase 4), allowing the association of **IRAK1** and consequently, **TRAF6** to the plasma membrane[200]. Next, phosphorylated IRAK1 and TRAF6 dissociate from the receptor and form a complex with **TAK1**, **TAB1, TAB2** and **TAB3**[174]. IRAK1 is then degraded and the remaining complex (consisting of TRAF6, TAK1, TAB1 and TAB2) translocate to the cytosol where it associates with the ubiquitin ligases **UBC13** (ubiquitin-conjugating enzyme 13) and **UEV1A** (ubiquitin-conjugating enzyme E2 variant 1)[201]. This leads to the ubiquitination of TRAF6 that induces the activation of TAK1[202]. In turn, TAK1 phosphorylates the IKK complex leading to phosphorylation and subsequent degradation of IκB. This allows NF-κB to translocate to the nucleus and induce expression of its targets genes.

Activation of NF-κB through DNA-damage

Although classical NF-κB is primarily a cytoplasmic pathway, DNA double strand breaks (DSB) can also activate the pathway in a NEMO-dependent manner[203–206]. Following exposure to DNA damage, free **NEMO** (not in a complex with IKKα and IKKβ) is translocated to the nucleus where it will be SUMOylated (by covalent modification with Small Ubiquitin-related MOdifier)[205]. The protein responsible for NEMO SUMOylation is **PIASγ** (protein inhibitor of activated STATγ)[207]. In fact, mutations in the residues that are SUMOylated impair nuclear accumulation of NEMO and, although it

has minimal impact on canonical NF-κB signalling, it completely abrogates DNA damage-induced NF-κB activation. Later, **PIDD** (p53-induced protein with a death domain) induces the formation of a nuclear signalling complex containing **RIP1** that also promotes SUMOylation of NEMO[208].

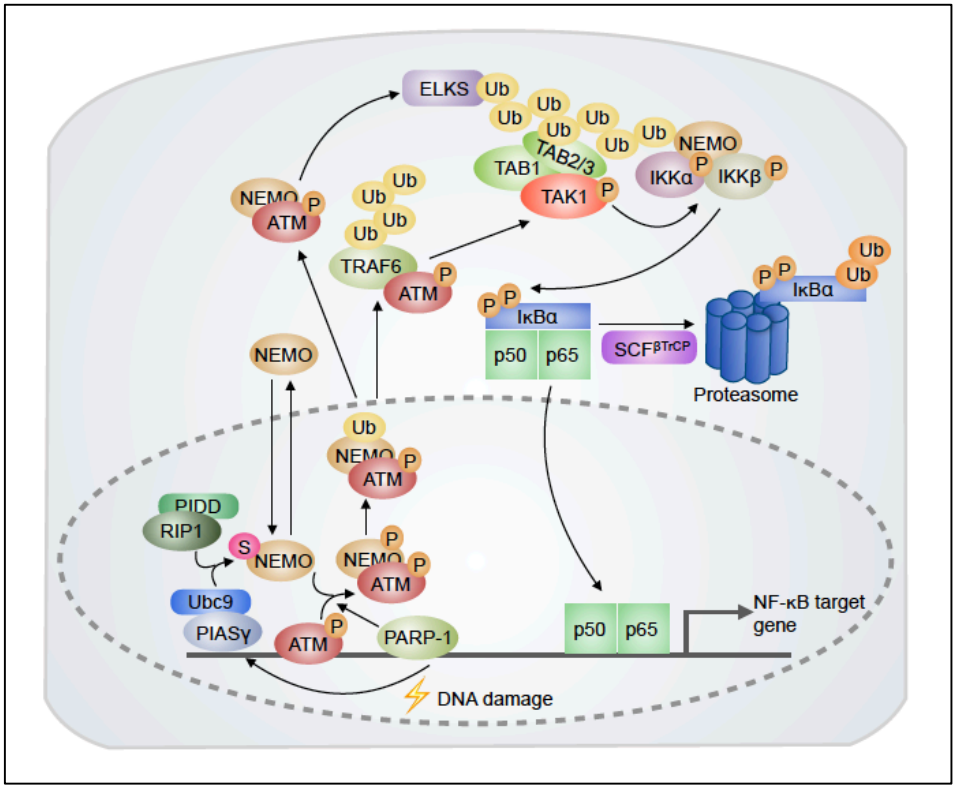

Figure I5 | NF-κB signalling cascades induced by DNA damage. In response to genotoxic treatments, NEMO translocates to the nucleus and is SUMOylated by PIASγ. The SUMOylation of NEMO can be facilitated by PARP-1 and/or PIDD/RIP1 complex. Nuclear NEMO forms a complex with ATM that phosphorylates NEMO promoting its monoubiquitination and subsequent cytoplasm export. Then, monoubiquitinated NEMO and ATM form a complex with ELKS which recruits TAK1 and the IKK complex though K63 ubiquitin chains, promoting their activation. ATM may also export to cytoplasm and form a complex with TRAF6, which leads to TRAF6 polyubiquitination that enhance IKK activation. Activated IKK phosphorylates IκBα and frees NF-κB for nuclear accumulation and activation of target genes.

Moreover, it has been shown that **PARP-1** (Poly-ADP ribose polymerase), which senses DNA strand breaks, is the responsible for assembling NEMO, PIASγ and the DNA-damage response activator, **ATM** (Ataxia-telangiectasia mutated)[209]. After being SUMOylated, NEMO is phosphorylated by ATM to

promote its ubiquitin-dependent nuclear export. At the same time, ATM is also exported in a NEMO-dependent manner to the cytoplasm where it associates with **ELKS** (protein rich in aminoacids E, L, K and S), which functions as an IKK complex activator. This results in the activation of NF-κB and the transcriptional activation of anti-apoptotic genes[206]. Different groups have now shown that ELKS ubiquitination is dependent on ATM and NEMO, and promotes the assembly of TAK1/TAB2/3 and NEMO/IKK complexes, thus activating NF-κB signaling[206,210] [**FIGURE I5**].

In addition, ATM activates **TRAF6** leading to Ubc13 polyubiquitination and generation of an ATM/TRAF6/cIAP1-complex that promotes TAK1 activation and NEMO monoubiquitination[211] [**FIGURE I5**].

I3.2 The IKK complex

The IKK complex is in fact a collection of complexes with apparent molecular size from 700 to 900 kD consisting of different subunits of the two catalytic active kinases, **IKKα** and **IKKβ**, and the regulatory subunit IKKγ (also called **NEMO** for NF-κB essential modulator)[212–216]. The sum of the molecular masses of these subunits is 220 kD, suggesting that the large IKK complex not only is oligomeric but also that other components are present in the complex. A further protein proposed as an essential regulatory subunit of the IKK complex is ELKS[217].

IκB kinase (IKK)

IKKα and IKKβ were identified as constituents of a protein complex that presents TNFα-induced IκBα specific kinase activity. Moreover, IKKα was also identified as a protein that interacts with NIK to activate the alternative NF-κB pathway. IKKα and IKKβ share 50% of sequence identity and 70% of protein structural similarity. These proteins contain a N-terminal **kinase domain** and a **scaffold/dimerisation domain (SDD)** located towards the C-terminus[218] that includes the regions previously characterised as leucine zipper (LZ) and helix-loop-helix (HLH) motifs. In the C-terminal part, it exists a **NEMO-binding domain (NBD)** that permits recognition and binding of IKKα and IKKβ to the regulatory subunit of the complex, NEMO[219,220]. Both proteins exhibit kinase activity towards IκBα, although IKKβ is much more efficient in phosphorylating IκBα than IKKα[221,222] [**FIGURE I6**].

Despite their homologies and the fact that they are part of the same complex, IKKα and IKKβ have non-overlapping functions mainly due to substrate specificities. IKKβ is the major IKK catalytic subunit for the phosphorylation of IκBα in response to pro-inflammatory stimuli such as TNFα. In contrast, IKKα phosphorylation is not critical for the activation of the classical IKK complex or for the activation of NF-κB by most pro-inflammatory stimuli[223,224]. In fact, IKKα$^{-/-}$ mice have intact IKK and NF-κB activation[223,225]. Nevertheless, there are situations in which active IKKα is more critical than IKKβ for NF-κB activation. For instance, p52/RelB nuclear translocation requires the kinase activity of IKKα but not that of IKKβ. Whereas the IKKβ dependent pathway is essential for activation of **innate immunity**[226,227], the IKKα-dependent pathway is more important for regulation of **adaptive immunity** and **lymphoid organogenesis**[228–230].

There is considerable evidence that phosphorylation of both IKKα and IKKβ at specific serine residues is required for their activation. In particular, both proteins contain an activation loop within the kinase domain, that is identical in sequence between both proteins, and is subject to phosphorylation resulting in a conformational change that leads to kinase activation[222,231]. Activating phosphorylation of IKKα takes place at serines S176/S180 whereas IKKβ is phosphorylated at serines S177/S181. Both serines are phosphorylated in vivo in response to pro-inflammatory cytokines[222]. Yet, for the time being, the molecular mechanisms of IKK activation are not fully understood. For instance, it was proposed that S176 of IKKα and S177 of IKKβ are the substrates for TAK1 activity and phosphorylation of the second residue is the result of IKK transphosphorylation[232]. It is likely that activation of IKK involves trans-autophosphorylation by its catalytic subunits IKKα and IKKβ, although different hypothesis have been postulated to regulate this initiating event: direct phosphorylation of one of the IKK catalytic subunits at the activation loop; IKK multimerization resulting in trans-autophosphorylation; and a conformational change induced by a PTM other than phosphorylation or through protein-protein interactions[233].

Another region involved in regulation of IKK activity is the **HLH motif**. Mutations within this motif decrease IKK activity without affecting complex assembly[214,221]. The HLH motif physically interacts with the kinase domain and seems to serve as an endogenous activator of IKK. C-terminal of the HLH motif, just before the NBD, IKKα and IKKβ contain a cluster of serines that are strongly phosphorylated during IKK activation. Phosphorylation at these sites requires IKK activity and it has a negative autoregulatory

function[222]. Given the transient nature of IKK activation, this autophosphorylation event may contribute to termination of IKK activity.

A few years ago, our group identified a truncated form of IKKα with a predicted molecular weight of 45 kD (**p45-IKKα**) that was present in different cell types but specifically activated in the nucleus of CRC cells (see details in section I2.4)[234]. This truncated form of IKKα is generated by the proteolytic cleavage of full length IKKα in the early endosomes by the action of cathepsins. The p45-IKKα form includes the kinase domain, but lacks some regulatory domains at the c-terminal region of the protein[235] [**FIGURE I6**].

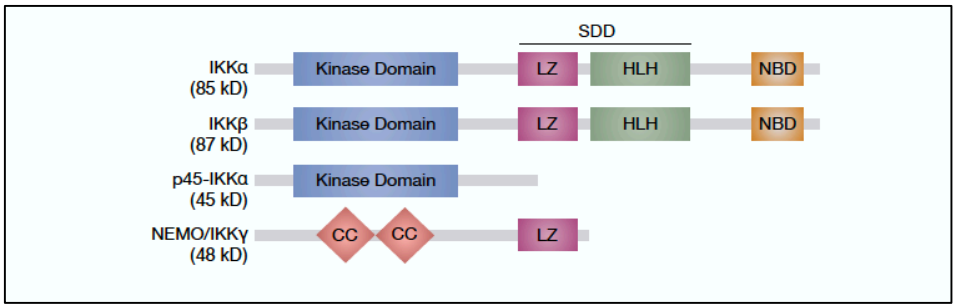

Figure I6 | Schematic representation of IKK structural organisation. IKKα and IKKβ possess a scaffold/dimerisation domain (SDD) containing a helix-loop-helix (HLH) and a leucine zipper (LZ) region, responsible for both homodimerisation and heterodimerisation of IKKα and IKKβ. They interact through their Nemo Binding Domain (NBD) with NEMO, which contains two coiled coil (CC) domains and a LZ. Truncated p45-IKKα includes the kinase domain but lacks the SDD and the NBD regions.

NEMO, the regulator of the IKK complex

NEMO is a 48 kD regulatory subunit and is the third component of the IKK complex. It was identified biochemically as a component of the IKKα/β-containing complex, and by genetic complementation of a cell line non-responsive to NF-κB-activating stimuli[215,236]. Structure-prediction algorithms predict that NEMO is primarily a helical protein with large stretches of **coiled-coil (CC)** structure, including a **LZ** domain in its C-terminus.

NEMO is essential for connecting the bound catalytic subunits to upstream activation in the classical NF-κB pathway. Consistent with its role in the assembly of a high-order IKK complex, NEMO itself forms multidimers, most likely tetramers[237]. Its oligomerisation depends on its N-terminal CC and LZ motifs. Biding of IKKβ (and probably that of IKKα) is conferred by the N-

terminal CC motif of NEMO recognised by the NBD of IKKβ[215,219]. Accordingly, a cell-permeable blocking NBD peptide prevents IKK activation[220]. These data and NEMO deletion[238,239] and loss-of-function (LOF) mutations[240] illustrate that IKK activation in classical NF-κB is absolutely dependent on NEMO.

TAK1

Transforming growth factor-β (TGF-β)-activated kinase 1 (TAK1, also called MAP3K7) was discovered in 1995 as a protein kinase that can be activated by **TGFβ**[241]. Since this original finding, TAK1 has been shown to be a critical mediator of the inflammatory response, as it was robustly activated by a wide variety of proinflammatory mediators such as TNFα, IL-1 and TLR[242,243]. This finding led to the identification of TAK1 as a component of an IKK activating complex[173]. As mentioned, TAK1 is bound to the accessory proteins **TAB1/2/3**[174,244] that are required for its recruitment to the TNFR1 signalling complex through protein-protein interactions. TAB1 constitutively binds to the N-terminus of TAK1, whereas TAB2 and TAB3 bind to the C-terminus in a context dependent manner. Although the upstream regulators of TAK1 depend on the type of stimulus, the interaction with TABs is an essential step for TAK1 autophosphorylation and activation[174,244–247].

Once activated, TAK1 is phosphorylated in T184 and T187[248–251]. In addition, **PKA** (protein kinase A)-mediated phosphorylation of TAK1 at S412 positively regulates TAK1 and is required for the activation of NF-κB[252,253]. Moreover, adding a higher level of complexity, it has been reported that phosphorylation at T187 and S412, are negatively regulated by protein phosphatases[254–258].

Several publications strongly suggest that TAK1 is also activated by **DNA-damage**, which is NEMO and RIP1 polyubiquitination-dependent [210,211,259].

Wnt signalling is another pathway that can activate TAK1, although the mechanisms are not well defined[260]. Ishitani and colleagues proposed that in the non-canonical Wnt pathway, CaMKII (Ca^{2+}/calmodulin-dependent protein kinase II) promotes TAK1-mediated activation of NLK (nemo-like kinase), which functions as a negative feedback regulator of Wnt signalling by suppressing transcriptional activity of β-catenin[261,262]. The same pathway is also involved in **osteoblast specificity** from bone marrow mesenchymal stem cells, in which the TAK1 pathway inactivates PPAR (peroxisome

proliferator-activated receptor) while simultaneously inducing RUNX2 (runt-related transcription factor 2)[263].

I3.3 Physiological IKKα functions

IKKα has several unique physiological roles, which involve NF-κB-independent, as well as NF-κB-dependent processes [**FIGURE I7**]. For instance, IKKα controls epidermal differentiation and skeletal morphogenesis independent of its kinase activity and NF-κB[224,225,264]. By contrast, proliferation of mammary epithelium during lactation and activation of the non-canonical p100 involve activation of the IKKα kinase function and modulation of NF-κB activity.

In the skin, IKKα knockout (KO) mice show a skin abnormality that is caused by defective keratinocyte differentiation and proliferation[224,264]. This phenotype can be rescued with a catalytically inactive IKKα mutant and involves the NF-κB-independent production of a not well-defined soluble factor[264]. In addition, epidermal IKKα interacts with SMAD2/3 after TGF-β stimulation to facilitate transcriptional activation of cell-cycle regulators promoting cell growth arrest and keratinocyte differentiation[265]. It was also shown that chromatin-bound IKKα at the promoter of 14- 3-3σ, which is a negative regulator of cell cycle, prevents Suv39h1 association leading to gene transcription in keratinocytes[266]. IKKα mutations or aberrant cytoplasmic localization of this kinase impose the generation of poorly differentiated SCC (Squamous Cell Carcinoma) and skin papillomas[267,268].

Together these observations underscore a pivotal role for IKKα in the regulation of **keratinocyte homeostasis and tumour suppression**.

Moreover, the phenotype of IKKα KO mice is not restricted to the skin since these animals display skeletal and craniofacial morphogenesis defects that can be largely rescued upon re-expression of epidermal-specific IKKα or kinase-dead (KD) IKKα. In a kinase-independent way, IKKα inhibits the expression of FGF8 (morphogen fibroblast growth factor), which is thought to be one of the mechanisms by which epidermal IKKα controls **mesoderm-derived morphogenesis**.

Specific functions for IKKα in p100 processing (see above) and **mammary gland differentiation**, which depend on its kinase activity, were revealed in mice expressing a non-responsive T-loop serine mutant of IKKα ($IKK\alpha^{AA/AA}$)[187,269]. In mammary gland development during pregnancy,

this IKKα mutation results in the same defects as disruption of RANK[m] signalling or that of cyclin D1 expression. IKKα may function as part of the classical IKK complex to confer RANK ligand-induced NF-κB activation, which in turn activates cyclin D1 expression and proliferation of mammary epithelial cells[269].

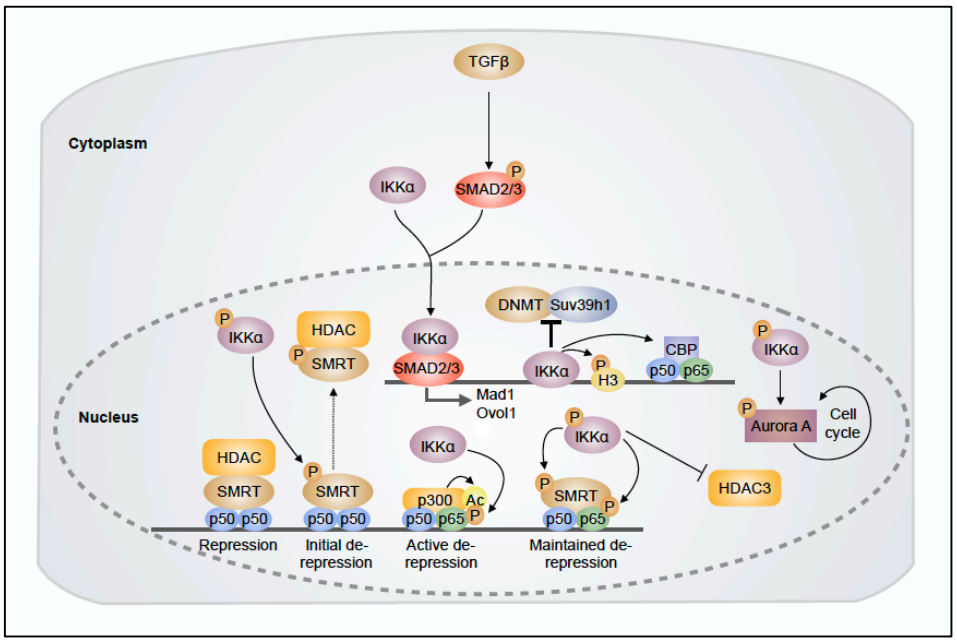

Figure I7 | Simplified representation of physiological IKKα functions. Nuclear IKKα phosphorylates Serine 10 on histone H3 facilitating the accessibility of transcriptional machinery to the chromatin. Moreover, it phosphorylates the histone acetylase CBP promoting its preferential binding to p65 leading to transcriptional activation. In human keratinocytes, IKKα prevents binding of epigenetic silencers Suv39h1 and Dnmt3a to the 14-3-3σ promoter and interacts with SMAD2/3 resulting in gene transcription. IKKα phosphorylates the nuclear co-repressor SMRT bound to p50 dimers inducing the displacement of SMRT and HDAC3. This recruits transcriptionally active p65/p50 dimers to specific gene promoters. IKKα phosphorylates p65 favouring p300 recruitment that acetylates p65, an event required for full gene transcription. Additionally, nuclear IKKα phosphorylates Aurora A, promoting cell cycle progression. Adapted from Espinosa et. al. 2011[270]. Arrows indicate activation/regulation/phosphorylation and dashed arrows indicate migration.

[m] RANK promotes proliferation and survival of mammary epithelial cells, and RANK loss or overexpression results in disrupted mammary gland development during pregnancy and impaired lactation[575,576]

Later, it was shown that IKKα can also be found in the nucleus in the absence of NEMO and IKKβ, where it acts at different levels to regulate NF-κB-dependent and –independent gene expression[271]. It was first shown that TNFα treatment induces the recruitment of IKKα, together with RelA and CBP (CREB-binding protein), onto the promoter of different NF-κB target genes, such as IκBα, IL-8 or IL-6, where it **phosphorylates S10 of histone H3**. This triggers subsequent CBP-mediated acetylation on K14 of H3, a crucial step in modulating chromatin accessibility and thus, NF-κB gene expression[272,273]. A similar situation was observed following LPS treatment in macrophages[274].

Furthermore, IKKα regulates additional steps of gene transcription including derepression of NF-κB target genes by **phosphorylation of SMRT** (Silencing mediator for retinoic acid and thyroid hormone receptor) repressor at S2410 thus creating a functional 14-3-3 binding domain that induces its nuclear export (together with HDAC3) and subsequent degradation[275].

On the other hand, it **phosphorylates chromatin-bound p65 at S536**, leading to p300 recruitment and subsequent acetylation of p65 at K310, an event necessary for full gene transcription[276]. However, the same phosphorylation event is required for triggering p65 proteasomal degradation, which facilitates termination of NF-κB-transcription of pro-inflammatory genes in macrophages[277]. There is also some data indicating that IKKα **phosphorylates PIAS1** in response to inflammatory stimuli allowing its association to the chromatin thus repressing transcriptional activity of NF-κB and termination of the inflammatory response[278].

It has also been described that IKKα is involved in **β-catenin** signalling pathway. In response to mitogenic stimuli, IKKα phosphorylates β-catenin and regulates expression of cyclin D1 through TCF[n] activity[279].

Last but not least, IKKα regulates the M phase of the cell cycle by inducing phosphorylation and activation of **Aurora A**, a mitotic kinase that regulate cell cycle progression[280].

[n] The TCF/LEF family is a group of transcription factors (TF) involved in the Wnt signalling pathway. They bind to DNA and recruit the co-activator β-catenin to enhancer elements of target genes.

I3.4 IKKα and cancer

It has long been known that the NF-κB pathway plays an important role in the development and maintenance of cancer, mainly associated with its function in inflammation. However, later discoveries have demonstrated that specific elements of the pathway can exert pro- or anti-tumorigenic effects independently of NF-κB [**FIGURE I8**]. For example, IKKα has tumour-suppressive roles in skin cancer as it acts as a major regulator of keratinocyte differentiation[223,264,265]. Other findings, however, argue that IKKα function can directly contribute to specific oncogenic functions[281,282].

Colorectal Cancer

For many years, different groups have investigated the role of IKKα in CRC. Indeed, our group was pioneer in demonstrating that in this tumour type IKKα is aberrantly activated and recruited to the promoter of different **Notch target genes,** such as *HES1*, *HES5* and *HERP2* [**FIGURE I8**]. Chromatin-bound IKKα constitutively phosphorylates **SMRT**, leading to its cytoplasmic export and the transcriptional activation of these genes. Conversely, IKKα inhibition, either pharmacologically or by expression of a dominant-negative form of the kinase, restores SMRT chromatin binding, inhibits Notch-dependent gene transcription, and reduces tumour size in a xenograft CRC model[283]. Similarly, IKKα can phosphorylate **N-CoR** (Nuclear Receptor Correpresor), a nuclear corepressor homologous to SMRT, creating a functional 14-3-3-binding domain and promoting its nuclear export[284] similar to that found for SMRT. More recently, we identified a nuclear active p45-IKKα form that is in a complex with full length non-phosphorylated IKKα and NEMO, and regulates the **phosphorylation of SMRT and Histone H3**. Activated p45-IKKα prevents apoptosis of CRC cells in vitro and is required for the maintenance of tumour growth in vivo. Moreover, BRAF activity is required and sufficient to induce p45-IKKα activation, which is TAK1-dependent[285] [**FIGURE I8**]. Consistent with the fact that p45-IKKα is generated in the endosomes by the action of cathepsins, inhibitors of endosomal acidification (such as chloroquine or bafilomycin A1) abolish p45-IKKα activation and suppress CRC cell growth both in vitro and in vivo.

In a different set of experiments, mice deficient in IKKα kinase activity were protected from intestinal tumour development, which was associated with an enhanced recruitment of **IFNγ (interferon γ)-producing M1-like myeloid cells** to the tumour. Polarization and accumulation of M1 macrophages in

the mutant mice is not cell autonomous but depends on the interaction between IKKα-mutant epithelial cells and mutant stromal cells[286].

Skin Cancer

Nuclear IKKα is clearly involved in skin cancer progression although some controversy exists about its pro or anti-tumorigenic functions. For instance, IKKα deletion in keratinocytes induces skin SCC in mice upregulating transcription of **EGFR ligands** and ligand activators, thus activating the EGFR-driven pathway[287]. Because IKKα supports 14-3-3σ expression (as discussed above) which negatively regulates the cell cycle phosphatase CDC25, in the absence of functional IKKα, cells aberrantly proliferate which results in the loss of skin homeostasis and increased cell transformation[266]. Other works also support and further explore this anti-tumorigenic functions, and suggest an association with the TGFβ pathway[265,288].

By contrast, in Basal Cell Carcinoma (BCC) nuclear IKKα is over-expressed and it directly binds to the ***LGR5*** **promoter,** upregulating its expression. This suggests that IKKα activity can contribute to oncogenic transformation not only through inflammatory-related signals but also through the regulation of stemness-related genes[289].

In a different study, our group identified that IKKα induces the chromatin release of **phosphorylated and SUMOylated IκBα (PS-IκBα)**, identified as a regulator of multiple developmental- and stemness-related genes such as HOX and IRX. IKKα activity on PS-IκBα induced its chromatin release, which was linked to oncogenic keratinocyte transformation[235] [**FIGURE I8**]. The mechanisms by which IKKα promotes PS-IκBα inactivation are primarily unknown, but we speculate that nuclear IKKα might phosphorylate PS-IκBα on non-canonical sites (without inducing IκBα degradation) or regulate specific editing enzymes, phosphatases, SUMO-proteases or specific PS-IκBα-interacting proteins.

Recently, it was shown that mice carrying an IKKα variant that specifically localizes to the nucleus of the keratinocytes develop more aggressive tumours in response to chemical carcinogens. Nuclear IKKα seems to promote tumorigenesis by regulating **c-Myc, Maspin,** and **Integrin-α6**, and tumours with nuclear IKKα mimic the characteristics of human skin tumours with high risk to metastasize[290]. These results are in agreement with previous findings of our group indicating that nuclear active IKKα plays

oncogenic and pro-metastatic role in SCC, being its detection predictive of higher metastatic capacity and worse patient outcome[291].

Breast Cancer

IKKα is required for estrogen-induced cell cycle progression of breast cancer cells through regulation of **E2F1**[292]. Moreover, in conjunction with **ERα** (Estrogen Receptor Alpha) and **SRC-3** (Steroid Receptor Coactivator 3), IKKα is necessary to activate transcription of estrogen-responsive genes that result in enhanced proliferation of breast cancer cells[293]. At the same time, IKKα can also cooperate with **Notch-1** to induce the transcriptional activation of ERα-dependent genes[294]. A similar cooperation between IKKα and Notch-1 was found in Acute T cell leukemia[295].

IKKα activity is also required for **ErbB2** [o]-induced tumorigenesis, and importantly the IKKα-activating cytokine RANKL has been shown to promote tumorigenesis and metastasis of mammary epithelial cells[296–298]. In addition, nuclear active IKKα, together with NIK, phosphorylate **p27/Kip1,** inducing its nuclear export, which results in enhanced cell proliferation[299] [**FIGURE I8**].

Prostate Cancer

In prostate cancer cells, IKKα phosphorylates and activates **mTORC1** downstream of activated AKT[p] [300,301]. In a similar fashion, IKKα associates with and enhances **mTORC2** kinase activity[302]. In castration-resistant prostate tumours, nuclear active IKKα represses the transcription of the metastasis-suppressor gene **Maspin** [**FIGURE I8**]. Indeed, accumulation of nuclear active IKKα in human and mouse prostate tumours correlates with metastatic progression, reduced Maspin expression, and infiltration of RANKL-expressing inflammatory cells[303]. It was claimed later that IKKα activation and nuclear translocation in this cancer cells is induced by LT (lymphotoxin) α and β produced by a population of tumour-infiltrating B

[o] Also known as HER2/neu, is amplified and/or overexpressed in 20-30% of invasive breast carcinomas[577]

[p] Activated AKT promotes proliferation, cell survival and cell growth in prostate cancer cells[578]

cells. These findings are in line with our recent results in SCC (for more details see skin cancer section).

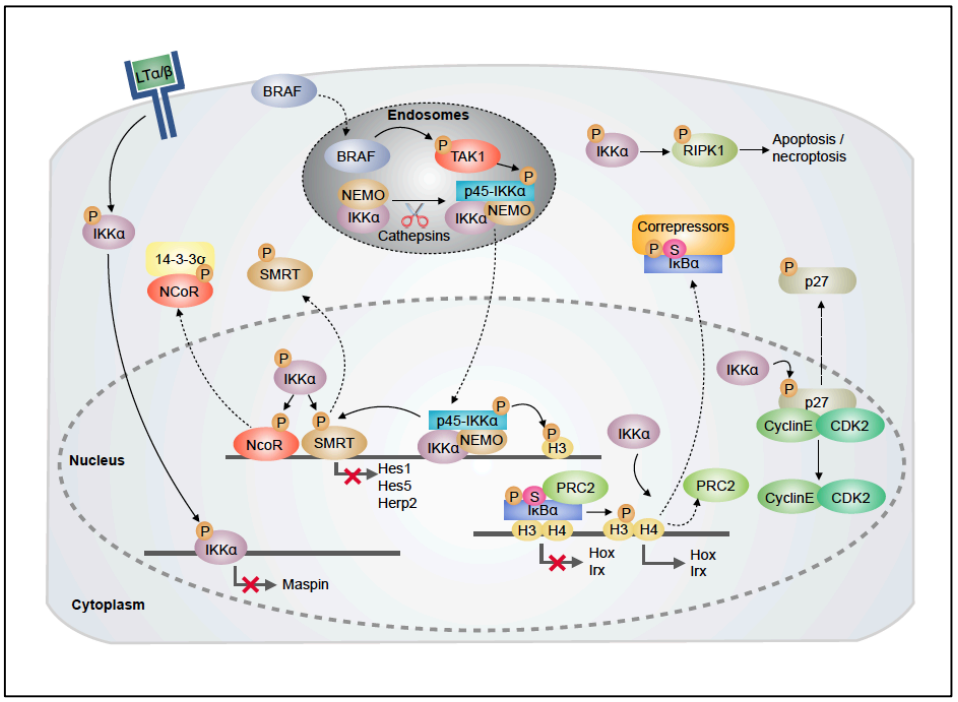

Figure I8 | Tumorigenic functions of IKKα. In CRC, IKKα phosphorylates the nuclear co-repressors N-CoR and SMRT, inducing its association from the chromatin and p45- IKKα is activated by BRAF and TAK1 in the endosomal compartment, and upon activation phosphorylates histone H3 and SMRT. Moreover, nuclear active IKKα contributes to chromatin release of phosphor-SUMO-IκBα, and stimulates the nuclear export of p27/Kip1 thereby supporting proliferation of tumour cells. IKKα regulates gene transcription of metastasis repressor Maspin in prostate cancer cells. IKKα also phosphorylates RIPK1 which is involved in apoptosis. Arrows indicate activation/regulation/phosphorylation, dashed arrows indicate migration and red cross indicates inactivation.

Liver Cancer

Hepatocellular carcinoma (HCC) is frequently developed in the context of chronic hepatitis characterized by liver inflammation and hepatocyte apoptosis[304]. In this context, NF-κB pathway can act as tumour promoter or tumour suppressor[304]. Luedde and colleagues demonstrated that IKKα and IKKβ regulate biliary homeostasis and promote hepatocellular carcinoma by phosphorylating **RIPK1** (Receptor-Interacting Protein Kinase 1), which is involved in both apoptosis and necroptosis (programmed necrotic cell death), independently of NF-κB[305] [**FIGURE I8**]. On the contrary, other

studies indicate that NEMO exerts a protective role against HCC through NF-κB-dependent and -independent pathways[306–309].

Lung cancer

In lung cancer, IKKα phosphorylates **CBP** and switches its binding preference from p53 to NF-κB. Thus, IKKα activity not only facilitates NF-κB-dependent gene expression, but also suppresses p53-induced gene transcription, leading to cell proliferation and tumour growth. In agreement with this finding, increased CBP phosphorylation and high levels of active IKKα are both detected in human lung tumour tissue compared to the adjacent normal tissue[310].

I3.5 NF-κB inhibition for cancer therapy

Given the relevant contribution of NF-κB and specific NF-κB members on tumour development and progression[311], this transcription factor and the upstream and downstream mediators are attractive targets for cancer prevention and therapy. However, because of the key role of NF-κB in such a wide spectrum of cellular biology, legitimate concerns have been raised regarding potential adverse effects that might result from its inhibition. Moreover, and as explained in previous sections, inhibiting or activating NF-κB may result in different and sometimes opposite effects depending on the cellular context. Thus, using NF-κB or elements of the pathway as therapeutic targets for cancer treatment should be differentially considered for each situation.

Numerous inhibitors of IKK and NF-κB activity have been reported, and their effects extensively reviewed[312–314]. Among them, we can find a variety of **natural products**[315,316], **biomolecular and peptide inhibitors**[317] and **synthetic small-molecule inhibitors** against IKK activity[314,318], which have taken the main focus in an effort to target the NF-κB pathway. Surprisingly, however, even though IKK inhibitors have served researchers for years as reliable tool compounds and have proved effect in a variety of experimental cancer models[285,318–320], they have not been able to move beyond animal studies and at present, no such drug has been clinically approved.

More realistic is the possibility of combining fine-tuned IKK inhibition with the more traditional chemotherapy protocols. For instance, IKK inhibitors are effective in sensitizing ovarian, colorectal and pancreatic cancer cells to

standard chemotherapy-induced death[321–324], through suppression of genes encoding antiapoptotic[325] and antioxidant molecules[326].

Another strategy is the **blockage of IκBα degradation** and thus, NF-κB nuclear translocation. In this sense, the first-in-class proteasome inhibitor bortezomib has emerged as an important treatment of B-cell lineage malignancies, such as multiple myeloma and relapsed/refractory mantle cell lymphoma[327,328].

A different issue is prevention and prophylactic therapy, and whether long-term suppression of low inflammation could reduce cancer risk. At this point, information is limited to Non Steroidal Anti-Inflammatory Drugs (NSAIDs), such as aspirin. Daily aspirin use at doses of 75 mg per day for 5 years or longer diminishes death due to several common cancers, such as colorectal, pancreatic and lung carcinomas[329]. The protumorigenic effects of this low but persistent inflammation could have been underestimated, since it is believed that about 20% of all cancers are linked to inflammation[330].

I4. Classical MAPK signalling pathway

The mitogen-activated protein kinases (MAPKs) are a family of serine-threonine kinases that play a key role in signal transduction and are known to participate in a diverse array of cellular programs, including differentiation, proliferation, cell division and cell death. MAPKs lie within protein kinase cascades, where each cascade consists of no fewer than three enzymes that are activated in series: a MAPK kinase kinase (MAPKKK), a MAPK kinase (MAPKK) and a MAP kinase (MAPK).

I4.1 RAS

Discoveries made in the 1980s revealed that the transforming activities of the rat-derived Harvey and Kirsten murine sarcoma retroviruses[331,332] contribute to cancer pathogenesis through a common set of genes termed *Ras* (for rat sarcoma virus)[333–335]. Soon thereafter, the use of recently developed techniques led to the identification of *Ras* genes as key players in cellular proliferation, differentiation and survival, as well as in experimental transformation and human tumour pathogenesis. The protein products of *Ras* oncogenes were named p21 due to its molecular weight, and were initially described to bind guanine nucleotides. Yet, four more years passed before it was proved that RAS proteins were indeed GTPases with the ability to associate to the inner side of the plasma membrane[336–338].

Unanswered by these first discoveries, however, was the signalling context in which RAS proteins operate: which proteins impart signals to RAS and how do activated RAS proteins pass signals to downstream targets within a cell? Despite there is still a lack of complete understanding of the normal and pathological functions of RAS, significant progress has been made in the past decades.

Initially, its ability to bind to the plasma membrane led to propose that RAS proteins are mediators of signal transduction. Consistently, EGF (Epidermal Growth Factor) was found to stimulate the ability of RAS to bind GTP thus leading to its activation[339]. Many RTK (Receptor tyrosine kinases) have been shown to activate RAS signalling, such as EGFR (EGF Receptor), ErbB2, IGF1R (Insulin Growth Factor Receptor) or VEGFR (Vascular Endothelial Growth Factor Receptor)[340]. Nowadays, the best-characterized route of RAS activation occurs at the plasma membrane and is mediated by

SOS (Son of Sevenless), a guanine nucleotide exchange factor (GEF). SOS stimulates the exchange of GDP bound to Ras by GTP that is required for a positive regulation of Ras activity. This nucleotide exchange allows RAS to interact directly with its target effectors, being the RAF kinase one the most important, which essentially regulates the ERK1/2 module. Regulation of both RAS and RAF is crucial for the proper maintenance of cell proliferation, as activating mutations in these genes lead to oncogenesis[341]. In addition, RAS can also activate other effectors such as the PI3K (phosphatidylinositol 3-kinases) pathway[342,343]. GAPs (GTPase activating proteins) are responsible for catalysing GTP hydrolysis, thus terminating RAS activation[344]. Among them we find NF1 (Neurofibromin 1), that functions as a negative regulator of RAS activation[345] [**FIGURE I9**].

In humans, there are three RAS proto-oncogenes that encode four RAS isoforms: HRAS, KRAS4A, KRAS4B[q] and NRAS. NRAS and/or HRAS-deficient animals develop normally and are viable[346–349]. In contrast, KRAS4B, but not KRAS4A, knockout mice died during embryogenesis[350,351].

I4.2 BRAF and its downstream effectors

Named for Rapidly Accelerated Fibrosarcoma (RAF), it was discovered over three decades ago as a retroviral oncogene, v-Raf[352] or v-MIL[353], possessing a serine/threonine kinase activity[354–356]. RAF family kinases were among the first oncoproteins to be described. They primarily act as signalling effectors downstream of RAS, and their close ties to cancer have fuelled a large number of studies.

There are three known mammalian RAF isoforms: ARAF, BRAF and CRAF that share structural homology but also display significant variations, both structural and functional. There are several conserved regions among all RAF proteins, designated as CR1, CR2 and CR3 (for Conserved Region). CR1 and CR2 in the N terminus are largely regulatory, whereas CR3 at the C-terminus encompasses the kinase domain[357–363]. The transforming v-RAF form contains a deletion of CR1 and CR2, resulting in a constitutively active form of RAF. Thus, the N-terminal half of RAF is considered to be a negative regulatory domain which helps in maintaining RAF in an inactive state in the absence of stimulation[364,365]. The common view is that the

[q] These two proteins arise from alternative RNA splicing of the KRAS gene. KRAS4B is the predominant splice variant expressed in many tissues, contributing to its focus in cancer studies.

catalytic domain of RAF is folded and bound to the N-terminal regulatory domain. The three RAF isoforms share a complex regulation by phosphorylation. ARAF and CRAF share five phosphorylation sites that are required to get activated[366,367]. BRAF contains four conserved phosphorylation sites and T598 and S601 are required for BRAF activation[368]. BRAF has a strong basal kinase activity in comparison with CRAF[367]. This difference could account for the fact that BRAF is frequently mutated in human cancer (most frequently V600E), whereas ARAF and CRAF mutations are difficult to find in tumours. In fact, single aminoacid changes are enough to stimulate BRAF kinase activity.

In their inactive state, all RAF proteins are found in the cytoplasm, with the N-terminal regulatory domain acting as an autoinhibitor of the C-terminal kinase domain. 14–3-3 dimers bind to phosphorylation sites present in both the N- and C-terminal regions and stabilize the autoinhibited state. Under normal signalling conditions, RAS activation recruits RAF proteins to the plasma membrane, which induces the release of 14-3-3 from the N-terminal binding site and facilitates the dephosphorylation of inhibitory sites as well as the phosphorylation of activating sites within the kinase domain. Importantly, many of the molecular mechanisms involved in RAF regulation directly impact BRAF **dimer formation** with CRAF, a key aspect of RAF activation and function[369–375]. RAF dimers are asymmetric: one of the kinases acts as an activator that stimulates the activity of the other partner kinase[376].

After activation, RAF proteins activate the MEK-ERK cascade. MEK proteins are activated by phosphorylation of two serine residues (S217 and S221 in MEK1 and MEK2) that are located in their activation segments. Once activated, MEK proteins phosphorylate ERK1 and ERK2 on threonine and tyrosine residues within their activation domains (T202 and Y204 in ERK1 and T185/Y187 in ERK2). After activation, ERK1/2 directly phosphorylates its substrates including both cytosolic and nuclear proteins. ERK is able to phosphorylate ELK1, which takes part of the serum response factor that regulates the expression of FOS; moreover, ERK phosphorylates c-JUN leading to the activation of the AP1 transcription factor, which is composed of FOS-JUN heterodimers[377]. As a result of the stimulation of these transcriptional regulators, key cell-cycle regulatory proteins are expressed which enable the cell to progress through the cell cycle[378]. Following catalytic activation, RAF signalling is subsequently attenuated by ERK-mediated feedback phosphorylation, which disrupts the RAS/RAF

interaction and releases RAF from the plasma membrane[379,380] [**FIGURE I9**].

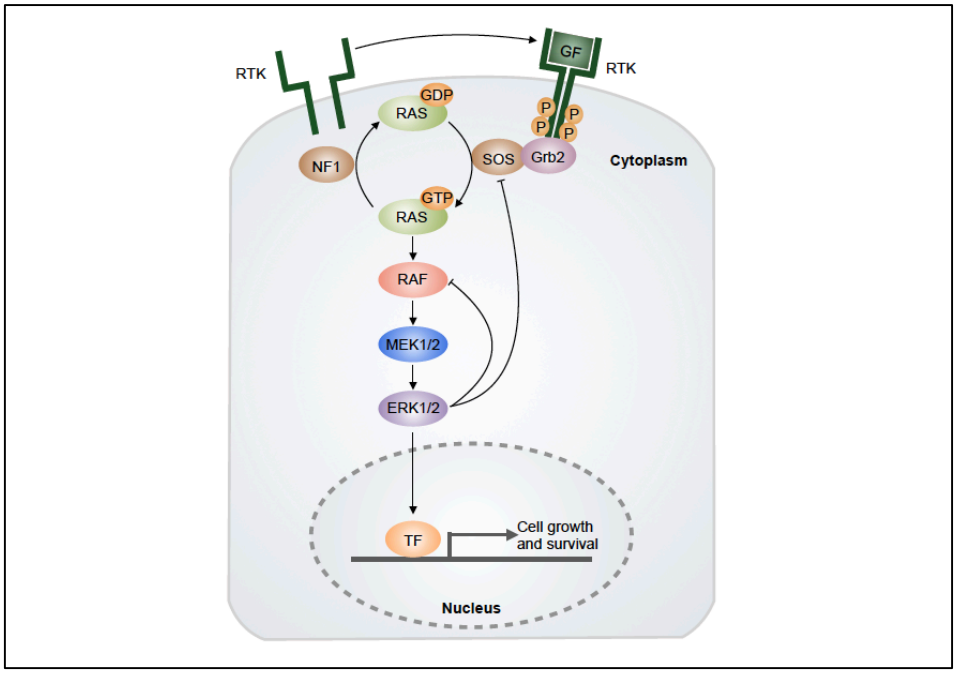

Figure I9 | MAPK signalling pathway downstream of KRAS and BRAF. Upon ligand binding, receptor tyrosine kinase (RTK) homodimerise leading to activation of intracellular kinase domain. Through the small adaptor proteins SOS and Grb2, KRAS signalling cascade is activated leading to increased cell proliferation. One of KRAS downstream targets is BRAF, that will subsequently activate MEK1/2 and ERK1/2 to activate several transcription factors (TF) responsible of cell growth and survival-related gene expression. To terminate signal transduction, ERK1/2 sends negative feedback loops to RAF and SOS, and NF1 hydrolyses GTP to GDP to inactivate RAS.

I4.3 MAPK signalling and cancer

Aberrant MAPK signalling in tumours

The MAPK cascade is a critical regulator of human cancer cell survival, dissemination and resistance to drug therapy. Constitutive MAPK pathway activation is found in 30% of all human cancers[381] as a result of molecular alterations in genes encoding key components of the pathway, such as RAS, BRAF or MEK, or upstream activation mediated by mutations or

amplification of cell-surface receptors, typically the EGFR. Deregulated signalling due to constitutive activation of the pathway leads to uncontrolled cell growth and survival, ultimately resulting in oncogenic transformation and progression.

Mutations in the RAS gene were first reported in cancer over 30 years ago, and numerous studies have since validated mutant RAS as a driver of tumour initiation and maintenance[382]. The predominantly mutated isoform is KRAS (85%) followed by NRAS (11%) and HRAS (4%). Missense gain-of-function mutations in all three RAS genes are found in 27% of all human cancers, with a high prevalence in CRC where it is found in almost 50% of the cases. 98% of the mutations are at one of the three mutational hotspots: G12, G13 and Q61 that compromise the GTP hydrolysis activity. To make things more complicated, RAS activation can also be driven by loss of GAPs, such as NF1, or persistent activation of GEFs, such as SOS1.

Human BRAF mutations are also found in a huge variety of cancers[383]. For instance, over 40 different missense mutations have been identified, although most of them are extremely rare[373]. The most common BRAF mutation (90% of total) is one in which thymidine is replaced by adenosine at nucleotide 1796[383], leading to the substitution of glutamic acid (E) for valine (V) at the 600 amino acid residue of the expressed protein, hence the identification of this mutation as **V600E**[r]. V600 can also be mutated to other residues, although at a much lower frequency (0,1 to 2%). From a molecular point of view, the consequence of this mutation is that the two regions in the kinase domain are forced apart into their active conformation. This is because the glutamate residue is larger than the valine one, and moreover is negatively charged instead of being hydrophobic[373]. BRAFV600E displays kinase activity about 500-fold greater than that of WT BRAF[373] and induces constitutive ERK signalling independently of RAS, evading normal mechanisms of pathway attenuation and stimulating proliferation, survival and transformation[384]. Under physiological conditions, signalling through RAS/RAF/MEK/ERK is regulated by ERK-mediated feedback inhibition[385]. Other mutations result in BRAF impaired kinase activity, which bind more tightly than WT BRAF to RAS-GTP and their activation of signalling is RAS dependent[386,387]. The highest incidence of BRAF mutations is in malignant melanoma (up to 70%)[388], and to a less extend in thyroid[389] (40%) and colorectal cancer (10-15%). Nonetheless, they also occur at low frequency

[r] As a result of a missing codon in the original BRAF sequence, V600E was initially designated as V599E and is identified as such in earlier literature[579] .

(1-3%) in a wide variety of other cancers. Mutations in ARAF have not been described up to date, whereas CRAF is rarely mutated[390], and MEK mutations have been hardly detected in human cancers.

Targeting MAPK members for cancer therapy

Target-based therapies are widely considered the future of cancer treatment and since the MAPK pathway is deregulated in a huge variety of tumours, much attention has been focused on its signalling effectors or its upstream activators as interesting targets for therapeutic intervention. Several strategies for inhibiting MAPK signalling have already been evaluated as cancer therapies. Promising therapeutic approaches include EGFR inhibitors or blocking antibodies, as well as inhibitors of downstream effectors such as BRAF or MEK. On the contrary, although it was originally believed that farnesyltransferase inhibitors would effectively inhibit RAS activation[391,392], clinically effective inhibitors of RAS have yet to be identified and no anti-RAS therapies have reached clinical application. On the one hand, recent studies have identified small molecules that directly bind to RAS disrupting crucial functions such as GDP-GTP regulation and interaction with its effectors[393,394]. Other molecules that block RAS interaction with the GEF SOS1[395,396] or its effectors[397] have also been identified. On the other hand, indirect approaches include: inhibition of enzymes that prevent membrane association of RAS[398] or that of proteins that facilitate RAS trafficking to the plasma membrane[399], inhibitors of downstream effector signalling (see details below) and small interfering or short hairpin RNA of mutant KRAS expression[400–402].

A different strategy to block aberrant activation of the MAPK pathway is the blockage of the upstream effector EGFR. Two predominant classes of EGFR inhibitors have been developed including **monoclonal antibodies** (mAbs) that block ligand binding to the extracellular domain of EGFR, such as cetuximab (Erbitux®) and panitumumab (Vectibix®), and **small molecule tyrosine kinase inhibitors** (TKIs) that target the receptor catalytic domain of EGFR, such as gefitinib (Iressa®) and erlotinib (Tarceva®). The only ones approved for the treatment of advanced colorectal cancer are cetuximab and panitumumab. Importantly, the clinical use of these antibodies is limited to individuals who do not harbour KRAS mutations[403] and the presence of BRAF mutations is also being considered as exclusion criteria for EGFR inhibitor treatment.

The fact that growth factor hyperactivity, and RAS/RAF mutations result in increased signalling through RAF, has converted RAF in an ideal target for therapeutic development. Sorafenib (Nexavar®, BAY 43-9006) was the first small molecule to undergo clinical investigation for the treatment of melanoma, one of the tumours with higher prevalence of BRAF mutations. It was initially known as a potent inhibitor of CRAF and it was found later to inhibit WT and mutant BRAF[404], as well as some other kinases. Unfortunately, sorafenib failed to yield a significant improvement in melanoma patient survival, although it is currently approved for clinical treatment of renal, hepatocellular and thyroid carcinomas[405–408]. The limited activity of sorafenib in tumours with BRAF mutation prompted the development of second-generation RAF inhibitors with greater sensitivity for mutant BRAF. Vemurafenib[409] (Zelboraf®, PLX4032) activity against mutant BRAFV600E mutation yielded intense excitement for melanoma therapy. It binds the ATP-binding domain of mutant BRAF monomer blocking MEK and ERK signalling[410], and in contrast to sorafenib, only inhibits cells harbouring BRAFV600E mutation. It is currently approved for the treatment of advanced melanoma patients harbouring BRAFV600E mutation.

Dabrafenib (Tafinar®, GSK2118436) has also shown positive response rates in metastatic melanoma, and indeed is clinically used alone or in combination with the MEK inhibitor trametinib to treat melanoma patients.

Other strategies involve the inhibition of MEK with the inhibitors trametinib (Mekinist®, GSK1120212) and cobimetinib (Cotellic®, XL518). Nowadays they are only approved for the treatment of melanoma alone or in combination with BRAF inhibitors.

Some of these therapies are used in combination with cytotoxic agents since they have proved to be a better approach that their use alone.

In contrast to the advanced development and evaluation of RAF and MEK inhibitors, there has been limited progress in the development of ERK1- and ERK2-selective inhibitors. This is partly due to the earlier assumption that, as ERK is the only known downstream target of MEK, no additive benefit would result from an ERK inhibitor compared to a MEK inhibitor. However, interest in the discovery and development of ERK inhibitors has recently emerged. This is in part due to the negative feedback loops that are promoted by small-molecule inhibitors and the development of resistance with RAF and MEK inhibitors that frequently involves recovery of ERK signalling. A few ERK inhibitors have been reported in the patent literature[411–415].

Resistance to MAPK signalling inhibition

The clinical success of even the most effective cancer therapies is uniformly limited by the development of **acquired drug resistance**. The mechanisms for drug resistance have been extensively studied, and although unexpected mechanisms appear from time to time, significant improvement has been made. Two common mechanisms of acquired drug resistance have been identified and, to date, have been most extensively studied. Mechanisms of resistance include **secondary mutations** in the drug target itself that abrogate the inhibitory activity of the drug and activation of **alternative signalling pathways** that bypass the original target [**FIGURE I10**].

Regarding anti-EGFR therapies, mechanisms of resistance include mutations in the KRAS, NRAS and BRAF genes, all of which lead to sustained activation of MAPK signalling independent of EGFR. The first piece of evidence of a secondary resistance mutation to a therapeutic antibody came when Montagut et al. elegantly demonstrated that colorectal cancer cells treated with cetuximab, develop a secondary EGFR mutation that impairs cetuximab but not EGFR ligand binding. Importantly enough, these cetuximab-resistant cells retained sensitivity to panitumumab, thus demonstrating that panitumumab binds a distinct EGFR epitope[416]. Recent studies have also identified signalling pathways that bypass EGFR and mediate cetuximab resistance, which include amplification of the closely related ERBB2 receptor and increased levels of the EGFR ligand heregulin[417,418].

Resistance to RAF inhibitors has also been a widely explored topic over the past few years. By 2010, different works demonstrated that RAF inhibitors suppress the ERK signalling in mutant BRAF cells but enhance ERK signalling in WT BRAF cells, a mechanism referred to as “the **RAF inhibitor paradox**” [**FIGURE I10**]. Substantial biochemical evidence suggests that the phenomenon is primarily the result of conformational changes, enhanced RAF dimerisation and transactivation induced by these drugs[419–421]. Some models explain this paradox as a response to the inhibition of the kinase activity of WT RAF by the drug either by relief of RAF autophosphorylation[422] or due to transactivation of CRAF[375]. At non-saturating concentrations, the inhibitors activate rather than inhibit the pathway, particularly in the presence of RAS mutations or activated upstream receptor kinases[423]. Villanueva *et al.* argue that resistance to BRAF inhibitors is mediated by enhanced IGF-IR/PI3K signalling[424] and in agreement with this finding, another report shows that in vemurafenib-

resistant cells the levels of AKT, a downstream effector of PI3K, are increased[425]. In addition, distinct mechanisms of MAPK activation have been found during BRAF inhibitor treatment. Mutually exclusive PDGFR beta RTK-mediated activation and RAS-mediated activation of the MAPK pathway were also found to account for resistance to BRAF inhibitors[426]. Moreover, expression of MAP3K8[427] or EGFR through SOX10 suppression[428] confers resistance to BRAF inhibition in BRAFV600E mutant cells. Another mechanism of resistance to vemurafenib relates to V600E alternative splicing[429].

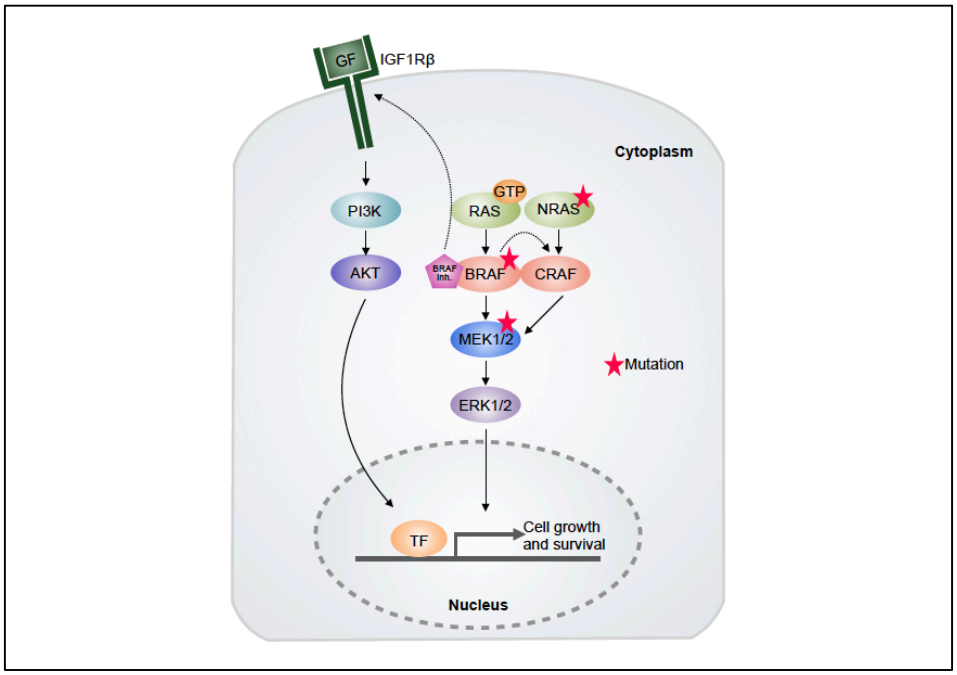

Figure I10 | Signalling pathways driving resistance to BRAF inhibitors. Following chronic BRAF inhibition, resistant cells evolve several compensatory mechanisms including activation of RTKs such as IGF-R1 and engagement of PI3K pathway. Another common mechanism is the transactivation of CRAF to activate downstream signalling. Activating mutations in MEK or NRAS can also appear, the latter will signal through CRAF.

Interestingly, there is evidence indicating that the tumour micro-environment confers resistance to BRAF inhibition therapy in melanoma through secretion of HGF[430] or FAK[431]. Accordingly co-inhibition of BRAF and FAK or HGF/MET abolished ERK reactivation and resulted in reversal of drug resistance[431]. To overcome BRAF inhibitor resistance, several efforts have been putted into developing novel therapeutic strategies including a new

pan-RAF inhibitor that also targets SRC[432] or compounds triggering ER stress[433], which have shown positive effects in patients who developed resistance to BRAF-selective inhibitors. It is worth noting that such paradoxical activation of ERK signalling has been observed with different ATP-competitive inhibitors of RAF, including vemurafenib and sorafenib, suggesting that their clinical application must be restricted to tumours harbouring activating mutations of BRAF.

Given that the majority of BRAF inhibitor resistance occurs through reactivation of MAPK, several MEK inhibitors were developed to be used alone or in combination with BRAF inhibitors in BRAF-mutant cells. Several studies reveal that BRAF inhibitor-resistant tumour cells are highly sensitive to MEK inhibition and demonstrate that targeted pharmacological MEK inhibition may be a highly effective therapeutic alternative in BRAF inhibitor-resistant tumour cells[434,435]. In light of these findings, focus has turned to dual inhibition of BRAF and its downstream target, MEK[436–438].

In summary, understanding the mechanisms of drug resistance through both in vitro models and human tumour tissues can clearly lead to the development of more effective targeted therapies, new therapeutic combinations or both. It will be important to personalize such approaches on the basis of the mechanisms of resistance of each individual tumour.

I5. DNA damage response pathway

I5.1 DNA damage and repair

The main objective for every life form is to deliver its genetic material intact and unchanged to the next generation. Constant assaults on the DNA by endogenous and environmental agents make this objective more difficult to achieve. Presence of DNA lesions can block genome replication and transcription, and in case of being repaired incorrectly or not repaired at all, they lead to mutations or wider-scale aberrations in the genome that threaten cell or organism viability. To counter this threat, cells have evolved mechanisms, collectively termed as the **DNA damage response (DDR),** to detect DNA lesions, signal its presence and mediate its repair[439–441]. Cells defective in these mechanisms generally display heightened sensitivity towards DNA-damaging agents and, as described below, such effects cause human disease like cancer. Although responses differ for different classes of DNA lesions, they usually occur by a common general programme. Like other signal transduction pathways, the DDR uses signal sensors, transducers and effectors. DDR signalling is activated by aberrant DNA structures induced by DNA damage or replication stress. The proteins that directly recognise the lesions are called sensors and activate the most upstream DDR kinases that will activate downstream effectors. The downstream effectors of the DDR kinases regulate a wide spectrum of cellular processes important for genomic stability, such as DNA replication, DNA repair and cell-cycle control. Although it displays a unique mechanism of activation, the DDR is a *bona fide* signal transduction pathway that is primarily driven by protein phosphorylation events.

Of the many types of DNA lesions, **DNA-single strand breaks (SSB)** arise both directly from disintegration of damaged sugars and indirectly from the excision repair of damaged bases. If they are not repaired, SSB can be converted into **double-strand breaks (DSB),** which are formed when both strands of the DNA duplex are broken. Regardless of their source, DSB are considered the most harmful lesions because they can drive genome rearrangements and cell death[442]. Other types of DNA lesions include apurinic site, deamination, mismatches, pyrimidine dimers, interstrand crosslink, bulky adducts, and intercalating agents[443].

Some DNA aberrations arise via **physiological processes** whereas others come from toxic environmental agents. Physiologically, some of the

mechanisms that can induce DNA lesions are: DNA mismatches occasionally introduced during DNA replication; DNA strand breaks caused by abortive topoisomerase I and II activity; DNA-base lesions caused by hydrolytic reactions and non-enzymatic methylations or DNA damage produced by reactive-oxygen compounds. On the other hand, the most pervasive environmental DNA-damaging agent is **ultraviolet (UV) light** that can induce ~100 lesions per exposed cell from residual UVA and UVB from the ozone layer. **Ionizing radiation (IR)** resulting from radioactive decay of naturally occurring compounds also generates various forms of DNA damage, the most toxic being DSB. But today, the most prevalent environmental cancer-causing chemicals are probably those produced by tobacco products, which trigger various types of cancer[444,445]. Cancer-causing DNA-damaging chemicals can also be found as contaminants of food, such as aflatoxins in the peanuts and peanuts butter and heterocyclic amines in over-cooked meats[446].

DNA-damage signalling and cell cycle checkpoints

One of the earliest events and key DDR-signalling components, is the recruitment of the protein kinases **ATM** (Ataxia telangiectasia mutated) and **ATR** (ATM- and Rad3-Related) to the damaged site, which orchestrate a large network of cellular processes to maintain genomic integrity [**FIGURE I11**].

Both ATM and ATR are activated by DNA damage, but their DNA-damage specificities are distinct and their functions are not redundant. Whereas ATM is primarily activated by DSBs, ATR responds to a broad spectrum of DNA damage, including DSBs, SSBs and a variety of DNA lesions that interfere with replication[447–449].

Following the detection of DSB, the histone variant H2A.X is targeted for phosphorylation in the chromatin close to the break site[450]. The phosphorylated form of H2A.X, known as **γH2A.X**, serves as a molecular beacon for the presence of damage thus marking nucleosomes in one or more megabases of the DNA surrounding the DSB[451]. γH2A.X is central in linking damaged chromatin to the DNA repair machinery, directing the recruitment of multiple DNA repair and signalling proteins into repair centres, microscopically visible nuclear aggregates known as “foci”.

To perform its chromatin-mediated functions, ATM has to specifically recognise the chromatin flanking DSBs, and **MDC1** is the key mediator of this process[452]. Through its BRCT (BRCA1 carboxy-terminal) domain,

MDC1 directly interacts with γH2A.X and is necessary for full-sized γH2A.X foci formation[453–455]. Activation of ATM also leads to phosphorylation of **KAP1** (for KRAB-interacting protein, but also known as TRIM28 or TIF1β) which is required for ATM-mediated global chromatin relaxation in response to DSB[456]. However how KAP1 mediates this response is still unknown.

The best characterised ATM/ATR targets are the protein kinases **CHK1** and **CHK2**[457,458]. Together with ATM and ATR, these checkpoint kinases reduce CDK (cyclin-dependent kinase) activity by various mechanisms, some of which involve activation of the p53 transcription factor[459–461]. CDKs inhibition slows down or arrests cell cycle progression at G1-S, intra-S and G2-M "cell cycle checkpoints" in order to increase the time available for DNA repair before replication or meiosis proceeds. In parallel, ATM and ATR enhance DNA repair by the recruitment of several repair factors to the site of damage, by inducing DNA-repair proteins transcriptionally or post-transcriptionally or activating these proteins by modulating its phosphorylation, acetylation, ubiquitination or SUMOylation[462]. If the above-mentioned events allow effective DNA repair, the DDR is inactivated leading to resumption of normal cell function. Alternatively, if the damage cannot be repaired, chronic DDR signalling triggers cell death by apoptosis or cellular senescence[463,464].

DNA-repair pathways

The wide diversity of DNA lesions, requires multiple and distinct DNA-repair mechanisms. Human cells have at least five primary pathways of DNA repair: **direct reversal**, **mismatch repair (MMR)**, **base excision repair (BER)**, **nucleotide excision repair (NER)**, and DSBs repair which include **non-homologous end-joining (NHEJ)**[465] and **homologous recombination (HR**)[466].

In NHEJ, DSBs are recognised by the Ku protein that then binds and activates the protein kinase DNA-PKcs (DNA-dependent protein kinase) and DNA ligase IV. Besides, it exists a less well characterised Ku-dependent NHEJ pathway, called **microhomology-mediated end-joining (MMEJ)** or alternative end-joining which results in sequence deletions[467]. Although both NHEJ and MMEJ are error-prone, they can operate in any phase of the cell cycle.

By contrast, HR is generally restricted to S and G2 because it uses sister-chromatid sequences as the template to mediate faithful repair. HR is always initiated by ssDNA generations through 5' resection of the DNA ends, which is promoted by various proteins including the MRE11-RAD50-NBS1 (MRN) complex. Subsequently, RAD51 and the BRCA1/2 (Breast cancer 1 and 2) proteins catalyse the binding of the ssDNA to the undamaged template, which will induce DNA ligation following the actions of polymerases, nucleases, helicases and other components. HR is also used to restart stalled replication forks and to repair interstrand DNA crosslinks.

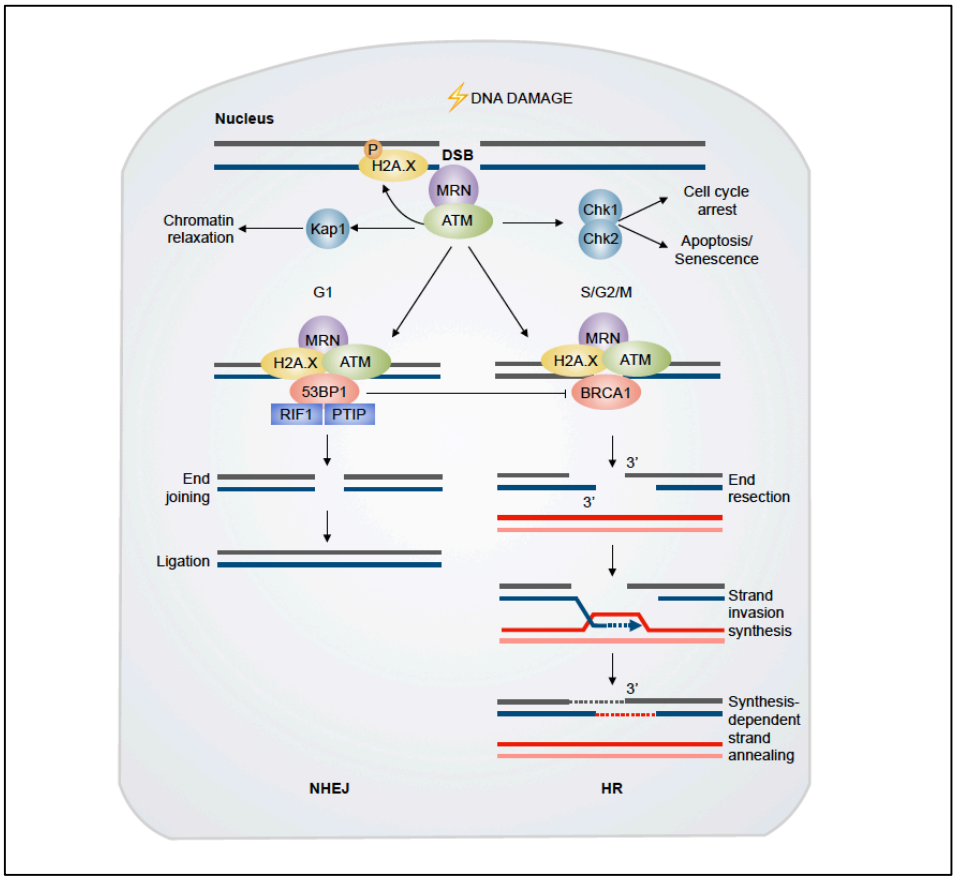

Figure I11 | Simplified model of DNA damage response signalling upon generation of DSBs. Upon DSB generation, MDC1 binding serves as a molecular platform to recruit ATM and H2A.X is phosphorylated. On the one hand, ATM phosphorylates KAP1 and Chk1/2 to induce cell cycle arrest and, if necessary, apoptosis. On the other hand, 53BP1 is phosphorylated and recruited to damaged foci to initiate NHEJ repair avoiding recruitment of BRCA1. In S/G2/M BRCA1 displaces 53BP1 to induce DNA end resection and repair of the DSB by HR.

I5.2 53BP1: Pro choice in DNA repair

More than two decades ago, 53BP1 was first described as a binding partner of the tumour suppressor protein p53[468]. Since then, 53BP1 studies have focus on its role in maintaining genomic integrity. Although the significance of the interaction with p53 remains largely unexplained, 53BP1 has emerged as a central component of chromatin-based DSB signalling[469,470]. 53BP1 is a direct reader of a DSB-specific histone code, which translates multiple site-specific histone modifications into efficient checkpoint signalling and DSB repair[471].

53BP1 is a large protein of 1972 amino acids with no apparent enzymatic activity but with interaction surfaces for numerous DSB-responsive proteins. Important structural elements in 53BP1 include the BRCT repeats that mediate the interactions between p53 and EXPAND1, the tandem Tudor domains that recognise specific histone marks, and 28 amino-terminal Ser/Thr-Gln (S/T-Q) sites, which are phosphorylated by ATM and/or ATR upon induction of DNA damage[469,472]. These phosphorylation sites are not required for 53BP1 recruitment to DNA damage foci, but mediate interactions with critical effectors of 53BP1 function.

When DSBs are detected, after the ATM-mediated phosphorylation of H2A.X and subsequent MDC1 recruitment, 53BP1 rapidly accumulates on the chromatin surrounding the break site[469,473,474]. Like most components of the DSB signalling pathway, 53BP1 recruitment can be monitored by microscopy by tracking the formation of subnuclear foci at damaged chromatin.

53BP1 is a key determinant of DSB repair pathway choice between NHEJ and HR[475–477] [**FIGURE I11**]. The decision of pathway selection is critical for the maintenance of genomic stability and is tightly controlled during different cell cycle phases[478]. A defining feature of the two pathways is whether they require DNA end-resection or not. HR depends entirely on the extensive resection of DNA surrounding the DSB to produce 3' single-stranded overhangs, whereas NHEJ efficiency greatly decreases upon DSB resection[479,480]. Therefore, a major determinant of pathway choice is the differential regulation of DNA end-resection during the cell cycle[481]. Although 53BP1 is not a core factor of the NHEJ[482,483], it antagonizes the resection of DSBs during the G1 phase of the cell cycle, preserving DSB ends and thereby favouring repair by NHEJ over HR. Upon entry into S phase, BRCA1 helps to switch the mode of DSB repair by excluding 53BP1-RIF1 complexes (see below for RIF1 details), thus enabling extensive DSB

resection and the initiation of HR. However, it remains unclear how 53BP1 is able to establish an effective barrier against DSB resection in G1. An important progress in understanding how 53BP1 functions to promote NHEJ came with the discovery of **RIF1** as an essential 53BP1 partner to block DSB resection in G1[399,484–487]. Consistent with this, RIF1 accumulates at damaged chromatin in a 53BP1-dependent manner[488]. The role for RIF1 downstream of 53BP1 was highly overlooked for a long time, in part due to phenotypic differences in mice models for RIF1 and 53BP1 deficiencies. Whereas *53bp1*$^{-/-}$ animals are viable but they exhibit radiosensitivity and immunodeficiency[489,490] *Rif1*$^{-/-}$ are embryonic lethal[491]. These differences were further reinforced by the discovery of other RIF1 functions that are independent of 53BP1[491–494]. At the same time, a second 53BP1 interacting protein was described: **PTIP**, which is involved in a different subset of 53BP1-dependent functions.

Apart from DSB pathway choice, 53BP1 is also essential to promote NHEJ of deprotected telomeres[495], and for coupling distal DNA ends generated during immunoglobulin long-range V(D)J recombination and class switch recombination (CSR), which is important for functional adaptive immune response[496–499].

I5.3 DNA damage and cancer: a close relationship

A major feature of cancer is **genome instability**[500], which accelerates the genetic alterations that drive tumour development[501,502]. For instance, in CRC genomic instability drives aberrant chromosomal rearrangements that drive oncogenic features. In addition, MMR defects cause MIN that predisposes to CRC[503], and CIN, which is seen in most sporadic solid tumours[24]. Most carcinogens operate by generating DNA damage and causing mutations[460,504].

The DDR plays an essential role in many aspects of cancer. Deficiencies in DDR mechanisms have been shown to be contributing factors in many stages of tumour development. Indeed, multiple hereditary cancer predispositions result from mutations in DNA repair genes[501,505]. One of the best-known examples is the defective allele of BRCA1 or BRCA2 genes, which encode for two proteins centrally involved in the repair of DNA DSBs by HR, that predispose women to develop breast and ovarian cancer[506,507]. Aberrant cell proliferation caused by oncogene activation or inactivation of certain tumour suppressors, causes DNA-replication stress and persistent

DNA damage formation[463,508,509]. In fact, the DDR pathway is commonly activated in early neoplastic lesions and likely protects against malignancy[508,509]. It has been suggested that defects on the DDR through mutational or epigenetic inactivation of its members, are selected during tumour development, thus allowing malignant progression. Therefore, it is not surprising that many malignant tumours show functional loss or deregulation of key proteins involved in the DDR and cell cycle regulation, like p53 and ATM[510], MRE11[511–513] or BRCA1/2[510]. Such mutations may allow pre-cancerous cells to breach the proliferation barrier posed by the DDR, thereby allowing the progression of pre-malignant lesions to malignant carcinomas.

I5.4 DNA damage repair inhibition for cancer treatment: PARP inhibitors as an example

Apart from its role in tumour suppression by preserving DNA integrity, DDR mechanisms play also a relevant function by attenuating the effectiveness of standard cancer treatments, such as radio- and chemotherapy. These treatments rely on the induction of DNA damage to proliferating cells including the highly proliferative cancer cells. However, some cancer cells resist the lethal effects of genotoxic cancer therapy in part by **activation of the DDR**[514–517]. Activation of DDR together with the fact that anti-cancer therapies are limited in dose and duration due to the numerous side effects that they produce makes that these therapies, though effective, often fail to be curative. Regulators of the DDR have therefore become attractive targets for cancer therapy primarily through two potential approaches. First, they have been used as chemo- or radio-sensitizers to increase the effectiveness of standard genotoxic treatments, and to prevent or overcome the development of resistance. Second, to exploit defects in DDR mechanisms as potentially targetable weaknesses through synthetic lethal approaches.

While defects in DDR components may, on the one hand, give cancer cells a growth advantage, as mentioned, allowing them to survive and proliferate despite oncogene-induced replication stress and genomic instability, they may also drive a reliance of cancer cells on any remaining DDR pathways in order to survive after DNA damage. Targeting of such remaining pathways may therefore be selectively toxic to cancer cells with mutations in certain DDR genes without affecting normal cells. The therapeutic potential of this approach was first demonstrated in cells harbouring **mutations in BRCA1**

and BRCA2, which were found to be highly sensitive to small molecule inhibitors of PARP (poly(ADP-ribose)-polymerase), a DDR protein that is involved in the detection and repair of DNA SSB by base excision repair[518,519]. Mechanistically, suppression of PARP leads to stalling of replication forks due to accumulation of unrepaired SSBs[520]. Stalled replication forks degrade into highly cytotoxic DSBs if they are not corrected by a proper mechanism, which is absent in BRCA1/2-mutated cells[520]. Since BRCA-mutated cells are incapable of HR, PARP inhibition results in genomic instability and cell death[521]. Thus, tumours that harbour a defect in HR (and likewise a defect in DSB repair) seem to be highly vulnerable to the effects of PARP inhibition. These findings led to the development of the first **PARP inhibitor, olaparib** (AZD-2281, Lynparza®), which was clinically approved by the FDA (Food and Drug Administration of USA) in 2014 for the treatment of advanced ovarian cancer with germline BRCA mutations.

Olaparib has since then shown promising results for the treatment of BRCA1/2 mutated breast or ovarian cancer in clinical trials[522–524].

Further studies have demonstrated that inhibition of other components of the DDR machinery can sensitise cancer cells to DNA damaging treatments [**TABLE I1**], including DNA-PKcs[525], ATM[526,527], ATR[528–531], or their downstream targets CHK1 and CHK2[532,533].

Cancer treatment	Type of DNA damage
Radiotherapy: - Ionising radiation	SSBs, DSB
Antimetabolites: - 5-Fluorouracil	Cytotoxic metabolite, inhibits base pairing leading to base damage and replication lesions
Topoisomerase inhibitors: - Camptothecins (Topo I) - Irinotecan (Topo I) - Etoposide (Topo II) - Antracyclins (Doxorubicin, epirubicin, daunorubicin) (Topo II)	SSBs, DSBs, replication lesions. Anthracyclines also generate free radicals
Platinum-based therapies (Oxaliplatin, carboplatin, cisplatin)	DSBs, DNA crosslinks, replication lesions, bulky DNA adducts

Table I1 | Examples of DNA-damaging agents used in cancer treatment and the type of DNA damage that they induce.

OBJECTIVES

OBJECTIVES

Our general objective was to study the functional contribution of IKKα to intestinal cancer initiation and progression, and to use this information to propose new therapeutic strategies for cancer therapy. This main objective is subdivided in specific subjects:

1. Investigate the requirement of IKKα in tumour initiation in a mouse model of intestinal tumorigenesis.
2. Investigate the mechanisms that mediate the addiction of intestinal adenomas to IKKα.
3. Identify possible p45-IKKα phosphorylation substrates.
4. Explore the functional relevance of p45-IKKα-dependent phosphorylations in cancer.
5. Study the possibility of inhibiting p45-IKKα activity as anticancer therapy.

MATERIALS AND METHODS

MM1. Animals

The classical vertebrate model used in biomedical research is the house mouse (*Mus musculus*), which shares around 95% of its genome with humans. Mice can be genetically manipulated to mimic human diseases or conditions and can be inbred to maintain uniformity within strains, allowing for more accurate and repeatable experiments. They have an accelerated lifespan and an entire life cycle can be studied within 2-3 years. And they are a cost-effective and efficient research tool (they are small, reproduce quickly and are relatively easy to house and transport).

In summary, these were the strains used:

Mouse strain	Description	Background	Reference
***Vilin*-Cre**	Constitutively active Cre recombinase under the control of the *Villin1* promoter: expressed in the intestinal epithelium	C57BL/6	534
***Ikkα*$^{FL/FL}$**	Deletion of *Ikkα*	C57BL/6	535
***Apc*$^{Min/+}$**	Truncated form of *Apc*. Animals develop adenomas in the small intestine predominantly.	C57BL/6	76
C57BL/6	Wild-type animals	C57BL/6	Jackson Laboratories

Table MM1 | Mouse strains.

For the generation of orthotopic xenografts mice, human tumours were perpetuated (>5 passages mice to mice) and kept crio-preserved for further experiments. In these experiments, equivalent pieces of individual tumours were implanted orthotopically in the wall of the cecum. After 4-5 weeks tumours were detectable by palpation, and the animals were randomly separated into the different groups of treatments. Vemurafenib (50mg/kg) was administered orally every day, 5-FU (50mg/kg) and irinotecan (50mg/kg) were administered every 4 days intravenously; and bafilomycin A1 (1mg/kg) and chloroquine were administered daily by intraperitoneal injection. After 21 days of treatment, mice were euthanized and the tumours collected, photographed, measured and processed for IHC analysis.

Animals were kept under pathogen-free conditions, and all animal work was conducted according to the guidelines from the Animal Care Committee at the Generalitat de Catalunya. These studies were approved by the Committee for Animal Experimentation at the Institute of Biomedical Research of Bellvitge (Barcelona).

MM2. Cell lines and reagents

All cells were grown in Dulbecco's modified Eagle's medium (DMEM) [Invitrogen] supplemented with 10% fetal bovine serum (FBS) [Biological Industries], 4.5 g/L glucose [Life Technologies], 2 mM L-glutamine [Biological Industries], 56 U/mL penicillin and 56 µg/mL streptomycin [Biological Industries]. Cells were grown in an incubator at 37°C and 5% CO_2.

For the cell treatments, the following compounds were used: BRAF inhibitor AZ626 [Selleckchem Ref. S2746], BRAF inhibitor vemurafenib [Selleckchem Ref. S1267], bafilomycin A1 [Sigma, Ref. B1793], TAK1 inhibitor 5Z-7-oxozeaneol [Selleckchem, Ref. 499610], MEK inhibitor Trametinib [Selleckchem, Ref. S2673], MG132 [Calbiochem, Ref. 474790], chloroquine [Sigma, Ref. C6628], 5-Fluorouracil [Accord, C.N 603544,3], irinotecan [Frasenius Kabi, C.N 687014,3], doxorubicin [Accord, Ref. 174247],BAY65-5811 [Bayer], TPCA [Sigma Ref. T1452].

For cell transfection and virus production human HEK293T were used [ATCC Ref. CRL-3216].

The panel of CRC cell lines used are Caco2 [ATCC Ref. HTB-37], DLD1 [ATCC Ref. CCL-221], HCT116 [ATCC Ref. CCL-247], HT29 [ATCC Ref. HTB-38D], LIM1215 [ECACC Ref. 10092301], SW480 [ATCC Ref. CCL-228] and WiDr [ATCC Ref. CCL-218].

WT and IKKα KO MEFs were kindly provided by Prof. Michael Karin laboratory, UCSD, La Jolla. And SV40-LT-immortalized $TRF2^{FL/FL}$ (Celli and de Lange, 2005) MEFs were kindly provided by Dr. Simon Boulton, The Francis Crick institute, London.

MM3. Intestine samples: paraffin embedding

The first step in the histological characterization of any tissue is the preparation of the sample. Fast and proper collection and preparation of the intestinal sample is essential to preserve the epithelial architecture. In this case, analyses of the intestines were performed using histological techniques to produce paraffin tissue blocks that allow fine sectioning.

Sample preparation

- Collect intestine in ice-cold phosphate buffered saline (PBS) [Biological Industries Ref. 02-023-1A]
- Remove fat and mesentery and flush carefully with help of a syringe

- Place in a cassette in "Swiss Roll" shape
- Fix in 4% paraformaldehyde (PFA) rocking overnight (O/N) at room temperature (RT) [Sigma Ref. P6148, 4% in PBS]
- 2x wash in PBS 15min rocking at RT
- 25% ethanol rocking 15min at RT [Merck Ref. 1.00983.2500]
- 50% ethanol rocking 15min at RT
- 75% ethanol rocking O/N at 4°C
- 90% ethanol rocking 30min at RT
- 3x absolute ethanol rocking 1h at RT
- 3x xylene rocking 1h at RT [VWR Ref. 28975.325]
- Place tissue in embedding mould and incubate in paraffin 1h at 65°C [Leica Ref. 39602004]
- Change paraffin and incubate O/N at 65°C
- Change paraffin and cool down at RT
- Store at 4°C

MM4. Haematoxylin and Eosin staining

Haematoxylin and Eosin (H&E) staining is the most broadly used staining in histopathology. Once a tissue specimen has been processed, H&E staining is generally performed to confirm the integrity of the tissue and its cellular composition and organisation.

Haematoxylin is a dark blue or violet stain that acts as a basic dye. It is positively charged and can react with negatively charged, basophilic cell components such as nucleic acids in the nucleus. Eosin us a red or pink stain that is anionic and acts as an acidic dye. It is negatively charged and can react with positively charged, acidophilic substances (also known as eosinophilic) substances, such as amino acid side chains. Most proteins in the cytoplasm and in the extracellular matrix are basic (positively charged due to arginine or lysine amino acidic residues), so they stain in varying shades of pink.

Starting material is usually 4% PFA-fixed 4µm paraffin sections:

<u>Dewax and rehydrate</u>

- Heat slides 1-2h at 65°C (if slides have been re-paraffined, place at 65°C the night before), until paraffin is melted
- Xylene I and II 15min each
- Absolute ethanol I and II 10min each
- 96% - 70% - 50% ethanol 10min each

- Distilled water 10min

Staining

- Haematoxylin 30sec [Merck Ref. 1092530500]
- Tap water 5min
- 80% ethanol 0.15% HCl 30sec
- Distilled water 30sec
- Ammonia water [NH_3(aq)] 0.3% 30sec
- Distilled water 30sec
- 96% ethanol 5min
- Eosin 3sec [Bio-Optica Ref. 05-10003/L]
- 3x absolute ethanol 1min each

Dehydrate and mount

- Absolute ethanol I and II 5min each
- Xylene I and II 5min each
- Mount in DPX [Merck Ref. 1.01979.0500]
- Pictures were obtained with an Olympus BX61 microscope, using the CellSens software

MM5. Immunohistochemistry

Immunohistochemistry (IHC) combines histological, immunological and biochemical techniques for the identification of specific tissue components by means of a specific antigen/antibody reaction tagged (directly or most commonly indirectly) with a visible label. IHC allows us to visualise the distribution and localisation of specific cellular components within cells and in the proper tissue context.

Starting material is usually 4% PFA-fixed 4µm paraffin sections:

Dewax and rehydrate

- Heat slides 1-2h at 65°C (if slides have been re-paraffined, place at 65°C the night before), until paraffin is melted
- Xylene I and II 15min each
- Absolute ethanol I and II 10min each
- 96% - 70% - 50% ethanol 10min each
- Distilled water 10min

Antigen retrieval

- Depending on the antibody, a different antigen retrieval protocol was used [see **Table MM2**]
    - Tris-EDTA (pH 8.0, 40mM Tris, 1mM EDTA) 50min at 100°C without pressure
    - Sodium citrate (pH 6.0) 3 min with pressure
- Retain in buffer 1h allowing cooling down to RT
- 3x wash in PBS rocking 5min at RT

Peroxidase blockage

- 0.3% H_2O_2 in PBS 20min rocking at RT [Sigma Ref. H1009-500ML]
- 3x wash in PBS rocking 5min at RT

Permeabilisation and blocking

For most of the antibodies, the permeabilisation and unspecific binding blockage is done simultaneously in one step.

- 0.3% Triton X-100 [Surfactant Amps, Thermo Scientific Ref. 28340], 1% bovine serum albumin (BSA) [Sigma Ref. 3912-500G] in PBS 1h at RT
- 3x wash in PBS rocking 5min at RT

Primary antibody

- Incubate overnight at 4°C in 0.05% BSA in PBS (see specific dilutions in **Table MM2**)
- 5x wash in PBS rocking 5min at RT

Secondary antibody

- Envision+ System HRP Labelled Polymer anti-Rabbit [Dako Ref. K4003] or anti-Mouse [Dako Ref. K4001] 90min at RT
- 5x wash in PBS rocking 5 min at RT

Develop (DAB)

- Develop with 3,3'-diaminobenzidine (DAB) [Dako Ref. K3468], which forms a very stable, brown end-product at the site of the target antigen
- 5x wash in PBS rocking 5 min at RT

Counterstaining and mounting

Samples were counterstained with haematoxylin, as follows:

- Distilled water 5min
- Haematoxylin 30sec

- Tap water 5min
- 80% ethanol 0.15% HCl 30sec
- Distilled water 30sec
- 50% - 70% - 96% ethanol 5min each
- Absolute ethanol I and II 5min each
- Xylene I and II 5min each
- Mount in DPX [Merck Ref. 1.01979.0500]
- Pictures were obtained with an Olympus BX61 microscope using the CellSens software and analysed using the Cell Profiler software[536] (www.cellprofiler.org)

Antibody	Company	Reference	Species	Dilution	Antigen retrieval
Ki67	Novocastra (Leica)	NCL-L-Ki67-MM1	Mouse	1:500	TE 50 min
ɣH2A.X	Cell Signalling	#2577	Rabbit	1:200	Citrate 3 min pressure
B-catenin	Sigma	C2206	Rabbit	1:500	TE 50 min
Cleaved caspase 3	Cell Signalling	#9661	Rabbit	1:200	Citrate 3 min Pressure

Table MM2 | Antibodies used in IHC

MM6. Murine crypt/adenoma cell isolation

Obtaining a population enriched in adenoma cells is of paramount importance to analyse cancer cells and the CSC compartment. Likewise, obtaining a cell suspension enriched in intestinal crypts is essential for analysing the ISC compartment. Both these enriched fractions can be used for analysis by IF, RNA extraction and qRT-PCR, flow cytometry and most importantly 3D culture that favours growth of cells with stem cell properties. Murine intestinal adenoma cells (MIACs) from the *Apc*$^{Min/+}$ mouse model are obtained through a combination of mechanic and enzymatic dissociation and intestinal crypts are obtained by mechanical dissociation. The protocol that we use was adapted from Sato et al. 2009 [101]:

Crypt isolation

- Collect the small intestine in ice-cold PBS with 5x antibiotics [Pen-Strep solution, Biological Industries Ref. 03-031-1B
- Remove fat and mesentery
- Cut open longitudinally
- Wash repeatedly in PBS 5x Pen/Strep until there are no remaining particles stuck to the intestine

- Carefully scrape the villi under a magnifying lens
- Collect villi-free tissue sections to PBS 5x Pen/Strep
- Wash 1x in PBS 5x Pen/Strep
- Cut the sections to 2-4mm pieces and transfer to 50mL tube
- Add 10mL PBS 5x Pen/Strep and pipet up and down with a 10mL pipette; remove supernatant and add fresh PBS; repeat until supernatant is clear; if tissue pellet is not settled by gravity, centrifuge 5min at 800 rpm at 4°C
- Add 10mL 2mM EDTA [Titriplex III, Merck Ref. 1370041000] in PBS 5x Pen/Strep
- Incubate 1-2h rocking at 4°C or 30min rocking at RT
- Let settle and remove supernatant
- Add 10mL PBS 5x Pen/Strep 10% FBS; pipet up and down 5-10 times and collect the supernatant after passing it through 100µm pore diameter nylon mesh (cell strainer) [Falcon Ref. 352360]
- Spin down the crypt fraction by centrifuging 10-20min at 800 rpm at 4°C to remove single cells (mostly lymphocytes)
- Resuspend crypt unit pellet in 5mL PBS 5x Pen/Strep and count

MIAC isolation

- Collect the small intestine in ice-cold PBS with 5x antibiotics [Pen-Strep solution, Biological Industries Ref. 03-031-1B
- Remove fat and mesentery
- Cut open longitudinally
- Wash repeatedly in PBS 5x Pen/Strep until there are no remaining particles stuck to the intestine
- Carefully scrape the villi under a magnifying lens (this step is not essential for MIAC isolation, but helps find small adenomas better)
- Dissect adenomas carefully with a blade under a magnifying lens
- Wash adenomas 3x in HBSS [Gibco Ref. 14025] 5x Pen/Strep rocking 5min at RT; let settle and discard the SN
- Incubate adenomas in 8mM EDTA in HBSS 5x Pen/Strep rocking 5min at RT
- Shake vigorously 3x 10 times: the supernatant is the first fraction (collect, add 5% FBS and keep on ice); keep the pellet for obtaining following fractions
- Cut the adenomas with a blade (to small pieces, do not mince them)

- Incubate adenoma pieces in 8 mM EDTA in HBSS 5x Pen/Strep rocking 20min at 4°C
- Shake vigorously 3x 10 times: the supernatant is the second fraction (collect, add 5% FBS and keep on ice); keep the pellet for obtaining following fractions
- Incubate adenoma pieces in 0.4 mg/mL Dispase I [Sigma Ref. D4818] in HBSS 5x Pen/Strep shaking 20min at 37°C
- Shake vigorously 3x 10 times
- Centrifuge all fractions 5min at 1200 rpm at 4°C; discard the SN
- Resuspend the pellet(s) in 1.25 mg/mL collagenase I [Sigma Ref. C0130] in HBSS 5x Pen/Strep shaking 20min at 37°C
- Shake vigorously 3x 10 times: the supernatant is the last fraction; centrifuge 5min at 1200 rpm at 4°C; discard the SN
- Resuspend the cells in ice-cold HBSS 5x Pen/Strep 140nM ROCK inhibitor [Y-27632, Sigma Ref. Y0503]
- Filter the cells through 100µm-70µm-40µm pore diameter cell strainers [Falcon Refs. 352360/50/40]
- Centrifuge 5min at 1200 rpm at 4°C; discard the SN
- Resuspend the cells in ice-cold HBSS 5x Pen/Strep 140nM ROCK inhibitor
- Count, checking viability by Trypan Blue dye exclusion

MM7. Human tumour cell isolation

Obtaining a population enriched in human cancer cells is of paramount importance to study cancer cells and the CSC compartment. This enriched fraction can be used for analysis by IF, RNA extraction and qRT-PCR, flow cytometry and most importantly 3D culture that favours growth of cells with stem cell properties and can be used for drug screening. Cells from the tumours are obtained through a combination of mechanic and enzymatic dissociation. The protocol that we use was adapted from Van De Wetering et al. 2015[104]:

Tumour isolation

- Collect the tumours in Advanced DMEM/F12 [Gibco Ref. 12634028] with 5x antibiotics [Pen-Strep solution, Biological Industries Ref. 03-031-1B
- Cut tumours into small pieces and incubate with 10 ml of: Collagenase II (1,5 mg/ml), Hyaluronidase (20 µg/ml) [Sigma, H3506] Ref. and ROCK inhibitor (10 µM) for 30 min at 37°C shaking

- Add 1 ml of FBS
- Filter the cells through 100 µm pore diameter cell strainer to remove large fragments
- Cells were subsequently spun at 1000 rpm for 3 min
- Resuspend the pellet in 1 ml of basal culture medium and pass the content to a eppendorf tube
- Centrifuge again at 1000 rpm
- Seed the cells at different dilutions depending on the pellet. Usually 1/10, 1/50 and 1/100.

MM8. Organoid/tumouroid culture and reagents

Once we have a crypt enriched suspension, isolated MIACs or isolated human tumour cells, we can seed them embedded in basement membrane matrices, such as Matrigel® [BD Biosciences, now Corning Ref. 354234], and in serum-free conditions. Cells that grow without serum and attachment to a plate are thought to have stem-cell characteristics. Indeed, these 3D cultures can be maintained indefinitely with serial passaging [537].

Seeding (adapted from Sato et al. 2009 [101])

- Optimal seeding conditions: 5.000-10.000 crypt units or 50.000 MIACs per 50 µl matrigel drop in 24-well plate with 500 µl complete organoid medium.
- Refresh growth factors (adding 50 µl to each well) every 2 days and change fresh complete organoid medium every 4 days.
- Composition of the **mouse** complete organoid/tumouroid medium:
  In Advanced DMEM/F12 [Gibco Ref. 12634028]
    - 100 U/mL Penicillin and 0.1 mg/mL Streptomycin [Pen/Strep Solution, Biological Industries Ref. 03-031-1B]
    - 2 mM L-Glutamine [Biological Industries Ref. 03-020-1B]
    - 1x B27 supplement [Gibco Ref. 17504044]
    - 1x N-2 supplement [Gibco Ref. 17502048]
    - 140 nM ROCK inhibitor [Y-27632, Sigma Ref. Y0503]
    - 100 ng/ml murine Noggin [Peprotech Ref. 250-38]
    - 100 ng/ml murine R-spondin1 [R&D Systems Ref. 3474-RS]
    - 50 ng/ml EGF [Sigma Ref. E9644]
    - 20 ng/ml basic FGF [Peptrotech Ref. 450-33B]

- Composition of the **human** complete tumouroid medium:

- 100 U/mL Penicillin, 0.1mg/mL Streptomycin and Primocin 100 µg/ml [Invivogen, Ref. Ant-pm-1]
- 2 mM L-Glutamine
- 1x B27 supplement
- 1x N-2 supplement
- 10 µM Rock inhibitor
- 100 ng/ml Recombinant Human Noggin [PeproTech, Ref. 120-10C]
- 100 ng/ml Recombinant Human R-spondin 1 [PeproTech, Ref. 120-38]
- 50 ng/ml EGF
- 10 mM N-acetilcisteine
- 1,25 mM Nicotinamide [Sigma, Ref. N3376]
- 0,5 µM A8301 (ALK inhibitor) [Sigma, Ref. SML0788]
- 3 µM SB202190 [Sigma, Ref. S70677]
- 10 nM Prostaglandin E2 [Tocris, Ref. 2296]
- 10 nM Gastrin I human [Tocris, 3006]

Passaging 3D cultures (adapted from VanDussen et al. 2012[538])

- With ice-cold 1mL tips, 7x pipet up and down both matrigel and medium in the well, making sure all the matrigel is dissolved
- Transfer to eppendorf tube placed on ice
- Add an extra 500µL of ice-cold DMEM-F12 (supplemented with antibiotics and L-glutamine, DF12++ hereon) to give volume
- Pass the suspension 4x through a 30G needle [yellow, BD Microlance Ref. 304000] placed in a 1mL syringe
- Depending on the organoid/spheroid count, splitting the culture 1/3 is recommended: divide in desired tubes and give volume with DF12++ to help wash matrigel out
- Centrifuge at 600g 5min at 4°C; discard the SN and keep the tubes constantly on ice
- On ice and with ice-cold tips resuspend each pellet in 50µL thawed matrigel
- Quickly place matrigel drops without bubbles onto pre-warmed (1-2h at 37°C) 24-well plate
- Incubate 1-2 minutes at RT
- Incubate 10-20 minutes at 37°C
- Add 450µL complete sphere medium (see composition above) on top of solidified matrigel drops

- Refresh factors at 3rd day and passage at 5th or 6th day is recommended
- To check culture viability, a Leica DFC295 microscope was used, and cells were imaged, if necessary, using the Leica Application Suite Image capture software. Sphere diameter was calculated using Fiji (Image J) software (https://fiji.sc)

MM9. Tumouroid immunostaining

Following a slightly modified protocol from Dow et. al 2015[82], for performing immunostaining of 3D structures grown in matrigel, cells were previously seeded onto round glass coverslips, so that they could be mounted on a slide in the last step.

Fixation

- Aspirate the medium and add 500µL 4% PFA /well; incubate 20min at RT
- 2x wash in PBS 3min at RT
- Add 500µL DTT buffer /well (100mM Tris pH9.4, 10mM DTT in H_2O). Incubate 25min at RT
- 3x wash in PBS 3min at RT

Permeabilisation

- Add 500µL permeabilisation buffer /well (0.5% Triton X-100 in PBS); incubate 10min at RT
- 3x wash in PBS 3min at RT

Blocking

- Add 500µL blocking buffer /well (2% BSA, 0.3% Triton X-100 in PBS); incubate at least 30min at RT, 1h is preferable (>2h at +4°C)

Primary antibody

- Without washing, add the primary antibodies diluted in blocking buffer, 500µL /well (See **Table MM3** for details)
- Incubate O/N at 4°C
- 3x wash in PBS 5min at RT
- 3x wash in 0.3% Triton X-100 in PBS 5min at RT

Secondary antibody

- Add directly labelled secondary antibodies (See **Table MM6** for details) in 0.05% BSA in PBS, 500µL /well; incubate 2h at RT, protected from light
- 3x wash in PBS 5min at RT, protected from light

Nuclei counterstaining and mounting

- Add 500µL DAPI 1:2000 in water / well [5mg/mL Invitrogen Ref. D1306]; incubate 10min at RT, protected from light
- 3x wash in PBS 5min at RT, protected from light
- Mount in ProLong® Diamond with DAPI [Thermo Scientific Ref. P36971] onto a slide
- Pictures were obtained with a TCS SP5 Upright Confocal Microscope, using the Leica Application Suite software and analysed using the Cell Profiler software[536] (www.cellprofiler.org)

Antibody	Company	Reference	Specie	Dilution
53BP1	BD Bioscience	612523	Mouse	1:2000
53BP1	Bethyl Laboratories	A300-272A	Rabbit	1:5000
γH2A.X	Merck Millipore	#2577	Mouse	1:600
RIF1	Santa Cruz Biotechnology	sc-65191	Goat	1:200
Cleaved caspase 3	Cell Signalling	#9661	Rabbit	1:200
p-IKK s180	Santa Cruz Biotechnology	sc-23470	Rabbit	1:200
Alexa Fluor 488 donkey anti-rabbit (2ary)	Invitrogen	A21202	Donkey	1:1000
Alexa Fluor 488 donkey anti-mouse (2ary)	Invitrogen	A21206	Donkey	1:1000
Alexa Fluor 546 donkey anti-rabbit (2ary)	Invitrogen	A10040	Donkey	1:1000
Alexa Fluor 546 donkey anti-goat (2ary)	Invitrogen	A11056	Donkey	1:1000

Table MM3 | Antibodies used in cell/tumouroid immunofluorescence

MM10. Cell immunofluorescence

Immunofluorescence is a technique that uses the specificity of antibodies to their antigen to conjugate fluorescent dyes to specific target protein within a cell. This allows the visualization of the distribution of the target molecule through the sample. For performing immunostaining in cell lines, cells were previously seeded onto glass coverslips, so that they could be mounted on a slide in the last step.

Fixation:

- Aspirate the medium and wash in PBS
- Fix the cells with cold methanol (previously kept at -20ºC) [VWR, Ref. 1 06018 2500] during 5 min at -20ºC
- 3X wash in PBS 5min at RT

Permeabilisation and blocking

- Add 1,5ml permeabilisation buffer/well (0,3% triton X-100, 1% BSA in PBS) and incubate at least 1h at RT.

Primary antibody

- Without washing, add the primary antibodies diluted in permeabilisation and blocking buffer, 200µl/cover glass (See **Table MM3** for details)
- Incubate O/N at 4ºC
- 3X wash in PBS 5min at RT

Secondary antibody

- Add directly labelled secondary antibodies in 1% BSA in PBS, 200µl/cover glass. Incubate 2h at RT, protected from light
- 3X wash in PBS 5min at RT, protected from light

Nuclei counterstaining and mounting

- Mount in ProLong® Diamond with DAPI onto a slide
- Pictures were obtained with a TCS SP5 Upright Confocal Microscope, using the Leica Application Suite software and analysed using the Cell Profiler software[536] (www.cellprofiler.org)

MM11. RNA isolation

Starting material was 3D culture adenoma cells (see above). Total RNA was extracted using the RNeasy Micro Kit [Qiagen Ref. 74004], following manufacturer's instructions, eluting in 18µL of RNase-free H_2O. Then, samples were quantified with a NanoDrop spectrophotometer [Thermo Scientific].

MM12. RNA sequencing and analysis

RNA sequencing (RNA-seq), also called whole transcriptome shotgun sequencing (WTSS), uses next-generation sequencing (NGS) to reveal the presence and quantity of RNA in a biological sample at a given moment in

time. In molecular biology, RNA-seq is used to analyse changes in the cellular transcriptome, for example it allows us to study differences in gene expression.

Total RNA from three biological replicates per condition was extracted (see above) and RNA concentration and integrity were determined using Agilent Bioanalyser [Agilent Technologies, G2939BA]. Libraries were prepared and sequenced at the CRG Genomics unit (Barcelona) using standard protocols on an Illumina HiSeq2500 with a read length of 50bp.

The pipeline used for the RNA-seq was the following:

- **Quality check** was performed by the CRG Genomics Unit using the FastQC1 (www.bioinformatics.babraham.ac.uk/projects/fastqc) that provides an overview of the quality of the data. The presence of ribosomal RNA in each sample was also checked using estimation from riboPicker4[539].
- **Reads were aligned** with STAR[540] (Spliced Transcripts Alignment to a Reference) to release 87 of the Mus musculus ENSEMBL version of the genome (GRMm38/mm10 assembly) . (ftp://ftp.ensembl.org/pub/release-87/fasta/mus_musculus/)
- **Differential expression analysis** was performed with DESeq2[541] (version 1.10.1) which is an R/Bioconductor[542] (www.r-project.org) package developed for analysing differential gene expression of count data.
    - Removing low counts: genes for which sum of counts across all samples were less than 2 were discarded for differential expression analysis. After this filtering of low counts, we carry on the analysis on 22,024 genes.
    - Differential expression analysis: by default, DESeq2 uses a Wald statistical test to detect differentially expressed genes. The comparisons were performed using this test, and p-values obtained were corrected for multiple testing using the Bonferroni-Hochberg/False Discovery Rate method.
    - Unsupervised analysis: hierarchical clustering analysis based on Euclidean distances of logged normalized counts between samples, along with a Principal Component Analysis to see how well samples relate to one another.

To represent de data, heatmaps were generated using R studio (https://www.rstudio.com/) and GSEA, statistical analysis was performed

with publicly available software from the Broad Institute (http://www.broadinstitute.org/gsea/index.jsp).

MM13. qRT-PCR

Quantitative real time polymerase chain reaction (qRT-PCR) is a technique based on the PCR used to amplify and simultaneously quantify a targeted DNA fragment, which has been previously reverse-transcribed from RNA sample to complementary DNA (cDNA). It enables both detection and quantification (as an absolute number of copies or relative amount when normalized to DNA input or additional normalizing genes) of one or more specific sequences in a DNA sample.

After RNA extraction (see above), RNAs were retrotranscribed using the First Strand cDNA Synthesis Kit [GE Healthcare Life Sciences Ref. 27-9261-01], following manufacturer's instructions. The product of the cDNA reaction was usually diluted 1:20 and used for subsequent PCR analysis. qRT-PCR was performed in the LightCycler480 system, using a SYBR Green I Master Kit [Roche Ref. 04887352001]. The primers used are listed in the table below:

Target	Specie	Sense (5'-3')	Antisense (5'-3')
B-actin	Mouse	GTGGGCCGCCCTAGGCACCAG	CTCTTTGATGTCACGCACGATTTC
Ascl2	Mouse	AGCATGGAAGCACACCTTG	AAGTGGACGTTTGCACCTTC
Lrig1	Mouse	CCAAAAGCTGCATGAGTTGA	GCACCACTGGTATCCTCGAT
Cdca7	Mouse	TCTGAGAGCTCTGCAAACGA	CAGAGAACAAGCCAGGGAAG

Table MM4 | qRT-PCR primers.

MM14. Mass Spectrometry

Mass spectrometry (MS) is technique that allows us to distinguish chemical entities with different mass-to-charge ratio. It is used in proteomics for the characterization and sequencing of proteins. This permits the study of cellular processes involving proteins such as cell signalling processes, structure of protein complexes or post-translational modifications. Usually components are first separated by liquid chromatography (LC) following coupled MS (LC-MS/MS) to enhance detection.

Lysates

- Cells were collected using a cell scrapper in a buffer containing 6M urea [Amersham Bioscience, Ref. 17-1319-01] and 200mM ABC (Ammoniumbicarbonat) [Fluka, Ref. 09830] plus Complete protease inhibitor cocktail [Complete Mini, Roche Ref. 04 693 124 001] and Phosphatase inhibitor cocktail (PhosSTOP, Roche Ref. 04 906 845 001].

Sample digestion and phosphopeptide enrichment

- Add 10 mM solution of DTT [Sigma, Ref. D9163] and let the reaction proceed for 1 hour at 37 °C.
- Prepare 20 mM IAM (Iodoacetamide) [Sigma, Ref. I1149] by mixing 100 µL 100 mM IAM with 400 µL 200 mM ABC. Add the appropriate volume of 20 mM IAM to the sample and alkylate for 30 minutes at room temperature in the dark
- Dilute samples with 200 mM ABC to have samples at 2M Urea before adding the endoprotease LysC. Dissolve a vial of LysC (10UA) [Wako, Ref. 129-02541] in 1mL of TEAB 50mM [Sigma, T7408] to have a solution of 2.4 µg/µL of LysC.
- Add the required amount of endoprotease LysC in the sample to have a 1:10 ratio enzyme:protein (w:w). You can dilute the enzyme with the appropriate volume of 200 mM ABC.
- Digest overnight at 37°C at 650 rpm in the thermo-mixer.
- Dilute samples with 200 mM ABC to have samples at less than 1M Urea before adding sequence-grade trypsin [Promega, ref. V5111].
- Add the required amount of sequence-grade trypsin in the sample to have a 1:10 ratio enzyme:protein (w:w). You can dilute the enzyme with the appropriate volume of 200 mM ABC.
- Stop the reaction by adding formic acid (10 % of final total volume) [Merck, Ref. 1.00264.0100].
- Enrich sample in phopshopeptides using Titanium Dioxide (TiO_2) beads [Titansphere, 5 µM, GL sciences Inc.].
- Clean up the sample with Hypersep C18 columns [Thermo Ref. 60108-305]:
    - **Column conditioning:** Activate the selected columns with methanol 100%
    - **Column equilibration:** Equilibrate the selected columns with 5 % formic acid in water.

    - **Sample loading:** Acidified samples are slowly loaded twice into the selected columns.
    - **Column wash:** Wash the selected columns with 5 % formic acid in water.
    - **Sample elution:** Elute the sample from the selected columns with 5 % formic acid in a 1:1 solution acetonitrile:water (v/v).
    - Evaporate the solvent of the eluted sample to dryness using a speed-vac system
    - For mass spectrometric analysis redissolve the sample in 0.1 % formic acid in water
- Evaporate the solvent of the samples with a speedvac
- Dissolve the samples in 0.1 % formic acid in water to a final concentration of ~1 mg/ml
- Samples are now ready to inject

Sample Injection

- 45% of each sample was injected in an Orbitrap Velos Pro with a 60min gradient using a 2cm Trap-column and 122cm 3µm column. Each sample was injected twice with the acquisition methods: DDA_TOP20_CID and DDA_TOP20_MSA. To avoid carry over, BSA runs were added between the samples. BSA controls were included both in the digestion and LCMSMS analysis for quality control.

Data analysis

- The data has been searched using an internal version of the search algorithm Mascot (http://www.matrixscience.com/) against a SP_Human (UniProt April 2015) database. Peptides have been filtered based on Ion score, only those peptides with an ion score>20 have been kept.
- Protein network was done using cytoscape software (www.cytoscape.org)

MM15. Western blot

Western blot (WB) is a widely used technique used in molecular biology to detect specific proteins in a sample. The sample material undergoes protein denaturation, followed by gel electrophoresis that will separate proteins based on its molecular weight. These results are then transferred to a membrane where proteins will be detected by specific antibodies that will be

detected by a secondary antibody which will allow the visualization of the protein.

Cell lysates

- Aspirate media
- 2X wash with PBS
- Add the suitable volume (depending on the number of cells) of the lysis buffer (0.5% Triton X-100, 1mM EDTA, 100 mM Na-orthovanadate, 0.25 mM PMSF in PBS) plus protease and phosphatase inhibitor cocktail
- Collect cells using a cell scrapper
- Incubate the mixture 20 min. on ice
- Centrifuge 10 min at maximum speed (13000 rpm)
- Collect supernatant to obtain soluble proteins
- Perform Bradford Assay to quantify protein
- Add 6X SDS-PAGE sample buffer + β-mercaptoethanol (BME) [Sigma, Ref. M-3148] to the supernatant
- Add 1X SDS-page sample buffer to the pellet to obtain insoluble proteins and sonicate 10 min in a Bioruptor®, medium setting
- Boil all samples at 95 ºC, 10 min.

Western Blot

- Electrophoresis and gel transfer: separate the samples by polyacrylamide gel electrophoresis (SDS-PAGE) and transfer to a PVDF membrane [Millipore Ref. IPVH00010].
- Block the PVDF membrane with 5% non-fat milk in TBS-T buffer (50mM Tris-HCl pH 8.0, 150 mM NaCl, 0.05% Tween 20 [VWR, Ref. 8.22184], in H_2O) rocking 1h at RT.
- Incubate the membrane with the primary antibody in blocking solution (see **Table MM5**) rocking O/N at 4°C.
- 5x wash in TBS-T buffer rocking 5min at RT.
- Incubate the membrane with the secondary antibody (HRP-conjugated) in blocking solution (see **Table MM5**) rocking 1h at RT.
- 5x wash in TBS-T buffer rocking 5min at RT.
- Incubate the membrane with ECL solution [Biological Industries Ref. 20-500-120] or [GE Healthcare RPN2232], that contains a chemiluminescent HRP substrate.
- Develop the chemiluminescent signal in an autoradiography film [GE Healthcare Ref. 28906835].

Antibody	Company	Reference	Specie	Dilution
p-IKK s180	Santa Cruz Biotechnology	sc-23470	Rabbit	1:1000
IKKα	Merck Millipore	OP133	Mouse	1:1000
p-Chk1 S345	Cell Signaling	#2348	Rabbit	1:1000
Chk1	Cell Signaling	#2360	Mouse	1:1000
p-KAP1 S824	Bethyl Laboratories	A300-767A	Rabbit	1:1000
KAP1	Cell Signaling	#4123	Rabbit	1:1000
ɣH2A.X	Cell Signaling	#2577	Rabbit	1:200
p-ERK 1/2	Cell Signaling	#4370	Rabbit	1:1000
ERK 1/2	Cell Signaling	#4696	Mouse	1:1000
Histone H3	Abcam	ab1791	Rabbit	1:10000
Lamin B	Santa Cruz Biotechnology	sc-6216	Goat	1:500
α-Tubulin	Sigma	T6074	Mouse	1:10000
IKKβ	Abcam	ab32135	Mouse	1:1000
NEMO	Santa Cruz Biotechnology	sc-8338	Rabbit	1:1000
Cleaved caspase 3	Cell Signalling	#9661	Rabbit	1:1000
p-ATM S1981	Merck Millipore	05-740	Mouse	1:1000
p-53BP1 S1618	Cell Signalling	#6209	Rabbit	1:1000
53BP1	Abcam	ab21083	Rabbit	1:1000
Anti-Rabbit-HRP (2ary)	DAKO	P0448	Goat	1:2000
Anti-Mouse-HRP (2ary)	DAKO	P0260	Rabbit	1:2000
Anti-Goat-HRP (2ary)	DAKO	P0449	Rabbit	1:2000

Table MM5 | Antibodies used in the WB.

MM16. Cell fractionation

Cell fractionation is the process to separate cellular components while preserving individual functions of each element. In our case, we use a protocol to separate proteins found in the cytoplasm, nucleus and chromatin/DNA. Once we obtain each fraction, proteins can be loaded in a gel following the WB protocol described above.

When processing up to $2 \cdot 10^6$ cells, use **bold** values.

- Prepare 1 ml of buffer A (10mM HEPES [Sigma, Ref. H-3375], 1.5mM MgCl2, 10mM KCl, 0.5mM DTT, 0.05% NP40) pH 7.9 per sample, adding the cocktail of usual protease inhibitors, keep on ice

- Add **300** / 600 µl of buffer A per large petri dish on ice and scrape thoroughly, leave on ice for 10 min
- Centrifuge at 4ºC at 3000 rpm for 10 min
- Remove supernatant and keep it (this will contain everything except large plasma membrane pieces, DNA and nucleoli), extract out 10 µl for Bradford assay
- Resuspend the pellet in **600** / 1200 µl of Buffer A (two times the amount you used at the beginning) for washing and centrifuge again at 4ºC at 3000 rpm for 10 min.
- On ice resuspend pellet in **150** / 300 µl of Buffer B and add 9.5 / 19 µl of 5M NaCl to give 300 mM NaCl (high salt helps lyse membranes and forces DNA into solution)
- Sonicate for 10 minutes on the Bioruptor, Medium setting (ensure at least 3/4th of the tubes are inside water bath)
- Leave on ice for 30 min
- Centrifuge at maximum speed (13000 rpm) for 20 min at 4ºC.
- The supernatant is the nuclei fraction
- Optional: If you want to obtain the chromatin fraction you can resuspend the remaining pellet in **150** / 300 µl of 1X Protein Buffer and sonicate it for 5' / 10' with the Bioruptor. Then you boil it 95 ºC, 10 minutes.

MM17. Viral production and shRNAs cell infection

Lentivirus production

Virus were produced by transient transfection of viral particles into HEK293T cells. Transfection is the process of introducing nucleic acids into cells. For this, we used PEI [Polyethylenimine, Linear, MW 25.000, Polysciences Inc. Ref. 23996]. PEI is a high-charge cationic polymer that readily binds highly anionic substrates, such as DNA and other negatively charged molecules. It works as a carrier vector.

- Transfection
    - Seed $2 \cdot 10^6$ HEK293T in a 100mm plate per condition the day before
    - Dilute 4µL PEI per µg of DNA into 1/10 of the final volume in serum-free DMEM (for example in 1mll in a 100mm plate)
    - Mix gently and incubate 5 min at RT

- Add 10µg of shRNA plasmid, 3µ of envelope plasmid (pMD2.G) and 7,5µg of packaging plasmid (dR8.2 dvpr), mix and incubate 20min at RT (see **Table MM6** for details)
- Add the solution to the culture plate or well
- Change medium after 24h. Remove medium with precipitates and add 6ml/plate of fresh medium

- Collection: Collect the media-containing virus 48h and 72h after transfection and filter the supernatant using a 0,45µm pore filter to remove any remaining cellular debris. At this point the supernatant can be stored at -80ºC for future use or used directly fresh to cells.

Cell infection and selection

- Plate the target cells in a 6-well plate, 24h prior to viral infection
- Remove media and replace with the virus-containing media plus 8µg/ml Polybrene
- After 24h remove medium and add fresh medium
- After 24h, cells were selected with puromycin for 72h. Puromycin concentration depends on the cell type, usually used between 1-2µg/ml
- Infected cells were then maintained in lower levels of puromycin (half of the concentration used for selection) until seeding for experimental purposes

Vector	Detailed name	Description	Reference
shIKKα 1	MISSION shRNA, TRCN0000000508 (human)	shRNA against the CDS of the human CHUK gene	Sigma
shIKKα 4	MISSION shRNA, TRCN0000199496 (human)	shRNA against the CDS of the human CHUK gene	Sigma
shControl	TRC2 pLKO.5-puro Non-mammalian shRNA Control Plasmid (SHC202)	Negative control containing a sequence that should not target any known human gene, but will engage RISC.	Sigma
shIKKβ	MISSION shRNA, TRCN00001897 (human)	shRNA against the CDS of the human IKBKB gene	Sigma
shNEMO	MISSION shRNA, TRCN000022146 (human)	shRNA against the CDS of the human IKBKG gene	Sigma
pMD2.G	pMD2.G plasmid #12259	Envelope expressing plasmid	Addgene
dR8.2 dvpr	pCMV-dR8.2 dvpr plasmid #8455 (human)	2nd generation lentiviral packaging plasmid	Addgene

Table MM6 | Vectors used for virus production.

MM18. Adenoviral infection

Deletion of floxed alleles in *Trf2*$^{FL/FL}$ cells was carried out with either Ad-GFP or Ad-GFP-Cre adenovirus (Vector Biolabs, ref. 1060 and 1700). Protein levels of TRF2 were checked by WB.

Before starting make sure to have a stock of cells at 70% confluence, more confluent cells will generate more aggregates and this can decrease infection efficiency

- Trypsinise cells and count them using a Neubauer chamber
- Separate $1{,}2 \cdot 10^6$ cells in a new eppendorf and centrifuge at 1200 rpm 5min
- Resuspend the pellet in 500µl OPTIMEM containing 2%FBS, polybrene 8µg/ml, and 150 MOI adenoviral particles
- Keep the cells in the incubator for 2h, mixing every 20min.
- Seed the cells in a 100mm plate
- Split cells the next day after infection, and use them for experiments 96h after infection to have full *Trf2* depletion and fused chromosomes

MM19. Peptide Nucleic Acid Fluorescence In Situ Hybridisation

Fluorescence in situ hybridization (FISH) is a molecular cytogenetic technique that uses fluorescent probes that bind only to sequences of the DNA with a high degree of complementarity. It is used in biomedical research to detect and localise specific DNA sequences within chromosomes. Peptide Nucleic Acid FISH (PNA-FISH) uses peptide nucleic acid probes which bind strongly to DNA, which we used to detect telomeric sequences.

<u>Methanol/acetic acid fixed metaphase spreads</u>

- Split cells 24 hours before harvest to be ~50% confluent at time of harvest.
- Incubate 3 hours in regular medium with 0.2 µg/ml of colcemid to arrest cells in metaphase. The effects of the colcemid [Roche, Ref. 10295892001] should be obvious at time of harvest (rounded, retractile cells with blebby membranes).
- Harvest cells by trypsinisation. Be gentle during harvesting, many of the dividing cells tend to lift off. Collect the wash supernatant to recapture cells that have floated off during the harvest. Neutralize

trypsin using the conditioned media to recover any floating mitotic cells found in the media. Spin everything down at 1200 rpm 5 minutes.

- Remove supernatant completely and resuspend in 5 ml of 0.075 M KCl (pre-warmed to 37ºC), be gentle to prevent lysis, this step swells the cells. Incubate for 15 minutes at 37ºC, invert tubes every 5-10 min to keep cells suspended.
- Spin the cells down, 5 min at 1200 rpm
- Decant the KCl, resuspend cells fully in the small volume of KCl that was left (by tapping).
- Drop by drop add 1 ml of cold fixative solution (3:1 Methanol and glacial acetic acid [Merck, Ref. 100063] prepared fresh) while the cells are slowly and gently mixed on a vortex.
- Add 9 ml more of fixative solution and store at 4ºC O/N or longer; cells can be kept at this stage indefinitely.
- When ready to drop, spin the cells down, 5 min at 1200 rpm
- Decant the fixative solution leaving a small volume of fixative solution left
- Immerse the glass slide in ice cold glacial acetic acid 45% and proceed immediately. Resuspend cells with the small volume of fixative solution and drop the resuspended cells from a couple of inches above the end of the wet slide tilted at a 45° angle.
- Place slides after dropping metaphases for 10 min on a humidified 37ºC chamber.
- Let the slides dry O/N, protected from light
- Check the slides under a regular light microscope for spreading efficiency. You should see many nuclei (all of the cytoplasmic membranes should be washed away or barely visible.) Well spread metaphase chromosomes should look like small black dots at low magnification. The arms of the chromosomes should be visible at higher magnifications. If the nuclei are too crowded or too sparse, you may need to dilute or concentrate your sample and drop the slide again.

<u>FISH</u>

- Rehydrate MetOH/Acetic acid spreads in PBS 5 minutes
- Perform the following optional steps:
    - Fix in 4% formaldehyde in PBS for 2 min (dilute from 37% commercial formaldehyde)
    - 3X wash in PBS 5 minutes each.

    - Treat with pepsin [Sigma, Ref. P6887] (1 mg/ml) @37ºC, 10 min. Pepsin prepared fresh in 10 mM glycine pH 2 and warmed up to 37ºC.
    - 2X wash in PBS 2 min each
    - Fix in 4% formaldehyde in PBS, 2 min.
- 3X wash in PBS 5 min each
- Dehydrate in ethanol series: 5 min in 70%, 95%, 100% at RT and air dry slides 20 min
- Place 100 µl of hybridization mix (10mM Tris-HCl pH 7,2, 70% formamide (deionised stock) [Sigma, Ref. 9037], 0,5% blocking reagent) containing the telomeric probe (see **Table MM7**) onto coverslips
- Denature on an 70ºC hot plate, 3 min.
- Hybridize O/N at 4°C
- Take off coverslip, wash slides in hybridization wash #1 (10mM Tris-HCl pH 7,2, 70% formamide [Sigma, Ref. 47671], 0,1% BSA that must be dissolved before adding formamide) 2X for 15 min, shaking
- Wash slides in hybridization wash #2 (0,1 M Tris-HCl pH 7,2, 0,15 M NaCl, 0,08% Tween-20) 3X for 5 min on shaker.
- Dehydrate in ethanol series: 5 min in 70%, 95%, 100% ethanol at RT and air-dry slides.
- Mount using ProLong Diamond with DAPI and store at -20°C protected from light.
- Chromosome images and telomere signals were captured using Zeiss Axio Imager M1 microscope equipped with an ORCA-ER camera (Hamamatsu) controlled by Volocity 4.3.2 software (Improvision).
- Following acquisition, images were imported into ImageJ (NIH) and Adobe Photoshop CS5 for manual quantitation

Probe	Sequence	Reference	Company	Dilution
TelG-Cy3	5'-(TTAGGG)3-3'	F1006	Bio-synthesis	1:10000

Table MM7 | Vectors used for virus production

MM20. IF-FISH

FISH probes can also we used to co-stain with antibodies, to visualise simultaneously DNA and proteins.

After finishing the Immunofluorescence protocol (see above), samples can be further processed to do FISH:

IF-FISH

- 3X wash in PBS 5 min each
- Fix the cells on the coverslips in 4% formaldehyde in PBS for 5 min (dilute from 37% commercial formaldehyde)
- 2X wash in PBS 5 min each
- Dehydrate in ethanol series: 5 min in 70%, 95%, 100% at RT and air dry slides 20 min (protected from light)
- Place 100 µl of hybridization mix containing the telomeric probe (see **Table MM7**) onto coverslips
- Denature with hybridisation mix at 70ºC by placing the slides on a heat block, 3 min
- Hybridise O/N at 4°C
- 2X wash in washing solution #1 15 min each
- 3X wash in PBS 5 min each
- Air dry at RT (protected from light) for 10 min
- Mount using ProLong Diamond with DAPI and store at -20°C protected from light.
- Chromosome images and fluorescent staining were captured using Zeiss Axio Imager M1 microscope equipped with an ORCA-ER camera (Hamamatsu) controlled by Volocity 4.3.2 software (Improvision).
- Following acquisition, images were quantified using cell profiler software

MM21. Laser microirradiation induced DNA damage

Laser microirradiation can be combined with IF analysis to study recruitment of endogenous proteins to laser-induced DNA damage tracks. Laser stripes can be visualised by positive controls like 53BP1, that mark sites of DNA breaks. In order to detect local recruitment of active IKKα to laser induced DNA damage, cells were processed as follows:

- HT29 cells were seeded on 35 mm glass bottom dish (Ibidi, 81158) and pre-sensitised for 48h with 10 µM BrdU.
- Cells were transferred to Olympus FV1000 confocal LSM with heated stage. Laser microirradition was performed in a stripe shape with a 405 nm laser focused through 40x objective (400mW at objective, 50 scans).
- 1 hour after DNA damage induction, cells were fixated and processed for IF (see above for protocol details)

MM22. Analysis of cellular DNA content by flow cytometry

Flow cytometry is an analytical cell-biology technique that utilizes light to count and profile cells in a heterogeneous suspension. It is a very potent technique that offers a "high-throughput" (for a large number of cells) automated quantification of fluorescent signals from individual cells.

Fixing cells:

- Trypsinise cells and 2X wash in PBS. Collect conditioned media if quantification of dead cells is required
- Resuspend $1 \cdot 10^6$ cells in 300 µl PBS
- Add 700 µl ice-cold (or -20°C) absolute Ethanol slowly while mixing by vortex. (Vortex during ethanol addition is crucial to avoid aggregates. The aggregates will be stable in the fixation). Samples can be stored in ethanol several weeks at 4°C
- Maintain ethanol fixation at least 2 hours on ice.

Propidium Iodide staining:

- Pellet cells at 5000 rpm (or high) in an eppendorf centrifuge.
- Manually aspirate supernatant up to pellet level. The high pellet spreading indicates pellet fragility and must handle with care, otherwise you will lose the cells
- Pellet twice with PBS
- Resuspend pellet with working solution (940 µl of PBS, 30 µl Solution A, 30 µl Solution B. Prepare this solution daily prior to use) and incubate 30 minutes at RT or preferable at 4°C overnight. The 4°C overnight incubation can be maintained for 48h or longer. You must check your cells for degradation
    - Solution A: Sodium citrate (38 mM), Propidium iodide (500 µg/ml in water) [Sigma, Ref. P4170]. Water solution stable 1 year at 4°C.
    - Solution B: RNase A [Qiagen, Ref. 50919501] 10 mg/ml in PBS. PBS solution stable at -20°C.

Analyse by flow cytometry

- Samples were analysed in a LSRFortessa analyser [BD Biosciences]

RESULTS: PART I

Ikkα deletion in the intestinal epithelium reduces tumour formation and proliferation

Since IKKα is not required for general NF-κB function, and previous studies suggested a crucial role in intestinal tumorigenesis, we now studied the specific contribution of intestinal epithelial IKKα to neoplastic transformation. We used a mice line carrying Cre recombinase under the control of *Villin* promoter (Villin-Cre). Since *Villin* is specifically expressed in the epithelial cells of the small and large intestine[543], crossing this line with the one containing loxP site-flanked *Ikkα*[535] resulted in tissue-specific deletion of the kinase. We then crossed intestinal-specific *Ikkα*$^{-/-}$ (*Ikkα* KO) mice with *Apc*$^{Min/+}$ mice to induce intestinal cell transformation in an *Ikkα*-deficient background [**FIGURE R1**].

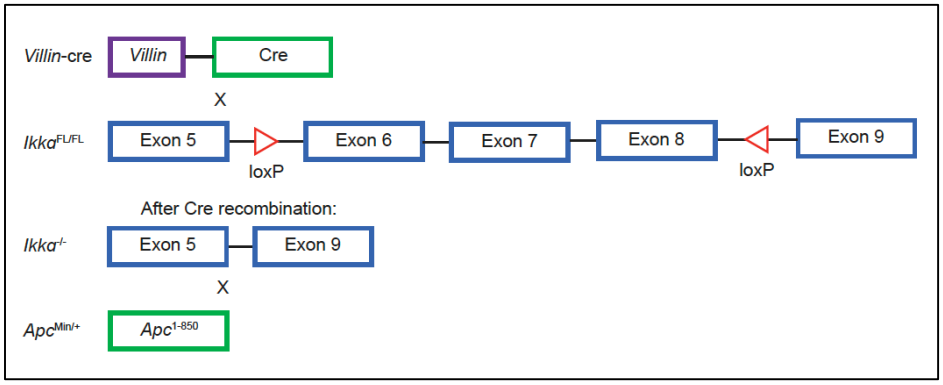

Figure R1 | Schematic representation of the strategy used to generate the compound mice used in our study. In brief, IKKα^{FL} mice were crossed with *Villin*-Cre (*Villin*-cre/*Ikkα*$^{FL/FL}$) and then with *Apc*$^{Min/+}$ mice. All mice were genotyped by PCR and animals were kept under pathogen-free conditions and manipulated according to the guidelines from Generalitat de Catalunya.

All different genotypes were born at the expected Mendelian ratios and showed no evident growth defects during the first 3 months of age, indicating that intestinal epithelial *Ikkα* was dispensable for tissue homeostasis (data not shown). Further analysis of 3-month-old animals carrying the $Apc^{Min/+}$ allele demonstrated that *Ikkα* deficiency cause a significant decrease in the number of tumours arising in the small intestine when compared with the $Ikk\alpha^{+/+}$ (IKKα WT) littermates or mice carrying one copy of the *Ikkα* gene ($IKK\alpha^{+/-}$, IKKα HET) [**FIGURE R2**].

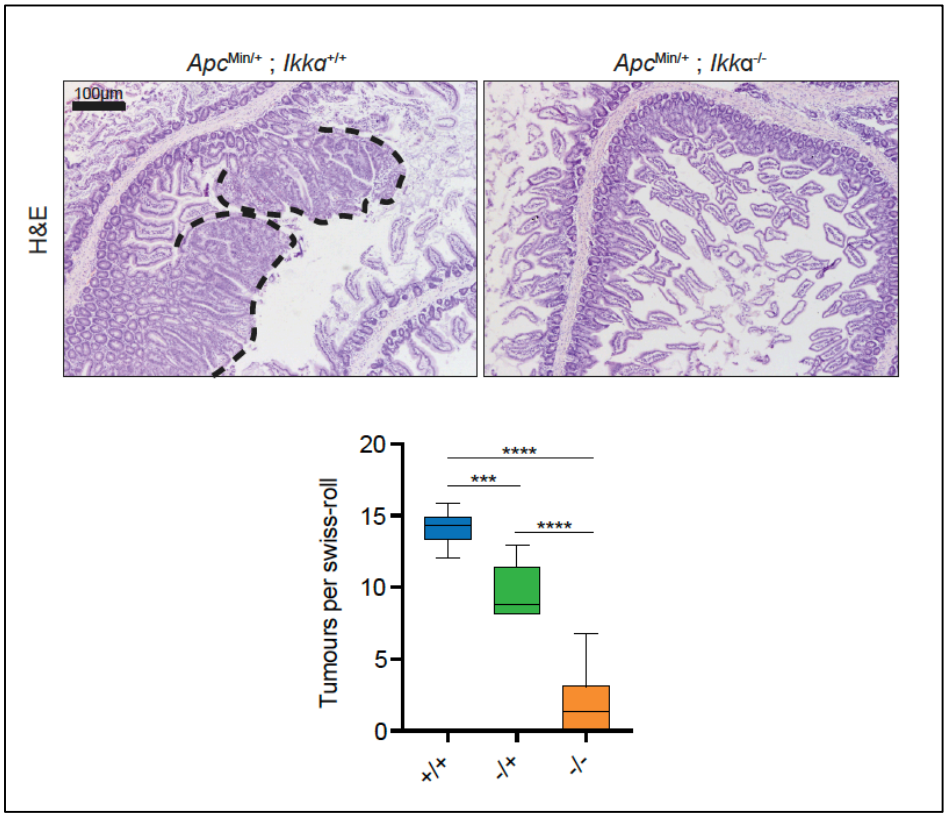

Figure R2 | *Ikkα* deficiency reduces tumour formation in the intestine of $Apc^{Min/+}$ mice. Representative images of H&E staining in $Apc^{Min/+}$;$Ikk\alpha^{+/+}$ and $Apc^{Min/+}$;$Ikk\alpha^{-/-}$ intestinal swiss rolls. Dashed lines delimited 2 different tumours present in the $Apc^{Min/+}$;$IKK\alpha^{+/+}$ image. Quantification of the tumour number is shown in the bottom panel (+/+:*Ikkα* WT, -/+: *Ikkα* HET, -/-: *Ikkα* KO). Graphs represent the average number of tumours per swiss roll from animals of each genotype. For statistical analysis, ordinary one-way ANOVA was used and the p-values are indicated as ***p<0.001, ****p<0.0001. Scale bar equals 50 µm.

Next, we studied the possibility that reduced proliferation of transformed cells might contribute to the observed phenotype. By immunohistochemical (IHC) analysis, we found that IKKα WT adenomas showed a significantly higher percentage of proliferating Ki67 positive cells when compared to the IKKα KO adenomas [**FIGURE R3**].

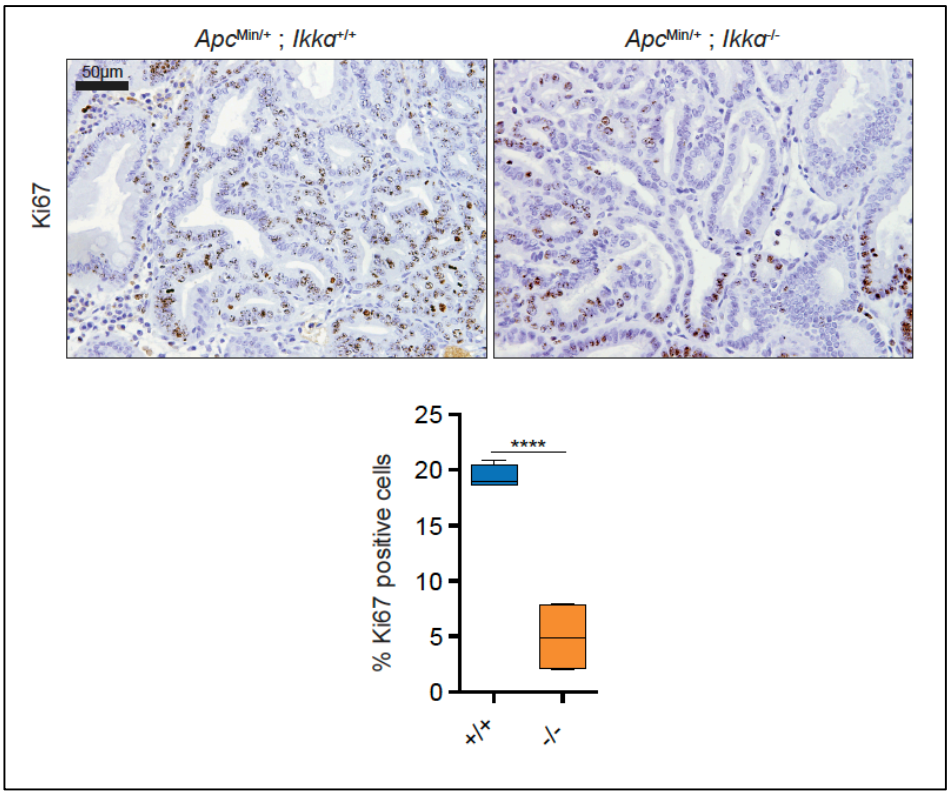

Figure R3 | *Ikkα*-deficient adenomas show decreased proliferation. Representative images of Ki67 IHC in $Apc^{Min/+}$, $Ikk\alpha^{+/+}$ and $Ikk\alpha^{-/-}$ adenomas. Quantification of Ki67 positive cells is shown in the bottom panel (+/+: *Ikkα* WT, -/-: *Ikkα* KO). Graphs represent the average number of tumours per swiss roll from animals of each genotype. For statistical analysis, unpaired t-test was used and the p-values are indicated as ****p<0.0001. Scale bar equals 50 μm.

In contrast, we consistently failed to detect any histological difference or changes in the number of Ki67 positive cells in the non-transformed intestinal mucosa of IKKα WT, HET or KO animals [**FIGURE R4**].

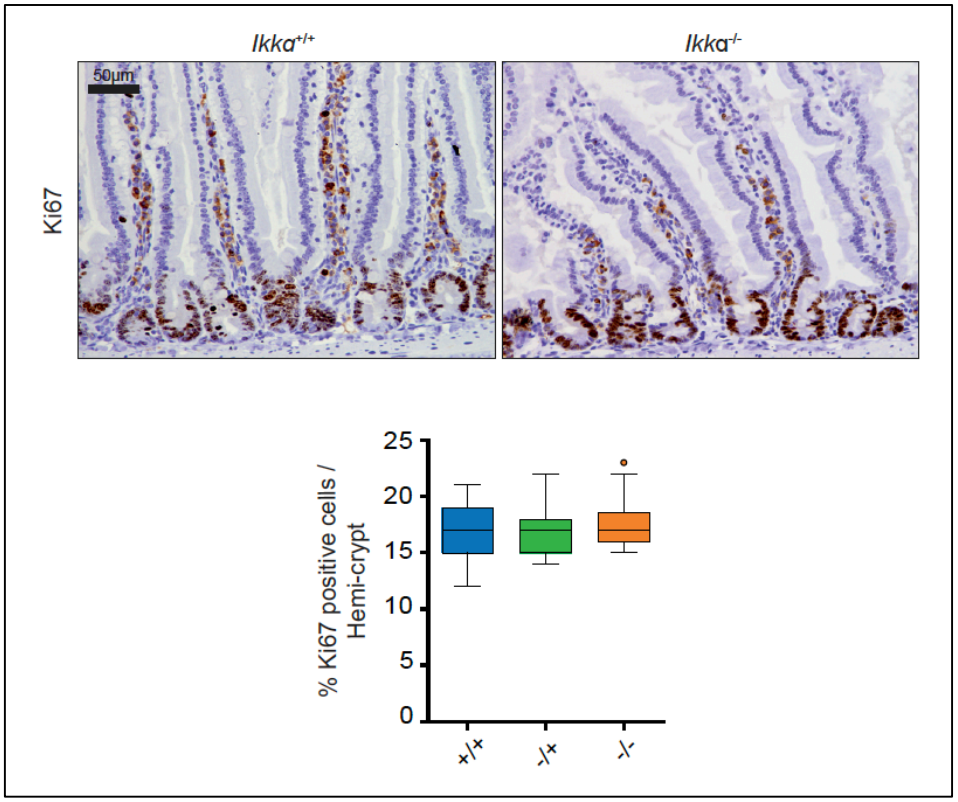

Figure R4 | *Ikkα* deficiency does not affect normal intestinal tissue homeostasis. Representative images of Ki67 IHC in *Ikkα*$^{+/+}$ and *Ikkα*$^{-/-}$ intestines. Quantification of the proliferating intestinal stem cell compartment per hemi-crypts is shown in the bottom panel (+/+:*Ikkα* WT, -/+: *Ikkα* HET, -/-: *Ikkα* KO). Graphs represent the average number of tumours per swiss roll from animals of each genotype. For statistical analysis, ordinary one-way ANOVA was used. Scale bar equals 50 µm.

To explore the possibility that decreased tumour number in the *Apc*$^{Min/+}$ IKKα KO mice was associated to increased apoptosis of the transformed cells, we checked the levels of cleaved caspase 3 in WT and IKKα KO *Apc*$^{Min/+}$ intestines. By IHC analysis, we observed very few cleaved caspase 3 positive areas within the tumours of both IKKα genotypes [**FIGURE R5**]. As positive control, we used irradiated intestines, which were consistently positive for cleaved caspase 3 (data not shown).

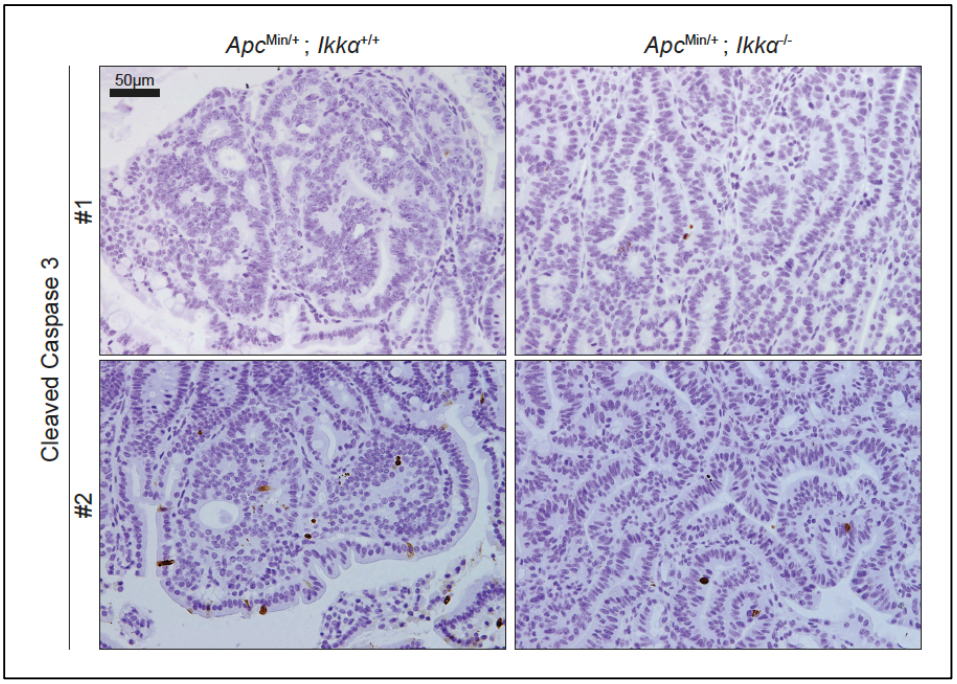

Figure R5 | *Ikkα* WT and KO adenomas do not show differences in apoptosis. Representative images of cleaved caspase 3 (ccas3) IHC in *Apc*$^{Min/+}$, *Ikkα*$^{+/+}$ and *Ikkα*$^{-/-}$ adenomas. Scale bar equals 50 µm.

Because active β-catenin plays a pivotal role in *Apc*-mutant tumour initiation and maintenance[544] and it was previously identified as a target of IKKα[279], we aimed to determine whether nuclear β-catenin levels were reduced in the IKKα KO background. By IHC analysis we found that IKKα KO tumours contain a significant decrease in the levels of nuclear β-catenin as compared with the IKKα controls [**FIGURE R6**].

These results indicate that **intestinal epithelial IKKα is essential for tumour initiation** and regulation of **tumour cell proliferation**, likely through regulation of β-catenin signalling, but it is dispensable for maintaining normal homeostasis and proliferation of the intestine, a situation that is clinically exploitable. Whether differences on β-catenin activation were due to direct phosphorylation by IKKα need to be further investigated.

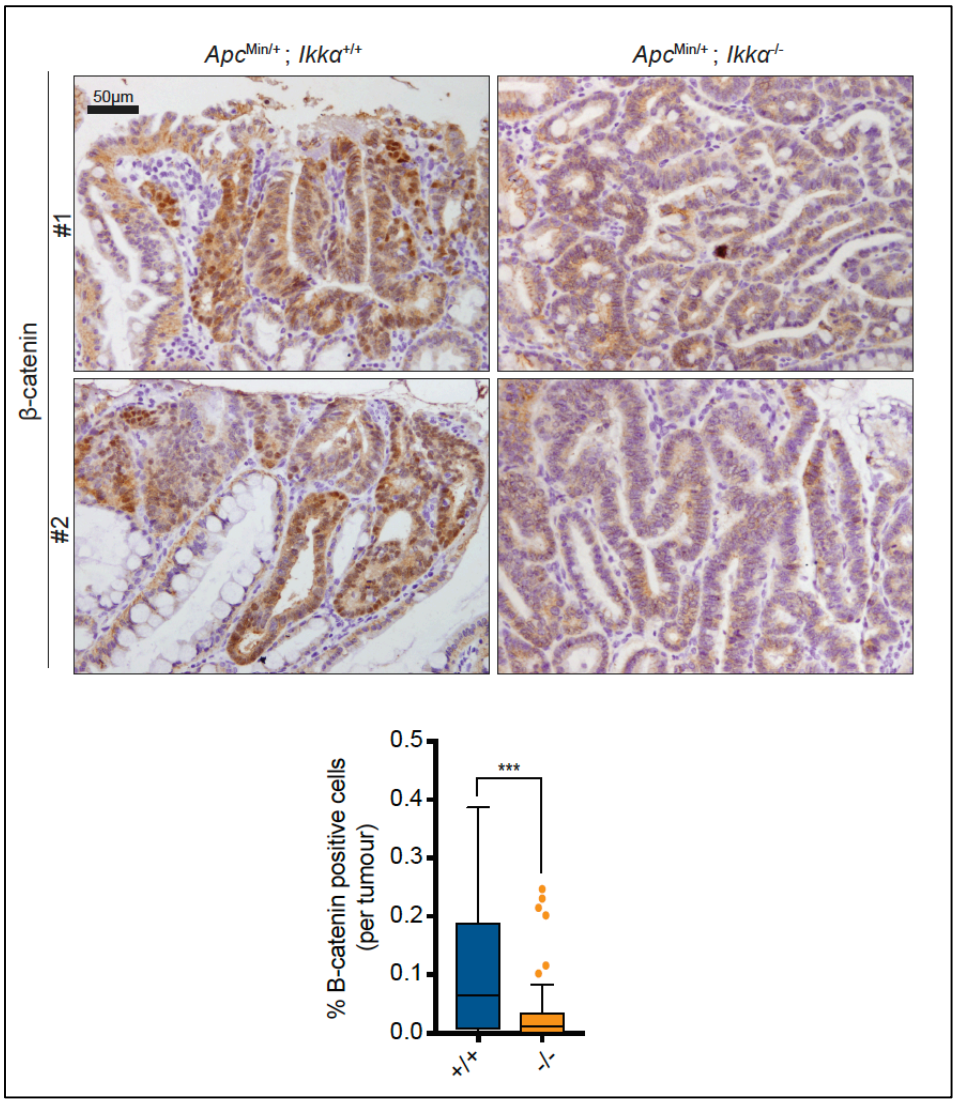

Figure R6 | *Ikkα*-deficient adenomas show decreased nuclear β-catenin. Representative images of β-catenin IHC in *Apc*$^{Min/+}$; *Ikkα*$^{+/+}$ and *Ikkα*$^{-/-}$ adenomas. Quantification of β-catenin positive nuclei per tumour is shown in the bottom panel (+/+:*Ikkα* WT, -/-: *Ikkα* KO). Graphs represent the average number of positive nuclei per tumour (n=40) from two different animals of each genotype. For statistical analysis, unpaired t-test was used and the p-values are indicated as ***p<0.001 and ****p<0.0001. Scale bar equals 50 µm.

Ikkα$^{-/-}$ tumouroids show a decrease in size and proliferation

The in vivo experiments described above provide strong evidence of the role of *Ikkα* in tumour formation in the *Apc*$^{Min/+}$ mouse model. To further investigate the contribution of *Ikkα* requirement in a pure intestinal epithelial tumour model, we used the *ex vivo* 3D culture system, in which single primary intestinal cells with tumour initiating capability generate spheroidal structures[101,103]. We will here refer to these tumour-spheroids as tumouroids. Consistent with our in vivo data, *Ikkα*$^{-/-}$;*Apc*$^{Min/+}$ adenoma cells generated tumouroids that were significantly smaller in size than IKKα WT counterparts [**FIGURE R7**]. This growth-deficient phenotype was much more pronounced in the initial cultures and attenuated after serial passaging of the tumouroid cultures. The significance of this result was confirmed by a careful quantification of sphere diameter [**FIGURE R7**].

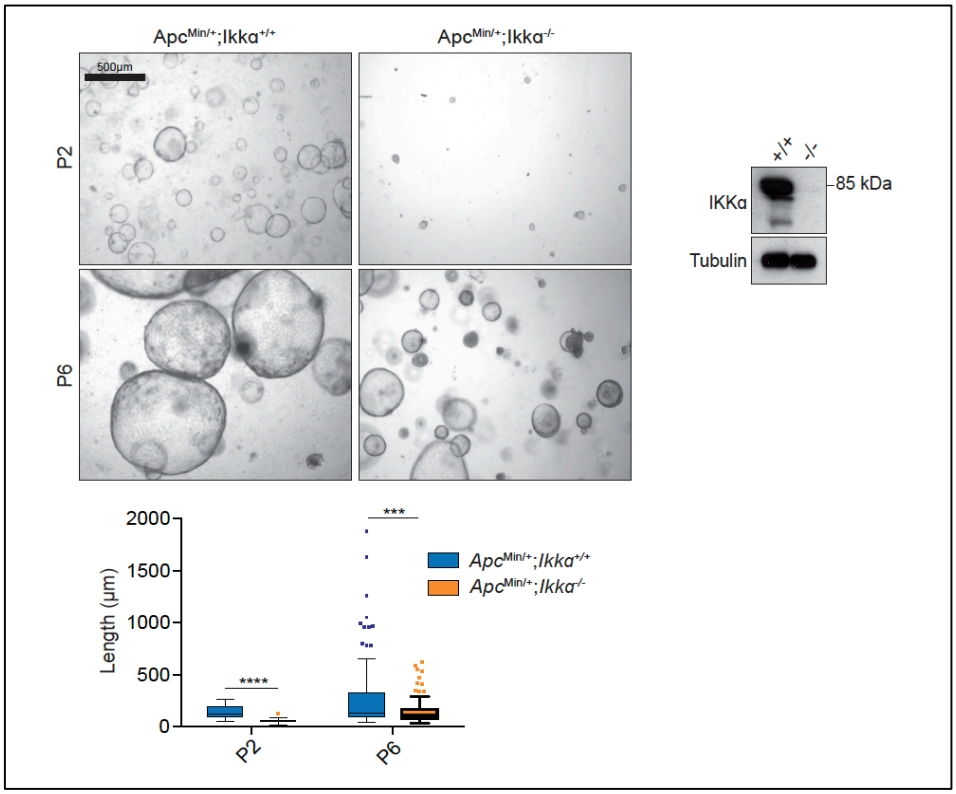

Figure R7 | *Ikkα*-deficient tumouroids are smaller than WT tumouroids. Representative images from tumouroid cultures and WB analysis to demonstrate the efficiency of IKKα deletion. P=passage. For statistical analysis, unpaired t-test was used and the p-values are indicated as ***p<0.001. Scale bar equals 500 µm.

Similar to that observed in the normal intestine, 3D organoid cultures, which were derived from non-transformed intestinal epithelial stem cells, showed no differences in their growing capacity when comparing *Ikkα*$^{+/+}$ and *Ikkα*$^{-/-}$ genotypes [**FIGURE R8**].

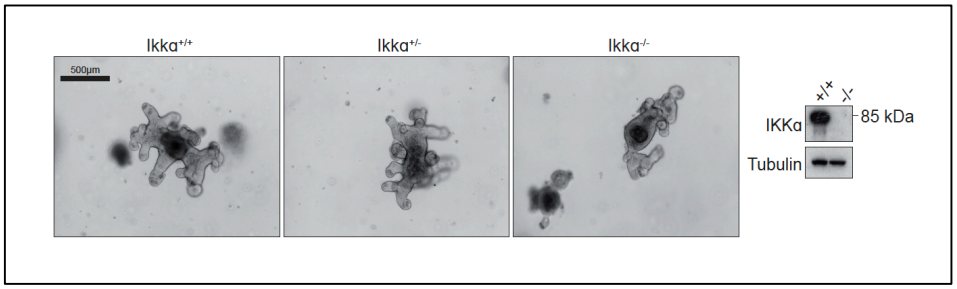

Figure R8 | *Ikkα* deletion does not affect growth of normal intestinal organoids. Representative images of organoid cultures of the indicated genotypes and WB analysis from the organoid cultures to demonstrate the efficiency of IKKα deletion. Scale bar equals 500 µm.

Immunofluorescence analysis of Ki67 expression demonstrated that *Ikkα*$^{-/-}$ tumouroids were almost depleted from proliferating cells compared with the *Ikkα*$^{+/+}$ structures [**FIGURE R9**].

These results identify epithelial ***Ikkα*** **as an important contributor to intestinal tumour initiation activity** ***ex vivo***.

.

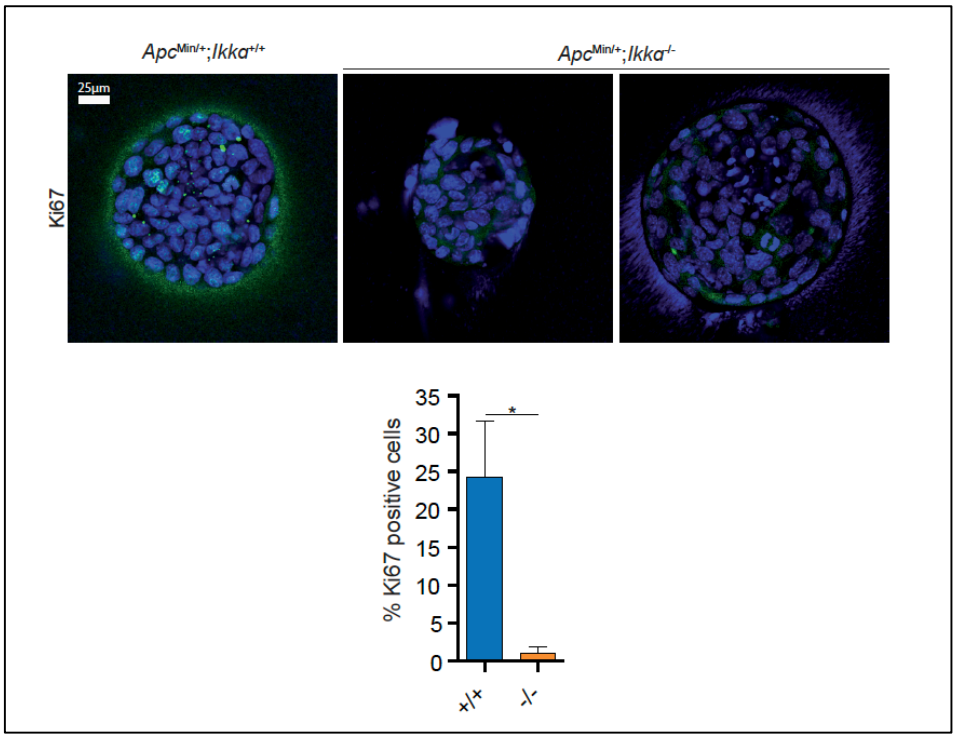

Figure R9 | *Ikkα* deficient tumouroids show decreased proliferation. Representative images of Ki67 staining in the *Apc*$^{Min/+}$;*Ikkα*$^{+/+}$ and *Apc*$^{Min/+}$;*Ikkα*$^{-/-}$ tumouroids from passage 6 (P6) grown in Matrigel®. Quantification of the percentage of Ki67 positive cells from 3 independent experiments, is shown in the bottom panel. Graph shows the average percentage and standard deviation of the mean. Magnification of images is indicated. For statistical analysis, unpaired t-test was used. P values are indicated as *p<0.05. Scale bar equals 25 μm.

IKKα governs tumouroid growth by regulating stem cell genes, and apoptosis and cell cycle related gene programs

We aimed to investigate the mechanisms underlying epithelial IKKα function in transformed cells by defining the transcriptional programs that depend on *IKKα* in the Apc$^{Min/+}$ tumouroids. We performed RNA-seq from *Apc*$^{Min/+}$ *Ikkα* WT (+/+) or *Ikkα* KO (-/-) tumouroid cells. Unsupervised cluster analysis demonstrated a clear co-segregation of WT and KO RNA samples **[FIGURE R10]**.

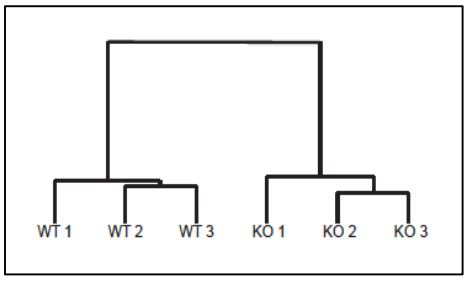

Figure R10 | Unsupervised hierarchical clustering. Analysis based on Euclidean distances of logged normalized counts between samples from 3 independent samples per genotype analysed.

Importantly, the transcriptional profile of *Ikkα* KO tumouroids showed a significant decrease in the levels of a previously defined intestinal stem cell (ISC) signature[545] [**FIGURE R12**], including genes essential for maintaining ISC function such as *Notch1*[546,547], *Cdca7*[548], *Lgr5*[549], *Ephb2*[119,550], *Ascl2*[551] or *Lrig1*[552], among others. We further confirmed these results by qRT-PCR of several of these genes in a different set of tumouroids from both genotypes [**FIGURE R11**].

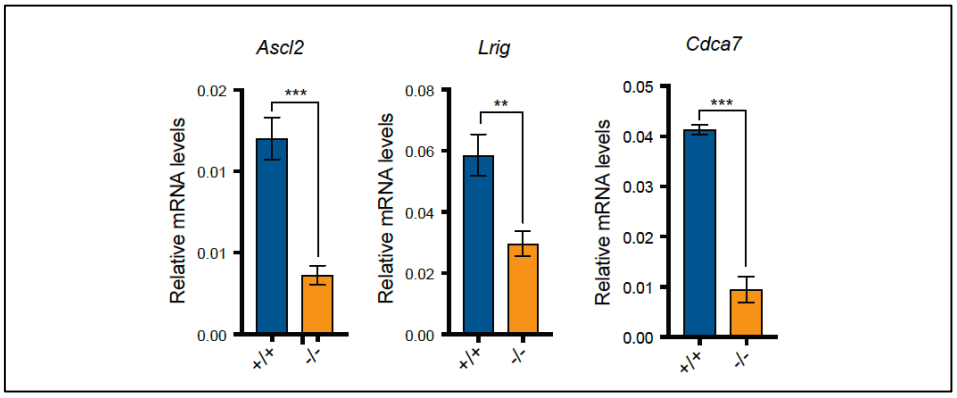

Figure R12 | *Ikkα*-deficient tumouroids show decreased expression of intestinal stem cell markers. qRT-PCRs show expression levels of *Ascl2*, *Lrig* and *Cdca7* in tumouroids from indicated genotypes (+/+:*Ikkα* WT, -/-: *Ikkα* KO), relative to β*actin*. For statistical analysis, unpaired t-test was used. P values are indicated as ***p*<0.01 and ****p*<0.001.

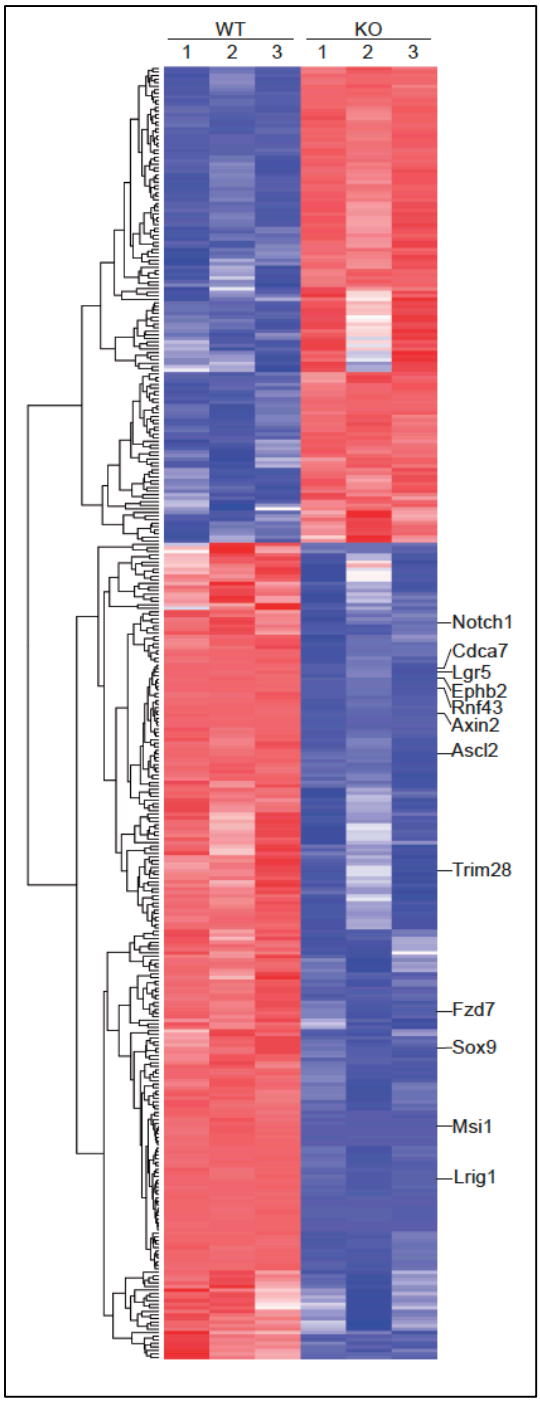

Figure R11 | *Ikka* KO tumouroids have decreased expression of genes involved in stem cell maintenance and function. RNA-seq heatmap showing differential expression of genes involved in intestinal stemness with scaled (*z*-score) columns. RNA-seq data is accessible at NCBI GEO database[580], accession GSE101415,

Gene Set Enrichment Analysis (GSEA), identified several pathways that were miss-regulated in IKKα deficient adenoma cells compared with IKKα WT. This apply to the apoptosis pathway that was significantly enriched in the absence of IKKα, including genes such as RIPK1, TRADD, FASLG, FAS and CASP8 among others. In contrast, IKKα-deficient adenomas showed a decrease in cell cycle related genes [**FIGURE R13**]. IKKα deficiency also leads to a decrease in the pro-tumorigenic MYC signature, whereas it did not correlate with a general reduction in canonical NF-κB signature, further suggesting that IKKα function in intestinal adenoma stem cells is mainly NF-κB independent [**FIGURE R14**].

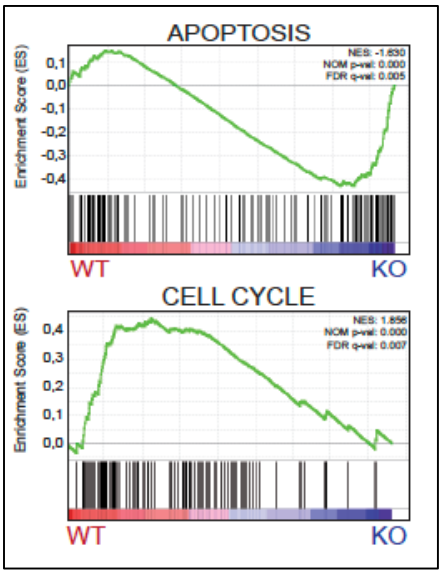

Figure R13 | GSEA plot. Differentially expressed genes from apoptotic- and cell cycle-related gene sets in *Ikkα* WT and KO tumouroids. NES: normalized enrichment score; NOM p-val: Normalized p-value; FDR q-val: false discovery rate q-value.

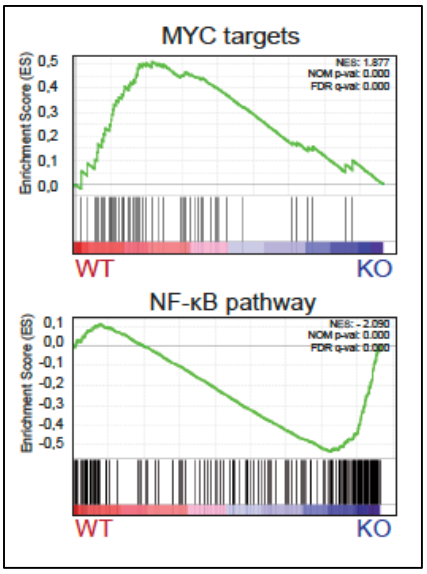

Figure R14 | GSEA plot. Differentially expressed genes from MYC- and NF- κB –related gene sets in *Ikkα* WT and KO tumouroids. NES: normalized enrichment score; NOM p-val: Normalized p-value; FDR q-val: false discovery rate q-value.

These results indicate that epithelial IKKα controls **transcription of stem cell signature** and are in agreement with our previous data indicating that IKKα regulates **cell survival and proliferation** in human CRC cells[234,285,553].

RESULTS: PART II

p45-IKKα is activated and translocated to the nucleus upon DNA damage

Previous work from our laboratory demonstrated that nuclear phosphorylated p45-IKKα is associated with advanced disease in human CRC. However, the role of p45-IKKα in tumour development and survival remains unexplored. To directly investigate the functional link between IKKα and tumour progression in CRC, we first focused on the identification of phosphorylation substrates of this kinase using an unbiased Liquid Chromatography-Tandem Mass spectrometry (LC-MS/MS) approach. We used the HT29 cell line that derives from human CRC which harbours the activating $BRAF^{V600E}$ mutation and contains high levels of activated p45-IKKα. In order to identify substrates that are phosphorylated downstream of BRAF but depend on IKKα, we infected HT29 cells with either control or IKKα short hairpin RNA (shRNA) which effectively depleted IKKα protein [**FIGURE R15**]. We then treated cells with the BRAF inhibitor AZ628 for 2 hours and released the inhibition for 30 minutes to allow a synchronous phosphorylation of downstream substrates of BRAF, including phosphorylation of IKKα itself and possible IKKα substrates. By LC-MS/MS analysis, we identified 53BP1 and KAP1 (also known as TRIM28 or TIF1β), which are important regulators of the DDR pathway, as candidate substrates of IKKα-dependent phosphorylation downstream of BRAF [**FIGURE R16**]. Of note, 53BP1 and KAP1 phosphorylations in response to DNA damage or vemurafenib-induced ERK activation have been recently reported in two different proteomic-based publications[554,555], supporting our data from the MS analysis.

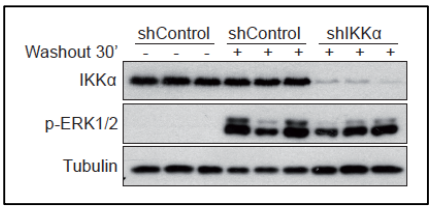

Figure R15 | WB for IKKα depletion and BRAF inhibitor effectiveness. HT29 cells were infected with shControl or shIKKα and selected for 72h with puromycin. To perform the experiment, cells were treated with the BRAF inhibitor AZ628 for 16h and washed out for 30 minutes in the indicated samples. Three biological replicates were done for each condition.

Protein Name	Site	Log2 FC	pvalue
53BP1	S265	1,2	0,03
	S1759/S176	2	0,03
KAP1 / TRIM28	S471/S47	0,8	0,005

Figure R16 | 53BP1 and KAP1 are candidate substrates for IKKα- and BRAF- dependent phosphorylations. Table shows MS results: phosphorylation sites, fold change (Log2) and *pvalue*.

To further investigate the possibility that BRAF and IKKα are functionally related to the DDR pathway, we induced DNA damage by exposing HT29 cells to Ultraviolet (UV) light and followed by WB analysis to check IKKα activity. Interestingly, we found that IKKα was robustly activated after UV treatment as well as other elements of the DDR pathway such as γH2A.X, Chk1 and KAP1^{556} [**FIGURE R17**].

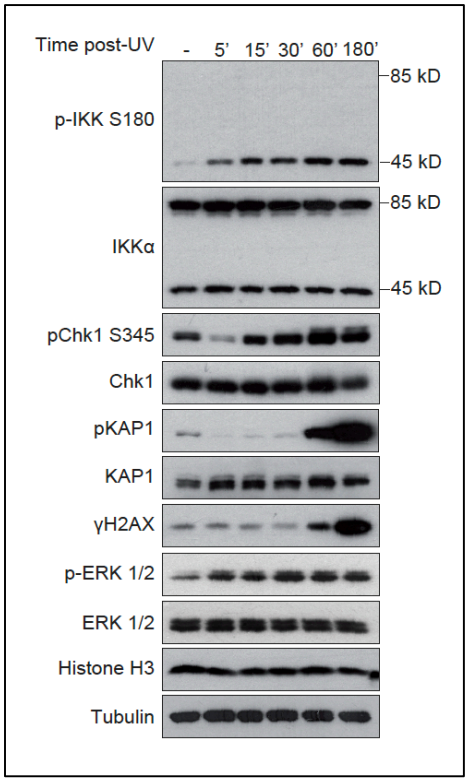

Figure R17 | p45-IKKα is activated after UV treatment. WB analysis of HT29 cells treated with UV light and analysed at the indicated time points after DNA damage exposure.

Similarly, IKKα was also activated with other stimuli that induce DNA damage such as ionizing radiation (IR) and the topoisomerase II inhibitor, etoposide [**FIGURE R18**].

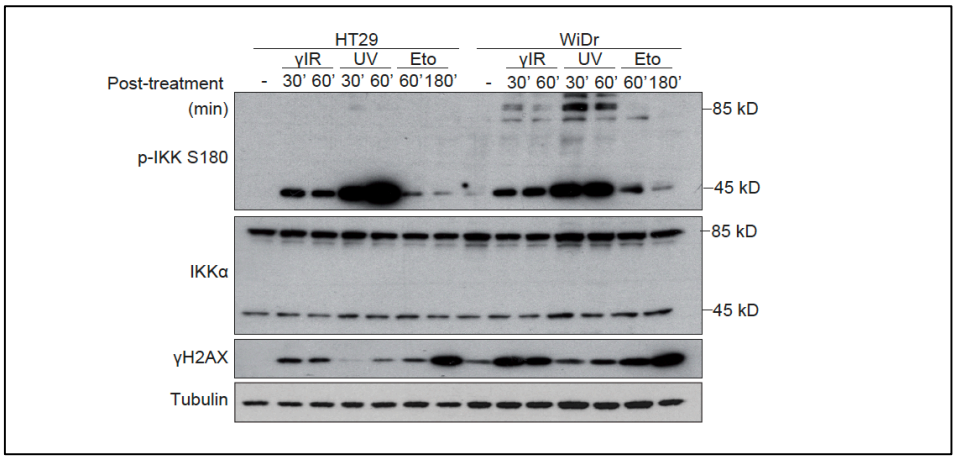

Figure R18 | p45-IKKα is activated after DNA damage induced by different stimuli. WB analysis of HT29 and WiDr cells following γ-IR (6Gy), UV (130mJ) or Etoposide (100 μM) treatments and collected at the indicated time points.

Next, we wondered whether DNA damage-dependent activation of IKKα was dependent on the presence of $BRAF^{V600E}$ mutation. To test this possibility, we used a panel of CRC cell lines carrying different mutations in KRAS (DLD1 and HCT116, codon 13 and SW480, codon 12), BRAF (HT29 and WiDR) or no mutations in these genes (LIM1215). After WB analysis, we found that all CRC cell lines activate p45-IKKα upon UV treatment, regardless of the mutations they harbour [**FIGURE R19**]. Remarkably, ERK1/2 that is a canonical mediator of BRAF and the canonical MAPK pathway was also phosphorylated after DNA damage induction, raising the possibility that BRAF was indeed activated by DNA damaging-agents.

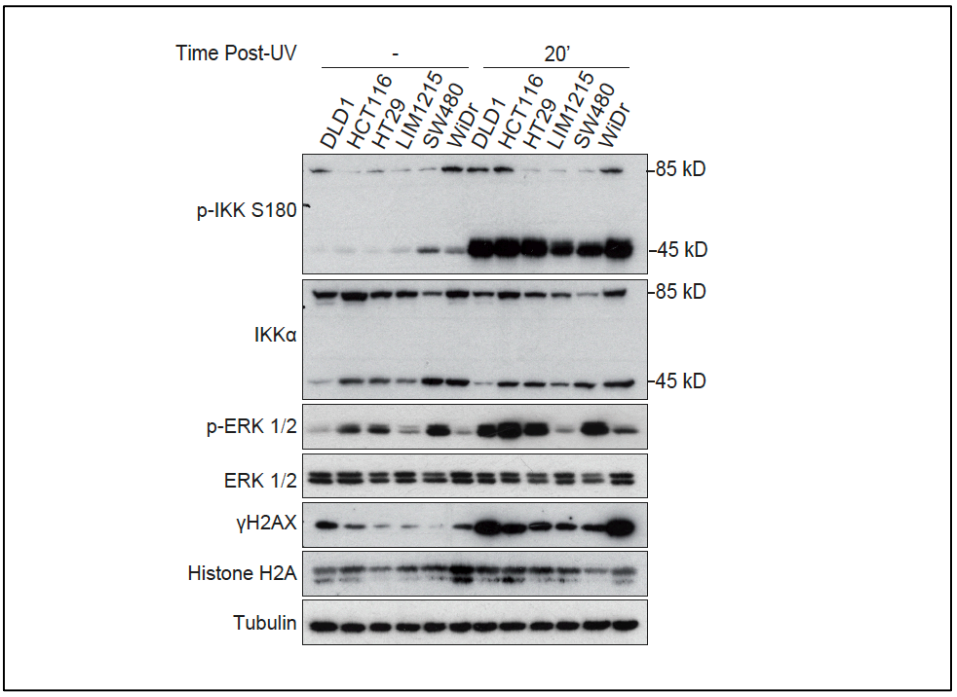

Figure R19 | p45-IKKα is activated after UV in all CRC cell lines tested. WB analysis of all listed CRC cell lines 30 minutes after UV.

Notably, p45-IKKα and ERK1/2 were both consistently activated even at low dose of UV light and independently of the time point analysed after DNA damage induction [**FIGURE R20**].

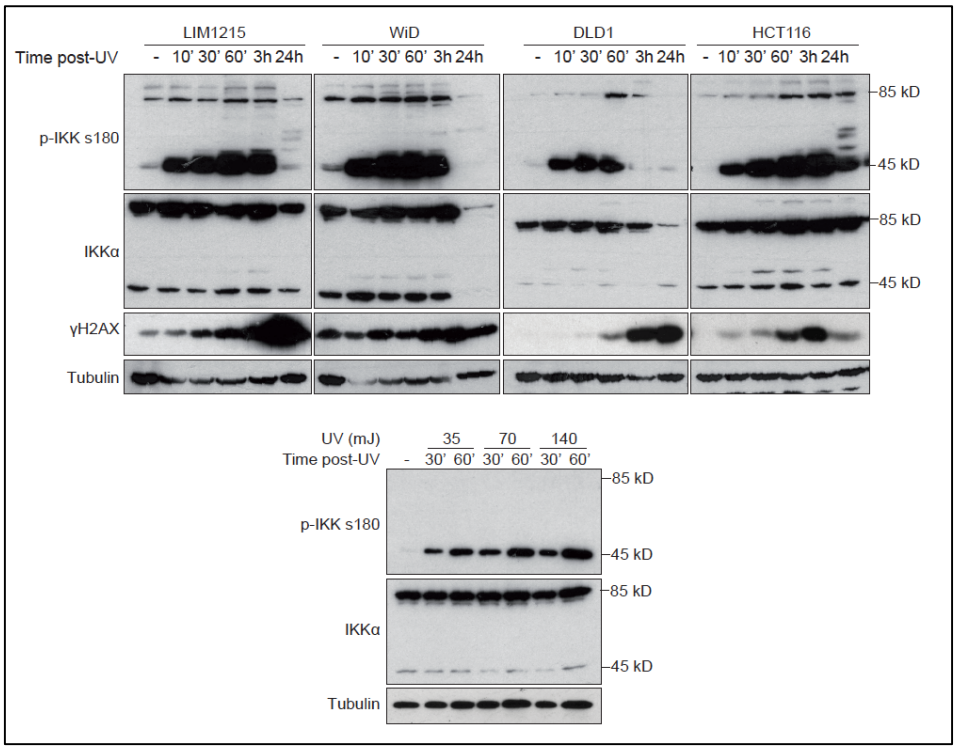

Figure R20 | p45-IKKα is consistently activated after DNA damage stimuli independently on the dose of UV light received. Upper panel: WB analysis of a panel of CRC cell lines at different time points after UV treatment. Lower panel: HT29 cell line treated at the indicated doses of UV analysed at the indicated time points by WB.

Given that the DDR signalling takes place mainly in the nucleus where damaged DNA is found, we assessed the subcellular localization of activated p45-IKKα upon DNA damage induction. By subcellular fractionation and WB analysis of HT29 cells at different time points after UV treatment [**FIGURE R21**], we observed that phosphorylated p45-IKKα was translocated to the nucleus soon after UV radiation, and levels of active p45-IKKα increased among time. Importantly, we did not detect IKKβ or NEMO in the nucleus of damaged cells, which demonstrates that these effects are independent of the previously described function of classical NF-κB in DNA damage response[557].

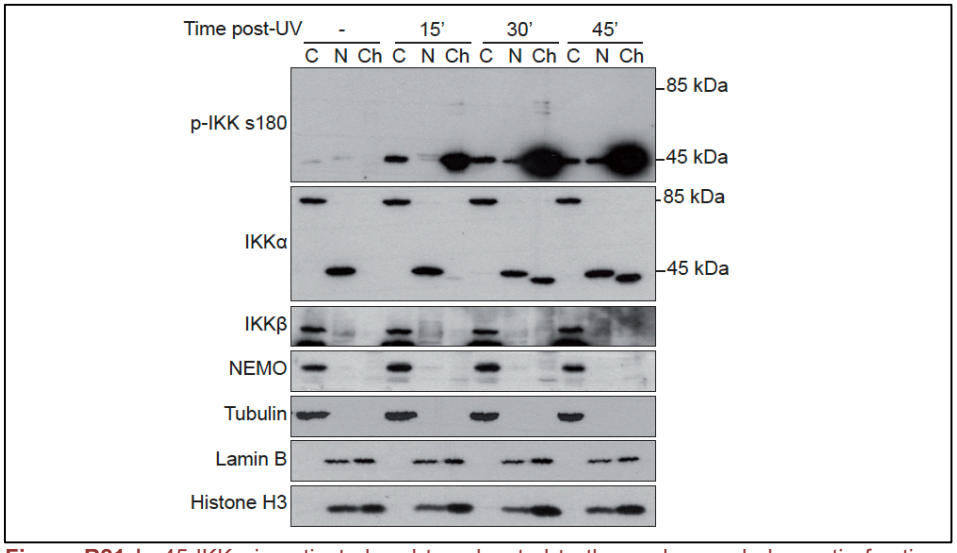

Figure R21 | p45-IKKα is activated and translocated to the nuclear and chromatin fractions after UV treatment. HT29 cells were processed to obtain the different subcellular fractions at the indicated time points after UV treatment, and then analysed by WB. C=Cytoplasm, N=Nucleus, Ch=Chromatin.

This result further suggests that p45-IKKα may have a putative role in DNA damage repair, but it does not prove that p45-IKKα is specifically recruited to the damaged sites where the DDR machinery is recruited. To formally test this possibility, we conducted immunofluorescence analysis to determine the localization of activated IKK in response to laser-induced DNA damage, to which 53BP1 has been previously shown to be recruited[469,473,474]. Importantly, we detected phosphorylated IKK colocalising with 53BP1 stripes after laser treatment [**FIGURE R22**].

Together these data indicate that **p45-IKKα is activated after DNA damage** and **active p45-IKKα is translocated to the nucleus and recruited to the sites of damaged DNA**.

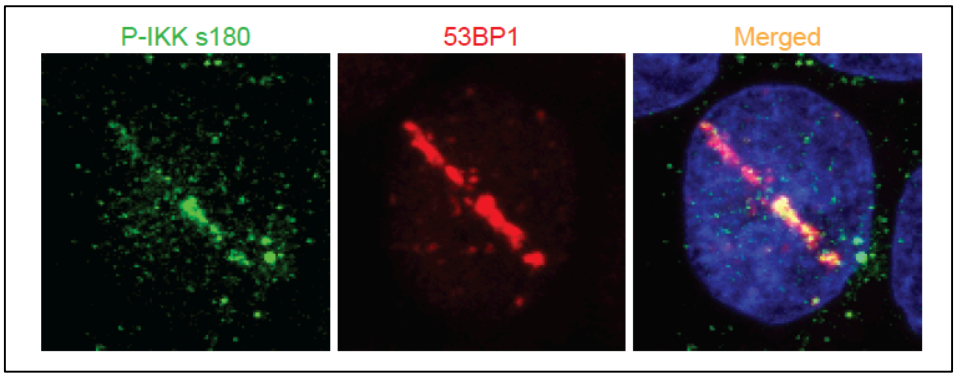

Figure R22 | Activated KKα is recruited to 53BP1 foci after laser-induced DNA damage. BrDU pre-sensitized HT29 cells were irradiated with a 405nm laser to induce localised DNA damage followed by a double immunostaining of P-IKK s180 and 53BP1.

BRAF is upstream of DNA damage induced p45-IKKα activation and the DDR pathway

Our initial mass spectrometry analysis that led to the identification of 53BP1 and TRIM28 as IKKα substrates was performed in CRC cells that had not been exposed to any DNA damaging agent. Thus, we sought to study if these same proteins or additional DDR elements were phosphorylated in an IKKα-dependent manner following DNA damage induction, when a massive increase in the levels of activated p45-IKKα is observed. To do so, HT29 cells were infected with control or IKKα shRNA, puromycin selected, and then treated (or not) with UV light for 30 minutes. Cells were then collected, enriched for phosphopeptides and analysed by mass spectrometry for the presence of differentially phosphorylated peptides in the selected experimental conditions [**FIGURE R23**].

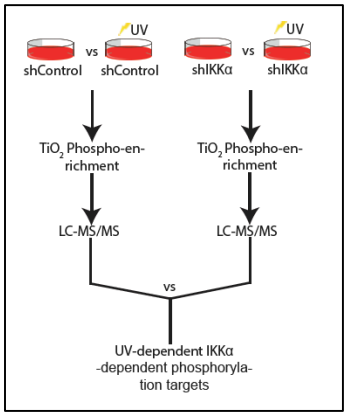

Figure R23 | Experimental design for the identification of IKKα targets in UV-treated cells. HT29 cells were transduced with shControl or shIKKα, puromycin-selected, treated with UV and collected 30 minutes after irradiation. Spectrometry analysis was focused on the identification of phosphorylated peptides specifically detected in the shControl/UV-treated cells.

Using this unbiased approach, we obtained a collection of peptides that were phosphorylated after DNA damage induction dependent on IKKα. Residues S1113 and S1618 of 53BP1 and S50 of KAP were significantly and consistently identified as phosphorylation substrates downstream of IKKα after UV treatment [**FIGURE R24**].

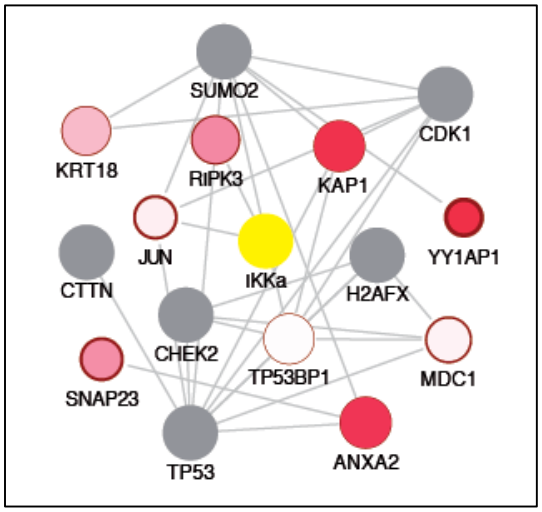

Figure R24 | Protein network of proteins that are significantly phosphorylated following UV treatment depending on IKKα. Note the presence of different elements of the DNA-damage response pathway including 53BP1 and KAP1/TRIM28. Red scale colour= Proteins found in the analysis. Red intensity indicates level of fold change. Grey= Proteins necessary to connect the network. Border thickness: indicative of statistical significance.

To gain further insight into the regulation of these elements by BRAF and p45-IKKα, we analysed by WB HT29 cells harvested at multiple time points after UV treatment in the absence or presence of BRAF inhibitor. Similar to what we previously described in non-stimulated cells[285], UV-induced activation of p45-IKKα was totally abrogated after BRAF inhibition [**FIGURE R25**].

Interestingly, one of the phosphorylation sites in 53BP1 that we identified as UV and IKKα dependent, is phosphorylation at S1618. It has been described that 53BP1 is phosphorylated at S1609 and S1618 during mitosis to impede binding of 53BP1 to the mitotic chromatin[558]. Given that this residue had been previously described, we took advantage of the commercially available antibody to detect this specific phosphorylation. Hence, we checked whether this phosphorylation is indeed dependent on BRAF and IKKα. As shown in [**FIGURE R25**], phosphorylation of 53BP1 is decreased upon BRAF inhibitor treatment in agreement with our MS data.

Importantly, not only phosphorylation of 53BP1 but also of other elements that are essential for the regulation of DNA-damage repair and the cellular check points were missregulated after BRAF inhibition. Specifically, BRAF inhibitor treatment precluded phosphorylation of Chk1 in response to UV treatment whereas phosphorylation of ATM and H2A.X (γH2A.X) were also attenuated. In addition, cells treated with BRAF inhibitor show increased levels of cleaved caspase 3 after UV compared to the control, indicating that inhibition of BRAF sensitizes CRC cells to DNA damage. Remarkably, inhibition of BRAF abolished the UV-dependent activation of p45-IKKα in all tested CRC cell lines [**FIGURE R26**].

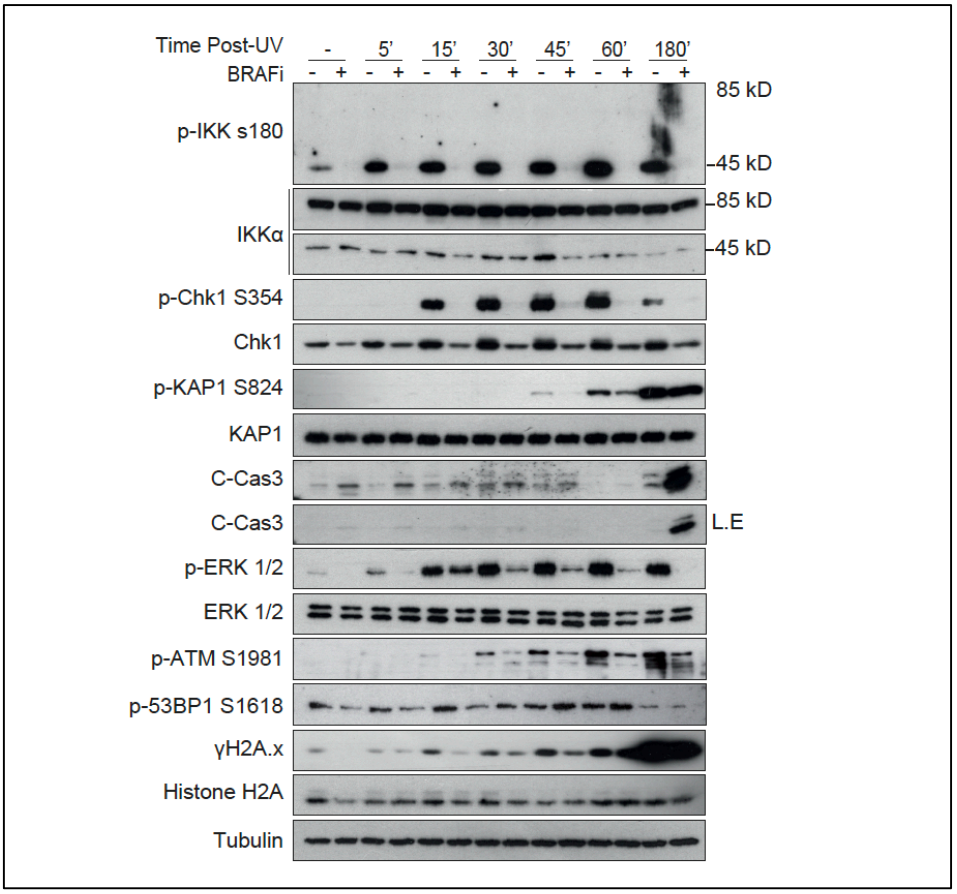

Figure R25 | BRAF inhibitor prevents UV-dependent ERK1/2, p45-IKKα and Chk1 phosphorylation, affects 53BP1 S1618 activation and increases cleaved Caspase 3 levels. Kinetic analysis of HT29 cells control or pre-treated for 16 hours with the BRAF inhibitor AZ628 (BRAFi), followed by UV exposure. HT29 cells were analysed by WB at the different time points indicated after UV treatment.

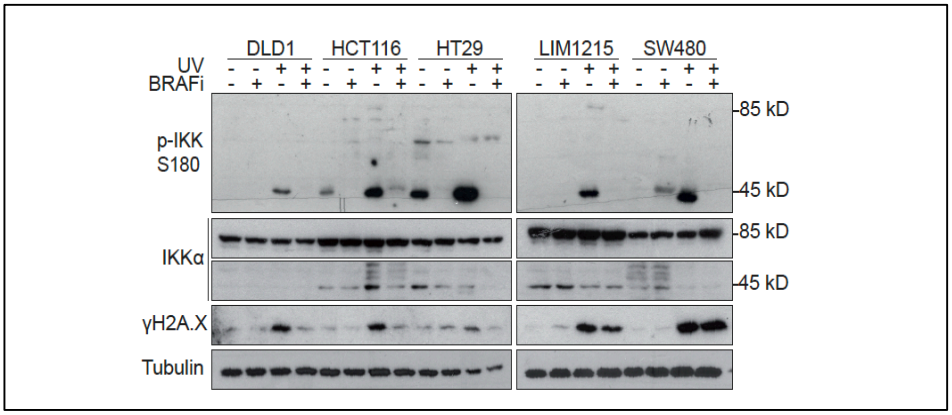

Figure R26 | Inhibition of DNA damage-mediated activation of p45-IKKα by BRAF inhibitor does not depend on BRAF V600E mutation. The indicated cell lines were left untreated or treated with BRAFi for 16 hours, and then irradiated with UV, as indicated. Cells were collected 30 minutes after treatment and analysed by WB.

We next assessed whether nuclear accumulation of p45-IKKα after DNA damage is controlled by BRAF. By subcellular fractionation and WB analysis of HT29 cells, we showed that nuclear translocation of p45-IKKα in response to DNA damage was abrogated by BRAF inhibition [**FIGURE R27**]. This demonstrates that BRAF not only controls p45-IKKα activation but also p45-IKKα nuclear translocation after DNA damage.

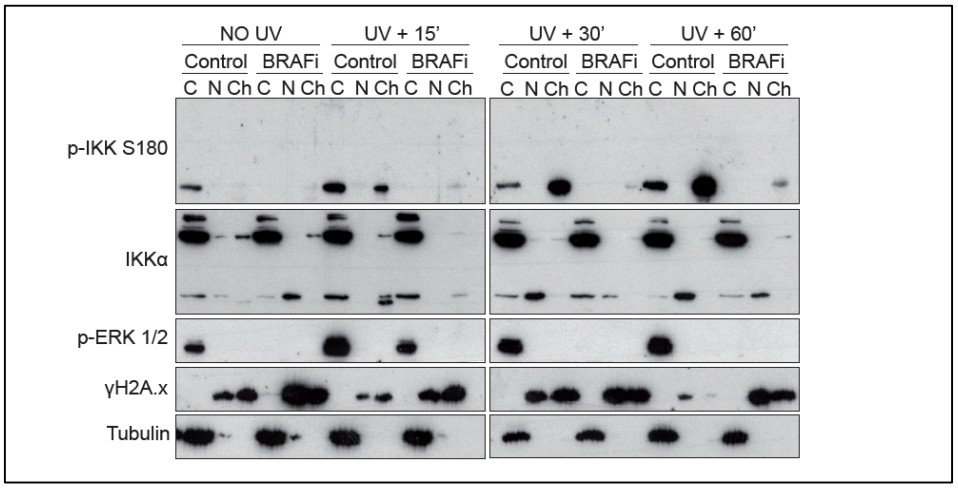

Figure R27 | DNA-damage induced nuclear translocation of p45-IKKα is abrogated after BRAF inhibition. HT29 cells were treated with AZ628 (10 μM) 16h, treated with UV (130mJ) and processed at the indicated time points to obtain the different subcellular fractions followed by WB analysis. C=Cytoplasm, N=Nucleus, Ch=Chromatin.

Previously, we demonstrated that in CRC cells, activation of p45-IKKα downstream of BRAF is dependent on TAK1[285], being TAK1 the principal kinase that activate the IKK complex in the NF-κB pathway[173]. To examine whether TAK1 was also required for the activation of p45-IKKα induced by DNA damage, we pre-treated HT29 cells with the TAK1 inhibitor 5z-7-oxozeaneol, exposed them to UV light and analysed the cell lysates by WB. As expected, inhibition of TAK1 reduced the levels of activated p45-IKKα after induction of DNA damage by UV [**FIGURE R28**].

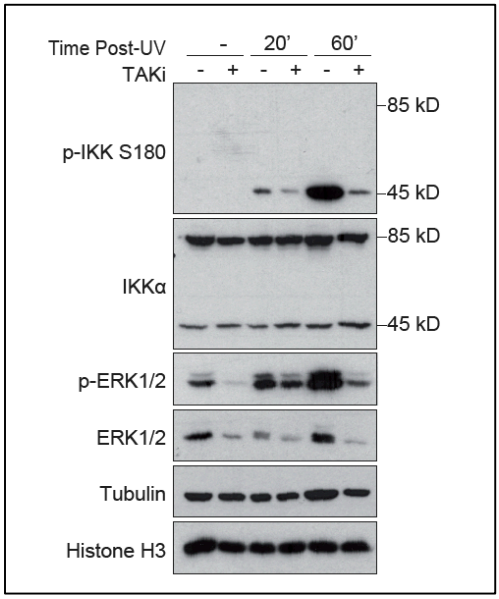

Figure R28 | TAK1 inhibitor prevents DNA damage dependent p45-IKKα activation. WB analysis of HT29 cells treated with the TAK1 inhibitor (5Z)-7-Oxozeaenol (10 μM) for 16 hours, then exposed to UV light and collected at the indicated time points.

Together, our analyses indicate that **IKKα regulates the phosphorylation of 53BP1 and TRIM28**, and demonstrate that **BRAF and TAK1 are upstream of DNA damage-dependent p45-IKKα activation**. Further, some elements of the DDR signalling, such as **ATM, γH2A.X and Chk1, are also regulated by BRAF activity**.

Inhibition of BRAF and TAK1 blocks 53BP1-mediated chromosome end-to-end fusions at dysfunctional telomeres

It has been previously shown that chromosomes fuse to each other upon telomere de-protection caused by depletion of the sheltering component TRF2[495,559]. Like DSB, deprotected telomeres activate ATM and accumulate 53BP1, which mediates NHEJ. To determine if BRAF and IKKα facilitate 53BP1-dependent NHEJ at dysfunctional telomeres, we used MEFs TRF2$^{FL/FL}$. Following CRE infection to induce TRF2 deletion, MEFs were left untreated or treated with BRAF, TAK1 or MEK inhibitors for 72 hours, and then cells were processed for metaphase visualization. We then performed Fluorescence In Situ Hybridization (FISH) analysis to detect telomeric regions, and cells were scored for the presence of chromosome end-to-end fusions. Interestingly, cells treated with either BRAF or TAK1 inhibitors showed a remarkable decrease in chromosome fusions compared to control cells or cells treated with MEK inhibitor [**FIGURE R29 and FIGURE R30**].

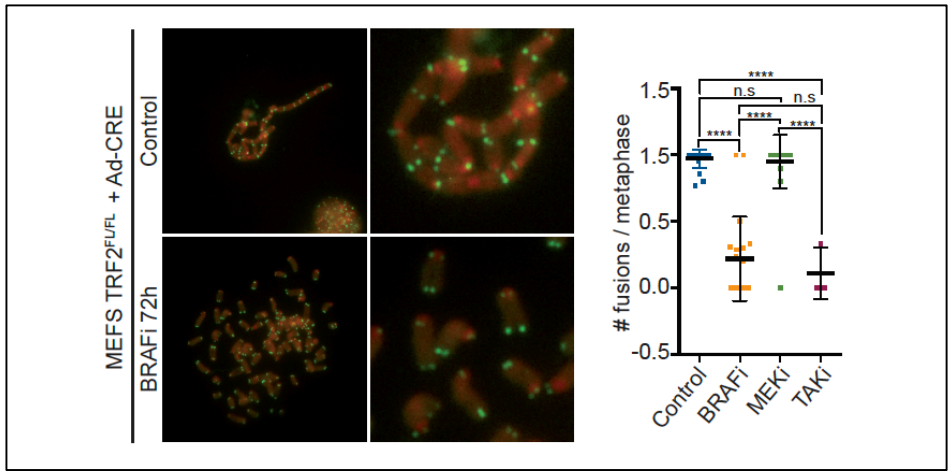

Figure R29 | BRAF and TAK1 inhibition preclude chromosome end-to-end fusions upon TRF2 depletion. Quantification of telomere fusions per metaphase in cells 96 hours after adenovirus GFP (Ad-GFP) or CRE (Ad-CRE) infection. Cells were treated for 72 hours with BRAFi (10 μM), MEKi (1 μM) and TAK1i (5 μM) prior to collection. For statistical analysis, one-way ANOVA was used. P values are indicated as ****p<0.0001.

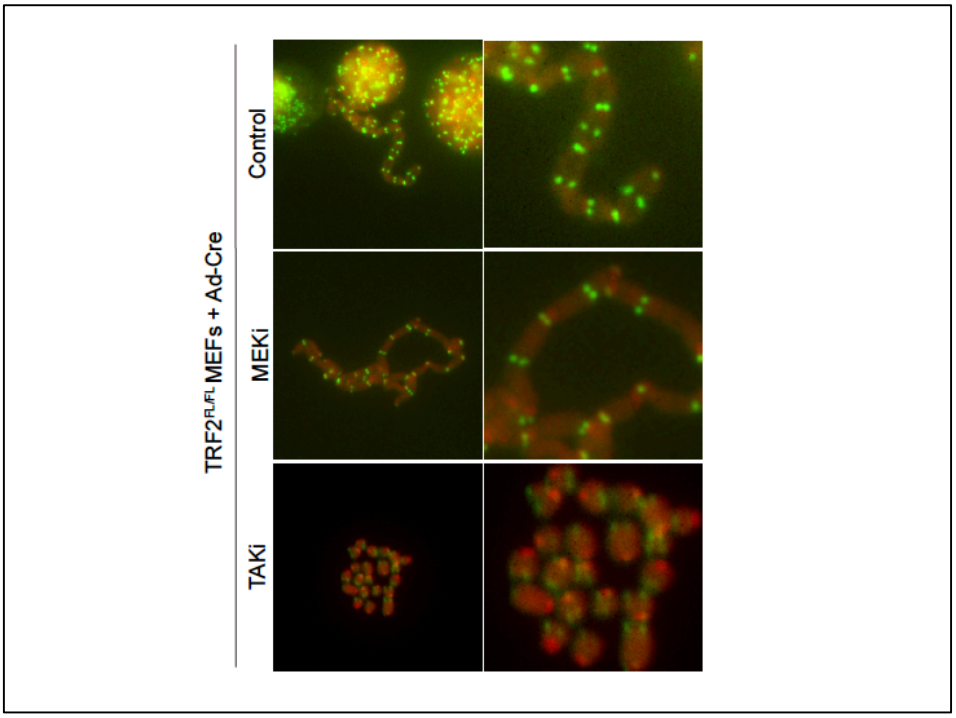

Figure R30 | BRAF and TAK1 inhibition preclude chromosome end-to-end fusions upon TRF2 depletion. Images of the indicated treatments from figure R29.

These results indicate that BRAF regulates NHEJ likely associated with altered BRAF/p45-IKKα and 53BP1 function but independent of the MEK/MAPK pathway.

Supporting this notion, we detected a significant decrease in the number of telomere-dysfunction-induced foci (TIFs) containing 53BP1 after BRAF inhibition [**FIGURE R31**], which could explain why chromosomes of dysfunctional telomeres do not fuse.

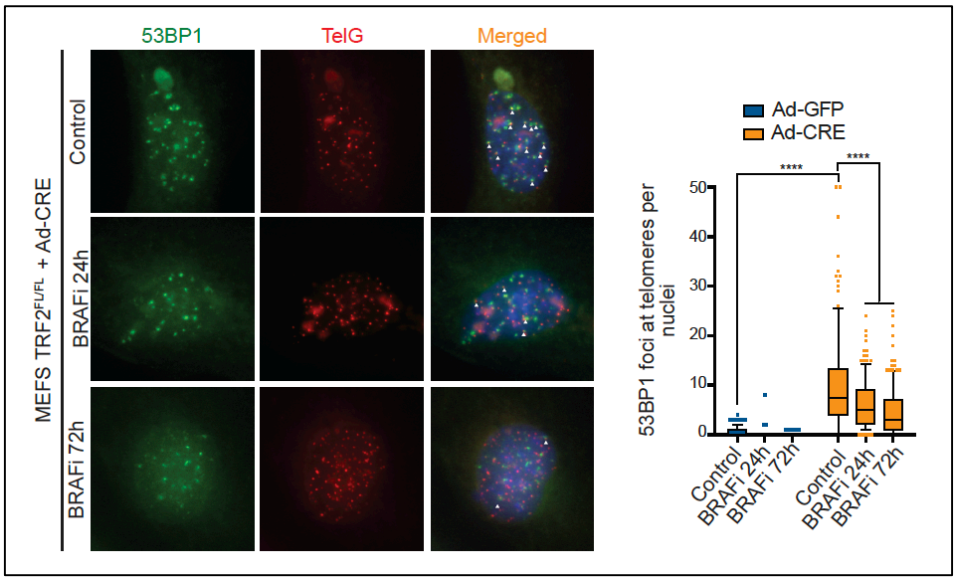

Figure R31 | BRAF inhibition prevents 53BP1 recruitment to deprotected telomeres. IF-FISH of 53BP1 and a telomeric probe in cells 96 hours after adenovirus GFP (Ad-GFP) or CRE (Ad-CRE) infection. Cells were treated for 24 and 72 hours with BRAF inhibitor AZ628 (10 μM) prior to collection. For statistical analysis, one-way ANOVA was used. P values are indicated as ****p<0.0001.

As previously mentioned, one feature that will dictate pathway choice and repair outcome, is the phase of the cell cycle that the cell is going through. Although NHEJ can happen at any point of the cell cycle, HR is more prone to occur during S and G2 phases, to guarantee genomic stability. To exclude the possibility that differences in cell cycle imposed by BRAF inhibition were at the base of defective chromosome fusion, we performed cell cycle analysis of TRF2$^{FL/FL}$ MEFs treated with the different drugs used for the experiment. Flow cytometry analysis showed that BRAF and MEK inhibition increases G1 phase where NHEJ is the only possibility to repair DSBs, while TAK1 inhibitor does not affect cell cycle progression [**FIGURE R32**]. These results strongly indicate that impairment of chromosome fusions following BRAF and TAK1 inhibition is not the result of cell cycle alterations.

These observations suggest that **53BP1 depends on BRAF and p45-IKKα to induce NHEJ at dysfunctional telomeres**.

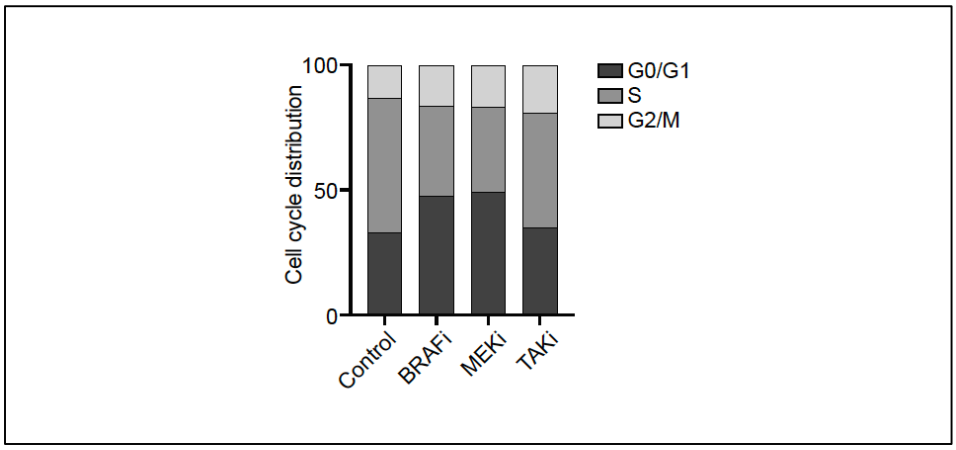

Figure R32 | Cell cycle profile of BRAF, MEK or TAK1 inhibited MEFs. Cell cycle analysis was performed in MEFs treated for 72h with BRAFi (10 μM), MEKi (1 μM) or TAKi (5 μM).

BRAF inhibition impairs RIF1 recruitment to 53BP1 foci and induces accumulation of DNA damage

Upon DNA damage, 53BP1 is accumulated near the sites of damage forming DNA damage foci that can be assessed by immunofluorescence[473]. In addition, association of RIF1 with specific phosphorylated forms of 53BP1 at DSB sites is functionally required for promoting 53BP1-dependent NHEJ[484]. We examined the requirement for BRAF in IR-dependent generation of 53BP1 and γH2A.x foci. Control and BRAF inhibitor-treated MEFS were IR-treated and then processed for 53BP1 and γH2A.x immunofluorescence (IF) at different time points [**FIGURE R33**]. We found that control and BRAF-inhibited cells show comparable number of foci 30 minutes after irradiation. By contrast, 24 hours after IR treatment, 53BP1 and γH2A.x foci only persisted in BRAF-inhibited cells suggesting that BRAF inhibition imposed a delay in DNA damage repair likely associated with 53BP1 dysfunction.

These results indicated that **BRAF activity is dispensable for 53BP1 recruitment to DSB sites but required for efficient DNA damage repair**

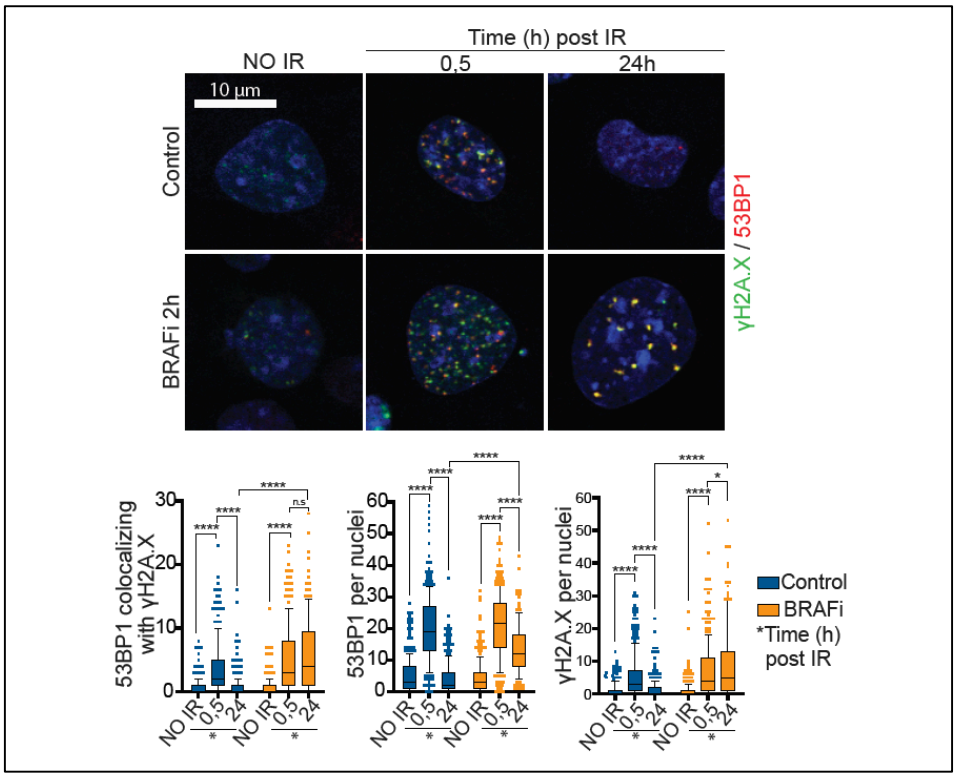

Figure R33 | BRAF inhibition prevents DNA damage foci resolution of γH2A.x and 53BP1. Representative images of a co-immunofluorescence (right panel) of 53BP1 and γH2A.x fixated at the indicated time points after γ-irradiation (2Gy). MEFS were treated with BRAF inhibitor AZ628 (10 µM). Quantification of the experiment is shown in the right panel. For statistical analysis, one-way ANOVA was used. P values are indicated as **p*<0.05 and *****p*<0.0001. Scale bar equals 10 µm.

As mentioned, association of RIF1 to 53BP1 is required for proper 53BP1 function in DNA repair[484]. Hence, we sought to determine whether RIF1 recruitment to 53BP1-containing DNA damage foci was affected upon BRAF inhibition, thus providing a mechanistic explanation for defective DNA-damage repair and 53BP1 foci persistence. Control and BRAF-inhibited MEFS where irradiated, and after 30 minutes cells were processed for 53BP1 and RIF1 IF [**FIGURE R34**]. We found that BRAF inhibition imposed a decrease in the number of RIF1 foci that colocalised with 53BP1, indicating that **BRAF activity was required for RIF1 recruitment to 53BP1 foci and the effective resolution of DSB after DNA damage**.

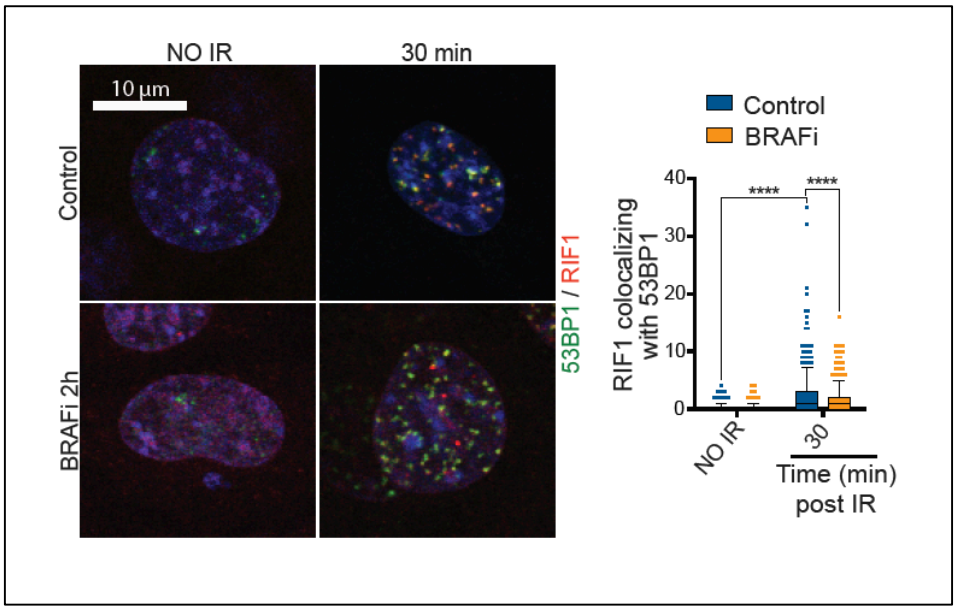

Figure R34 | BRAF inhibition precludes RIF1 recruitment to 53BP1 foci. Representative images of a co-immunofluorescence (left panel) of 53BP1 and RIF1 fixated 30 minutes after γ-irradiation (2Gy). MEFS were treated with BRAF inhibitor AZ628 (10 µM). Quantification of the experiment is shown in the right panel. For statistical analysis, unpaired t-test was used. P values are indicated as ****p<0.0001. Scale bar equals 10 µm.

IKKα inhibition reproduces the effects of BRAF inhibition in the DDR pathway

To extend our observations beyond BRAF inhibition, we sought to study the effect of IKKα inhibition or downregulation on the DDR and 53BP1 function. As a first approach, we transduced HT29 cells with two different shRNA targeting IKKα or control shRNA and, after selection, we treated them with UV and processed for WB at different time points after DNA damage induction [**FIGURE R35**]. Knocking down IKKα led to a decrease in the levels of phosphorylated Chk1 and H2A.X when compared to control cells as previously found in BRAF-inhibited cells.

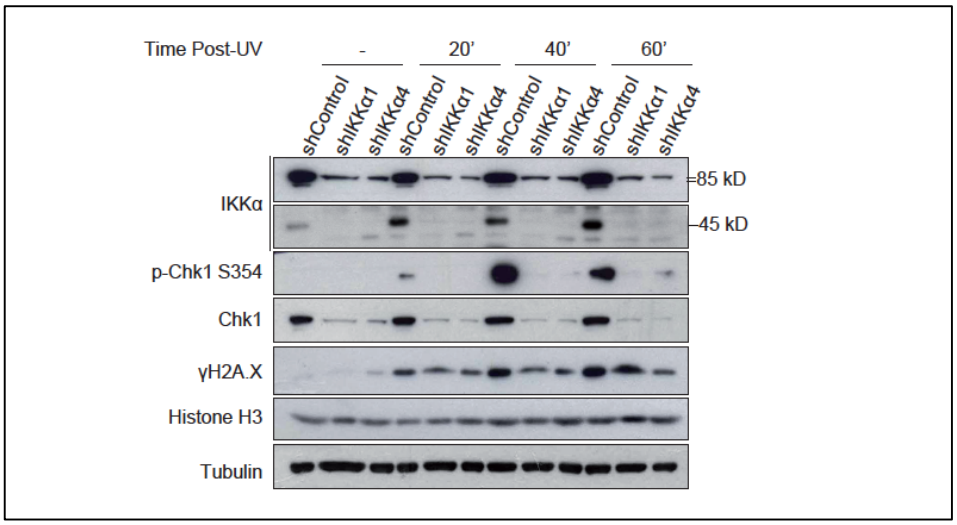

Figure R35 | IKKα downregulation inhibits Chk1 phosphorylation and decreases levels of γH2A.X after DNA damage. HT29 cells were infected with the indicated shRNAs and selected with puromycin for 72 hours. Cells were then treated with UV light and analysed by WB at the indicated time points after DNA damage induction.

Previous reports had already linked cell survival upon DNA damage and ATM activation with canonical NF-κB signalling leading to increased cell survival[204,206]. To exclude the possibility that BRAF and p45-IKKα were in fact regulating the same mechanisms of cell survival related with canonical NF-κB, we knocked down IKKβ and NEMO which are essential to activate NF-κB signalling, and tested the effect on p-Chk1 or γH2A.X levels after UV exposure. We did not detect any alteration of p-Chk1 or H2A.X phosphorylation in response to UV after IKKβ or NEMO/IKKγ depletion, which demonstrates that these events are independent of conventional NF-κB [**FIGURE R36**]. Similarly, blockage of IKKβ through two different pharmacological inhibitors did not affect phosphorylation of these elements related with activation of the DDR. The efficiency of the inhibitors was confirmed by the accumulation of P-IkBα. Indeed, TPCA only affected p-Chk1 levels at higher doses which also inhibit IKKα [**FIGURE R37 and R38**].

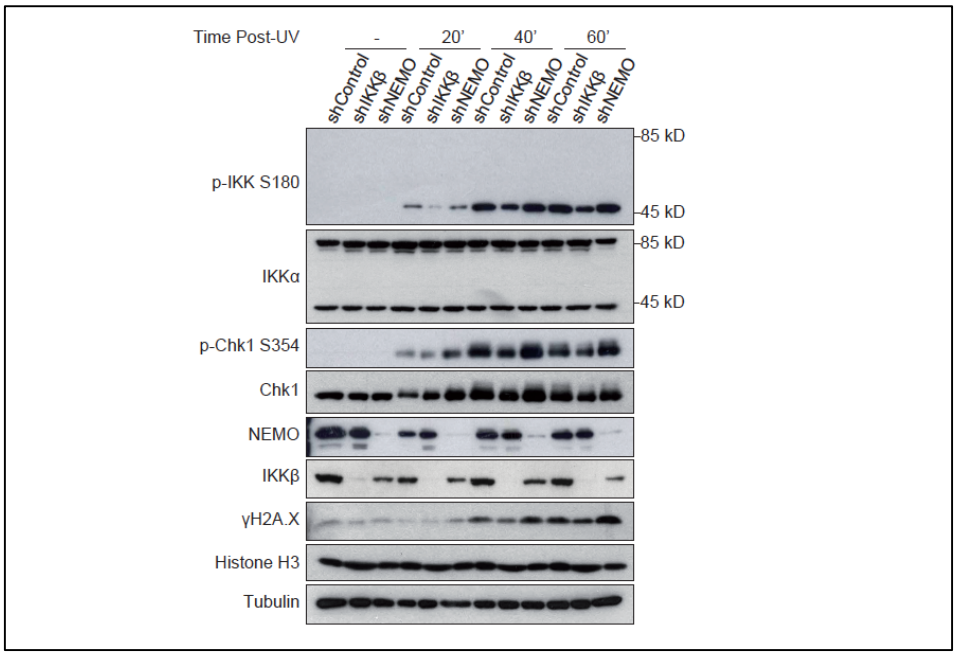

Figure R36 | IKKβ nor NEMO downregulation affect the phosphorylation of Chk1 or γH2A.X after DNA damage**.** HT29 cells were infected with the indicated shRNAs and selected with puromycin for 72 hours. Then, cells were treated with UV light and analysed by WB at the indicated time points after DNA damage induction.

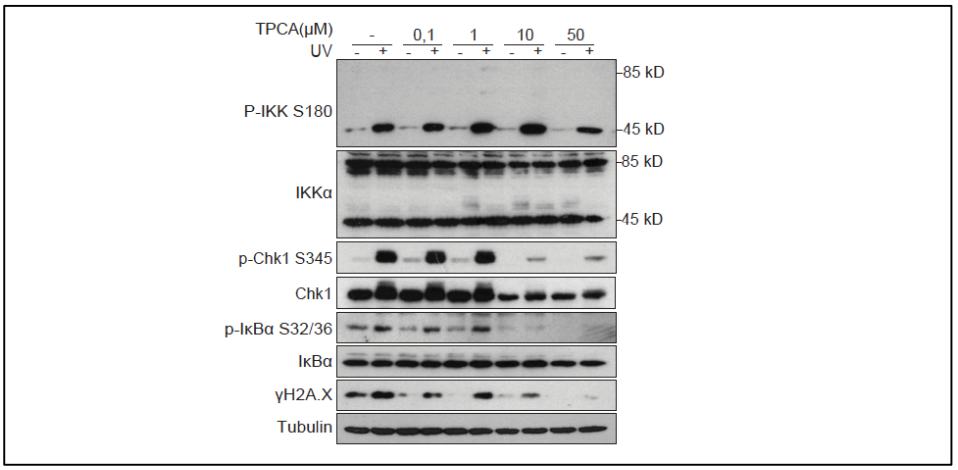

Figure R37 | IKK inhibitor prevents DNA damage induced Chk1 phosphorylation only at doses that inhibit IKKα. WB analysis of HT29 cells treated with the IKK inhibitor TPCA at the indicated concentrations (IC_{50} IKKα= 400 nM, IC_{50} IKKβ= 17,9 nM) for 16 hours, followed by exposure to UV light and collected 30 min after DNA damage induction.

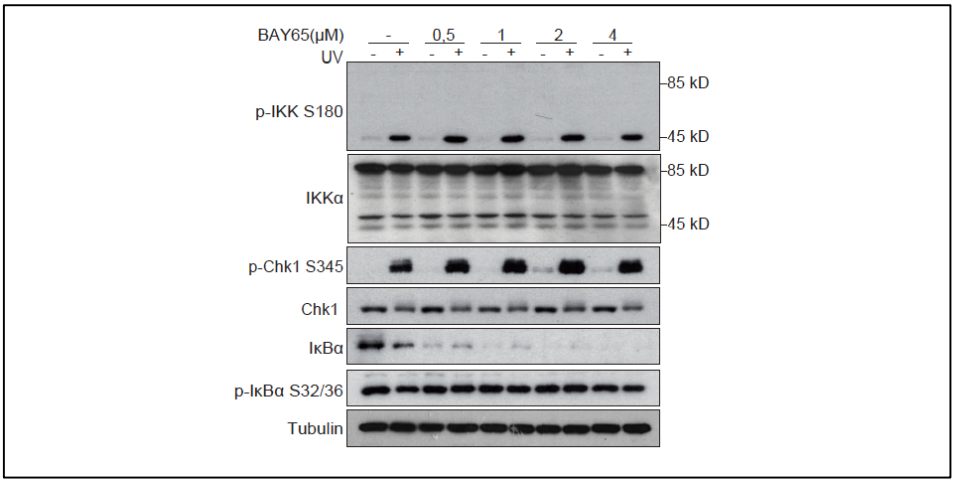

Figure R38 | IKKβ inhibitor BAY65, does not affect Chk1 phosphorylation induced by DNA damage**.** WB analysis of HT29 cells treated with BAY65 at the indicated concentrations for 16 hours followed by UV exposure and collected 30 min after DNA damage induction.

Furthermore, to study if IKKα also affects RIF1 recruitment to 53BP1 foci, we used IKKα knockout (KO) MEFS to asses RIF1 and 53BP1 by immunofluorescence [**FIGURE R39]**. Importantly, MEFs IKKα KO have no detectable IKKα protein as shown by WB. Consistent with our findings using BRAF inhibitor, MEFs IKKα KO show impaired capacity to recruit RIF1 to 53BP1 damaged foci after irradiation compared to WT MEFs.

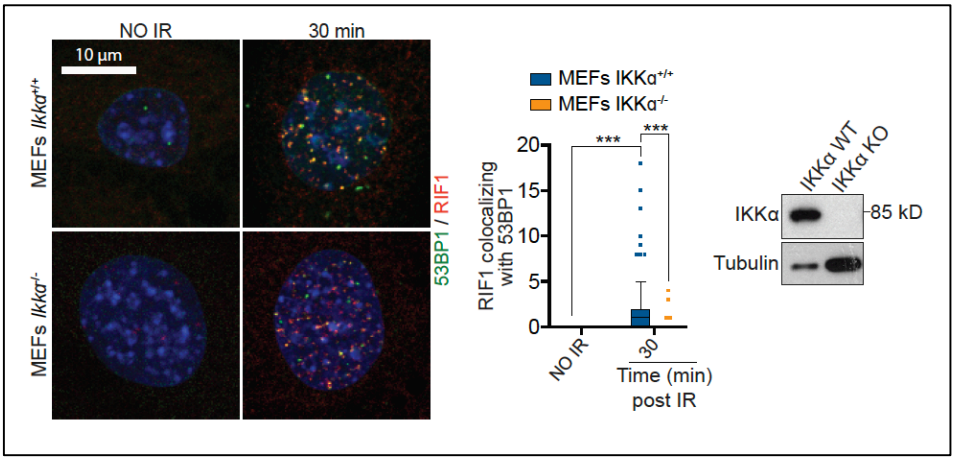

Figure R39 | IKKα deficiency precludes RIF1 recruitment to 53BP1 foci. Representative images of co-immunofluorescence analysis (left panel) of 53BP1 and RIF1 30 min after γ-irradiation (2Gy). Quantification of RIF1 foci colocalising with 53BP1 is shown in the right panel. For statistical analysis, two-way ANOVA was used and the p-values are indicated as ***p<0.001. Scale bar equals 10 μm.

Together these findings establish a **contribution of IKKα in regulating the DNA damage response.**

BRAF inhibition synergies the effect of standard chemotherapy on an in vivo human CRC PDX model

Current protocols for CRC treatment mostly rely on DNA-damaging chemotherapy leading to apoptosis of tumour cells. Based on that, we hypothesized that inhibition of BRAF or IKKα might increase chemotherapy effectiveness by preventing effective DNA damage repair in tumour cells after therapy. We tested this possibility using patient-derived CRC tumours that were disaggregated to culture them as tumouroids in 3D cultures[104], and/or implanted othotopically in nude mice to confirm the results in an in vivo setting [**FIGURE R40**].

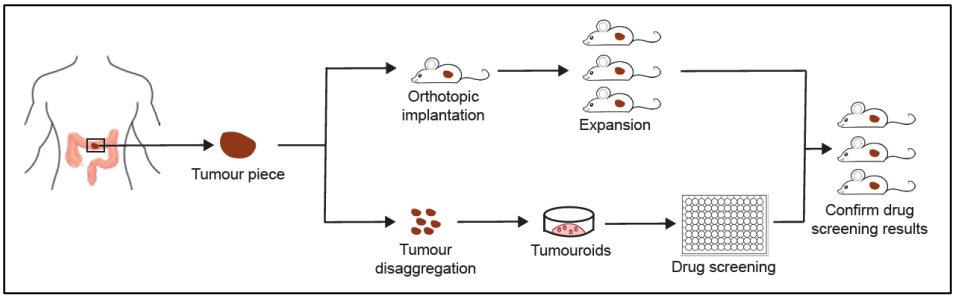

Figure R40 | Schematic representation of the experimental design used. After tumour collection, one part of the tumour piece was disaggregated and seeded in Matrigel® as tumouroids to test different drug combinations. The other part of the tumour was implanted orthotopically in mice, expanded and used for the selected experiment.

Tumouroids were treated with low doses of the cytotoxic agents 5-Fluorouracil (5-FU) plus Irinotecan in addition to BRAF inhibitor. Analysis of these tumouroids by IF, demonstrated that the **combined treatment induced a massive accumulation of DNA damage,** as determined by accumulation of γH2A.X, **that led to cell apoptosis**, as indicated by the higher levels of cleaved caspase 3 in this group of treatments [**FIGURE R41**].

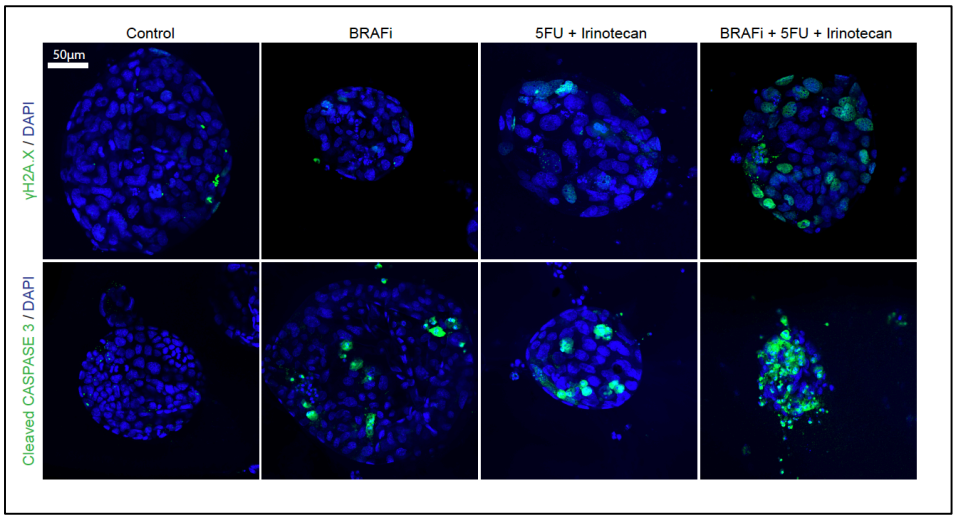

Figure R41 | BRAF inhibition in combination with 5FU+Irinotecan increases DNA-damage accumulation and induction of apoptosis. A patient-derived tumouroid was treated with AZ628 (10 µM) and/or 5FU (50 µg/ml) + Irinotecan (20 µg/ml) for 24 hours prior to IF analysis. Figure shows representative images of γH2A.X and Cleaved Caspase 3 immunostaining. Scale bar equals 50 µm.

We then extended our observations beyond cell culture and moved to an in vivo setting by using a patient-derived orthotopic xenograft (PDOX) model for CRC. Mice were treated with the standard chemotherapeutic regime 5-FU plus Irinotecan, alone or in combination with the clinically approved BRAF inhibitor, vemurafenib[560]. Consistent with our previous findings, **the combination of 5-FU and irinotecan with vemurafenib, significantly reduced the tumour burden** [**FIGURE R42**].

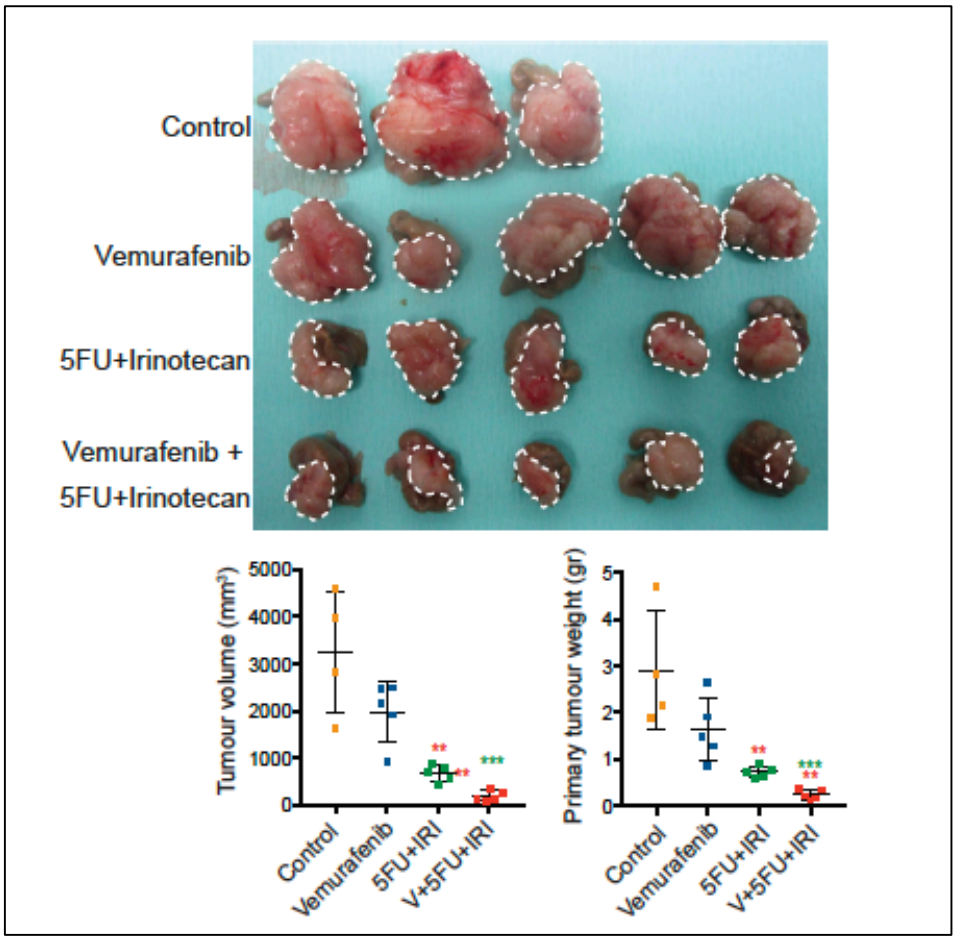

Figure R42 | Combination of vemurafenib with 5FU+irinotecan increases effectiveness against tumour growth**.** Photograph of primary CRC tumours recovered at the end of the experiment with the indicated treatments. Below the photograph, the quantification of the experiment is provided. Statistical analysis was performed by unpaired t test comparing the different treatments with control animals (red asterisks) or with animals treated with 5FU+Irinotecan (green asterisks). *p<0,05; **p<0.01; ***p<0.001. 5FU: 5-Fluorouracil, IRI: Irinotecan, V: Vemurafenib. This experiment was performed in collaboration with Dr. Alberto Villanueva.

Importantly, we obtained comparable results by treating the PDOX model with 5-FU plus Irinotecan in combination with inhibitors of endosomal acidification, bafilomycin A1 and chloroquine, that inhibit p45-IKKα activation, as we have previously shown[285]. Treatment of tumouroids with low doses of the cytotoxic agents (5-FU+Irinotecan) led to a dose-dependent cell death of tumour cells that was significantly enhanced by addition of chloroquine or bafilomycin A1 [**FIGURE R43**].

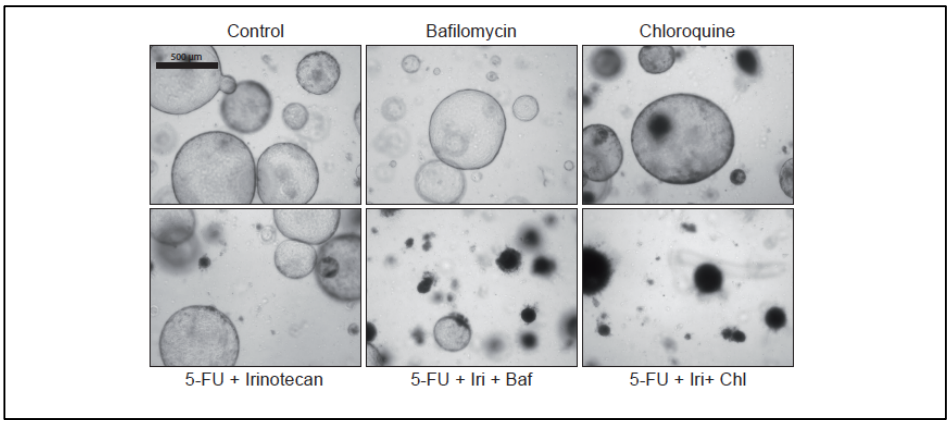

Figure R43 | Combination of bafilomycin A1 or chloroquine with 5FU+Irinotecan collapse tumouroid viability. Patient-derived tumouroids were treated with bafilomycin A1 (20 nM) or chloroquine (10 µM) and/or 5FU+Irinotecan (Iri) (50 µg/ml and 20 µg/ml, respectively) for 72 hours. Representative images at the end of the experiment are shown after the indicated treatments. A representative experiment from n>3 is shown. Scale bar equals 500 µm.

Moreover, analysis of these tumouroids by IF and treatment of PDOX mice with chloroquine or bafilomycin in combination with 5FU+Irinotecan show comparable results with BRAF inhibition. This demonstrates that the effects obtained by inhibiting BRAF depend on p45-IKKα [**FIGURE R44 and R45**].

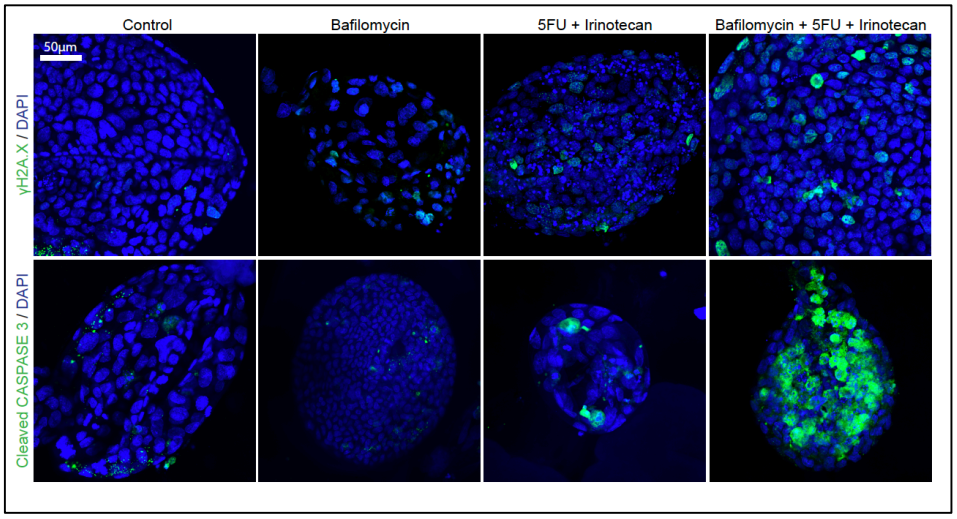

Figure R44 | Bafilomycin treatment in combination with 5FU+Irinotecan increases DNA-damage accumulation and induction of apoptosis**.** A patient-derived tumouroid was treated with bafilomycin (20 nM) and/or 5FU + Irinotecan (50 µg/ml and 20 µg/ml) for 24 hours prior to IF analysis. Figure shows representative images of γH2A.X and Cleaved Caspase 3 immunostaining. Scale bar equals 50 µm.

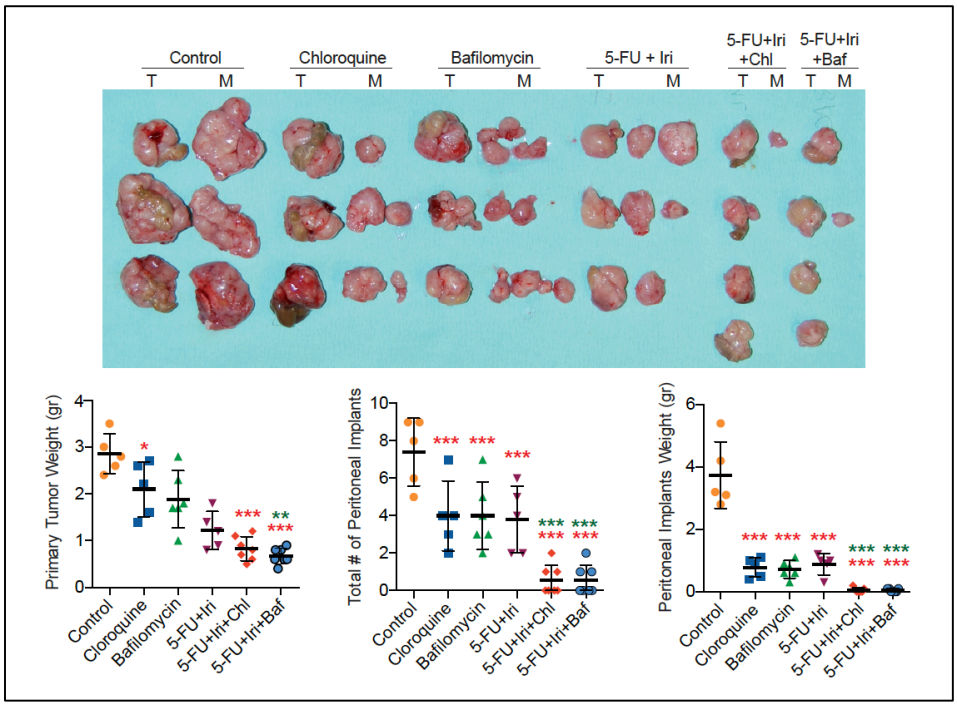

Figure R45 | Combination of bafilomycin or chloroquine with 5FU+Irinotecan increases effectiveness against tumour growth. Photograph of primary CRC tumours recovered at the end of the experiment with the indicated treatments. T refers to the primary tumour and M to the peritoneal implants. Primary tumour weight, total number of peritoneal implants and total weigh of the peritoneal implants obtained with the different treatments. Statistical analysis was performed by T-test comparing the different treatments with control animals (red asterisks) or with animals treated with 5-FU+Irinotecan (green asterisks); *p<0.05; **p<0.01; ***p<0.001. This experiment was performed in collaboration with Dr. Alberto Villanueva and Dr. Pol Margalef.

Further, we analysed the tumour tissue by Immunohistochemistry (IHC), and in agreement with our previous data, the addition of vemurafenib to the treatment, increased the levels of γH2A.X suggestive of increased DNA damage [**FIGURE R46**].

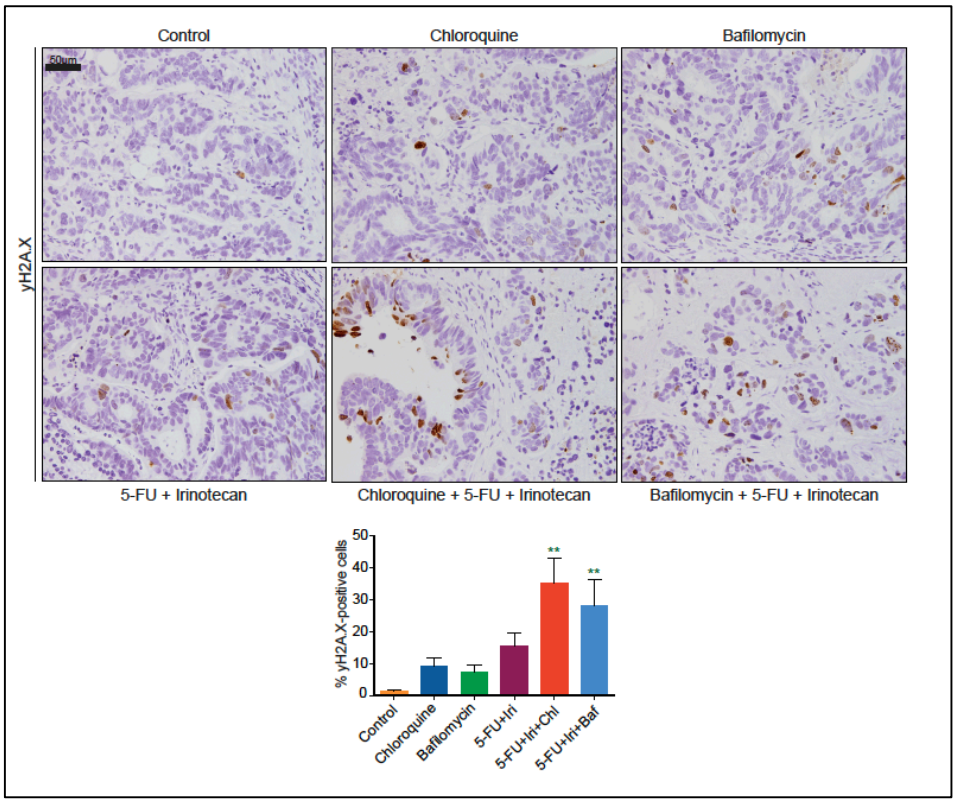

Figure R46 | Combination of bafilomycin or chloroquine with 5FU+irinotecan increases DNA damage in CRC cells in vivo. IHC analysis of γH2A.X in the tumoural tissue recovered at the end of the experiment shown in figure R45. Statistical analysis was performed by one-way ANOVA. Green asterisks indicate comparison of the different treatments with animals treated with 5-FU+Irinotecan. P values are indicated as **p<0.01. Scale bar equals 50 µm.

Moreover, by WB analysis we have seen that doxorubicin is the chemotherapeutic agent that increases the most p45-IKKα activation. Consistent with this finding, combination of doxorubicin and BRAF inhibitor AZ628 induce tumouroids collapse, compared with the single combinations that does not affect tumouroid viability [**FIGURE R47**]. This opens a new therapeutic opportunity for using doxorubicin in CRC cells, since until now CRC have demonstrated to be highly resistant to anthracyclines such as doxorubicin[561].

These findings establish for the first time a rationale for using composed therapies involving **inhibition of BRAF together with DNA-damaging agents in anti-CRC therapies independent of the BRAF mutational status of the tumour.**

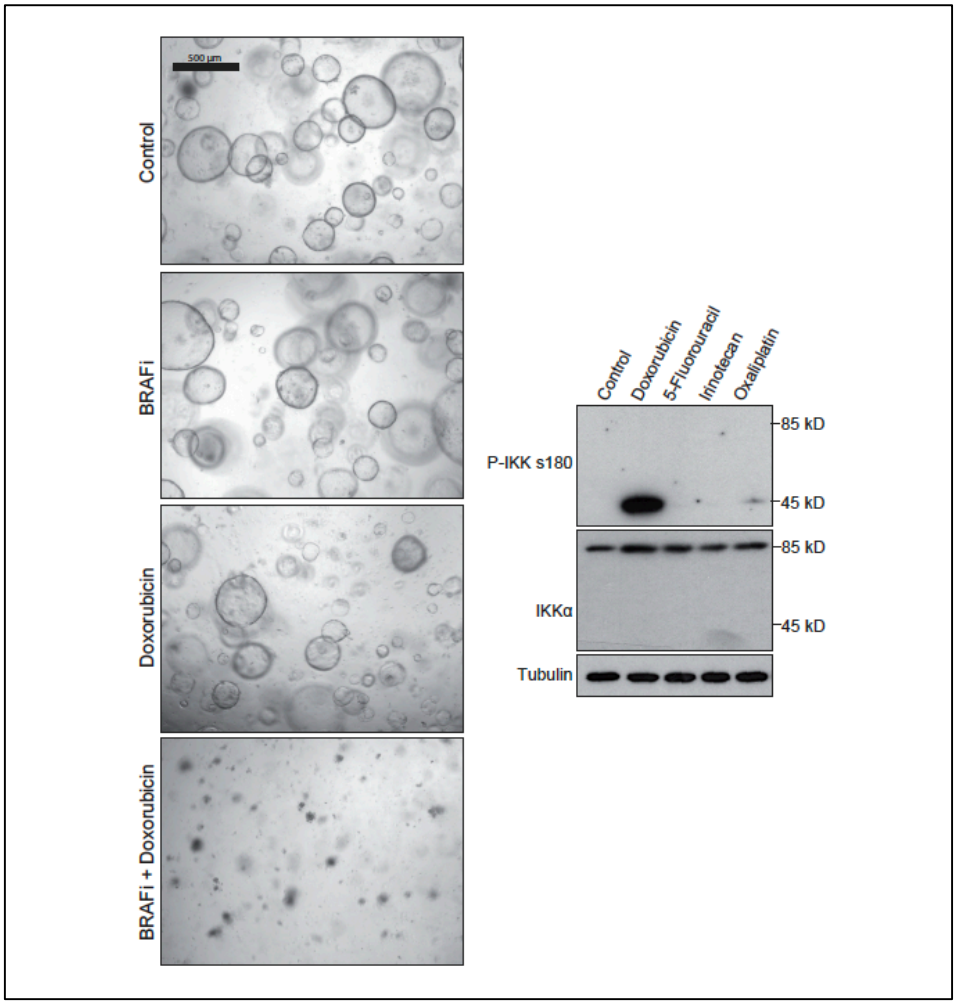

Figure R47 | Combination of BRAFi with Doxorubicin collapse tumouroid viability. Patient-derived tumouroids were treated with BRAFi (10 µM) and/or Doxorubicin (4 µg/ml for 72 hours. Representative images at the end of the experiment are shown after the indicated treatments. A representative experiment from n>3 is shown. Scale bar equals 500 µm.

DISCUSSION

DISCUSSION

As mentioned in the introduction, activation of NF-kB elements is a recurrent observation in most types of cancer. However, general inhibitors of NF-kB or the IKK complex are extremely toxic, which has precluded their clinical development for many years. Importantly, in the first part of this work, we have demonstrated that in vivo, IKKα is essential for intestinal tumorigenesis while dispensable for intestinal tissue homeostasis. Our previous investigations already demonstrated that IKKα is at the top of various mechanisms related with colorectal cancer progression, and detection of active IKKα in the nucleus of cancer cells is associated with poor prognosis, not only in CRC patients but also in patients with SSC[234,283,291]. However, the mechanistic bases supporting these observations are primarily unknown, and very few studies have delved into IKKα contribution to tumour initiation. To answer the second question, we generated a compound mouse model for tumour initiation carrying a mutation in *Apc* (*Apc*$^{Min/+}$) and lacking IKKα specifically in intestinal epithelial cells (*Villin*-Cre;*Ikkα*$^{FL/FL}$).

We show that IKKα-deficient intestinal cells have a decreased capacity to form adenomas, and the few adenomas arising in this background display a significant reduction in cell proliferation. Importantly, intestinal-specific IKKα deficiency did not affect normal intestinal crypt proliferation[15] or tissue homeostasis. Surprisingly, stem cell activity was highly reduced in the transformed IKKα-deficient adenoma cells indicating the existence of differences in the stemness program of normal and transformed cells that need to be investigated and could be therapeutically exploited [**FIGURE D1**].

As mentioned in the introduction, *Apc*$^{Min/+}$ mice mainly develop adenomas in the small intestine that rarely progress to invasive carcinomas. This highly differs from the human disease, where APC mutated adenomas are formed in the colon and they confer high risk of developing CRC[74,562]. Although it still remains unclear, these differences between mouse and human might be due to differential expression of Wnt pathway genes in the two organisms[563]. Despite these variances, countless years of research support that APC mutated mouse model recapitulates its human disease counterpart (FAP) and it is a good tool to study early tumorigenesis in the intestinal tissue. Nevertheless, it would be important to develop mouse models of sporadic and advanced colon cancer to test IKKα contribution to

advances CRC and metastasis in vivo. This would give further insights into the mechanisms by which IKKα participates in tumour maintenance and progression, and would help to understand IKKα-related mechanisms of intestinal tumorigenesis and therapy resistance. A paradigmatic model for CRC would be the ones including the following features: (1) a model that develops few tumours involving the colon epithelium, (2) the tumours are fuelled by somatic alterations of genes known to be involved in human CRC and (3) the tumours follow the canonical pathway from adenoma-carcinoma-metastasis sequence. Attending to these criteria, one of the best models up to date is the one described in 2015 by Scott Lowe laboratory's that was generated by crossing mice harbouring an inducible shRNA against *Apc*, with mice with a conditional *Kras* mutant and a *p53* null allele (sh*Apc*;*Kras*^{G12D};*p53*$^{fl/fl}$;*Lgr*5-CreER). Using this model, the group demonstrated the possibility of generating *Apc* mutated adenomas that develop in the colon and progress to carcinomas upon introduction of *Kras* and *p53* mutations.

From a clinical point of view, uncovering the role of IKKα in tumour initiation and/or progression at the mechanistic level would help to potentially develop preventive and/or curative drugs. Indeed, we already have data revealing the importance of IKKα in tumour maintenance and progression.

Moreover, the observation that IKKα is totally dispensable for normal NF-κB activation[223] but also for normal intestinal homeostasis might facilitate re-evaluating the pre-existing idea that IKK inhibition is therapeutically inappropriate due to its extreme toxicity[564]. In this same direction, our results obtained from in vitro cultured normal intestinal stem cells (ISC) and stem cell-enriched adenoma cells, strongly suggest that normal and transformed stem cells are differentially addicted to IKKα, which open a window for therapeutic interventions. As mentioned, we found that in vivo, IKKα KO tumouroids are significantly smaller when compared to the WT counterparts, which is in part explained by the decrease in proliferating cells marked with Ki67. Importantly, intestinal crypts of both IKKα WT and KO mice were able to generate organoids, demonstrating that IKKα KO non-transformed cells do not have any defect in their ISC pool and they are fully functional.

Our results also reinforce the potential of using organoids and tumouroids as a research tool to further validate experimental results generated from cell lines, since they better recapitulate in vivo observations. State-of-the-art techniques, such as CRISPR/Cas9 for targeted genome-editing, have brought interesting advances such as the introduction of specific mutations of the most commonly mutated colorectal cancer genes (*APC*, *KRAS* and/or

PI3KCA, P53 and *SMAD4*) into organoids derived from normal human intestinal epithelium[105,106]. Mutant organoids can be selected by removing individual growth factors from the culture medium and, for instance, quadruple mutants grow independently of stem-cell-niche factors. Taking into account our results, we are now in the process of deleting IKKα and other elements of the NF-kB pathway (by CRISPR/Cas9) in mouse-derived and human-derived tumouroids to study the impact of IKKα deletion at different stages of the disease. It would be also interesting to study whether IKKα is required at any specific point of CRC progression and related with the sequential acquisition of mutations that are known to occur in this type of cancer. To further investigate its carcinogenic capacities, engineered tumouroids could be implanted in mice and tested for their capacity to engraft and generate metastasis.

Furthermore, by RNA-seq analysis, our results demonstrate that intestinal epithelial IKKα exerts a cell autonomous function in the intestinal adenoma stem cells affecting proliferation and stemness. It would be interesting to study whether IKKα directly mediates expression of particular ISC genes specifically in the oncogenic background and, if so, which are the factors that regulate this differential behaviour. ChIP-seq experiments of IKKα and potential cofactors from normal and transformed organoids will help to explore the underlying mechanisms.

Another open question is whether the reduced expression of stemness associated genes in the IKKα-deficient tumouroids is associated with a reduction in the pool of stem cells in the *Apc*$^{Min/+}$;Ikk*α* mice tumours. Currently, the most accepted approach to determine ISC content is by lineage tracing of *Lgr5* positive cells. Therefore, it would be helpful to cross the Lgr5-EGFP-ires-creERT2 mice with the *Apc*$^{Min/+}$:Ikk*α* WT or KO mice and follow the ISC population in the control and the IKKα-depleted background. Furthermore, this should be extended to other systems where stem cells are well characterised, such as the skin or the hematopoietic system, which would probably help to the understanding of other types of cancer such as leukaemia or SCC.

Although there exists some controversy, it is worth discussing the differential role of IKKα as a tumour suppressor or as an oncogene depending on the type of malignancy. Hu and colleagues very elegantly demonstrated that IKKα is essential for keratinocyte differentiation in the skin and, in accordance, epithelial-specific IKKα deletion induces tumour development. In contrast, we and others[281] have shown that IKKα is necessary for tumour development and progression in the intestine but also

in skin lesions such as SSC. This is of clinical relevance since therapeutic intervention leading to IKKα inhibition would cause adverse effects in particular tissues. It is still not clear the reason why IKKα has such different roles in tumorigenesis, and this is still subject of further study. One possibility is that IKKα, in some specific tissues, has a most prevalent role than in others to maintain homeostasis and, if it is usually mutated or downregulated, this would result in total loss of homeostasis and tumours would arise. On the other hand, in tissues where IKKα has not a pivotal role, when overactivated by different cytokines and other mediators due to increased inflammation or some other responses, this would tend to induce tumorigenesis. Importantly, our data support the concept that IKKα is a plausible target for the development of new anti-cancer therapies which CRC patients could benefit. Further investigation on the upstream and downstream effectors of cancer-associated IKKα activity will provide valuable information for the design of better and more selective therapies against human CRC.

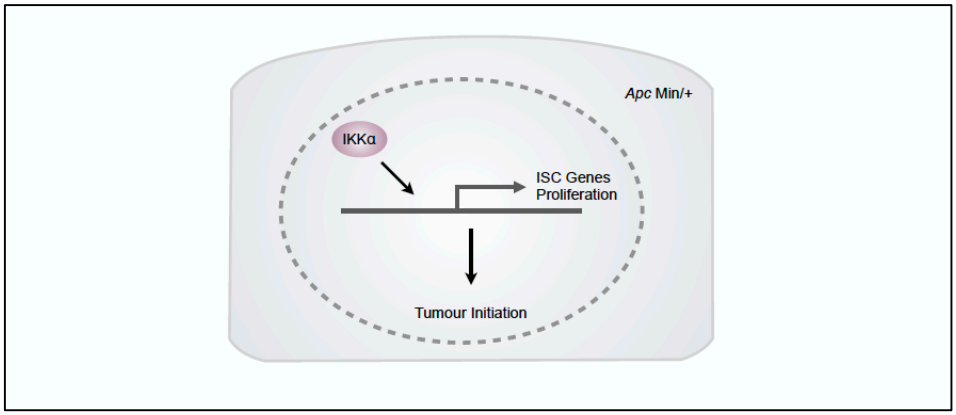

Figure D1 | Working model 1: IKKα controls tumour initiation by regulating stemness and proliferation-related genes.

In the second part of this thesis, we focused on studying the mechanisms by which p45-IKKα[234,285] induces cancer cell survival and which are the elements involved in this process [**FIGURE D2**]. We anticipated the participation of specific targets that might be phosphorylated downstream of IKKα in CRC cells. To validate this possibility, we performed mass spectrometry analysis searching for peptides phosphorylated after BRAF activation in the presence of IKKα. Importantly, 53BP1 and KAP1, two proteins that are closely related to the DNA damage response machinery, were phosphorylated downstream of BRAF only in the presence of IKKα.

This finding prompted us to study a potential role of IKKα in the regulation of the DNA damage response and its putative application to cancer therapy. By WB analysis we demonstrated that p45-IKKα is highly activated and translocated to the nucleus upon DNA damage, and this effect is observed in response to treatment with different DNA damaging agents, including those used in standard anti-cancer treatments such as UV, γIR or doxorubicin. Similar results were obtained using a panel of different CRC cell lines indicating that this is a general response to DNA damage and is not restricted to cells carrying specific mutations. In addition, the dose of UV does not affect p45-IKKα activation in contrast to other reports that claim that different doses of UV activated p53 differently[565]. In the same set of experiments, we show that ERK1/2 is also activated after DNA damage induction further suggesting that BRAF is upstream of p45-IKKα activation after DNA damage, as we next demonstrated using specific inhibitors.

Previous relevant publications indicated that NF-κB can be activated in response to DNA damage and genotoxic stress by a mechanism that involve NEMO nuclear translocation and its ATM-dependent phosphorylation[207,210,525]. However, we have here unequivocally demonstrated that activation of p45-IKKα is independent of “classical” NF-κB since it is independent of NEMO and IKKβ, and it does not involve their nuclear translocation upon induction of DNA damage. Moreover, downregulation of NEMO or IKKβ does not affect the levels of p-Chk1, γH2A.X or ATM in CRC cells in contrast to inhibition of BRAF or downregulation of IKKα. But why NF-κB is not activated in CRC cells? Although we do not have a definitive answer, we previously demonstrated that the main active form of IKK in CRC cells is IKKα, and more specifically a truncated form of the kinase that we called p45-IKKα. In previous work from our laboratory we demonstrated that p45-IKKα does not activate NF-κB but rather participate in specific nuclear functions that we are now trying to uncover. In contrast, our unpublished results indicate that lymphoma cells fail to activate p45-IKKα but rather activate the canonical IKK complex and NF-κB in response to comparable stimuli. Thus, it is possible that different cell types selectively activate p45-IKKα or canonical NF-κB pathway through mechanism that we will investigate in the near future. One possible explanation could rely on the differential activity of cathepsins, that truncate IKKα, in the endosomal compartment of epithelial or hematopoietic cells.

Another question that this work opens is how p45-IKKα is activated in response to DNA damage. Because the response is fast, the more plausible hypothesis is that a specific factor such as BRAF directly phosphorylates

p45-IKKα following its activation by upstream elements such as EGFR. Indeed, there are several publications that demonstrate that EGFR is transactivated after DNA damaging stimuli such as UV and γ-IR[566]. In this regard, we have preliminary results indicating that inhibition of EGFR, with small molecules or monoclonal antibodies, differentially affect p45-IKKα phosphorylation after UV treatment. This suggests that EGFR is activated in a ligand-independent manner after DNA damage, inducing BRAF and p45-IKKα. Moreover, conditioned media from irradiated cells does not induce p45-IKKα activation, demonstrating that it is not through secretion of soluble factors. However, more work needs to be done to further address this question.

In an effort to confirm the contribution of p45-IKKα to the DNA damage response, we analysed p45-IKKα recruitment to damaged sites. For this, we induced localised DNA damage in cancer cells with a 405nm laser, followed by IF analysis of p-IKK S180 together with 53BP1, which is known to associate to the sites of damage[471]. Importantly, we found positive colocalisation between both proteins, demonstrating that activated IKKα is recruited to damaged DNA together with 53BP1. However, these experiments need to be improved, as we did not detect 53BP1 recruitment to all the generated DNA damage stripes and results were highly variable from cell to cell. One possibility of improvement would be to perform live imaging of GFP- or mCherry-tagged IKKα following UV radiation or treatment with other damaging agents. This strategy would also allow us to define the kinetics of IKKα and 53BP1 recruitment in response to particular insults. Our trial of tagging IKKα with a mCherry fusion protein in its N-terminal part mainly failed due to the fact that our tagged protein lost its ability to translocate to the nucleus upon DNA damage induction. One possible explanation for this phenotype is that mCherry imposed a conformational change to IKKα in the chimeric protein that makes it no longer functional in terms of nuclear translocation. Another possibility is that mCherry is interfering with the ability of IKKα to associate with adaptor proteins or modifiers required for its shuttling. Our future strategy involves the use of alternative tags or to directly incorporate the tag at the c-terminus of the p45-kD form.

Another important question that aroused from our data is whether 53BP1 and KAP1 are direct substrates of IKKα and whether this function is specifically achieved after DNA damage induction. Although our first MS experiments were performed in the absence of any treatment, we have to consider that CRC cells have high genetic instability and thus a persistent

activation of the DNA damage response. The second set of experiments mainly support a DNA-damage specific function for IKKα since we consistently found that 53BP1 and KAP1 phosphorylation occurred after UV treatment and significantly decreased in cells IKKα knocked down. However, it is important to take into account that the experimental design also contain some limitations such as the time point after UV induction that was selected for analysis and the strategy followed to generate the data.

For example, we arbitrarily decided to obtain cell lysates 30 minutes after DNA damage induction. Since DDR is a dynamic response we have probably lost the first events of the DDR cascade as well as the final stages of DNA repair. Likely reflecting this bias, we did not detect well-characterised phosphorylation events of the cascade such as p-ATM or γH2A.X, although this could also be due to technical artefacts imposed by non-productive fragmentation of specific proteins regions (some digestion products are too small or too big to be detected) or the presence of unstable phospho-residues. Importantly, to generate our list of candidates as IKKα substrates, we initially compared the phosphorylation levels after UV exposure in both backgrounds (shC and shIKKα) and selected the ones that were induced in control cells but failed to do so in the condition of IKKα downregulation. Although we all agreed with the rationale of the analysis, we should also consider the possibility that some phosphorylated peptides failed to be increased after UV treatment because they were already phosphorylated in the untreated IKKα downregulated cells. In our case, this is not a further concern since we directly validate the phosphorylation levels of the selected targets in either condition by WB.

On the other hand, the fact that we detected two well-known ATM downstream targets as differentially phosphorylated depending on IKKα expression, opens the possibility that IKKα is in fact directly phosphorylating ATM. Although our analysis did not identify ATM as a candidate substrate for IKKα, it is possible that the detection of ATM peptides was missed due to the particularities of the experimental approach, as mentioned above. Indeed, we confirmed by WB that inhibition of BRAF (that blocks p45-IKKα activation) affects ATM phosphorylation after UV treatment. Further studies, such a kinase assay with IKKα and ATM, will be performed to explore this possibility.

Phosphorylation of 53BP1 at T1692 and S1618 occurs during mitosis and help to exclude 53BP1 from the chromatin thus attenuating the DNA damage response[567]. Phosphorylation at these particular residues blocks the interaction of the UDR (Ubiquitination-dependent recruitment) motif with

nucleosomes containing ubiquitinated H2A and impede binding of 53BP1 to mitotic chromatin, avoiding mitotic lesions. Protein phosphatase PP4C/R3β removes these phosphorylations to allow recruitment of 53BP1 to the chromatin in G1 phase. In this scenario, it is reasonable to speculate that phosphorylation at S1618 downstream of IKK is necessary for a fine regulation of the entire DNA damage response and the release of 53BP1 from the chromatin. It could also be that single phosphorylation at S1618 in the absence of T1692 has a different effect on 53BP1 activity and, for example, does not affect 53BP1 recruitment to damaged chromatin, like our IF results suggest. A third possibility is that downregulation of IKKα might impose an increase in phosphorylation of 53BP1 at S1618 under "basal" conditions in cancer cells with high levels of genomic instability and constant DNA damage, and not being further induced after UV treatment. In this scenario, IKKα would be negatively regulating S1618 phosphorylation.

In a recent report, Kubiniok and colleagues studied the phosphoproteomic profile of CRC cells treated or not with vemurafenib, to better understand the paradoxical activation of ERK in cells treated with BRAF inhibitors[419]. Intriguingly, in their MS analysis they identified phosphorylations in 53BP1 that are BRAF dependent, thus further supporting our results. Interestingly, Poulikakos et al identified phosphorylation of 53BP1 at S1114 to be dependent on BRAF, whereas we identified S1113 to be UV and IKKα dependent. This difference in one position could be due to a technical effect of the mass spectrometer, since it is sometimes not that accurate and could differ from one position. The same phosphorylations in KAP1 and MDC1 are also found in their analysis. This data provides strong evidence for our findings.

As mentioned above, previous work from our laboratory uncovered that activation of p45-IKKα is prevented by BRAF or TAK1 inhibition. p45-IKKα is the result of a proteolytic cleavage of full length IKKα which is mediated by endosomal cathepsins. Hence, we previously demonstrated that inhibitors of the endosomal acidification also preclude p45-IKKα phosphorylation. In the current work, we have confirmed our results using different drugs that modulate p45-IKKα activation: BRAF, TAK1 and endosomal acidification inhibitors as well as genetic tools such as shRNAs. Using these approximations, we have demonstrated that BRAF inhibition and IKKα knock down both prevented UV-dependent Chk1 phosphorylation and affected the DDR pathway. In relation with this observation, Zhang and colleagues[568,569] elegantly demonstrated that upon extensive DNA damage Chk1 is ubiquitinated by Fbx6 and consequently degraded, terminating

checkpoint signalling. Protein levels of Chk1 and Fbx6 showed an inverse correlation in cancer cells and impairment of Chk1 degradation is associated with cancer cell resistance to chemotherapy. Therefore, we speculated that this decrease in Chk1 phosphorylation levels could be due to an extensive accumulation of DNA damage after inhibition of IKK activity. To confirm this hypothesis, we plan to do WB analysis of UV induced and IKKα inhibited cells treated with the proteasome inhibitor MG132.

Finally, to further investigate the impact of IKKα-mediated phosphorylation on 53BP1 function, we took advantage of a system that induces dysfunctionality of telomeres, which will activate NHEJ. In most organisms, the end of chromosomes is organised into telomeres that comprise stretches of short-tandem repeats terminating in a 3' protruding ssDNA overhang. Because chromosome ends structurally resemble DSB, there is a specific shelterin complex that is responsible of preventing chromosome fusion by the same mechanism of DDR signalling and NHEJ[570]. TRF2 is one of the components of the shelterin complex, and its loss is sufficient to induce telomere fusions through the activation of ATM[570]. After TRF2 depletion, Mre11, p-ATM, γH2A.X, 53BP1, and RIF1 accumulate at the chromosome ends thus inducing 53BP1-mediated NHEJ. The cytological structures formed by the DNA damage factors are referred to as Telomere dysfunction Induced Foci (TIFs). To test IKKα function in this context, we used MEFS with inducible *Trf2* deletion to promote telomere NHEJ. We demonstrated that BRAF and TAK1 but not MEK inhibition prevent telomere fusions upon TRF2 deletion. This experiment demonstrates that blockage of p45-IKKα upstream kinases is sufficient to block 53BP1 function on NHEJ thus preventing telomere fusions. Further investigation is required to directly demonstrate the contribution of IKKα in TIFs formation induced by 53BP1.

Another way to check 53BP1 function is by IF looking at formation of 53BP1 foci at damaged chromatin after DNA damage. Importantly, we found that after irradiation, control and BRAFi treated cells have the same capacity and kinetics for 53BP1 recruitment, and also for induction of γH2A.X foci. Intriguingly, 24 hours after irradiation BRAF inhibited cells are no able to repair DNA damage as seen by persistent foci detection, compared to control cells (that efficiently resolve DNA damage thus losing γH2A.X foci). In other words, IKKα-mediated phosphorylation of 53BP1 does not affect its recruitment but it does affect its ability to repair damaged DNA.

To move a step further in the investigation of 53BP1 by IKKα, we tested the possibility that IKKα–dependent phosphorylation of 53BP1 may affect association with its partner RIF1, whose recruitment to DNA-damaged foci

is essential for 53BP1 function[484]. We found that BRAF inhibition decreases recruitment of RIF1 to 53BP1 foci, which could explain the loss of functionality. In agreement with this observation, it was previously found that RIF1 binds to 53BP1 when phosphorylated at specific residues within the consensus S/T-Q in its amino-terminal half. It could be a possibility that particular phosphorylation events on 53BP1 dependent on IKKα are important for RIF1 binding. In fact, S1114 is located within this domain.

Why 53BP1 recruitment after BRAF inhibition is impaired at dysfunctional telomeres but it is not at IR-induced foci? We have to take into account that the type of DNA damage is very different, and therefore the signalling and the requirements to activate each pathway might be slightly changed. Deprotected telomeres induce endogenous DNA damage while γ-IR is an exogenous stimulus that may activate additional signals. Moreover, we have found that ATM phosphorylation is decreased, but not lost, upon BRAF inhibition and therefore the few phosphorylated protein left could be enough to induce 53BP1 recruitment.

To demonstrate that the effects that we see with the BRAF inhibitor are mediated by IKKα inactivation, we took two alternative strategies to block IKKα: genetic or pharmacologic inhibition. Using specific shRNA against IKKα or inhibiting IKKα activity by treatment with bafilomycin A1 or chloroquine (as we previously demonstrated). IKKα knockdown led to reduced p-Chk1, p-ATM and γH2A.X, although the effect was not as striking as the one detected after BRAF inhibition. These results suggest a higher efficacy of the BRAF inhibitor on IKKα inactivation or that BRAF exert other activities on the DDR pathway that are not mediated by IKKα. The fact that IKKα KO MEFs present impaired recruitment of RIF1 at the same extend as treatment with BRAF inhibitor, suggests that IKKα knockdown is not sufficient and the remaining IKKα protein is enough to phosphorylate its substrates.

To improve the knock down experiments, it would be of paramount importance to generate CRISPR/Cas9 knock out cells for IKKα. With this technique, we could generate total KO cells avoiding the unpredictable effects of residual IKKα protein. Although, to date we failed to generate IKKα knock out lines using this strategy, we are currently repeating these experiments using different sets of guide DNA. We really believe that IKKα KO CRC lines would be important tools for future experiments deciphering IKKα function.

In the last part of this work, we moved to an in vivo patient-derived xenograft model of human CRC that validated our in vitro results. Our data demonstrates that BRAF/IKKα pathway is important for 53BP1 function and DNA damage repair. Likewise, inhibition of this pathway after DNA-damage induction increased apoptosis in CRC cells. This can be extrapolated to clinical applications using chemotherapeutic agents that induce DNA damage together with BRAF inhibitors currently available in the clinics.

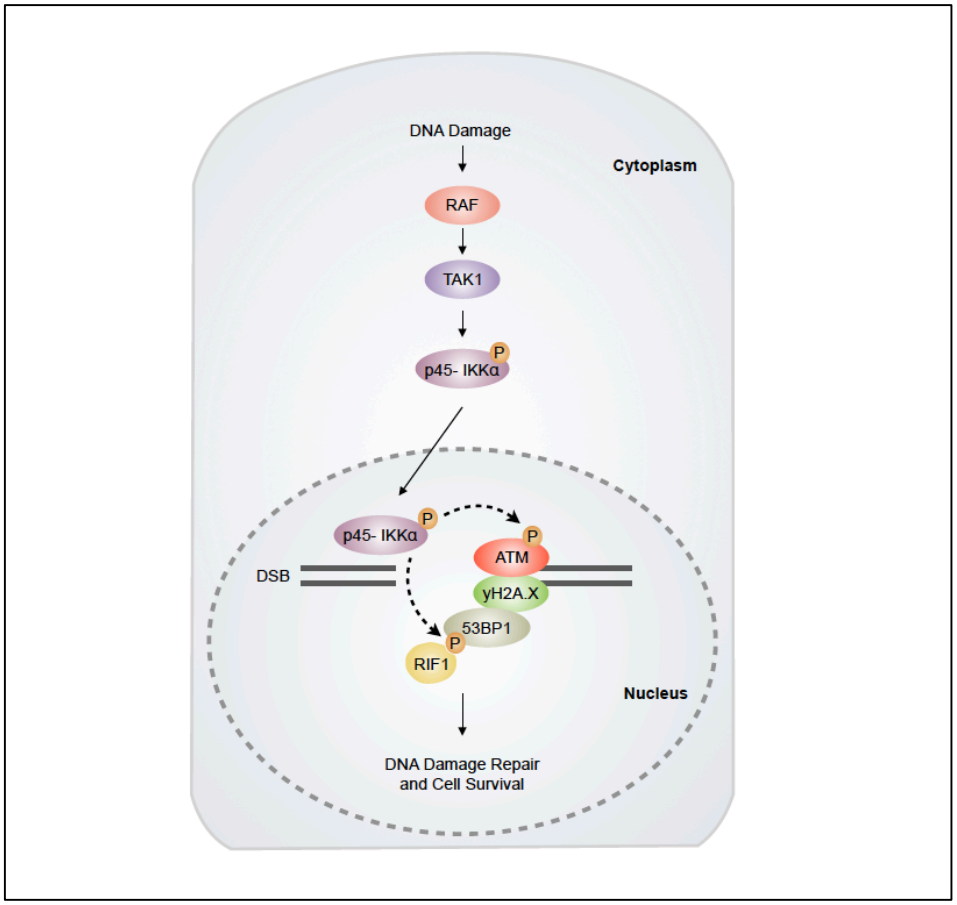

Figure D2 | Working model 2: p45-IKKα role in the DDR pathway. Upon DNA damage induction, BRAF and TAK1 induce p45-IKKα activation and nuclear translocation. In the nuclear compartment, p45-IKKα regulates phosphorylation of 53BP1, directly or through ATM, which is important to repair DNA damage and maintain cancer cell survival.

We first tested this possibility ex vivo, using tumouroids derived from patients. Remarkably, combination of BRAF inhibition with first-line chemotherapy 5FU+Irinotecan highly increased the levels of DNA damage

assessed by γH2A.X staining, leading to enhanced apoptosis. Next, we performed the same combinations in mice bearing the same tumours and interestingly, the combination of vemurafenib plus 5FU+Irinotecan significantly decreased the primary tumour weight and volume. Metastases could not be assessed in this experiment due to the small number of metastasis observed in the controls. Interestingly, we found the same results with drugs that block p45-IKKα activity, chloroquine and bafilomycin A1.

These results open a new therapeutic opportunity for CRC patients. First-line treatments for advanced CRC patients include 5-FU with leucovorin and irinotecan or oxaliplatin[571,572], alone or combined with EGFR-targeted agents[144]. However, the high percentage of KRAS and BRAF mutations in CRC (~50% and 15% respectively) make most of the patients resistant to anti-EGFR antibodies, and only about 15% can benefit from the treatment. We now provide strong data that demonstrates that DNA-damaging agents sensitize cancer cells to BRAF inhibitors, regardless of its mutational status. This opens a new scenario, in which not only patients carrying mutations in $BRAF^{V600E}$ might benefit from these inhibitors as it was previously anticipated and tested[420,423]. Furthermore, this can be extended to adjuvant and neoadjuvant therapies involving chemotherapy or radiation that are commonly used to facilitate subsequent surgical interventions.

Other tumours that are known to rely on IKKα and BRAF activity could also benefit from these findings. For example, around 50% of melanomas are known to harbour BRAF mutations and indeed, vemurafenib is being used to successfully treat melanoma patients, although most of them develop therapeutic resistances. Our expectation is that treating melanoma patients, which are being treated with vemurafenib or a combination of vemurafenib plus MEK inhibitors, with novel protocols including DNA-damaging agents such as chemotherapy or radiation might improve the therapeutic benefit of BRAF/MAPK inhibition, thus increasing patient survival.

In summary, results from the second part of this work provide a new role for BRAF and IKKα in tumour formation and therapy resistance, and provide strong mechanistic data for combining chemotherapy with BRAF inhibitors, thus opening new therapeutic opportunities not only to CRC patients, but hopefully to other cancer patients.

CONCLUSIONS

CONCLUSIONS

Part I

1. Intestinal-specific deletion of IKKα does not affect intestinal homeostasis, but reduces tumour initiation in the *Apc*$^{Min/+}$ mouse model.
2. IKKα is necessary to regulate proliferation of tumour cells but does not affect the proliferating compartment of normal intestinal crypts.
3. IKKα is essential for the growth and proliferation of primary adenoma cells in 3D cultures but not for the growth of normal intestinal stem cells.
4. IKKα controls transcription of a stem cell signature in adenoma cells.
5. IKKα regulates apoptosis and cell cycle related gene programs.

Part II

1. p45-IKKα regulates phosphorylation of the DDR elements 53BP1 and KAP1.
2. p45-IKKα is activated and translocated to the nucleus upon DNA damage induction.
3. BRAF and TAK1 regulate UV-dependent activation of p45-IKKα.
4. Activation of ATM, H2A.X and Chk1 is reduced upon BRAF inhibition.
5. BRAF and TAK1 inhibition prevent 53BP1-mediated chromosome fusions at dysfunctional telomeres.
6. BRAF inhibition and IKKα deficiency prevent RIF1 recruitment to DNA damage foci in irradiated cells.
7. BRAF inhibition induces accumulation of DNA damage in irradiated cells.
8. IKKα, but not NEMO or IKKβ, downregulation affects activation of Chk1 and H2A.X.

9. Inhibition of BRAF or p45-IKKα synergises with chemotherapeutic agents to induce DNA damage and apoptosis of CRC cells in vitro.
10. Inhibition of BRAF or p45-IKKα synergises with chemotherapeutic agents that induce DNA damage to reduce tumour growth in a human CRC PDX model.

BIBLIOGRAPHY

1. Ito, S. The enteric surface coat on cat intestinal microvilli. *J. Cell Biol.* **27,** 475–491 (1965).
2. Specian, R. D. & Oliver, M. G. Functional biology of intestinal goblet cells. *Am. J. Physiol.* **260,** C183-93 (1991).
3. Pelaseyed, T. *et al.* The mucus and mucins of the goblet cells and enterocytes provide the first defense line of the gastrointestinal tract and interact with the immune system. *Immunol. Rev.* **260,** 8–20 (2014).
4. Shan, M. *et al.* Mucus Enhances Gut Homeostasis and Oral Tolerance by Delivering Immunoregulatory Signals. *Science (80-.).* **342,** 447–453 (2013).
5. JARVI, O. & KEYRILAINEN, O. On the cellular structures of the epithelial invasions in the glandular stomach of mice caused by intramural application of 20-methylcholantren. *Acta Pathol. Microbiol. Scand. Suppl.* **39,** 72–3 (1956).
6. von Moltke, J., Ji, M., Liang, H.-E. & Locksley, R. M. Tuft-cell-derived IL-25 regulates an intestinal ILC2–epithelial response circuit. *Nature* **529,** 221–225 (2015).
7. Howitt, M. R. *et al.* Tuft cells, taste-chemosensory cells, orchestrate parasite type 2 immunity in the gut. *Science (80-.).* **351,** 1329–1333 (2016).
8. Gerbe, F. *et al.* Intestinal epithelial tuft cells initiate type 2 mucosal immunity to helminth parasites. *Nature* **529,** 226–230 (2016).
9. Schwalbe, G. Beiträge zur Kenntniss der Drüsen in den Darmwandungen, in's Besondere der Brunner'schen Drüsen. *Arch. für mikroskopische Anat.* **8,** 92–140 (1872).
10. Paneth, J. Ueber die secernirenden Zellen des Dünndarm-Epithels. *Arch. Mikrosk. Anat.* **31,** 113–191 (1888).
11. Deckx, R. J., Vantrappen, G. R. & Parein, M. M. Localization of lysozyme activity in a Paneth cell granule fraction. *Biochim. Biophys. Acta* **139,** 204–7 (1967).
12. Ouellette, A. J., Miller, S. I., Henschen, A. H. & Selsted, M. E. Purification and primary structure of murine cryptdin-1, a Paneth cell defensin. *FEBS Lett.* **304,** 146–148 (1992).
13. Bevins, C. L. & Salzman, N. H. Paneth cells, antimicrobial peptides and maintenance of intestinal homeostasis. *Nat. Rev. Microbiol.* **9,** 356–368 (2011).
14. Clevers, H. C. & Bevins, C. L. Paneth Cells: Maestros of the Small Intestinal Crypts. *Annu. Rev. Physiol.* **75,** 289–311 (2013).
15. Cheng, H. & Leblond, C. P. Origin, differentiation and renewal of the four main epithelial cell types in the mouse small intestine III. Entero-endocrine cells. *Am. J. Anat.* **141,** 503–519 (1974).
16. J, F. *et al.* GLOBOCAN 2012, Cancer Incidence and Mortality Worldwide : IARC CancerBase. *International Agency for Research on Cancer 2014* (2014). Available at: http://globocan.iarc.fr/.
17. Casimiro, C. [Etiopathogenic factors in colorectal cancer. Nutritional and life-style aspects. 2]. *Nutr. Hosp.* **17,** 128–38
18. Shike, M. Diet and lifestyle in the prevention of colorectal cancer: an overview. *Am. J. Med.* **106,** 11S–15S; discussion 50S–51S (1999).

19. Ferlay, J. *et al.* Cancer incidence and mortality worldwide: Sources, methods and major patterns in GLOBOCAN 2012. *Int. J. Cancer* **136,** E359–E386 (2015).
20. Cheng, L. Aberrant crypt foci as microscopic precursors of colorectal cancer. *World J. Gastroenterol.* **9,** 2642 (2003).
21. Siu, I. M., Pretlow, T. G., Amini, S. B. & Pretlow, T. P. Identification of dysplasia in human colonic aberrant crypt foci. *Am. J. Pathol.* **150,** 1805–13 (1997).
22. Maskens, A. P. Histogenesis of adenomatous polyps in the human large intestine. *Gastroenterology* **77,** 1245–51 (1979).
23. Konstantakos, A. K., Siu, I. M., Pretlow, T. G., Stellato, T. A. & Pretlow, T. P. Human aberrant crypt foci with carcinoma in situ from a patient with sporadic colon cancer. *Gastroenterology* **111,** 772–7 (1996).
24. Lengauer, C., Kinzler, K. W. & Vogelstein, B. Genetic instabilities in human cancers. *Nature* **396,** 643–649 (1998).
25. Nowak, M. A. *et al.* The role of chromosomal instability in tumor initiation. *Proc. Natl. Acad. Sci.* **99,** 16226–16231 (2002).
26. Sinicrope, F. A. *et al.* Prognostic Impact of Microsatellite Instability and DNA Ploidy in Human Colon Carcinoma Patients. *Gastroenterology* **131,** 729–737 (2006).
27. Weisenberger, D. J. *et al.* CpG island methylator phenotype underlies sporadic microsatellite instability and is tightly associated with BRAF mutation in colorectal cancer. *Nat. Genet.* **38,** 787–793 (2006).
28. Ogino, S. *et al.* CpG island methylator phenotype, microsatellite instability, BRAF mutation and clinical outcome in colon cancer. *Gut* **58,** 90–96 (2009).
29. Carethers, J. M. & Jung, B. H. Genetics and Genetic Biomarkers in Sporadic Colorectal Cancer. *Gastroenterology* **149,** 1177–1190.e3 (2015).
30. Fearon, E. R. *et al.* A genetic model for colorectal tumorigenesis. *Cell* **61,** 759–67 (1990).
31. Bienz, M. & Clevers, H. Linking colorectal cancer to Wnt signaling. *Cell* **103,** 311–20 (2000).
32. Morin, P. J. *et al.* Activation of beta-catenin-Tcf signaling in colon cancer by mutations in beta-catenin or APC. *Science* **275,** 1787–90 (1997).
33. Powell, S. M. *et al.* APC mutations occur early during colorectal tumorigenesis. *Nature* **359,** 235–237 (1992).
34. Kinzler, K. W. & Vogelstein, B. Lessons from hereditary colorectal cancer. *Cell* **87,** 159–70 (1996).
35. Goss, K. H. & Groden, J. Biology of the Adenomatous Polyposis Coli Tumor Suppressor. *J. Clin. Oncol.* **18,** 1967–1979 (2000).
36. Clevers, H. Wnt/β-Catenin Signaling in Development and Disease. *Cell* **127,** 469–480 (2006).
37. Berx, G., Nollet, F. & van Roy, F. Dysregulation of the E-cadherin/catenin complex by irreversible mutations in human carcinomas. *Cell Adhes. Commun.* **6,** 171–84 (1998).
38. Bailey, T. *et al.* Altered cadherin and catenin complexes in the Barrett's esophagus-dysplasia-adenocarcinoma sequence: correlation with disease progression and dedifferentiation. *Am. J. Pathol.* **152,** 135–44 (1998).

39. Downward, J. Targeting RAS signalling pathways in cancer therapy. *Nat. Rev. Cancer* **3,** 11–22 (2003).
40. Markowitz, S. *et al.* Inactivation of the type II TGF-beta receptor in colon cancer cells with microsatellite instability. *Science* **268,** 1336–8 (1995).
41. Vogelstein, B. *et al.* Allelotype of colorectal carcinomas. *Science (80-.).* **244,** (1989).
42. Calon, A. *et al.* Dependency of Colorectal Cancer on a TGF-β-Driven Program in Stromal Cells for Metastasis Initiation. *Cancer Cell* **22,** 571–584 (2012).
43. Fearon, E. R. *et al.* Identification of a chromosome 18q gene that is altered in colorectal cancers. *Science* **247,** 49–56 (1990).
44. Sui, X. *et al.* p53 controls colorectal cancer cell invasion by inhibiting the NF-κB-mediated activation of Fascin. *Oncotarget* **6,** 22869–79 (2015).
45. Bunz, F. *et al.* Disruption of p53 in human cancer cells alters the responses to therapeutic agents. *J. Clin. Invest.* **104,** 263–9 (1999).
46. Benhattar, J., Cerottini, J.-P., Saraga, E., Metthez, G. & Givel, J.-C. p53 mutations as a possible predictor of response to chemotherapy in metastatic colorectal carcinomas. *Int. J. Cancer* **69,** 190–192 (1996).
47. Sottoriva, A. *et al.* A Big Bang model of human colorectal tumor growth. *Nat. Genet.* **47,** 209–216 (2015).
48. March, H. N. *et al.* Insertional mutagenesis identifies multiple networks of cooperating genes driving intestinal tumorigenesis. *Nat. Genet.* **43,** 1202–1209 (2011).
49. Muzny, D. M. *et al.* Comprehensive molecular characterization of human colon and rectal cancer. *Nature* **487,** 330–337 (2012).
50. Vogelstein, B. *et al.* Cancer Genome Landscapes. *Science (80-.).* **339,** 1546–1558 (2013).
51. Chung, D. C. & Rustgi, A. K. DNA mismatch repair and cancer. *Gastroenterology* **109,** 1685–1699 (1995).
52. Thibodeau, S., Bren, G. & Schaid, D. Microsatellite instability in cancer of the proximal colon. *Science (80-.).* **260,** (1993).
53. Ionov, Y., Peinado, M. A., Malkhosyan, S., Shibata, D. & Perucho, M. Ubiquitous somatic mutations in simple repeated sequences reveal a new mechanism for colonic carcinogenesis. *Nature* **363,** 558–561 (1993).
54. Grady, W. M., Rajput, A., Lutterbaugh, J. D. & Markowitz, S. D. Detection of aberrantly methylated hMLH1 promoter DNA in the serum of patients with microsatellite unstable colon cancer. *Cancer Res.* **61,** 900–2 (2001).
55. Boland, C. R. & Goel, A. Microsatellite instability in colorectal cancer. *Gastroenterology* **138,** 2073–2087.e3 (2010).
56. Jasperson, K. W., Tuohy, T. M., Neklason, D. W. & Burt, R. W. Hereditary and familial colon cancer. *Gastroenterology* **138,** 2044–58 (2010).
57. Grady, W. M. Genetic testing for high-risk colon cancer patients. *Gastroenterology* **124,** 1574–1594 (2003).
58. Lynch, H. T. & de la Chapelle, A. Hereditary Colorectal Cancer. *N. Engl. J. Med.* **348,** 919–932 (2003).
59. Kerber, R. A., Neklason, D. W., Samowitz, W. S. & Burt, R. W. Frequency of Familial Colon Cancer and Hereditary Nonpolyposis Colorectal Cancer (Lynch Syndrome) in a Large Population Database. *Fam. Cancer* **4,** 239–

244 (2005).
60. Hampel, H. *et al.* Feasibility of Screening for Lynch Syndrome Among Patients With Colorectal Cancer. *J. Clin. Oncol.* **26,** 5783–5788 (2008).
61. Peltomäki, P. *et al.* Microsatellite Instability Is Associated with Tumors That Characterize the Hereditary Non-Polyposis Colorectal Carcinoma Syndrome. *Cancer Res.* **53,** (1993).
62. Bronner, C. E. *et al.* Mutation in the DNA mismatch repair gene homologue hMLH 1 is associated with hereditary non-polyposis colon cancer. *Nature* **368,** 258–261 (1994).
63. Kastrinos, F. & Syngal, S. Inherited colorectal cancer syndromes. *Cancer J.* **17,** 405–15 (2011).
64. Loeb, L. A., Loeb, K. R. & Anderson, J. P. Multiple mutations and cancer. *Proc. Natl. Acad. Sci. U. S. A.* **100,** 776–81 (2003).
65. Markowitz, S. TGF-beta receptors and DNA repair genes, coupled targets in a pathway of human colon carcinogenesis. *Biochim. Biophys. Acta* **1470,** M13-20 (2000).
66. Rubinfeld, B. *et al.* Association of the APC gene product with beta-catenin. *Science (80-.).* **262,** (1993).
67. Munemitsu, S., Albert, I., Souza, B., Rubinfeld, B. & Polakis, P. Regulation of intracellular beta-catenin levels by the adenomatous polyposis coli (APC) tumor-suppressor protein. *Proc. Natl. Acad. Sci. U. S. A.* **92,** 3046–50 (1995).
68. Su, L., Vogelstein, B. & Kinzler, K. Association of the APC tumor suppressor protein with catenins. *Science (80-.).* **262,** (1993).
69. Ikeda, S. *et al.* Axin, a negative regulator of the Wnt signaling pathway, forms a complex with GSK-3β and β-catenin and promotes GSK-3β-dependent phosphorylation of β-catenin. *EMBO J.* **17,** 1371–1384 (1998).
70. Kishida, S. *et al.* Axin, a negative regulator of the Wnt signaling pathway, directly interacts with adenomatous polyposis coli and regulates the stabilization of β-catenin. *J. Biol. Chem.* **273,** 10823–10826 (1998).
71. Sakanaka, C., Weiss, J. B. & Williams, L. T. Bridging of beta-catenin and glycogen synthase kinase-3beta by axin and inhibition of beta-catenin-mediated transcription. *Proc. Natl. Acad. Sci. U. S. A.* **95,** 3020–3 (1998).
72. Liu, C. *et al.* Control of β-catenin phosphorylation/degradation by a dual-kinase mechanism. *Cell* **108,** 837–847 (2002).
73. Guinney, J. *et al.* The consensus molecular subtypes of colorectal cancer. *Nat. Med.* **21,** 1350–1356 (2015).
74. Groden, J. *et al.* Identification and characterization of the familial adenomatous polyposis coli gene. *Cell* **66,** 589–600 (1991).
75. Moser, A. R., Pitot, H. C. & Dove, W. F. A dominant mutation that predisposes to multiple intestinal neoplasia in the mouse. *Science* **247,** 322–4 (1990).
76. Su, L. K. *et al.* Multiple intestinal neoplasia caused by a mutation in the murine homolog of the APC gene. *Science* **256,** 668–70 (1992).
77. Halberg, R. B. *et al.* Tumorigenesis in the multiple intestinal neoplasia mouse: Redundancy of negative regulators and specificity of modifiers. *Proc. Natl. Acad. Sci.* **97,** 3461–3466 (2000).
78. Hinoi, T. *et al.* Mouse model of colonic adenoma-carcinoma progression

based on somatic Apc inactivation. *Cancer Res.* **67,** 9721–9730 (2007).
79. Robanus-Maandag, E. C. *et al.* A new conditional Apc-mutant mouse model for colorectal cancer. *Carcinogenesis* **31,** 946–952 (2010).
80. Shibata, H. Rapid Colorectal Adenoma Formation Initiated by Conditional Targeting of the Apc Gene. *Science (80-.).* **278,** 120–123 (1997).
81. Hung, K. E. *et al.* Development of a mouse model for sporadic and metastatic colon tumors and its use in assessing drug treatment. *Proc. Natl. Acad. Sci.* **107,** 1565–1570 (2010).
82. Dow, L. E. *et al.* Apc Restoration Promotes Cellular Differentiation and Reestablishes Crypt Homeostasis in Colorectal Cancer. *Cell* **161,** 1539–1552 (2015).
83. Hung, K. E. *et al.* Development of a mouse model for sporadic and metastatic colon tumors and its use in assessing drug treatment. *Proc. Natl. Acad. Sci.* **107,** 1565–1570 (2010).
84. Janssen, K. *et al.* APC and oncogenic KRAS are synergistic in enhancing Wnt signaling in intestinal tumor formation and progression. *Gastroenterology* **131,** 1096–1109 (2006).
85. Sansom, O. J. *et al.* Loss of Apc allows phenotypic manifestation of the transforming properties of an endogenous K-ras oncogene in vivo. *Proc. Natl. Acad. Sci.* **103,** 14122–14127 (2006).
86. Marsh, V. *et al.* Epithelial Pten is dispensable for intestinal homeostasis but suppresses adenoma development and progression after Apc mutation. *Nat. Genet.* **40,** 1436–1444 (2008).
87. Deming, D. A. *et al.* PIK3CA and APC mutations are synergistic in the development of intestinal cancers. *Oncogene* **33,** 2245–2254 (2014).
88. Leystra, A. A. *et al.* Mice Expressing Activated PI3K Rapidly Develop Advanced Colon Cancer. *Cancer Res.* **72,** 2931–2936 (2012).
89. Muñoz, N. M. *et al.* Transforming growth factor beta receptor type II inactivation induces the malignant transformation of intestinal neoplasms initiated by Apc mutation. *Cancer Res.* **66,** 9837–9844 (2006).
90. Takaku, K. *et al.* Intestinal tumorigenesis in compound mutant mice of both Dpc4 (Smad4) and Apc genes. *Cell* **92,** 645–56 (1998).
91. Sodir, N. M. *et al.* Smad3 Deficiency Promotes Tumorigenesis in the Distal Colon of *Apc* $^{Min/+}$ Mice. *Cancer Res.* **66,** 8430–8438 (2006).
92. Hamamoto, T. *et al.* Compound disruption of smad2 accelerates malignant progression of intestinal tumors in apc knockout mice. *Cancer Res.* **62,** 5955–61 (2002).
93. Muller, P. A. J. *et al.* Mutant p53 Drives Invasion by Promoting Integrin Recycling. *Cell* **139,** 1327–1341 (2009).
94. Okayasu, I. *et al.* Dysplasia and carcinoma development in a repeated dextran sulfate sodium-induced colitis model. *J. Gastroenterol. Hepatol.* **17,** 1078–83 (2002).
95. Hidalgo, M. *et al.* Patient-Derived Xenograft Models: An Emerging Platform for Translational Cancer Research. *Cancer Discov.* **4,** (2014).
96. Vidal, A. *et al.* Lurbinectedin (PM01183), a New DNA Minor Groove Binder, Inhibits Growth of Orthotopic Primary Graft of Cisplatin-Resistant Epithelial Ovarian Cancer. *Clin. Cancer Res.* **18,** (2012).
97. Cutz, J.-C. *et al.* Establishment in Severe Combined Immunodeficiency

Mice of Subrenal Capsule Xenografts and Transplantable Tumor Lines from a Variety of Primary Human Lung Cancers: Potential Models for Studying Tumor Progression–Related Changes. *Clin. Cancer Res.* **12,** (2006).
98. Kalscheuer, H. *et al.* A Model for Personalized in Vivo Analysis of Human Immune Responsiveness. *Sci. Transl. Med.* **4,** 125ra30-125ra30 (2012).
99. Garrido-Laguna, I. *et al.* Tumor Engraftment in Nude Mice and Enrichment in Stroma- Related Gene Pathways Predict Poor Survival and Resistance to Gemcitabine in Patients with Pancreatic Cancer. *Clin. Cancer Res.* **17,** 5793–5800 (2011).
100. Eirew, P. *et al.* Dynamics of genomic clones in breast cancer patient xenografts at single-cell resolution. *Nature* **518,** 422–426 (2014).
101. Sato, T. *et al.* Single Lgr5 stem cells build crypt–villus structures in vitro without a mesenchymal niche. *Nature* **459,** 262–265 (2009).
102. Jung, P. *et al.* Isolation and in vitro expansion of human colonic stem cells. *Nat. Med.* **17,** 1225–1227 (2011).
103. Sato, T. *et al.* Long-term Expansion of Epithelial Organoids From Human Colon, Adenoma, Adenocarcinoma, and Barrett's Epithelium. *Gastroenterology* **141,** 1762–1772 (2011).
104. Van De Wetering, M. *et al.* Prospective derivation of a living organoid biobank of colorectal cancer patients. *Cell* **161,** 933–945 (2015).
105. Matano, M. *et al.* Modeling colorectal cancer using CRISPR-Cas9–mediated engineering of human intestinal organoids. *Nat. Med.* **21,** 256–62 (2015).
106. Drost, J. *et al.* Sequential cancer mutations in cultured human intestinal stem cells. *Nature* **521,** 43–47 (2015).
107. Dick, J. E. Stem cell concepts renew cancer research. *Blood* **112,** 4793–4807 (2008).
108. Clevers, H. The cancer stem cell: premises, promises and challenges. *Nat. Med.* **17,** 313–319 (2011).
109. Visvader, J. E. & Lindeman, G. J. Cancer stem cells in solid tumours: accumulating evidence and unresolved questions. *Nat. Rev. Cancer* **8,** 755–768 (2008).
110. Dick, J. E. Stem cell concepts renew cancer research. *Blood* **112,** 4793–4807 (2008).
111. Colak, S. & Medema, J. P. Cancer stem cells - important players in tumor therapy resistance. *FEBS J.* **281,** 4779–4791 (2014).
112. Barker, N. *et al.* Crypt stem cells as the cells-of-origin of intestinal cancer. *Nature* **457,** 608–611 (2009).
113. Shimokawa, M. *et al.* Visualization and targeting of LGR5+ human colon cancer stem cells. *Nature* **545,** 187–192 (2017).
114. Melo, F. de S. e *et al.* A distinct role for Lgr5+ stem cells in primary and metastatic colon cancer. *Nature* **543,** 676–680 (2017).
115. Shimokawa, M. *et al.* Visualization and targeting of LGR5+ human colon cancer stem cells. *Nature* **545,** 187–192 (2017).
116. Ricci-Vitiani, L. *et al.* Identification and expansion of human colon-cancer-initiating cells. *Nature* **445,** 111–115 (2007).
117. O'Brien, C. A. *et al.* A human colon cancer cell capable of initiating tumour

growth in immunodeficient mice. *Nature* **445,** 106–110 (2007).
118. Zhu, L. *et al.* Prominin 1 marks intestinal stem cells that are susceptible to neoplastic transformation. *Nature* **457,** 603–607 (2009).
119. Merlos-Suárez, A. *et al.* The Intestinal Stem Cell Signature Identifies Colorectal Cancer Stem Cells and Predicts Disease Relapse. *Cell Stem Cell* **8,** 511–524 (2011).
120. Nishimura, S., Wakabayashi, N., Toyoda, K., Kashima, K. & Mitsufuji, S. Expression of Musashi-1 in human normal colon crypt cells: a possible stem cell marker of human colon epithelium. *Dig. Dis. Sci.* **48,** 1523–9 (2003).
121. Murayama, M. *et al.* Musashi-1 suppresses expression of Paneth cell-specific genes in human intestinal epithelial cells. *J. Gastroenterol.* **44,** 173–182 (2009).
122. Potten, C. S. *et al.* Identification of a putative intestinal stem cell and early lineage marker; musashi-1. *Differentiation* **71,** 28–41 (2003).
123. Sureban, S. M. *et al.* Knockdown of RNA Binding Protein Musashi-1 Leads to Tumor Regression In Vivo. *Gastroenterology* **134,** 1448–1458.e2 (2008).
124. Li, D. *et al.* Msi-1 is a Predictor of Survival and a Novel Therapeutic Target in Colon Cancer. *Ann. Surg. Oncol.* **18,** 2074–2083 (2011).
125. Rezza, A. *et al.* The overexpression of the putative gut stem cell marker Musashi-1 induces tumorigenesis through Wnt and Notch activation. *J. Cell Sci.* **123,** 3256–3265 (2010).
126. Kreso, A. *et al.* Self-renewal as a therapeutic target in human colorectal cancer. *Nat. Med.* **20,** 29–36 (2013).
127. Jay, P., Berta, P. & Blache, P. Expression of the Carcinoembryonic Antigen Gene Is Inhibited by SOX9 in Human Colon Carcinoma Cells. *Cancer Res.* **65,** 2193–2198 (2005).
128. Darido, C. *et al.* Defective Claudin-7 Regulation by Tcf-4 and Sox-9 Disrupts the Polarity and Increases the Tumorigenicity of Colorectal Cancer Cells. *Cancer Res.* **68,** 4258–4268 (2008).
129. Abdel-Samad, R. *et al.* MiniSOX9, a dominant-negative variant in colon cancer cells. *Oncogene* **30,** 2493–2503 (2011).
130. Lü, B. *et al.* Analysis of SOX9 Expression in Colorectal Cancer. *Am. J. Clin. Pathol.* **130,** 897–904 (2008).
131. Matheu, A. *et al.* Oncogenicity of the Developmental Transcription Factor Sox9. *Cancer Res.* **72,** 1301–1315 (2012).
132. Huang, E. H. *et al.* Aldehyde dehydrogenase 1 is a marker for normal and malignant human colonic stem cells (SC) and tracks SC overpopulation during colon tumorigenesis. *Cancer Res.* **69,** 3382–9 (2009).
133. Pang, R. *et al.* A subpopulation of CD26 + cancer stem cells with metastatic capacity in human colorectal cancer. *Cell Stem Cell* **6,** 603–615 (2010).
134. Nakanishi, Y. *et al.* Dclk1 distinguishes between tumor and normal stem cells in the intestine. *Nat. Genet.* **45,** 98–103 (2012).
135. Asfaha, S. *et al.* Krt19(+)/Lgr5(-) Cells Are Radioresistant Cancer-Initiating Stem Cells in the Colon and Intestine. *Cell Stem Cell* **16,** 627–38 (2015).
136. Neumann, J. *et al.* SOX2 expression correlates with lymph-node metastases and distant spread in right-sided colon cancer. *BMC Cancer*

11, 518 (2011).
137. Gao, W. *et al.* Isolation and Phenotypic Characterization of Colorectal Cancer Stem Cells With Organ-Specific Metastatic Potential. *Gastroenterology* **145,** 636–646.e5 (2013).
138. Wu, Z. *et al.* TPO-Induced Metabolic Reprogramming Drives Liver Metastasis of Colorectal Cancer CD110+ Tumor-Initiating Cells. *Cell Stem Cell* **17,** 47–59 (2015).
139. Van Cutsem, E. *et al.* ESMO consensus guidelines for the management of patients with metastatic colorectal cancer. *Ann. Oncol.* **27,** 1386–1422 (2016).
140. Asmis, T. *et al.* Strategies of sequential therapies in unresectable metastatic colorectal cancer: a meta-analysis. *Curr. Oncol.* **21,** 318 (2014).
141. Cohen, M. H., Gootenberg, J., Keegan, P. & Pazdur, R. FDA Drug Approval Summary: Bevacizumab Plus FOLFOX4 as Second-Line Treatment of Colorectal Cancer. *Oncologist* **12,** 356–61 (2007).
142. Verdaguer, H., Tabernero, J. & Macarulla, T. Ramucirumab in metastatic colorectal cancer: evidence to date and place in therapy. *Ther. Adv. Med. Oncol.* **8,** 230–42 (2016).
143. Patel, A. & Sun, W. Ziv-aflibercept in metastatic colorectal cancer. *Biologics* **8,** 13–25 (2014).
144. Van Cutsem, E. *et al.* Cetuximab and Chemotherapy as Initial Treatment for Metastatic Colorectal Cancer. *N. Engl. J. Med.* **360,** 1408–1417 (2009).
145. Bokemeyer, C. *et al.* Fluorouracil, Leucovorin, and Oxaliplatin With and Without Cetuximab in the First-Line Treatment of Metastatic Colorectal Cancer. *J. Clin. Oncol.* **27,** 663–671 (2009).
146. Douillard, J.-Y. *et al.* Randomized, phase III trial of panitumumab with infusional fluorouracil, leucovorin, and oxaliplatin (FOLFOX4) versus FOLFOX4 alone as first-line treatment in patients with previously untreated metastatic colorectal cancer: the PRIME study. *J. Clin. Oncol.* **28,** 4697–705 (2010).
147. Amado, R. G. *et al.* Wild-Type *KRAS* Is Required for Panitumumab Efficacy in Patients With Metastatic Colorectal Cancer. *J. Clin. Oncol.* **26,** 1626–1634 (2008).
148. Karapetis, C. S. *et al. K-ras* Mutations and Benefit from Cetuximab in Advanced Colorectal Cancer. *N. Engl. J. Med.* **359,** 1757–1765 (2008).
149. Boland, P. M. & Fakih, M. The emerging role of neoadjuvant chemotherapy for rectal cancer. *J. Gastrointest. Oncol.* **5,** 362–73 (2014).
150. Pita-Fernández, S. *et al.* Intensive follow-up strategies improve outcomes in nonmetastatic colorectal cancer patients after curative surgery: a systematic review and meta-analysis. *Ann. Oncol.* **26,** 644–656 (2015).
151. Sen, R. & Baltimore, D. Multiple nuclear factors interact with the immunoglobulin enhancer sequences. *Cell* **46,** 705–716 (1986).
152. Ben-Neriah, Y. & Karin, M. Inflammation meets cancer, with NF-κB as the matchmaker. *Nat. Immunol.* **12,** 715–723 (2011).
153. Simmonds, R. E. & Foxwell, B. M. Signalling, inflammation and arthritis: NF-κB and its relevance to arthritis and inflammation. *Rheumatology* **47,** 584–590 (2008).
154. Barnes, P. J. & Adcock, I. M. NF-kappa B: a pivotal role in asthma and a

new target for therapy. *Trends Pharmacol Sci* **18,** 46–50 (1997).
155. Schütze, S. & Schneider-Brachert, W. Impact of TNF-R1 and CD95 Internalization on Apoptotic and Antiapoptotic Signaling. in 63–85 (Springer, Berlin, Heidelberg, 2009). doi:10.1007/400_2008_23
156. Smith, C. A., Farrah, T. & Goodwin, R. G. The TNF receptor superfamily of cellular and viral proteins: Activation, costimulation, and death. *Cell* **76,** 959–962 (1994).
157. Hsu, H., Xiong, J. & Goeddel, D. V. The TNF receptor 1-associated protein TRADD signals cell death and NF-κB activation. *Cell* **81,** 495–504 (1995).
158. Hsu, H., Huang, J., Shu, H.-B., Baichwal, V. & Goeddel, D. V. TNF-Dependent Recruitment of the Protein Kinase RIP to the TNF Receptor-1 Signaling Complex. *Immunity* **4,** 387–396 (1996).
159. Boldin, M. P. *et al.* Self-association of the "death domains" of the p55 tumor necrosis factor (TNF) receptor and Fas/APO1 prompts signaling for TNF and Fas/APO1 effects. *J. Biol. Chem.* **270,** 387–91 (1995).
160. Boldin, M. P. *et al.* A novel protein that interacts with the death domain of Fas/APO1 contains a sequence motif related to the death domain. *J. Biol. Chem.* **270,** 7795–8 (1995).
161. Pobezinskaya, Y. L. *et al.* The function of TRADD in signaling through tumor necrosis factor receptor 1 and TRIF-dependent Toll-like receptors. *Nat. Immunol.* **9,** 1047–1054 (2008).
162. Chen, N.-J. *et al.* Beyond tumor necrosis factor receptor: TRADD signaling in toll-like receptors. *Proc. Natl. Acad. Sci.* **105,** 12429–12434 (2008).
163. Ermolaeva, M. A. *et al.* Function of TRADD in tumor necrosis factor receptor 1 signaling and in TRIF-dependent inflammatory responses. *Nat. Immunol.* **9,** 1037–1046 (2008).
164. Varfolomeev, E. *et al.* IAP Antagonists Induce Autoubiquitination of c-IAPs, NF-κ B Activation, and TNFα-Dependent Apoptosis. *Cell* **131,** 669–681 (2007).
165. Mahoney, D. J. *et al.* Both cIAP1 and cIAP2 regulate TNFalpha-mediated NF-kappaB activation. *Proc. Natl. Acad. Sci. U. S. A.* **105,** 11778–83 (2008).
166. Vince, J. E. *et al.* IAP Antagonists Target cIAP1 to Induce TNFα-Dependent Apoptosis. *Cell* **131,** 682–693 (2007).
167. Haas, T. L. *et al.* Recruitment of the Linear Ubiquitin Chain Assembly Complex Stabilizes the TNF-R1 Signaling Complex and Is Required for TNF-Mediated Gene Induction. *Mol. Cell* **36,** 831–844 (2009).
168. Rahighi, S. *et al.* Specific Recognition of Linear Ubiquitin Chains by NEMO Is Important for NF-κB Activation. *Cell* **136,** 1098–1109 (2009).
169. Tokunaga, F. *et al.* Involvement of linear polyubiquitylation of NEMO in NF-κB activation. *Nat. Cell Biol.* **11,** 123–132 (2009).
170. Gerlach, B. *et al.* Linear ubiquitination prevents inflammation and regulates immune signalling. *Nature* **471,** 591–596 (2011).
171. Ikeda, F. *et al.* SHARPIN forms a linear ubiquitin ligase complex regulating NF-κB activity and apoptosis. *Nature* **471,** 637–641 (2011).
172. Zhao, Q. & Lee, F. S. Mitogen-activated protein kinase/ERK kinase kinases 2 and 3 activate nuclear factor-kappaB through IkappaB kinase-alpha and

IkappaB kinase-beta. *J. Biol. Chem.* **274,** 8355–8 (1999).
173. Wang, C. *et al.* TAK1 is a ubiquitin-dependent kinase of MKK and IKK. *Nature* **412,** 346–51 (2001).
174. Ishitani, T. *et al.* Role of the TAB2-related protein TAB3 in IL-1 and TNF signaling. *EMBO J.* **22,** 6277–6288 (2003).
175. Sakurai, H., Miyoshi, H., Mizukami, J. & Sugita, T. Phosphorylation-dependent activation of TAK1 mitogen-activated protein kinase kinase kinase by TAB1. *FEBS Lett.* **474,** 141–145 (2000).
176. Karin, M. & Ben-Neriah, Y. Phosphorylation Meets Ubiquitination: The Control of NF-κB Activity. *Annu. Rev. Immunol.* **18,** 621–663 (2000).
177. Wertz, I. E. *et al.* De-ubiquitination and ubiquitin ligase domains of A20 downregulate NF-κB signalling. *Nature* **430,** 694–699 (2004).
178. Brummelkamp, T. R., Nijman, S. M. B., Dirac, A. M. G. & Bernards, R. Loss of the cylindromatosis tumour suppressor inhibits apoptosis by activating NF-κB. *Nature* **424,** 797–801 (2003).
179. Kovalenko, A. *et al.* The tumour suppressor CYLD negatively regulates NF-κB signalling by deubiquitination. *Nature* **424,** 801–805 (2003).
180. Trompouki, E. *et al.* CYLD is a deubiquitinating enzyme that negatively regulates NF-κB activation by TNFR family members. *Nature* **424,** 793–796 (2003).
181. Keusekotten, K. *et al.* OTULIN antagonizes LUBAC signaling by specifically hydrolyzing met1-linked polyubiquitin. *Cell* **153,** 1312–1326 (2013).
182. Chen, Z. J. Ubiquitin signalling in the NF-kappaB pathway. *Nat. Cell Biol.* **7,** 758–65 (2005).
183. Coope, H. J. CD40 regulates the processing of NF-kappaB2 p100 to p52. *EMBO J.* **21,** 5375–5385 (2002).
184. Claudio, E., Brown, K., Park, S., Wang, H. & Siebenlist, U. BAFF-induced NEMO-independent processing of NF-κB2 in maturing B cells. *Nat. Immunol.* **3,** 958–965 (2002).
185. Dejardin, E. *et al.* The Lymphotoxin-β Receptor Induces Different Patterns of Gene Expression via Two NF-κB Pathways. *Immunity* **17,** 525–535 (2002).
186. Vaira, S. *et al.* RelB is the NF-kappaB subunit downstream of NIK responsible for osteoclast differentiation. *Proc. Natl. Acad. Sci. U. S. A.* **105,** 3897–902 (2008).
187. Senftleben, U. *et al.* Activation by IKKα of a second, evolutionary conserved, NF-kB signaling pathway. *Science (80-.).* **293,** 1495–1499 (2001).
188. Liao, G., Zhang, M., Harhaj, E. W. & Sun, S.-C. C. Regulation of the NF-κB-inducing kinase by tumor necrosis factor receptor-associated factor 3-induced degradation. *J. Biol. Chem.* **279,** 26243–26250 (2004).
189. He, J. Q. *et al.* Rescue of TRAF3-null mice by p100 NF-kappa B deficiency. *J. Exp. Med.* **203,** 2413–8 (2006).
190. He, J. Q., Saha, S. K., Kang, J. R., Zarnegar, B. & Cheng, G. Specificity of TRAF3 in its negative regulation of the noncanonical NF-κB pathway. *J. Biol. Chem.* **282,** 3688–3694 (2007).
191. Vallabhapurapu, S. *et al.* Nonredundant and complementary functions of

TRAF2 and TRAF3 in a ubiquitination cascade that activates NIK-dependent alternative NF-κB signaling. *Nat. Immunol.* **9,** 1364–1370 (2008).
192. Vince, J. E. *et al.* IAP Antagonists Target cIAP1 to Induce TNFα-Dependent Apoptosis. *Cell* **131,** 682–693 (2007).
193. Xiao, G., Harhaj, E. W. & Sun, S. C. NF-κB-inducing kinase regulates the processing of NF-κB2 p100. *Mol. Cell* **7,** 401–409 (2001).
194. Betts, J. C. & Nabel, G. J. Differential regulation of NF-kappaB2(p100) processing and control by amino-terminal sequences. *Mol. Cell. Biol.* **16,** 6363–71 (1996).
195. Solan, N. J., Miyoshi, H., Carmona, E. M., Bren, G. D. & Paya, C. V. RelB Cellular Regulation and Transcriptional Activity Are Regulated by p100. *J. Biol. Chem.* **277,** 1405–1418 (2002).
196. Zarnegar, B., Yamazaki, S., He, J. Q. & Cheng, G. Control of canonical NF-kappaB activation through the NIK-IKK complex pathway. *Proc. Natl. Acad. Sci. U. S. A.* **105,** 3503–3508 (2008).
197. Martin, M. U. & Wesche, H. Summary and comparison of the signaling mechanisms of the Toll/interleukin-1 receptor family. *Biochim. Biophys. Acta* **1592,** 265–80 (2002).
198. Yamamoto, M. & Akira, S. TIR Domain-Containing Adaptors Regulate TLR Signaling Pathways. in *Mechanisms of Lymphocyte Activation and Immune Regulation X* **560,** 1–9 (Springer US, 2005).
199. Yamamoto, M. Role of Adaptor TRIF in the MyD88-Independent Toll-Like Receptor Signaling Pathway. *Science (80-.).* **301,** 640–643 (2003).
200. Takeda, K. & Akira, S. TLR signaling pathways. *Semin. Immunol.* **16,** 3–9 (2004).
201. Deng, L. *et al.* Activation of the IkappaB kinase complex by TRAF6 requires a dimeric ubiquitin-conjugating enzyme complex and a unique polyubiquitin chain. *Cell* **103,** 351–61 (2000).
202. Wang, C. *et al.* TAK1 is a ubiquitin-dependent kinase of MKK and IKK. *Nature* **412,** 346–51 (2001).
203. Li, N. & Karin, M. Ionizing radiation and short wavelength UV activate NF-κB through two distinct mechanisms. *Cell Biol.* **95,** 13012–13017 (1998).
204. Biton, S. & Ashkenazi, A. NEMO and RIP1 Control Cell Fate in Response to Extensive DNA Damage via TNF-α Feedforward Signaling. *Cell* **145,** 92–103 (2011).
205. Huang, T. T., Feinberg, S. L., Suryanarayanan, S. & Miyamoto, S. The zinc finger domain of NEMO is selectively required for NF-kappa B activation by UV radiation and topoisomerase inhibitors. *Mol. Cell. Biol.* **22,** 5813–5825 (2002).
206. Wu, Z.-H., Shi, Y., Tibbetts, R. S. & Miyamoto, S. Molecular Linkage Between the Kinase ATM and NF-κB Signaling in Response to Genotoxic Stimuli. *Science (80-.).* **311,** (2006).
207. Mabb, A. M., Wuerzberger-Davis, S. M. & Miyamoto, S. PIASy mediates NEMO sumoylation and NF-κB activation in response to genotoxic stress. *Nat. Cell Biol.* **8,** 986–993 (2006).
208. Janssens, S., Tinel, A., Lippens, S. & Tschopp, J. PIDD Mediates NF-κB activation in response to DNA damage. *Cell* **123,** 1079–1092 (2005).

209. Stilmann, M. *et al.* A Nuclear Poly(ADP-Ribose)-Dependent Signalosome Confers DNA Damage-Induced IκB Kinase Activation. *Mol. Cell* **36,** 365–378 (2009).
210. Wu, Z. H. *et al.* ATM- and NEMO-dependent ELKS ubiquitination coordinates TAK1-Mediated IKK activation in response to genotoxic stress. *Mol. Cell* **40,** 75–86 (2010).
211. Hinz, M. *et al.* A cytoplasmic ATM-TRAF6-cIAP1 module links nuclear DNA damage signaling to ubiquitin-mediated NF-κB activation. *Mol. Cell* **40,** 63–74 (2010).
212. DiDonato, J. A., Hayakawa, M., Rothwarf, D. M., Zandi, E. & Karin, M. A cytokine-responsive IκB kinase that activates the transcription factor NF-κB. *Nature* **388,** 548–554 (1997).
213. Mercurio, F. IKK-1 and IKK-2: Cytokine-Activated IκB Kinases Essential for NF-B Activation. *Science (80-.).* **278,** 860–866 (1997).
214. Zandi, E., Rothwarf, D. M., Delhase, M., Hayakawa, M. & Karin, M. The IκB kinase complex (IKK) contains two kinase subunits, IKK?? and IKK??, necessary for Iκb phosphorylation and NF-κB activation. *Cell* **91,** 243–252 (1997).
215. Rothwarf, D. M., Zandi, E., Natoli, G. & Karin, M. IKK- γ is an essential regulatory subunit of the IκB kinase complex.
216. Chen, Z. J., Parent, L. & Maniatis, T. Site-specific phosphorylation of IkappaBalpha by a novel ubiquitination-dependent protein kinase activity. *Cell* **84,** 853–862 (1996).
217. Sigala, J. L. D. Activation of Transcription Factor NF-κB Requires ELKS, an I B Kinase Regulatory Subunit. *Science (80-.).* **304,** 1963–1967 (2004).
218. Xu, G. *et al.* Crystal structure of inhibitor of κB kinase β. *Nature* **472,** 325–330 (2011).
219. May, M. J., Marienfeld, R. B. & Ghosh, S. Characterization of the IκB-kinase NEMO binding domain. *J. Biol. Chem.* **277,** 45992–46000 (2002).
220. May, M. J. Selective Inhibition of NF-kappa B Activation by a Peptide That Blocks the Interaction of NEMO with the Ikappa B Kinase Complex. *Science (80-.).* **289,** 1550–1554 (2000).
221. Zandi, E., Chen, Y. & Karin, M. Direct phosphorylation of IkappaB by IKKalpha and IKKbeta: discrimination between free and NF-kappaB-bound substrate. *Science* **281,** 1360–3 (1998).
222. Delhase, M. Positive and Negative Regulation of IκB Kinase Activity Through IKK Subunit Phosphorylation. *Science (80-.).* **284,** 309–313 (1999).
223. Hu, Y. *et al.* Abnormal morphogenesis but intact IKK activation in mice lacking the IKKalpha subunit of IkappaB kinase. *Science* **284,** 316–20 (1999).
224. Takeda, K. *et al.* Limb and skin abnormalities in mice lacking IKKalpha. *Science (80-.).* **284,** 313–316 (1999).
225. Li, Q. *et al.* IKK1-deficient mice exhibit abnormal development of skin and skeleton. *Genes Dev.* **13,** 1322–1328 (1999).
226. Senftleben, U., Li, Z. W., Baud, V. & Karin, M. IKKβ is essential for protecting T cells from TNFα-induced apoptosis. *Immunity* **14,** 217–230 (2001).

227. Alcamo, E. *et al.* Targeted mutation of TNF receptor I rescues the RelA-deficient mouse and reveals a critical role for NF-kappa B in leukocyte recruitment. *J. Immunol.* **167,** 1592–1600 (2001).
228. Poljak, L., Carlson, L., Cunningham, K., Kosco-Vilbois, M. H. & Siebenlist, U. Distinct activities of p52/NF-kappa B required for proper secondary lymphoid organ microarchitecture: functions enhanced by Bcl-3. *J. Immunol.* **163,** 6581–8 (1999).
229. Caamano, J. H. *et al.* Nuclear factor (NF)-kB2 (p100/p52) is required for normal splenic microarchitecture and B cell-mediated immune responses. *J.Exp.Med.* **187,** 185–196 (1998).
230. Yamada, T. *et al.* Abnormal immune function of hemopoietic cells from alymphoplasia (aly) mice, a natural strain with mutant NF-kappa B-inducing kinase. *J. Immunol.* **165,** 804–12 (2000).
231. Johnson, L. N., Noble, M. E. M. & Owen, D. J. *Active and inactive protein kinases: Structural basis for regulation*. *Cell* **85,** 149–158 (1996).
232. Zhang, J., Clark, K., Lawrence, T., Peggie, M. W. & Cohen, P. An unexpected twist to the activation of IKKβ: TAK1 primes IKKβ for activation by autophosphorylation. *Biochem. J.* **461,** 531–537 (2014).
233. Hacker, H. & Karin, M. Regulation and Function of IKK and IKK-Related Kinases. *Sci. STKE* **2006,** re13-re13 (2006).
234. Margalef, P. *et al.* A Truncated Form of IKKα Is Responsible for Specific Nuclear IKK Activity in Colorectal Cancer. *Cell Rep.* **2,** 840–854 (2012).
235. Mulero, M. C. *et al.* Chromatin-bound IκBα regulates a subset of polycomb target genes in differentiation and cancer. *Cancer Cell* **24,** 151–166 (2013).
236. Yamaoka, S. *et al.* Complementation cloning of NEMO, a component of the IκB kinase complex essential for NF-κB activation. *Cell* **93,** 1231–1240 (1998).
237. Tegethoff, S., Behlke, J. & Scheidereit, C. Tetrameric oligomerization of IkappaB kinase gamma (IKKgamma) is obligatory for IKK complex activity and NF-kappaB activation. *Mol. Cell. Biol.* **23,** 2029–41 (2003).
238. Rudolph, D. *et al.* Severe liver degeneration and lack of NF-kappaB activation in NEMO/IKKgamma-deficient mice. *Genes Dev.* **14,** 854–62 (2000).
239. Schmidt-Supprian, M. *et al.* NEMO/IKK gamma-deficient mice model incontinentia pigmenti. *Mol. Cell* **5,** 981–92 (2000).
240. Kenwrick, S. J. *et al.* Genomic rearrangement in NEMO impairs NF-kappaB activation and is a cause of incontinentia pigmenti. The International Incontinentia Pigmenti (IP) Consortium. *Nature* **405,** 466–472 (2000).
241. Yamaguchi, K. *et al.* Identification of a member of the MAPKKK family as a potential mediator of TGF-β signal transduction. *Science (80-.).* **270,** 2008–2011 (1995).
242. Sakurai, H., Shigemori, N., Hasegawa, K. & Sugita, T. TGF-β-Activated Kinase 1 Stimulates NF-κB Activation by an NF-κB-Inducing Kinase-Independent Mechanism. *Biochem. Biophys. Res. Commun.* **243,** 545–549 (1998).
243. Ninomiya-Tsuji, J. *et al.* The kinase TAK1 can activate the NIK-I kappaB as well as the MAP kinase cascade in the IL-1 signalling pathway. *Nature* **398,**

252–256 (1999).
244. Cheung, P. C. F., Nebreda, A. R. & Cohen, P. TAB3, a new binding partner of the protein kinase TAK1. *Biochem. J.* **378,** 27–34 (2004).
245. Kanayama, A. *et al.* TAB2 and TAB3 activate the NF-κB pathway through binding to polyubiquitin chains. *Mol. Cell* **15,** 535–548 (2004).
246. Shibuya, H. *et al.* TAB1: an activator of the TAK1 MAPKKK in TGF-beta signal transduction. *Science* **272,** 1179–82 (1996).
247. Takaesu, G. *et al.* TAB2, a Novel Adaptor Protein, Mediates Activation of TAK1 MAPKKK by Linking TAK1 to TRAF6 in the IL-1 Signal Transduction Pathway. *Mol. Cell* **5,** 649–658 (2000).
248. Yu, Y. *et al.* Phosphorylation of Thr-178 and Thr-184 in the TAK1 T-loop is required for interleukin (IL)-1-mediated optimal NFκB and AP-1 activation as well as IL-6 gene expression. *J. Biol. Chem.* **283,** 24497–24505 (2008).
249. Kishimoto, K., Matsumoto, K. & Ninomiya-Tsuji, J. TAK1 mitogen-activated protein kinase kinase kinase is activated by autophosphorylation within its activation loop. *J. Biol. Chem.* **275,** 7359–7364 (2000).
250. Scholz, R. *et al.* Autoactivation of transforming growth factor β-activated kinase 1 is a sequential bimolecular process. *J. Biol. Chem.* **285,** 25753–25766 (2010).
251. Singhirunnusorn, P., Suzuki, S., Kawasaki, N., Saiki, I. & Sakurai, H. Critical roles of threonine 187 phosphorylation in cellular stress-induced rapid and transient activation of transforming growth factor-??-activated kinase 1 (TAK1) in a signaling complex containing TAK1-binding protein TAB1 and TAB2. *J. Biol. Chem.* **280,** 7359–7368 (2005).
252. Kobayashi, Y. *et al.* Prostaglandin E2 enhances osteoclastic differentiation of precursor cells through protein kinase A-dependent phosphorylation of TAK1. *J. Biol. Chem.* **280,** 11395–11403 (2005).
253. Ouyang, C. *et al.* Transforming growth factor (TGF)-??-activated kinase 1 (TAK1) activation requires phosphorylation of serine 412 by protein kinase A catalytic subunit ?? (PKAC??) and X-linked protein kinase (PRKX). *J. Biol. Chem.* **289,** 24226–24237 (2014).
254. Zheng, H. *et al.* The dual-specificity phosphatase DUSP14 negatively regulates tumor necrosis factor- and interleukin-1-induced nuclear factor-??B activation by dephosphorylating the protein kinase TAK1. *J. Biol. Chem.* **288,** 819–825 (2013).
255. Kajino, T. *et al.* Protein phosphatase 6 down-regulates TAK1 kinase activation in the IL-1 signaling pathway. *J. Biol. Chem.* **281,** 39891–39896 (2006).
256. Hanada, M. *et al.* Regulation of the TAK1 Signaling Pathway by Protein Phosphatase 2C. *J. Biol. Chem.* **276,** 5753–5759 (2001).
257. Li, M. G. *et al.* Regulation of the interleukin-1-induced signaling pathways by a novel member of the protein phosphatase 2C family (PP2Cε). *J. Biol. Chem.* **278,** 12013–12021 (2003).
258. Sung, I. K., Joon, H. K., Wang, L. & Choi, M. E. Protein phosphatase 2A is a negative regulator of transforming growth factor-β1-induced TAK1 activation in mesangial cells. *J. Biol. Chem.* **283,** 10753–10763 (2008).
259. Yang, Y. *et al.* A Cytosolic ATM/NEMO/RIP1 Complex Recruits TAK1 To Mediate the NF- κB and p38 Mitogen-Activated Protein Kinase

(MAPK)/MAPK-Activated Protein 2 Responses to DNA Damage. *Mol. Cell. Biol.* **31,** 2774–2786 (2011).
260. Dai, L., Aye Thu, C., Liu, X. Y., Xi, J. & Cheung, P. C. F. TAK1, more than just innate immunity. *IUBMB Life* **64,** 825–834 (2012).
261. Ishitani, T. *et al.* The TAK1-NLK-MAPK-related pathway antagonizes signalling between beta-catenin and transcription factor TCF. *Nature* **399,** 798–802 (1999).
262. Ishitani, T. *et al.* The TAK1-NLK Mitogen-Activated Protein Kinase Cascade Functions in the Wnt-5a/Ca2+ Pathway To Antagonize Wnt/ -Catenin Signaling. *Mol. Cell. Biol.* **23,** 131–139 (2003).
263. Takada, I. *et al.* A histone lysine methyltransferase activated by non-canonical Wnt signalling suppresses PPAR-γ transactivation. *Nat. Cell Biol.* **9,** 1273–1285 (2007).
264. Hu, Y. *et al.* IKKalpha controls formation of the epidermis independently of NF-kappaB. *Nature* **410,** 710–4 (2001).
265. Descargues, P. *et al.* IKKalpha is a critical coregulator of a Smad4-independent TGFbeta-Smad2/3 signaling pathway that controls keratinocyte differentiation. *Proc. Natl. Acad. Sci. U. S. A.* **105,** 2487–92 (2008).
266. Zhu, F. *et al.* IKKα Shields 14-3-3σ, a G2/M Cell Cycle Checkpoint Gene, from Hypermethylation, Preventing Its Silencing. *Mol. Cell* **27,** 214–227 (2007).
267. Liu, B. *et al.* A critical role for I kappaB kinase alpha in the development of human and mouse squamous cell carcinomas. *Proc. Natl. Acad. Sci. U. S. A.* **103,** 17202–7 (2006).
268. Park, E. *et al.* Reduction in IkappaB kinase alpha expression promotes the development of skin papillomas and carcinomas. *Cancer Res.* **67,** 9158–9168 (2007).
269. Cao, Y. *et al.* IKKα provides an essential link between RANK signaling and cyclin D1 expression during mammary gland development. *Cell* **107,** 763–775 (2001).
270. Espinosa, L., Bigas, A. & Mulero, M. C. Alternative nuclear functions for NF-κB family members. *Am. J. Cancer Res.* **1,** 446–59 (2011).
271. Huang, W.-C. & Hung, M.-C. Beyond NF-κB activation: nuclear functions of IκB kinase α. *J. Biomed. Sci.* **20,** 3 (2013).
272. Anest, V. *et al.* A nucleosomal function for IκB kinase-α in NF-κB-dependent gene expression. *Nature* **423,** 659–663 (2003).
273. Yamamoto, Y., Verma, U. N., Prajapati, S., Kwak, Y.-T. & Gaynor, R. B. Histone H3 phosphorylation by IKK-α is critical for cytokine-induced gene expression. *Nature* **423,** 655–659 (2003).
274. Gye, Y. P. *et al.* NIK is involved in nucleosomal regulation by enhancing histone H3 phosphorylation by IKKα. *J. Biol. Chem.* **281,** 18684–18690 (2006).
275. Hoberg, J. E. *et al.* SMRT derepression by the IkappaB kinase alpha: a prerequisite to NF-kappaB transcription and survival. *Mol. Cell* **16,** 245–55 (2004).
276. Hoberg, J. E., Popko, A. E., Ramsey, C. S. & Mayo, M. W. IκB kinase a-mediated derepression of SMRT potentiates acetylation of RelA/p65 by

p300. *Mol Cell Biol* **26,** 457–471 (2006).
277. Lawrence, T., Bebien, M., Liu, G. Y., Nizet, V. & Karin, M. IKKα limits macrophage NF-κB activation and contributes to the resolution of inflammation. *Nature* **434,** 1138–1143 (2005).
278. Liu, B. *et al.* Proinflammatory Stimuli Induce IKKα-Mediated Phosphorylation of PIAS1 to Restrict Inflammation and Immunity. *Cell* **129,** 903–914 (2007).
279. Albanese, C. *et al.* IKKalpha regulates mitogenic signaling through transcriptional induction of cyclin D1 via Tcf. *Mol. Biol. Cell* **14,** 585–99 (2003).
280. Prajapati, S. *et al.* IKK?? regulates the mitotic phase of the cell cycle by modulating Aurora A phosphorylation. *Cell Cycle* **5,** 2371–2380 (2006).
281. Colomer, C., Marruecos, L., Vert, A., Bigas, A. & Espinosa, L. NF-κB Members Left Home: NF-κB-Independent Roles in Cancer. *Biomed. 2017, Vol. 5, Page 26* **5,** 26 (2017).
282. Liu, S., Chen, Z., Zhu, F. & Hu, Y. IκB kinase alpha and cancer. *J. Interferon Cytokine Res.* **32,** 152–8 (2012).
283. Fernandez-Majada, V. *et al.* Nuclear IKK activity leads to dysregulated Notch-dependent gene expression in colorectal cancer. *Proc. Natl. Acad. Sci.* **104,** 276–281 (2007).
284. Fernández-Majada, V. *et al.* Aberrant Cytoplasmic Localization of N-CoR in Colorectal Tumors. *Cell Cycle* **6,** 1748–1752 (2007).
285. Margalef, P. *et al.* BRAF-induced tumorigenesis is IKKα-dependent but NF-κB-independent. *Sci. Signal.* **8,** (2015).
286. Göktuna, S. I. *et al.* IKKα Promotes Intestinal Tumorigenesis by Limiting Recruitment of M1-like Polarized Myeloid Cells. *Cell Rep.* **7,** 1914–1925 (2014).
287. Liu, B. *et al.* IKKα Is Required to Maintain Skin Homeostasis and Prevent Skin Cancer. *Cancer Cell* **14,** 212–225 (2008).
288. Marinari, B. *et al.* The tumor suppressor activity of IKKalpha in stratified epithelia is exerted in part via the TGF-beta antiproliferative pathway. *Proc. Natl. Acad. Sci. U. S. A.* **105,** 17091–6 (2008).
289. Jia, J. *et al.* LGR5 expression is controled by IKKα in basal cell carcinoma through activating STAT3 signaling pathway. *Oncotarget* **7,** 27280–94 (2016).
290. Alameda, J. P. *et al.* Deciphering the role of nuclear and cytoplasmic IKKα in skin cancer. *Oncotarget* **7,** 29531–47 (2016).
291. Toll, A. *et al.* Active nuclear IKK correlates with metastatic risk in cutaneous squamous cell carcinoma. *Arch. Dermatol. Res.* **307,** 721–729 (2015).
292. Tu, Z. *et al.* IKKα regulates estrogen-induced cell cycle progression by modulating E2F1 expression. *J. Biol. Chem.* **281,** 6699–6706 (2006).
293. Park, K. J., Krishnan, V., O'Malley, B. W., Yamamoto, Y. & Gaynor, R. B. Formation of an IKKα-dependent transcription complex is required for estrogen receptor-mediated gene activation. *Mol. Cell* **18,** 71–82 (2005).
294. Hao, L. *et al.* Notch-1 activates estrogen receptor-alpha-dependent transcription via IKKalpha in breast cancer cells. *Oncogene* **29,** 201–213 (2010).

295. Vilimas, T. *et al.* Targeting the NF-κB signaling pathway in Notch1-induced T-cell leukemia. *Nat. Med.* **13,** 70–77 (2007).
296. Tan, W. *et al.* Tumour-infiltrating regulatory T cells stimulate mammary cancer metastasis through RANKL–RANK signalling. *Nature* **470,** 548–553 (2011).
297. Gonzalez-Suarez, E. *et al.* RANK ligand mediates progestin-induced mammary epithelial proliferation and carcinogenesis. *Nature* **468,** 103–7 (2010).
298. Schramek, D. *et al.* Osteoclast differentiation factor RANKL controls development of progestin-driven mammary cancer. *Nature* **468,** 98–102 (2010).
299. Zhang, W. *et al.* A NIK-IKKα Module Expands ErbB2-Induced Tumor-Initiating Cells by Stimulating Nuclear Export of p27/Kip1. *Cancer Cell* **23,** 647–659 (2013).
300. Dan, H. C. *et al.* Akt-dependent activation of mTORC1 complex involves phosphorylation of mTOR (mammalian target of rapamycin) by IκB kinase α (IKKα). *J. Biol. Chem.* **289,** 25227–25240 (2014).
301. Dan, H. C., Adli, M. & Baldwin, A. S. Regulation of mammalian target of rapamycin activity in PTEN-inactive prostate cancer cells by IKKα. *Cancer Res.* **67,** 6263–9 (2007).
302. Dan, H. C., Antonia, R. J. & Baldwin, A. S. PI3K/Akt promotes feedforward mTORC2 activation through IKKα. *Oncotarget* **7,** 21064–21075 (2016).
303. Luo, J.-L. *et al.* Nuclear cytokine-activated IKKα controls prostate cancer metastasis by repressing Maspin. *Nature* **446,** 690–694 (2007).
304. Motola-Kuba, D., Zamora-Valdés, D., Uribe, M. & Méndez-Sánchez, N. Hepatocellular carcinoma. An overview. *Ann. Hepatol. Off. J. Mex. Assoc. Hepatol.* **5,** 16–24 (2006).
305. Koppe, C. *et al.* IκB kinaseα/β control biliary homeostasis and hepatocarcinogenesis in mice by phosphorylating the cell-death mediator receptor-interacting protein kinase 1. *Hepatology* **64,** 1217–1231 (2016).
306. Aigelsreiter, A. *et al.* NEMO expression in human hepatocellular carcinoma and its association with clinical outcome. *Hum. Pathol.* **43,** 1012–1019 (2012).
307. Ehlken, H. *et al.* Death receptor-independent FADD signalling triggers hepatitis and hepatocellular carcinoma in mice with liver parenchymal cell-specific NEMO knockout. *Cell Death Differ.* **21,** 1–12 (2014).
308. Kondylis, V. *et al.* NEMO Prevents Steatohepatitis and Hepatocellular Carcinoma by Inhibiting RIPK1 Kinase Activity-Mediated Hepatocyte Apoptosis. *Cancer Cell* **28,** 582–598 (2015).
309. Luedde, T. *et al.* Deletion of NEMO/IKKγ in Liver Parenchymal Cells Causes Steatohepatitis and Hepatocellular Carcinoma. *Cancer Cell* **11,** 119–132 (2007).
310. Huang, W.-C., Ju, T.-K., Hung, M.-C. & Chen, C.-C. Phosphorylation of CBP by IKKα Promotes Cell Growth by Switching the Binding Preference of CBP from p53 to NF-κB. *Mol. Cell* **26,** 75–87 (2007).
311. Karin, M., Cao, Y., Greten, F. R. & Li, Z.-W. NF-κB IN CANCER: FROM INNOCENT BYSTANDER TO MAJOR CULPRIT. *Nat. Rev. Cancer* **2,** 301–310 (2002).

312. Gilmore, T. D. & Garbati, M. R. Inhibition of NF-κB Signaling as a Strategy in Disease Therapy. in *Current topics in microbiology and immunology* **349,** 245–263 (2010).
313. Gilmore, T. D. & Herscovitch, M. Inhibitors of NF-κB signaling: 785 and counting. *Oncogene* **25,** 6887–6899 (2006).
314. Karin, M., Yamamoto, Y. & Wang, Q. M. The IKK NF-κB system: a treasure trove for drug development. *Nat. Rev. Drug Discov.* **3,** 17–26 (2004).
315. Folmer, F., Jaspars, M., Dicato, M. & Diederich, M. Marine natural products as targeted modulators of the transcription factor NF-??B. *Biochem. Pharmacol.* **75,** 603–617 (2008).
316. Ríos, J. L., Recio, M. C., Escandell, J. M. & Andújar, I. Inhibition of transcription factors by plant-derived compounds and their implications in inflammation and cancer. *Curr. Pharm. Des.* **15,** 1212–1237 (2009).
317. Habineza Ndikuyeze, G. *et al.* A phase I clinical trial of systemically delivered NEMO binding domain peptide in dogs with spontaneous activated B-cell like diffuse large B-cell lymphoma. *PLoS One* **9,** e95404 (2014).
318. Lee, D. F. & Hung, M. C. Advances in targeting IKK and IKK-related kinases for cancer therapy. *Clinical Cancer Research* **14,** 5656–5662 (2008).
319. Lam, L. T. *et al.* Small molecule inhibitors of I??B kinase are selectively toxic for subgroups of diffuse large B-cell lymphoma defined by gene expression profiling. *Clin. Cancer Res.* **11,** 28–40 (2005).
320. Schön, M. *et al.* KINK-1, a novel small-molecule inhibitor of IKKβ, and the susceptibility of melanoma cells to antitumoral treatment. *J. Natl. Cancer Inst.* **100,** 862–875 (2008).
321. Mabuchi, S. *et al.* Inhibition of NFkappaB increases the efficacy of cisplatin in in vitro and in vivo ovarian cancer models. *J. Biol. Chem.* **279,** 23477–85 (2004).
322. Cusack, J. C. *et al.* Enhanced chemosensitivity to CPT-11 with proteasome inhibitor PS-341: Implications for systemic nuclear factor-κB inhibition. *Cancer Res.* **61,** 3535–3540 (2001).
323. Shah, S. A. *et al.* 26S proteasome inhibition induces apoptosis and limits growth of human pancreatic cancer. *J. Cell. Biochem.* **82,** 110–22 (2001).
324. Bold, R. J., Virudachalam, S. & McConkey, D. J. Chemosensitization of pancreatic cancer by inhibition of the 26S proteasome. *J. Surg. Res.* **100,** 11–7 (2001).
325. Nakanishi, C. & Toi, M. Nuclear factor-kappaB inhibitors as sensitizers to anticancer drugs. *Nat. Rev. Cancer* **5,** 297–309 (2005).
326. Kiessling, M. K. *et al.* Inhibition of constitutively activated nuclear factor-K,B induces reactive oxygen species- and iron-dependent cell death in cutaneous T-cell lymphoma. *Cancer Res.* **69,** 2365–2374 (2009).
327. Doss, S., Hay, N. & Sutcliffe, F. NICE guidance on bortezomib and thalidomide for first-line treatment of multiple myeloma. *Lancet Oncol.* **12,** 837–838 (2011).
328. Amschler, K. *et al.* NF-kappaB inhibition through proteasome inhibition or IKKbeta blockade increases the susceptibility of melanoma cells to cytostatic treatment through distinct pathways. *J. Invest. Dermatol.* **130,**

1073–1086 (2010).
329. Rothwell, P. M. *et al.* Effect of daily aspirin on long-term risk of death due to cancer: Analysis of individual patient data from randomised trials. *Lancet* **377,** 31–41 (2011).
330. Coussens, L. M. & Werb, Z. Inflammation and cancer. *Nature* **420,** 860–867 (2002).
331. Harvey, J. J. An Unidentified Virus which causes the Rapid Production of Tumours in Mice. *Nature* **204,** 1104–1105 (1964).
332. Kirsten, W. H. & Mayer, L. A. Morphologic responses to a murine erythroblastosis virus. *J. Natl. Cancer Inst.* **39,** 311–35 (1967).
333. Ellis, R. W., DeFeo, D., Furth, M. E. & Scolnick, E. M. Mouse cells contain two distinct ras gene mRNA species that can be translated into a p21 onc protein. *Mol. Cell. Biol.* **2,** 1339–45 (1982).
334. DeFeo, D. *et al.* Analysis of two divergent rat genomic clones homologous to the transforming gene of Harvey murine sarcoma virus. *Proc. Natl. Acad. Sci. U. S. A.* **78,** 3328–32 (1981).
335. Chang, E. H., Gonda, M. A., Ellis, R. W., Scolnick, E. M. & Lowy, D. R. Human genome contains four genes homologous to transforming genes of Harvey and Kirsten murine sarcoma viruses. *Proc. Natl. Acad. Sci. U. S. A.* **79,** 4848–52 (1982).
336. Shih, T. Y., Papageorge, A. G., Stokes, P. E., Weeks, M. O. & Scolnick, E. M. Guanine nucleotide-binding and autophosphorylating activities associated with the p21src protein of Harvey murine sarcoma virus. *Nature* **287,** 686–691 (1980).
337. Sweet, R. W. *et al.* The product of ras is a GTPase and the T24 oncogenic mutant is deficient in this activity. *Nature* **311,** 273–5 (1984).
338. Gibbs, J. B., Sigal, I. S., Poe, M. & Scolnick, E. M. Intrinsic GTPase activity distinguishes normal and oncogenic ras p21 molecules. *Proc. Natl. Acad. Sci. U. S. A.* **81,** 5704–8 (1984).
339. Kamata, T. & Feramisco, J. R. Epidermal growth factor stimulates guanine nucleotide binding activity and phosphorylation of ras oncogene proteins. *Nature* **310,** 147–150 (1984).
340. Lemmon, M. A. & Schlessinger, J. Cell signaling by receptor tyrosine kinases. *Cell* **141,** 1117–1134 (2010).
341. Karnoub, A. E. & Weinberg, R. A. Ras oncogenes: split personalities. *Nat. Rev. Mol. Cell Biol.* **9,** 517–531 (2008).
342. Rodriguez-Viciana, P. *et al.* Phosphatidylinositol-3-OH kinase as a direct target of Ras. *Nature* **370,** 527–32 (1994).
343. Pacold, M. E. *et al.* Crystal structure and functional analysis of Ras binding to its effector phosphoinositide 3-kinase gamma. *Cell* **103,** 931–43 (2000).
344. Boguski, M. S. & McCormick, F. Proteins regulating Ras and its relatives. *Nature* **366,** 643–654 (1993).
345. Xu, G. *et al.* The neurofibromatosis type 1 gene encodes a protein related to GAP. *Cell* **62,** 599–608 (1990).
346. Potenza, N. *et al.* Replacement of K-Ras with H-Ras supports normal embryonic development despite inducing cardiovascular pathology in adult mice. *EMBO Rep.* **6,** 432–7 (2005).
347. Koera, K. *et al.* K-Ras is essential for the development of the mouse

embryo. *Oncogene* **15,** 1151–1159 (1997).
348. Umanoff, H., Edelmann, W., Pellicer, A. & Kucherlapati, R. The murine N-ras gene is not essential for growth and development. *Proc. Natl. Acad. Sci. U. S. A.* **92,** 1709–13 (1995).
349. Esteban, L. M. *et al.* Targeted genomic disruption of H-ras and N-ras, individually or in combination, reveals the dispensability of both loci for mouse growth and development. *Mol. Cell. Biol.* **21,** 1444–1452 (2001).
350. Johnson, L. N., Noble, M. E. & Owen, D. J. Active and inactive protein kinases: structural basis for regulation. *Cell* **85,** 149–58 (1996).
351. Koera, K. *et al.* K-ras is essential for the development of the mouse embryo. *Oncogene* **15,** 1151–9 (1997).
352. Rapp, U. R. *et al.* Structure and biological activity of v-raf, a unique oncogene transduced by a retrovirus (malignant transformation/transduction/molecular cloning). *Biochemistry* **80,** 4218–4222 (1983).
353. Jansen, H. W., Ruckert, B., Lurz, R. & Bister, K. Two unrelated cell-derived sequences in the genome of avian leukemia and carcinoma inducing retrovirus MH2. *EMBO J.* **2,** 1969–1975 (1983).
354. Bonner, T. *et al.* The human homologs of the raf (mil) oncogene are located on human chromosomes 3 and 4. *Science* **223,** 71–4 (1984).
355. Jansen, H. *et al.* Homologous cell-derived oncogenes in avian carcinoma virus MH2 and murine sarcoma virus 3611. *Nature* **307,** 281–284 (1984).
356. Moelling, K., Heimann, B., Beimling, P., Rapp, U. R. & Sander, T. Serine- and threonine-specific protein kinase activities of purified gag-mil and gag-raf proteins. *Nature* **312,** 558–561 (1984).
357. Brtva, T. R. *et al.* Two distinct Raf domains mediate interaction with Ras. *J. Biol. Chem.* **270,** 9809–9812 (1995).
358. Chuang, E. *et al.* Critical Binding and Regulatory Interactions between Ras and Raf Occur through a Small, Stable N-Terminal Domain of Raf and Specific Ras Effector Residues. *Mol. Cell. Biol.* **14,** 5318–5325 (1994).
359. Daub, M. *et al.* The RafC1 cysteine-rich domain contains multiple distinct regulatory epitopes which control Ras-dependent Raf activation. *Mol. Cell. Biol.* **18,** 6698–710 (1998).
360. Luo, Z., Diaz, B., Marshall, M. S. & Avruch, J. An intact Raf zinc finger is required for optimal binding to processed Ras and for ras-dependent Raf activation in situ. *Mol. Cell. Biol.* **17,** 46–53 (1997).
361. Ghosh, S. & Bell, R. M. Identification of discrete segments of human Raf-1 kinase critical for high affinity binding to Ha-Ras. *J. Biol. Chem.* **269,** 30785–30788 (1994).
362. Zhang, X. F. *et al.* Normal and oncogenic p21ras proteins bind to the amino-terminal regulatory domain of c-Raf-1. *Nature* **364,** 308–313 (1993).
363. Tzivion, G., Luo, Z. & Avruch, J. A dimeric 14-3-3 protein is an essential cofactor for Raf kinase activity. *Nature* **394,** 88–92 (1998).
364. Stanton, V. P., Nichols, D. W., Laudano, A. P. & Cooper, G. M. Definition of the human raf amino-terminal regulatory region by deletion mutagenesis. *Mol. Cell. Biol.* **9,** 639–647 (1989).
365. Ishikawa, F. *et al.* Identification of a transforming activity suppressing sequence in the c-raf oncogene. *Oncogene* **3,** 653–8 (1988).

366. Fabian, J. R., Daar, I. 0 & Morrison, D. K. Critical Tyrosine Residues Regulate the Enzymatic and Biological Activity of Raf-1 Kinase. *Mol. Cell. Biol.* **13,** 7170–7179 (1993).
367. Mason, C. S. *et al.* Serine and tyrosine phosphorylations cooperate in Raf-1, but not B-Raf activation. *EMBO J.* **18,** 2137–48 (1999).
368. Zhang, B. H. & Guan, K. L. Activation of B-Raf kinase requires phosphorylation of the conserved residues Thr598 and Ser601. *EMBO J.* **19,** 5429–39 (2000).
369. Farrar, M. A., Alberola-lla, J. & Perlmutter, R. M. Activation of the Raf-1 kinase cascade by coumermycin-induced dimerization. *Nature* **383,** 178–181 (1996).
370. Luo, Z. *et al.* Oligomerization activates c-Raf-1 through a Ras-dependent mechanism. *Nature* **383,** 181–185 (1996).
371. Weber, C. K., Slupsky, J. R., Andreas Kalmes, H. & Rapp, U. R. Active ras induces heterodimerization of cRaf and BRaf. *Cancer Res.* **61,** 3595–3598 (2001).
372. Rushworth, L. K., Hindley, A. D., Neill, E. O. ' & Kolch, W. Regulation and Role of Raf-1/B-Raf Heterodimerization. *Mol. Cell. Biol.* **26,** 2262–2272 (2006).
373. Wan, P. T. . C. *et al.* Mechanism of activation of the RAF-ERK signaling pathway by oncogenic mutations of B-RAF. *Cell* **116,** 855–867 (2004).
374. Garnett, M. J., Rana, S., Paterson, H., Barford, D. & Marais, R. Wild-type and mutant B-RAF activate C-RAF through distinct mechanisms involving heterodimerization. *Mol. Cell* **20,** 963–969 (2005).
375. Heidorn, S. J. *et al.* Kinase-Dead BRAF and Oncogenic RAS Cooperate to Drive Tumor Progression through CRAF. *Cell* **140,** 209–221 (2010).
376. Hu, J. *et al.* Allosteric activation of functionally asymmetric RAF kinase dimers. *Cell* **154,** 1036–1046 (2013).
377. Yordy, J. S. & Muise-Helmericks, R. C. Signal transduction and the Ets family of transcription factors. *Oncogene* **19,** 6503–6513 (2000).
378. Pruitt, K. & Der, C. J. Ras and Rho regulation of the cell cycle and oncogenesis. *Cancer Letters* **171,** 1–10 (2001).
379. Dougherty, M. K. *et al.* Regulation of Raf-1 by direct feedback phosphorylation. *Mol. Cell* **17,** 215–224 (2005).
380. Ritt, D. A., Monson, D. M., Specht, S. I. & Morrison, D. K. Impact of feedback phosphorylation and Raf heterodimerization on normal and mutant B-Raf signaling. *Mol. Cell. Biol.* **30,** 806–19 (2010).
381. Hoshino, R. *et al.* Constitutive activation of the 41-/43-kDa mitogen-activated protein kinase signaling pathway in human tumors. *Oncogene* **18,** 813–822 (1999).
382. Cox, A. D. & Der, C. J. Ras history. *Small GTPases* **1,** 2–27 (2010).
383. Davies, H. *et al.* Mutations of the BRAF gene in human cancer. *Nature* **417,** 949–954 (2002).
384. Yao, Z. *et al.* BRAF Mutants Evade ERK-Dependent Feedback by Different Mechanisms that Determine Their Sensitivity to Pharmacologic Inhibition. *Cancer Cell* **28,** 370–383 (2015).
385. Lito, P. *et al.* Relief of Profound Feedback Inhibition of Mitogenic Signaling by RAF Inhibitors Attenuates Their Activity in BRAFV600E Melanomas.

Cancer Cell **22,** 668–682 (2012).
386. Nieto, P. *et al.* A Braf kinase-inactive mutant induces lung adenocarcinoma. *Nature* **548,** 239–243 (2017).
387. Yao, Z. *et al.* Tumours with class 3 BRAF mutants are sensitive to the inhibition of activated RAS. *Nature* **548,** 234 (2017).
388. Long, G. V. *et al.* Prognostic and clinicopathologic associations of oncogenic BRAF in metastatic melanoma. *J. Clin. Oncol.* **29,** 1239–1246 (2011).
389. Kimura, E. T. *et al.* High prevalence of BRAF mutations in thyroid cancer: Genetic evidence for constitutive activation of the RET/PTC-RAS-BRAF signaling pathway in papillary thyroid carcinoma. *Cancer Res.* **63,** 1454–1457 (2003).
390. Emuss, V., Garnett, M., Mason, C. & Marais, R. Mutations of C-RAF are rare in human cancer because C-RAF has a low basal kinase activity compared with B-RAF. *Cancer Res.* **65,** 9719–9726 (2005).
391. Kohl, N. E. *et al.* Selective Inhibition of ras-Dependent Transformation by a Farnesyltransferase Inhibitor. *Source Sci. New Ser. J. Immunol. Eur. J. Immunol Infect. Immun. J. Exp. Med* **260,** 1934–1937 (1993).
392. Gibbs, J. B., Oliff, A. & Kohl, N. E. Farnesyltransferase inhibitors: Ras research yields a potential cancer therapeutic. *Cell* **77,** 175–178 (1994).
393. Hunter, J. C. *et al.* In situ selectivity profiling and crystal structure of SML-8-73-1, an active site inhibitor of oncogenic K-Ras G12C. *Proc. Natl. Acad. Sci.* **111,** 8895–8900 (2014).
394. Ostrem, J. M., Peters, U., Sos, M. L., Wells, J. A. & Shokat, K. M. K-Ras(G12C) inhibitors allosterically control GTP affinity and effector interactions. *Nature* **503,** 548–551 (2013).
395. Maurer, T. *et al.* Small-molecule ligands bind to a distinct pocket in Ras and inhibit SOS-mediated nucleotide exchange activity. *Proc. Natl. Acad. Sci.* **109,** 5299–5304 (2012).
396. Sun, Q. *et al.* Discovery of small molecules that bind to K-Ras and inhibit Sos-mediated activation. *Angew. Chemie - Int. Ed.* **51,** 6140–6143 (2012).
397. Shima, F. *et al.* In silico discovery of small-molecule Ras inhibitors that display antitumor activity by blocking the Ras-effector interaction. *Proc Natl Acad Sci U S A* **110,** 8182–8187 (2013).
398. Cox, A. D., Der, C. J. & Philips, M. R. Targeting RAS Membrane Association: Back to the Future for Anti-RAS Drug Discovery? *Clin. Cancer Res.* **21,** 1819–1827 (2015).
399. Zimmermann, M., Lottersberger, F., Buonomo, S. B., Sfeir, A. & de Lange, T. 53BP1 Regulates DSB Repair Using Rif1 to Control 5' End Resection. *Science (80-.).* **339,** 700–704 (2013).
400. Pecot, C. V. *et al.* Therapeutic Silencing of KRAS Using Systemically Delivered siRNAs. *Mol. Cancer Ther.* **13,** 2876–2885 (2014).
401. Xue, W. *et al.* Small RNA combination therapy for lung cancer. *Proc. Natl. Acad. Sci.* **111,** E3553–E3561 (2014).
402. Kamerkar, S. *et al.* Exosomes facilitate therapeutic targeting of oncogenic KRAS in pancreatic cancer. *Nature* **546,** 498–503 (2017).
403. De Roock, W. *et al.* Effects of KRAS, BRAF, NRAS, and PIK3CA mutations on the efficacy of cetuximab plus chemotherapy in chemotherapy-

refractory metastatic colorectal cancer: A retrospective consortium analysis. *Lancet Oncol.* **11,** 753–762 (2010).
404. Wilhelm, S. M. *et al.* BAY 43-9006 exhibits broad spectrum oral antitumor activity and targets the RAF/MEK/ERK pathway and receptor tyrosine kinases involved in tumor progression and angiogenesis. *Cancer Res.* **64,** 7099–7109 (2004).
405. Llovet, J. M. *et al.* Sorafenib in Advanced Hepatocellular Carcinoma. *N. Engl. J. Med.* **359,** 378–390 (2008).
406. Escudier, B. *et al.* Sorafenib for treatment of renal cell carcinoma: Final efficacy and safety results of the phase III treatment approaches in renal cancer global evaluation trial. *J. Clin. Oncol.* **27,** 3312–3318 (2009).
407. de Castroneves, L. A. *et al.* Sorafenib for the Treatment of Progressive Metastatic Medullary Thyroid Cancer: Efficacy and Safety Analysis. *Thyroid* **26,** 414–419 (2016).
408. Shen, Y.-C. *et al.* Clinical Trials in Hepatocellular Carcinoma: An Update. *Liver Cancer* **2,** 345–364 (2013).
409. Flaherty, K. T. *et al.* Inhibition of Mutated, Activated BRAF in Metastatic Melanoma. *N. Engl. J. Med.* **363,** 809–819 (2010).
410. Yang, H. *et al.* Antitumor activity of BRAF inhibitor vemurafenib in preclinical models of BRAF-mutant colorectal cancer. *Cancer Res.* **72,** 779–789 (2012).
411. Hatzivassiliou, G. *et al.* ERK Inhibition Overcomes Acquired Resistance to MEK Inhibitors. *Mol Cancer Ther.* **11,** 1143–54 (2012).
412. Aronov, A. M. *et al.* Structure-guided design of potent and selective pyrimidylpyrrole inhibitors of extracellular signal-regulated kinase (ERK) using conformational control. *J. Med. Chem.* **52,** 6362–6368 (2009).
413. Ohori, M. *et al.* Identification of a selective ERK inhibitor and structural determination of the inhibitor-ERK2 complex. *Biochem. Biophys. Res. Commun.* **336,** 357–363 (2005).
414. Herrero, A. *et al.* Small Molecule Inhibition of ERK Dimerization Prevents Tumorigenesis by RAS-ERK Pathway Oncogenes. *Cancer Cell* **28,** 170–182 (2015).
415. Morris, E. J. *et al.* Discovery of a novel ERK inhibitor with activity in models of acquired resistance to BRAF and MEK inhibitors. *Cancer Discov.* **3,** 742–750 (2013).
416. Montagut, C. *et al.* Identification of a mutation in the extracellular domain of the Epidermal Growth Factor Receptor conferring cetuximab resistance in colorectal cancer. *Nat. Med.* **18,** 221–223 (2012).
417. Yonesaka, K. *et al.* Activation of ERBB2 Signaling Causes Resistance to the EGFR-Directed Therapeutic Antibody Cetuximab. *Sci. Transl. Med.* **3,** 99ra86-99ra86 (2011).
418. Bertotti, A. *et al.* A molecularly annotated platform of patient- derived xenografts ('xenopatients') identifies HER2 as an effective therapeutic target in cetuximab-resistant colorectal cancer. *Cancer Discov.* **1,** 508–523 (2011).
419. Poulikakos, P. I., Zhang, C., Bollag, G., Shokat, K. M. & Rosen, N. RAF inhibitors transactivate RAF dimers and ERK signaling in cells with wild-type BRAF. *Nature* **464,** 427–30 (2010).

420. Hatzivassiliou, G. *et al.* RAF inhibitors prime wild-type RAF to activate the MAPK pathway and enhance growth. *Nature* **464,** 431–435 (2010).
421. Kopetz, S. *et al.* PLX4032 in metastatic colorectal cancer patients with mutant BRAF tumors . *J. Clin. Oncol.* **28:15s,** (suppl;abstr 3534) (2010).
422. Holderfield, M. *et al.* RAF Inhibitors Activate the MAPK Pathway by Relieving Inhibitory Autophosphorylation. *Cancer Cell* **23,** 594–602 (2013).
423. Bollag, G. *et al.* Clinical efficacy of a RAF inhibitor needs broad target blockade in BRAF-mutant melanoma. *Nature* **467,** 596–599 (2010).
424. Villanueva, J. *et al.* Acquired Resistance to BRAF Inhibitors Mediated by a RAF Kinase Switch in Melanoma Can Be Overcome by Cotargeting MEK and IGF-1R/PI3K. *Cancer Cell* **18,** 683–695 (2010).
425. Su, F. *et al.* Resistance to selective BRAF inhibition can be mediated by modest upstream pathway activation. *Cancer Res.* **72,** 969–978 (2012).
426. Nazarian, R. *et al.* Melanomas acquire resistance to B-RAF(V600E) inhibition by RTK or N-RAS upregulation. *Nature* **468,** 973–977 (2010).
427. Johannessen, C. M. *et al.* COT drives resistance to RAF inhibition through MAP kinase pathway reactivation. *Nature* **468,** 968–972 (2010).
428. Sun, C. *et al.* Reversible and adaptive resistance to BRAF(V600E) inhibition in melanoma. *Nature* **508,** 118–122 (2014).
429. Poulikakos, P. I. *et al.* RAF inhibitor resistance is mediated by dimerization of aberrantly spliced BRAF(V600E). *Nature* **480,** 387–390 (2011).
430. Straussman, R. *et al.* Tumour micro-environment elicits innate resistance to RAF inhibitors through HGF secretion. *Nature* **487,** 500–504 (2012).
431. Hirata, E. *et al.* Intravital imaging reveals how BRAF inhibition generates drug-tolerant microenvironments with high integrin β1/FAK Signaling. *Cancer Cell* **27,** 574–588 (2015).
432. M.R., G. *et al.* Paradox-breaking RAF inhibitors that also target SRC are effective in drug-resistant BRAF mutant melanoma. *Cancer Cell* **27,** 85–96 (2015).
433. Cerezo, M. L. *et al.* Compounds Triggering ER Stress Exert Anti-Melanoma Effects and Overcome BRAF Inhibitor Resistance Compounds Triggering ER Stress Exert Anti-Melanoma Effects and Overcome BRAF Inhibitor Resistance. *Cancer Cell* **29,** 805–819 (2016).
434. Solit, D. B. *et al.* BRAF mutation predicts sensitivity to MEK inhibition. *Nature* **439,** 358–362 (2006).
435. Marusiak, A. A. *et al.* Mixed lineage kinases activate MEK independently of RAF to mediate resistance to RAF inhibitors. *Nat. Commun.* **5,** 3901 (2014).
436. Haling, J. R. *et al.* Structure of the BRAF-MEK Complex Reveals a Kinase Activity Independent Role for BRAF in MAPK Signaling. *Cancer Cell* **26,** 402–413 (2014).
437. Lito, P. *et al.* Disruption of CRAF-Mediated MEK Activation Is Required for Effective MEK Inhibition in KRAS Mutant Tumors. *Cancer Cell* **25,** 697–710 (2014).
438. Hatzivassiliou, G. *et al.* Mechanism of MEK inhibition determines efficacy in mutant KRAS- versus BRAF-driven cancers. *Nature* **501,** 232–236 (2013).
439. Harrison, J. C. & Haber, J. E. Surviving the Breakup: The DNA Damage Checkpoint. *Annu. Rev. Genet.* **40,** 209–235 (2006).

440. Rouse, J. & Jackson, S. P. Interfaces between the detection, signaling, and repair of DNA damage. *Science (80-.).* **297,** 547–551 (2002).
441. Harper, J. W. & Elledge, S. J. The DNA Damage Response: Ten Years After. *Mol. Cell* **28,** 739–745 (2007).
442. Bennett, C. B., Lewis, A. L., Baldwin, K. K. & Resnick, M. A. Lethality induced by a single site-specific double-strand break in a dispensable yeast plasmid. *Proc. Natl. Acad. Sci.* **90,** 5613–5617 (1993).
443. Helleday, T., Eshtad, S. & Nik-Zainal, S. Mechanisms underlying mutational signatures in human cancers. *Nat. Rev. Genet.* **15,** 585–598 (2014).
444. Risk Factors_ Tobacco - National Cancer Institute.
445. Blackadar, C. B. Historical review of the causes of cancer. *World J. Clin. Oncol.* **7,** 54 (2016).
446. Wogan, G. N., Hecht, S. S., Felton, J. S., Conney, A. H. & Loeb, L. A. Environmental and chemical carcinogenesis. *Seminars in Cancer Biology* **14,** 473–486 (2004).
447. Shiloh, Y. ATM and related protein kinases: safeguarding genome integrity. *Nat. Rev. Cancer* **3,** 155–168 (2003).
448. Cimprich, K. A. & Cortez, D. ATR: an essential regulator of genome integrity. *Nat. Rev. Mol. Cell Biol.* **9,** 616–627 (2008).
449. Maréchal, A. & Zou, L. DNA damage sensing by the ATM and ATR kinases. *Cold Spring Harb. Perspect. Biol.* **5,** (2013).
450. Misteli, T. & Soutoglou, E. The emerging role of nuclear architecture in DNA repair and genome maintenance. *Nat. Rev. Mol. Cell Biol.* **10,** 243–254 (2009).
451. Rogakou, E. P., Pilch, D. R., Orr, A. H., Ivanova, V. S. & Bonner, W. M. DNA double-stranded breaks induce histone H2AX phosphorylation on serine 139. *J. Biol. Chem.* **273,** 5858–68 (1998).
452. Lou, Z. *et al.* MDC1 maintains genomic stability by participating in the amplification of ATM-dependent DNA damage signals. *Mol. Cell* **21,** 187–200 (2006).
453. Stewart, G. S., Wang, B., Bignell, C. R., Taylor, A. M. R. & Elledge, S. J. MDC1 is a mediator of the mammalian DNA damage checkpoint. *Nature* **421,** 961–966 (2003).
454. Lee, M. S., Edwards, R. A., Thede, G. L. & Glover, J. N. M. Structure of the BRCT Repeat Domain of MDC1 and Its Specificity for the Free COOH-terminal End of the γ-H2AX Histone Tail. *J. Biol. Chem.* **280,** 32053–32056 (2005).
455. Stucki, M. *et al.* MDC1 directly binds phosphorylated histone H2AX to regulate cellular responses to DNA double-strand breaks. *Cell* **123,** 1213–1226 (2005).
456. Ziv, Y. *et al.* Chromatin relaxation in response to DNA double-strand breaks is modulated by a novel ATM- and KAP-1 dependent pathway. *Nat. Cell Biol.* **8,** 870–876 (2006).
457. Matsuoka, S., Huang, M. & Elledge, S. J. Linkage of ATM to cell cycle regulation by the Chk2 protein kinase. *Science* **282,** 1893–7 (1998).
458. Liu, Q. *et al.* Chk1 is an essential kinase that is regulated by Atr and required for the G2/M DNA damage checkpoint. *Genes Dev.* **14,** 1448–

1459 (2000).
459. Bartek, J. & Lukas, J. DNA damage checkpoints: from initiation to recovery or adaptation. *Current Opinion in Cell Biology* **19,** 238–245 (2007).
460. Kastan, M. B. & Bartek, J. Cell-cycle checkpoints and cancer. *Nature* **432,** 316–323 (2004).
461. Riley, T., Sontag, E., Chen, P. & Levine, A. Transcriptional control of human p53-regulated genes. *Nat. Rev. Mol. Cell Biol.* **9,** 402–412 (2008).
462. Huen, M. S. & Chen, J. The DNA damage response pathways: at the crossroad of protein modifications. *Cell Res.* **18,** 8–16 (2008).
463. Halazonetis, T. D., Gorgoulis, V. G. & Bartek, J. An Oncogene-Induced DNA Damage Model for Cancer Development. *Science (80-.).* **319,** 1352–1355 (2008).
464. Campisi, J. & d'Adda di Fagagna, F. Cellular senescence: when bad things happen to good cells. *Nat. Rev. Mol. Cell Biol.* **8,** 729–740 (2007).
465. Lieber, M. R. The mechanism of human nonhomologous DNA End joining. *Journal of Biological Chemistry* **283,** 1–5 (2008).
466. San Filippo, J., Sung, P. & Klein, H. Mechanism of Eukaryotic Homologous Recombination. *Annu. Rev. Biochem.* **77,** 229–257 (2008).
467. McVey, M. & Lee, S. E. MMEJ repair of double-strand breaks (director's cut): deleted sequences and alternative endings. *Trends in Genetics* **24,** 529–538 (2008).
468. Iwabuchi, K., Bartel, P. L., Li, B., Marraccino, R. & Fields, S. Two cellular proteins that bind to wild-type but not mutant p53. *Proc. Natl. Acad. Sci. U. S. A.* **91,** 6098–102 (1994).
469. Rappold, I., Iwabuchi, K., Date, T. & Chen, J. Tumor suppressor p53 binding protein 1 (53BP1) is involved in DNA damage-signaling pathways. *J. Cell Biol.* **153,** 613–20 (2001).
470. Bothmer, A. *et al.* Regulation of DNA End Joining, Resection, and Immunoglobulin Class Switch Recombination by 53BP1. *Mol. Cell* **42,** 319–329 (2011).
471. Panier, S. & Boulton, S. J. Double-strand break repair: 53BP1 comes into focus. *Nat. Rev. Mol. Cell Biol.* **15,** 7–18 (2013).
472. Xia, Z., Morales, J. C., Dunphy, W. G. & Carpenter, P. B. Negative Cell Cycle Regulation and DNA Damage-inducible Phosphorylation of the BRCT Protein 53BP1. *J. Biol. Chem.* **276,** 2708–2718 (2001).
473. Anderson, L., Henderson, C. & Adachi, Y. Phosphorylation and Rapid Relocalization of 53BP1 to Nuclear Foci upon DNA Damage. *Mol. Cell. Biol.* **21,** 1719–1729 (2001).
474. Schultz, L. B., Chehab, N. H., Malikzay, A. & Halazonetis, T. D. p53 Binding Protein 1 (53BP1) Is an Early Participant in the Cellular Response to DNA Double-Strand Breaks. *J. Cell Biol.* **151,** 1381–1390 (2000).
475. Bouwman, P. *et al.* 53BP1 loss rescues BRCA1 deficiency and is associated with triple-negative and BRCA-mutated breast cancers. *Nat. Struct. Mol. Biol.* **17,** 688–695 (2010).
476. Bunting, S. F. *et al.* 53BP1 inhibits homologous recombination in brca1-deficient cells by blocking resection of DNA breaks. *Cell* **141,** 243–254 (2010).
477. Chapman, J. R., Taylor, M. R. G. & Boulton, S. J. Playing the End Game:

DNA Double-Strand Break Repair Pathway Choice. *Molecular Cell* **47,** 497–510 (2012).
478. Chapman, J. R., Sossick, A. J., Boulton, S. J. & Jackson, S. P. BRCA1-associated exclusion of 53BP1 from DNA damage sites underlies temporal control of DNA repair. *J. Cell Sci.* **125,** 3529–3534 (2012).
479. Heyer, W.-D., Ehmsen, K. T. & Liu, J. Regulation of Homologous Recombination in Eukaryotes. *Annu. Rev. Genet.* **44,** 113–139 (2010).
480. Dynan, W. S. & Yoo, S. Interaction of Ku protein and DNA-dependent protein kinase catalytic subunit with nucleic acids. *Nucleic Acids Research* **26,** 1551–1559 (1998).
481. Symington, L. S. & Gautier, J. Double-Strand Break End Resection and Repair Pathway Choice. *Annu. Rev. Genet.* **45,** 247–271 (2011).
482. Iwabuchi, K. *et al.* 53BP1 contributes to survival of cells irradiated with X-ray during G1 without Ku70 or Artemis. *Genes to Cells* **11,** 935–948 (2006).
483. Nakamura, K. *et al.* Genetic dissection of vertebrate 53BP1: A major role in non-homologous end joining of DNA double strand breaks. *DNA Repair (Amst).* **5,** 741–749 (2006).
484. Chapman, J. R. *et al.* RIF1 Is Essential for 53BP1-Dependent Nonhomologous End Joining and Suppression of DNA Double-Strand Break Resection. *Mol. Cell* **49,** 858–871 (2013).
485. Escribano-Díaz, C. *et al.* A Cell Cycle-Dependent Regulatory Circuit Composed of 53BP1-RIF1 and BRCA1-CtIP Controls DNA Repair Pathway Choice. *Mol. Cell* **49,** 872–883 (2013).
486. Di Virgilio, M. *et al.* Rif1 Prevents Resection of DNA Breaks and Promotes Immunoglobulin Class Switching. *Science (80-.).* **339,** 711–715 (2013).
487. Feng, L., Fong, K. W., Wang, J., Wang, W. & Chen, J. RIF1 counteracts BRCA1-mediated end resection during DNA repair. *J. Biol. Chem.* **288,** 11135–11143 (2013).
488. Silverman, J., Takai, H., Buonomo, S. B. C., Eisenhaber, F. & de Lange, T. Human Rif1, ortholog of a yeast telomeric protein, is regulated by ATM and 53BP1 and functions in the S-phase checkpoint. *Genes Dev.* **18,** 2108–2119 (2004).
489. Morales, J. C. *et al.* Role for the BRCA1 C-terminal repeats (BRCT) protein 53BP1 in maintaining genomic stability. *J. Biol. Chem.* **278,** 14971–14977 (2003).
490. Mochan, T. A., Venere, M., DiTullio, R. A. & Halazonetis, T. D. 53BP1, an activator of ATM in response to DNA damage. *DNA Repair* **3,** 945–952 (2004).
491. Buonomo, S. B. C., Wu, Y., Ferguson, D. & De Lange, T. Mammalian Rif1 contributes to replication stress survival and homology-directed repair. *J. Cell Biol.* **187,** 385–398 (2009).
492. Cornacchia, D. *et al.* Mouse Rif1 is a key regulator of the replication-timing programme in mammalian cells. *EMBO J.* **31,** 3678–3690 (2012).
493. Yamazaki, S. *et al.* Rif1 regulates the replication timing domains on the human genome. *EMBO J.* **31,** 3667–77 (2012).
494. Xu, D. *et al.* Rif1 provides a new DNA-binding interface for the Bloom syndrome complex to maintain normal replication. *EMBO J.* **29,** 3140–3155

(2010).
495. Dimitrova, N., Chen, Y.-C. M., Spector, D. L. & de Lange, T. 53BP1 promotes non-homologous end joining of telomeres by increasing chromatin mobility. *Nature* **456,** 524–528 (2008).
496. Difilippantonio, S. *et al.* 53BP1 facilitates long-range DNA end-joining during V(D)J recombination. *Nature* **456,** 529–533 (2008).
497. Manis, J. P. *et al.* 53BP1 links DNA damage-response pathways to immunoglobulin heavy chain class-switch recombination. *Nat. Immunol.* **5,** 481–487 (2004).
498. Reina-San-Martin, B., Chen, J., Nussenzweig, A. & Nussenzweig, M. C. Enhanced intra-switch region recombination during immunoglobulin class switch recombination in 53BP1-/- B cells. *Eur. J. Immunol.* **37,** 235–239 (2007).
499. Ward, I. M. *et al.* 53BP1 is required for class switch recombination. *J. Cell Biol.* **165,** 459–464 (2004).
500. Stratton, M. R., Campbell, P. J. & Futreal, P. A. The cancer genome. *Nature* **458,** 719–724 (2009).
501. Negrini, S., Gorgoulis, V. G. & Halazonetis, T. D. Genomic instability — an evolving hallmark of cancer. *Nat. Rev. Mol. Cell Biol.* **11,** 220–228 (2010).
502. Hanahan, D. & Weinberg, R. A. Hallmarks of cancer: The next generation. *Cell* **144,** 646–674 (2011).
503. Jiricny, J. The multifaceted mismatch-repair system. *Nat. Rev. Mol. Cell Biol.* **7,** 335–346 (2006).
504. Wang, H. H. *et al.* Replication protein A2 phosphorylation after DNA damage by the coordinated action of ataxia telangiectasia-mutated and DNA-dependent protein kinase. *Cancer Res.* **61,** 8554–8563 (2001).
505. Goode, E. L., Ulrich, C. M. & Potter, J. D. Polymorphisms in DNA repair genes and associations with cancer risk. *Cancer Epidemiol. Biomarkers Prev.* **11,** 1513–1530 (2002).
506. Pal, T. *et al.* BRCA1 and BRCA2 mutations account for a large proportion of ovarian carcinoma cases. *Cancer* **104,** 2807–2816 (2005).
507. Levy-Lahad, E. & Friedman, E. Cancer risks among BRCA1 and BRCA2 mutation carriers. *Br. J. Cancer* **96,** 11–15 (2007).
508. Bartkova, J. *et al.* DNA damage response as a candidate anti-cancer barrier in early human tumorigenesis. *Nature* **434,** 864–870 (2005).
509. Gorgoulis, V. G. *et al.* Activation of the DNA damage checkpoint and genomic instability in human precancerous lesions. *Nature* **434,** 907–913 (2005).
510. Kandoth, C. *et al.* Mutational landscape and significance across 12 major cancer types. **502,** 333–339 (2013).
511. Ottini, L. *et al.* MRE11 expression is impaired in gastric cancer with microsatellite instability. *Carcinogenesis* **25,** 2337–2343 (2004).
512. Bartkova, J. *et al.* Aberrations of the MRE11-RAD50-NBS1 DNA damage sensor complex in human breast cancer: MRE11 as a candidate familial cancer-predisposing gene. *Mol. Oncol.* **2,** 296–316 (2008).
513. Choudhury, A. *et al.* MRE11 expression is predictive of cause-specific survival following radical radiotherapy for muscle-invasive bladder cancer. *Cancer Res.* **70,** 7017–7026 (2010).

514. Karnitz, L. M. *et al.* Gemcitabine-induced activation of checkpoint signaling pathways that affect tumor cell survival. *Mol Pharmacol* **68,** 1636–1644 (2005).
515. Myers, K., Gagou, M. E., Zuazua-Villar, P., Rodriguez, R. & Meuth, M. ATR and Chk1 Suppress a Caspase-3–Dependent Apoptotic Response Following DNA Replication Stress. *PLoS Genet.* **5,** e1000324 (2009).
516. Woods, D. & Turchi, J. J. Chemotherapy induced DNA damage response Convergence of drugs and pathways. *Cancer Biol. Ther.* **14,** 379–389 (2013).
517. Bao, S. *et al.* Glioma stem cells promote radioresistance by preferential activation of the DNA damage response. *Nature* **444,** 756–760 (2006).
518. Bryant, H. E. *et al.* Specific killing of BRCA2-deficient tumours with inhibitors of poly(ADP-ribose) polymerase. *Nature* **434,** 913–917 (2005).
519. Farmer, H. *et al.* Targeting the DNA repair defect in BRCA mutant cells as a therapeutic strategy. *Nature* **434,** 917–921 (2005).
520. Helleday, T. The underlying mechanism for the PARP and BRCA synthetic lethality: Clearing up the misunderstandings. *Molecular Oncology* **5,** 387–393 (2011).
521. Rouleau, M., Patel, A., Hendzel, M. J., Kaufmann, S. H. & Poirier, G. G. PARP inhibition: PARP1 and beyond. *Nat. Rev. Cancer* **10,** 293–301 (2010).
522. Fong, P. C. *et al.* Inhibition of Poly(ADP-Ribose) Polymerase in Tumors from *BRCA* Mutation Carriers. *N. Engl. J. Med.* **361,** 123–134 (2009).
523. Audeh, M. W. *et al.* Oral poly(ADP-ribose) polymerase inhibitor olaparib in patients with BRCA1 or BRCA2 mutations and recurrent ovarian cancer: a proof-of-concept trial. *Lancet* **376,** 245–251 (2010).
524. Tutt, A. *et al.* Oral poly(ADP-ribose) polymerase inhibitor olaparib in patients with BRCA1 or BRCA2 mutations and advanced breast cancer: a proof-of-concept trial. *Lancet* **376,** 235–244 (2010).
525. Zhao, Y. *et al.* Preclinical Evaluation of a Potent Novel DNA-Dependent Protein Kinase Inhibitor NU7441. *Cancer Res.* **66,** 5354–5362 (2006).
526. Rainey, M. D., Charlton, M. E., Stanton, R. V. & Kastan, M. B. Transient Inhibition of ATM Kinase Is Sufficient to Enhance Cellular Sensitivity to Ionizing Radiation. *Cancer Res.* **68,** 7466–7474 (2008).
527. Golding, S. E. *et al.* Dynamic inhibition of ATM kinase provides a strategy for glioblastoma multiforme radiosensitization and growth control. *Cell Cycle* **11,** 1167–1173 (2012).
528. Fokas, E. *et al.* Targeting ATR in vivo using the novel inhibitor VE-822 results in selective sensitization of pancreatic tumors to radiation. *Cell Death Dis.* **3,** e441 (2012).
529. Pires, I. M. *et al.* Targeting radiation-resistant hypoxic tumour cells through ATR inhibition. *Br. J. Cancer* **107,** 291–299 (2012).
530. Prevo, R. *et al.* The novel ATR inhibitor VE-821 increases sensitivity of pancreatic cancer cells to radiation and chemotherapy. *Cancer Biol. Ther.* **13,** 1072–1081 (2012).
531. Huntoon, C. J. *et al.* ATR Inhibition Broadly Sensitizes Ovarian Cancer Cells to Chemotherapy Independent of BRCA Status. *Cancer Res.* **73,** 3683–3691 (2013).

532. Blasina, A. *et al.* Breaching the DNA damage checkpoint via PF-00477736, a novel small-molecule inhibitor of checkpoint kinase 1. *Mol. Cancer Ther.* **7,** 2394–2404 (2008).
533. Mitchell, C. *et al.* Poly(ADP-ribose) polymerase 1 modulates the lethality of CHK1 inhibitors in carcinoma cells. *Mol. Pharmacol.* **78,** 909–17 (2010).
534. El Marjou, F. *et al.* Tissue-specific and inducible Cre-mediated recombination in the gut epithelium. *genesis* **39,** 186–193 (2004).
535. Gareus, R. *et al.* Normal epidermal differentiation but impaired skin-barrier formation upon keratinocyte-restricted IKK1 ablation. *Nat. Cell Biol.* **9,** 461–469 (2007).
536. Carpenter, A. E. *et al.* CellProfiler: image analysis software for identifying and quantifying cell phenotypes. *Genome Biol.* **7,** R100 (2006).
537. Fatehullah, A., Tan, S. H. & Barker, N. Organoids as an in vitro model of human development and disease. *Nat. Cell Biol.* **18,** 246–254 (2016).
538. VanDussen, K. L. *et al.* Notch signaling modulates proliferation and differentiation of intestinal crypt base columnar stem cells. *Development* **139,** 488–497 (2012).
539. Schmieder, R., Lim, Y. W. & Edwards, R. Identification and removal of ribosomal RNA sequences from metatranscriptomes. *Bioinformatics* **28,** 433–435 (2012).
540. Dobin, A. *et al.* STAR: Ultrafast universal RNA-seq aligner. *Bioinformatics* **29,** 15–21 (2013).
541. Love, M. I., Huber, W. & Anders, S. Moderated estimation of fold change and dispersion for RNA-seq data with DESeq2. *Genome Biol.* **15,** 550 (2014).
542. Huber, W. *et al.* Orchestrating high-throughput genomic analysis with Bioconductor. *Nat. Methods* **12,** 115–121 (2015).
543. Madison, B. B. *et al.* cis elements of the villin gene control expression in restricted domains of the vertical (crypt) and horizontal (duodenum, cecum) axes of the intestine. *J. Biol. Chem.* **277,** 33275–33283 (2002).
544. Van de Wetering, M. *et al.* The β-catenin/TCF-4 complex imposes a crypt progenitor phenotype on colorectal cancer cells. *Cell* **111,** 241–250 (2002).
545. Muñoz, J. *et al.* The Lgr5 intestinal stem cell signature: robust expression of proposed quiescent '+4' cell markers. *EMBO J* **31,** 3079–3091 (2012).
546. Fre, S., Bardin, A., Robine, S. & Louvard, D. Notch signaling in intestinal homeostasis across species: the cases of Drosophila, Zebrafish and the mouse. *Exp Cell Res* **317,** 2740–2747 (2011).
547. Riccio, O. *et al.* Loss of intestinal crypt progenitor cells owing to inactivation of both Notch1 and Notch2 is accompanied by derepression of CDK inhibitors p27Kip1 and p57Kip2. *EMBO Rep* **9,** 377–383 (2008).
548. Guiu, J. *et al.* Identification of Cdca7 as a novel Notch transcriptional target involved in hematopoietic stem cell emergence. *J Exp Med* **211,** 2411–2423 (2014).
549. Barker, N. *et al.* Identification of stem cells in small intestine and colon by marker gene Lgr5. *Nature* **449,** 1003–1007 (2007).
550. Batlle, E. *et al.* Beta-catenin and TCF mediate cell positioning in the intestinal epithelium by controlling the expression of EphB/ephrinB. *Cell* **111,** 251–263 (2002).

551. van der Flier, L. G. *et al.* Transcription factor achaete scute-like 2 controls intestinal stem cell fate. *Cell* **136,** 903–912 (2009).
552. Wong, V. W. *et al.* Lrig1 controls intestinal stem-cell homeostasis by negative regulation of ErbB signalling. *Nat Cell Biol* **14,** 401–408 (2012).
553. Fernández-Majada, V. *et al.* Nuclear IKK activity leads to dysregulated notch-dependent gene expression in colorectal cancer. *Proc Natl Acad Sci U S A* **104,** 276–281 (2007).
554. Kubiniok, P., Lavoie, H., Therrien, M. & Thibault, P. Time-resolved Phosphoproteome Analysis of Paradoxical RAF Activation Reveals Novel Targets of ERK. *Mol. Cell. Proteomics* **16,** 663–679 (2017).
555. Winter, M. *et al.* Deciphering the acute cellular phosphoproteome response to irradiation with X-rays, protons and carbon ions. *Mol. Cell. Proteomics* **16,** mcp.M116.066597 (2017).
556. Ciccia, A. & Elledge, S. J. The DNA Damage Response: Making It Safe to Play with Knives. *Molecular Cell* **40,** 179–204 (2010).
557. McCool, K. W. & Miyamoto, S. DNA damage-dependent NF-κB activation: NEMO turns nuclear signaling inside out. *Immunol. Rev.* **246,** 311–326 (2012).
558. Lee, D. H. *et al.* Dephosphorylation Enables the Recruitment of 53BP1 to Double-Strand DNA Breaks. *Mol. Cell* **54,** 512–525 (2014).
559. Sfeir, A. & de Lange, T. Removal of Shelterin Reveals the Telomere End-Protection Problem. *Science (80-.).* **336,** 593–597 (2012).
560. fda & cder. HIGHLIGHTS OF PRESCRIBING INFORMATION.
561. Hu, T., Li, Z., Gao, C.-Y. & Cho, C. H. Mechanisms of drug resistance in colon cancer and its therapeutic strategies. *World J. Gastroenterol.* **22,** 6876–89 (2016).
562. Lynch, H. T., Lynch, J. F., Lynch, P. M. & Attard, T. Hereditary colorectal cancer syndromes: Molecular genetics, genetic counseling, diagnosis and management. in *Familial Cancer* **7,** 27–39 (2008).
563. Leedham, S. J. *et al.* A basal gradient of Wnt and stem-cell number influences regional tumour distribution in human and mouse intestinal tracts. *Gut* **62,** 83–93 (2013).
564. Wullaert, A., Bonnet, M. C. & Pasparakis, M. NF-κB in the regulation of epithelial homeostasis and inflammation. *Cell Res.* **21,** 146–158 (2011).
565. Latonen, L., Taya, Y. & Laiho, M. UV-radiation induces dose-dependent regulation of p53 response and modulates p53-HDM2 interaction in human fibroblasts. *Oncogene* **20,** 6784–6793 (2001).
566. Rodemann, H. P., Dittmann, K. & Toulany, M. Radiation-induced EGFR-signaling and control of DNA-damage repair. *International Journal of Radiation Biology* **83,** 781–791 (2007).
567. Yuan, T. L. *et al.* Development of siRNA payloads to target KRAS-Mutant cancer. *Cancer Discov.* **4,** 1182–1197 (2014).
568. Zhang, Y.-W. *et al.* Genotoxic Stress Targets Human Chk1 for Degradation by the Ubiquitin-Proteasome Pathway. *Mol. Cell* **19,** 607–618 (2005).
569. Zhang, Y.-W. *et al.* The F box protein Fbx6 regulates Chk1 stability and cellular sensitivity to replication stress. *Mol. Cell* **35,** 442–53 (2009).
570. de Lange, T. Shelterin: the protein complex that shapes and safeguards human telomeres. *Genes Dev.* **19,** 2100–2110 (2005).

571. Aparicio, J. *et al.* FOLFOX alternated with FOLFIRI as first-line chemotherapy for metastatic colorectal cancer. *Clin. Colorectal Cancer* **5,** 263–7 (2005).
572. Masi, G. *et al.* First-line 5-fluorouracil/folinic acid, oxaliplatin and irinotecan (FOLFOXIRI) does not impair the feasibility and the activity of second line treatments in metastatic colorectal cancer. *Ann. Oncol.* **17,** 1249–1254 (2006).
573. Ha, H., Han, D. & Choi, Y. TRAF-Mediated TNFR-Family Signaling. in *Current Protocols in Immunology* **Chapter 11,** Unit11.9D (John Wiley & Sons, Inc., 2009).
574. Malinin, N. L., Boldin, M. P., Kovalenko, A. V. & Wallach, D. MAP3K-related kinase involved in NF-KB induction by TNF, CD95 and IL-1. *Nature* **385,** 540–544 (1997).
575. Gonzalez-Suarez, E. *et al.* RANK Overexpression in Transgenic Mice with Mouse Mammary Tumor Virus Promoter-Controlled RANK Increases Proliferation and Impairs Alveolar Differentiation in the Mammary Epithelia and Disrupts Lumen Formation in Cultured Epithelial Acini. *Mol. Cell. Biol.* **27,** 1442–1454 (2007).
576. Fata, J. E. *et al.* The Osteoclast Differentiation Factor Osteoprotegerin-Ligand Is Essential for Mammary Gland Development. *Cell* **103,** 41–50 (2000).
577. Borg, Å. *et al.* HER2/neu AMPLIFICATION AND COMEDO TYPE BREAST CARCINOMA. *The Lancet* **333,** 1268–1269 (1989).
578. Majumder, P. K. & Sellers, W. R. Akt-regulated pathways in prostate cancer. *Oncogene* **24,** 7465–7474 (2005).
579. Garnett, M. J. & Marais, R. Guilty as charged: B-RAF is a human oncogene. *Cancer Cell* **6,** 313–319 (2004).
580. Edgar, R., Domrachev, M. & Lash, A. E. Gene Expression Omnibus: NCBI gene expression and hybridization array data repository. *Nucleic Acids Res.* **30,** 207–10 (2002).